



**Defining a Role for SNARE Proteins in
Dendritic Cell Secretion**

A thesis submitted for the degree of Ph.D.

By

Laura Collins B.Sc. (Hons)

January 2014

Based on research carried out at

School of Biotechnology,

Dublin City University,

Dublin 9

Ireland

Under the Supervision of Dr. Christine Loscher

Declaration

I hereby certify that this material, which I now submit for assessment on the programme of study leading to the award of Doctor of Philosophy is entirely my own work, and that I have exercised reasonable care to ensure that the work is original, and does not to the best of my knowledge breach any law of copyright, and has not been taken from the work of others save and to the extent that such work has been cited and acknowledged within the text of my work.

Signed: _____(Candidate) ID No.: 54485807 Date: _____

TABLE OF CONTENTS

Table of Contents	iii
Abstract	ix
Abbreviations	x
Acknowledgements	xiii
Publications	xv
Chapter 1	1
General Introduction	1
1.0 The Immune System	2
1.1 Overview of Innate and Adaptive Immunity	2
1.2 Linking the Innate and Adaptive: The Dendritic Cell.....	3
1.3 Engagement of Pathogen Recognition Receptors (PRRs) in DCs is a critical step in the induction of the adaptive immune response.	4
1.3.1 Toll-like Receptors (TLRs).....	4
1.3.2 TLR location – Critical to their Function	5
1.4 Mature DCs – potent inducers of effector T cell responses.....	7
1.4.1 Migration to Lymphoid Organs – A Role for Chemokines.....	7
1.4.2 Signal 1 - Antigen Presentation - MHC Class I and II	8
1.4.3 Signal 2 – Co-Stimulation molecules CD80/CD86.....	9
1.4.4 Signal 3 – Cytokine polarisation.....	9
1.5 Cytokines and Chemokines as Targets in Inflammatory Disease.....	11
1.6 Protein Trafficking	12
1.6.1 Cytokine Secretion.....	12
1.7 SNAREs	13
1.7.1 SNARE Structure.....	14
1.7.2 SNARE Functions.....	16
1.8 SNAREs and their Role in Disease.....	18
1.9 SNAREs in Immune cells	18
1.9.1. Neutrophils.....	18
1.9.1 Mast Cells	19
1.9.2 Natural Killer Cells.....	20
1.9.3 Macrophage	21
1.9.4. Dendritic Cell.....	23
1.10 Project Aims and Objectives.....	24

Chapter 2 Materials and Methods	25
2.1 Materials.....	26
2.1.1 Cell Culture Materials and Reagents	26
2.1.2 Enzyme Linked ImmunoSorbent Assay Reagents.....	27
2.1.3 Flow Cytometry Reagents	27
2.1.4 FACS Aria Reagents.....	28
2.1.5 RNA Isolation and cDNA synthesis Reagents	28
2.1.6 Polymerase Reaction Chain Reaction Reagents	28
2.1.7 Quantitative Reverse Transcriptase Polymerase Chain Primers.....	29
2.1.8 Protein Purification Reagents	30
2.1.9 Antibodies used for Western and Immunofluorescence	30
2.1.10 Immunofluorescence Reagents	30
2.1.11 Immunofluorescence Secondary antibodies	31
2.2 Methods.....	32
2.2.1 Stock Solutions and Buffers	32
2.3 Cell Culture Techniques.....	32
2.3.1 Cell Enumeration and Viability Assessment	33
2.3.2 JAWS II Dendritic Cell Line.....	35
2.3.3 Isolation and Culture of Bone Marrow-Derived Dendritic Cells.....	35
2.3.3.1 Day 1 – Bone Marrow Harvest.....	35
2.3.3.2 Day 4 – Feeding Cells.....	36
2.3.3.4 Day 7 – Counting and Plating Cells.....	36
2.3.4 Cryogenic Preservation of Cell Stocks	36
2.3.5 Revival of Frozen Stocks.....	37
2.3.6 Toll-Like Receptor Activation.....	37
2.3.7 Cytotoxicity Assay.....	38
2.4 Enzyme Linked Immunosorbant Assay (ELISA)	39
2.4.1 Detection of Cytokines, IL-6, IL-10, TNF-alpha, IL-12p40, IL-12-70, IL-23 and IL-27p28	40
2.4.2 Detection of Cytokines, IL-1beta and IFN-gamma.....	40
2.4.3 Detection of Chemokines, MIP-1 and MIP-2	41
2.5 Flow Cytometry	41
2.5.1 Cell Surface Staining.....	43
2.5.2 Cell Viability.....	44

2.6	Quantitative Polymerase Chain Reaction (qPCR).....	45
2.6.1	RNase Free Working Environment.....	45
2.6.2	RNA Isolation.....	46
2.6.3	RNA Integrity Analysis and Quantification by Spectrometry.....	46
2.6.4	RNA Integrity Analysis by Gel Electrophoresis.....	47
2.6.5	Reverse Transcription (RT) – complementary DNA (cDNA) Synthesis ..	47
2.6.6	Reverse Transcriptase Polymerase Chain Reaction (RT-PCR).....	48
2.6.7	Temperature Gradients	49
2.6.8	Primer Efficiency Curves.....	50
2.6.9	Quantitative Reverse Transcriptase Polymerase Chain Reaction (qRT-PCR).....	51
2.7	Western Blotting	53
2.7.1	Isolation of Whole cell Lysates	53
2.7.3	SDS Denaturing Polyacrylamide Gel Electrophoresis	53
2.7.4	Protein Transfer	54
2.7.6	Immunoblotting and Detection	54
2.8	Inhibition of intracellular protein STX-3	55
2.9	RNAi	56
2.9.1	siRNA	56
2.10	<i>In vivo</i> Mouse Models of Disease	57
2.10.1	DSS Model of Colitis.....	57
2.10.2	<i>Citrobacter Rodentium</i> Model.....	58
2.11	Immunofluorescence	58
2.11.1	Coverslips	59
2.11.2	Fixation	60
2.11.3	Intracellular SNARE Staining	60
2.12	STX11 ^{-/-} <i>IN VITRO</i> STUDY	60
2.13	STX11 ^{-/-} BMDC T-Cell Co-Culture	61
2.13.1	Isolation of Splenocytes.....	61
2.13.2	CD4 ⁺ T-Cell Magnetic Particle Isolation.....	61
2.13.3	Proliferation Analysis using CFSE Dye	62
2.13.4	BMDC T-Cell Co-Culture	62
2.14	Statistical Analysis	63
Chapter 3	64

Characterisation of JAWSII Dendritic Cells.....	64
3.1 Introduction	65
3.2 Results	68
3.2.1 The Doses of the TLR Ligands used on JAWSII DCs Have No Significant Effect on Cell Viability.....	68
3.2.2 JAWSII DCs Time Dependently Secrete Pro-Inflammatory Cytokines in response to the TLR4 ligand, Lipopolysaccharide (LPS)	68
3.2.3 Comparison of Cytokine and Chemokine Secretion from JAWSII DCs and BMDCs Following Activation with the TLR2 ligand, Peptidoglycan (PGN)	69
3.2.4 Comparison of Cytokine and Chemokine Secretion from JAWSII DCs and BMDCs Following Activation with the TLR3 ligand, Polyinosinic-Polycytidylic Acid (Poly (I:C)).....	70
3.2.5 Comparison of Cytokine and Chemokine Secretion from JAWSII DCs and BMDCs Following Activation with the TLR4 ligand, Lipopolysaccharide (LPS)	71
3.2.6 Comparison of Cytokine and Chemokine Secretion from JAWSII DCs and BMDCs Following Activation with the TLR5 ligand, Flagellin	72
3.2.7 Comparison of Cytokine and Chemokine Secretion from JAWSII DCs and BMDCs Following Activation with the TLR7 ligand, Loxoribine.....	73
3.2.8 Comparison of Cytokine and Chemokine Secretion from JAWSII DCs and BMDCs Following Activation with the TLR9 ligand, CpG Oligodeoxynucleotides (CpG ODN).....	74
3.2.9 Comparison of Cell Surface Marker Expression on JAWSII DCs and BMDCs Following Activation with the TLR2 ligand, Peptidoglycan (PGN).....	75
3.2.10 Comparison of Cell Surface Marker Expression on JAWSII DCs and BMDCs Following Activation with the TLR3 ligand, Polyinosinic-Polycytidylic (Poly (I:C)).....	76
3.2.11 Comparison of Cell Surface Marker Expression on JAWSII DCs and BMDCs Following Activation with the TLR4 ligand, Lipopolysaccharide (LPS)	77
3.2.12 Comparison of Cell Surface Marker Expression on JAWSII DCs and BMDCs Following Activation with the TLR5 ligand, Flagellin	78
3.2.13 Comparison of Cell Surface Marker Expression on JAWSII DCs and BMDCs Following Activation with the TLR7 ligand, Loxoribine.....	78
3.2.14 Comparison of Cell Surface Marker Expression on JAWSII DCs and BMDCs Following Activation with the TLR9 ligand, CpG oligodeoxynucleotides (CPG ODN).....	79
3.3 Discussion	114
Chapter 4	121

SNARE Expression during Immune Activation	121
4.1 Introduction	122
4.2 Results	124
4.2.1 Insurance of Removal of genomic DNA	124
4.2.2 Expression of SNARE mRNA during LPS Activation	125
4.2.3 Identification of Robust Endogenous Control for RTY-qPCR.....	125
4.2.4 Primer Optimisation.....	126
4.2.7 mRNA Expression of SNAREs in JAWS DCs Following Time Dependant Activation with a TLR Ligand; TLR2 Peptidoglycan, TLR4 Lipopolysaccharide and TLR7 Loxoribine	126
4.2.7.1 mRNA Expression of Qa-SNAREs, STX2, STX3, STX4, STX5, STX7, STX11, STX12 and STX16	127
4.2.7.2 mRNA Expression of Qbc SNARE SNAP23	128
4.2.7.3 mRNA Expression of Qb-SNAREs, VTI1a and VTI1b.....	129
4.2.7.4 mRNA Expression of Qc SNARE, STX6	129
4.2.7.5 mRNA Expression of VAMP2, VAMP3, VAMP4, VAMP7 and VAMP8	129
4.2.8 mRNA Expression of Pro-Inflammatory Cytokines and Chemokines in the Colon in a DSS Induced Colitis Model.....	131
4.2.9 mRNA Expression of SNAREs in the Colon Following Induction of DSS induced Colitis Model	133
4.2.10 mRNA Expression of Pro-Inflammatory Cytokines and Chemokines in the Colon following Infection with T <i>Citrobacter rodentium</i>	135
4.2.11 mRNA Expression of SNAREs in the Colon following infection with <i>Citrobacter rodentium</i>	136
4.3 Discussion	169
Chapter 5	177
Functional Roles for STX3 and STX11	177
5.1 Introduction	178
5.2 Results	180
5.2.1 Re-cap of STX3 mRNA Expression and JAWS II and BMDC cytokine and chemokine secretion data	180
5.2.2 Knockdown of STX3 Significantly Decreases the Secretion of IL-6 and MIP-1 alpha from JAWSII DCs.....	181
5.2.2 Neutralisation of STX3 with a STX3 Specific Antibody Significantly Decreases the Secretion of IL-6 from JAWS II DCs	182

5.2.3	Immunofluorescent analysis of the SNARE STX3 Translocates to the plasma membrane only in IL-6 secreting JAWSII DCs and BMDCs	183
5.2.4	Members of the IL-12 Family are Significantly Up-Regulated in <i>Stx11</i> ^{-/-} BMDCs Compared to Wild Type	184
5.2.5	IFN- gamma Is Significantly Up-Regulated in <i>Stx11</i> ^{-/-} BMDCs Compared to Wild Type	186
5.2.6	Chemokines are Significantly Up-regulated in <i>Stx11</i> ^{-/-} BMDCs Compared to WT	187
5.2.7	Cytokines IL-6, IL-10 and TNF-alpha From <i>Stx11</i> ^{-/-} BMDCs Compared to WT	188
5.2.8	Higher Basal Level Surface Marker Expression on <i>Stx11</i> ^{-/-} BMDCs Compared to WT and Modulation of the Dendritic Cell Marker CD11c	189
5.2.8	STX11 Expression is significantly up-regulated at the same timepoint IFN-gamma is up-regulated	193
5.2.9	WT BMDCs Up-regulate Their Expression of Surface markers when Differentiated in the Presence of IFN-Gamma	194
5.2.10	WT BMDCs Up-regulate Their Expression of IL-12 when Differentiated in the Presence of IFN-Gamma.....	195
5.2.11	The addition of an Anti-IFN-Gamma Neutralizing Antibody to <i>Stx11</i> ^{-/-} BMDCs Resulted in a Phenotype Similar to WT BMDCs	196
5.2.11	Expression of the Maturation Marker CCR5 is Down-regulated in <i>Stx11</i> ^{-/-} BMDCs and Reversed in the Presence of an Anti-IFN-Gamma Antibody	197
5.2.12	Expression of PD-L1 is Up-regulated in <i>Stx11</i> ^{-/-} BMDCs and Reversed in the Presence of an Anti-IFN-Gamma Antibody	198
5.2.12	<i>Stx11</i> ^{-/-} BMDCs have Impaired Ability to Prime T cells By inhibition of cytokine Secretion.....	198
Chapter 6	239
General Discussion	239
6.1 General Discussion	240
Appendices	249
Appendix A	Media and Buffers	250
Appendix B	Primer Temperature Gradients.....	254
Appendix C	STX 3 Transfection Data	255
Appendix D	STX-11 Expression in WT and <i>STX-11</i> ^{-/-} BMDCs.....	256
Bibliography	257

ABSTRACT

The role of dendritic cells (DCs) in directing the immune response as they are a source of cytokines which can promote T cell survival and T helper cell differentiation. While it has become evident that soluble-N-ethylmaleimide-sensitive-factor accessory-protein receptors (SNARE) are involved in membrane fusion and ultimately cytokine release, little is known about which members of this family facilitate the secretion of specific cytokines from DCs. The importance of research into SNAREs was highlighted by the 2013 Nobel Prize for Physiology and Medicine to the researchers involved in discovery of these essential proteins.

We established a cell model of cytokine and chemokine secretion from DCs using the cell line JAWSII DCs and primary bone marrow-derived DCs (BMDCs) which were stimulated with a panel of TLR ligands that we correlated with differential SNAREs expression. We also examined SNARE expression, *in vivo*, in two models of experimental colitis was examined and we identified two candidate SNAREs, STX3 and STX11, to investigate further.

We showed that STX3 mRNA levels correlated with IL-6 and MIP-1 α release from JAWSII DCs. Abolishment of STX3 from DCs, by two separate means, RNAi and a neutralising antibody, resulted in attenuation of IL-6 levels and to some extent MIP-1 α levels. Analysis of subcellular location showed translocation of STX3 to the cell membrane only in DCs secreting IL-6 or MIP-1 α , indicating a role for it in trafficking of these immune mediators. We also investigated the role of STX11 using DCs from STX11 deficient mice. These cells portrayed a more mature phenotype compared with wildtype (WT) BMDCs, with increased production of the IL-12 family of cytokines, increased expression of co-stimulatory surface markers and reduced levels of CD11c in unstimulated cells. We established that this phenotype was due to uncontrolled production of IFN- γ , a known DC maturation stimulus, and identified STX11 as a regulator of IFN- γ secretion. These findings may lead to a better understanding of the pathogenesis of the autosomal recessive disorder of immune dysregulation, familial hemophagocytic lymphohistiocytosis type-4 (FHL-4), which is characterised by over production of cytokines and higher number of activated lymphocytes due to STX11 deficiency.

ABBREVIATIONS

ADP	Adenosine Diphosphate
ANOVA	Analysis of Variance
AP-1	Activator Protein-1
APC	Allophycocyanin
APC	Antigen Presenting Cell
APS	Ammonium Persulphate
ATP	Adenosine Triphosphate
ASA	Acetylsalicylic Acid
BCA	Bicinchoninic Acid
BD	Becton Dickinson
BMDCs	Bone Marrow-Derived Dendritic Cells
BSA	Bovine Serum Albumin
BSU	Biological Services Unit
CCR	C-C Chemokine Receptor
CD	Cluster of Differentiation
CFDE-SE	Carboxyfluoresceindiacatatesuccinimidyl Ester
CFSE	Carboxyfluorescein Succinimidyl Ester
CIA	Collagen-Induced Arthritis
CpG ODN	CpG oligodeoxynucleotides
CTL	Cytotoxic T Lymphocyte
CTP	Cytidine Triphosphate
DAMPs	Damage-Associated Molecular Patterns
DCs	Dendritic Cells
DDAI	Daily Disease Activity
DEPC	Diethylpyrocarbonate
DMSO	Dimethyl Sulphoxide
DNA	Deoxyribonucleic Acid
ds	Double stranded
DSS	Dextran Sulphate Sodium
DTT	Dithiothreitol
EAE	Experimental autoimmune encephalitis
EDTA	Ethylenediaminetetraacetic Acid
ELISA	Enzyme Linked Immunosorbant Assay
ER	Endoplasmic Reticulum
FACS	Fluorescence Activated Cell Sorting
FBS	Fetal Bovine Serum
FHL-4	Familial Hemophagocytic Lymphohistiocytosis
FITC	Fluorescein Isothiocyanate
GAPDH	Glyceraldehyde 3-Phosphate Dehydrogenase
GM-CSF	Granulocyte-macrophage colony stimulating factor
GTP	Guanosine Triphosphate
HBSS	Hanks Balanced Salt Solution
HEPES	4-(2-hydroxyethyl)-1 piperazineethanesulfonic Acid
HRP	Horseradish Peroxidase
IB	Immunoblotted
IBD	Inflammatory bowel disease
IFN	Interferon

IL	Interleukin
IRFs	IFN Response Factors
KCl	Potassium Chloride
KO	Knock out
LPS	Lipopolysaccharide
Mal	MyD88 Adaptor-Like
MAPK	Mitogen-Activated Protein Kinases
MC38	Murine Colon Carcinoma
MCP	Monocyte-Chemotactic protein
MEM	Minimum Essential Medium
MFI	Mean Fluorescence Intensity
MHC	Major Histocompatibility complex
MIP	Macrophage inflammatory protein
MIQE	Minimum information for publication of quantitative real-time PCR experiments
mRNA	Messenger Ribonucleic acid
MTS	3-4,5-dimethylthiazol-2-yl)-5-(3-carboxymethoxyphenyl)-2-(4-sulfophenyl)-2H-tetrazolium inner salt
MUNC	Mammalian Uncoordinated
NFκB	Nuclear factor <i>kappa</i> -light-chain-enhancer of activated <i>B</i> cells
NK	Natural Killer
NLRs	Nucleotide-Binding Domain and Leucine-Rich Repeat Containing Receptors
NSF	N-ethylmaleimide-sensitive factor
NTP	Nucleoside Triphosphate
OCT	Optimal Cutting Temperature
PAF	Paraformaldehyde
PAGE	Polyacrylamide Electrophoresis
PAM	Palmitoyl-3-cysteine-serine-lysine-4
PAMPs	Pathogen associated molecular patterns
PBS	Phosphate Buffered Saline
PCR	Polymerase Chain Reaction
PE	Phycoerythrin
PES	Phenazineethosulfate
PGN	Peptidoglycan
PGRPs	Peptidoglycan recognition proteins
PI	Propidium Iodide
PMTs	Photomultiplier Tubes
Poly (I:C)	Polyinosinic-polycytidylic acid
PPR	pattern-recognition receptors
QPCR	Quantitative Polymerase Chain Reaction
RA	Rheumatoid arthritis
RIG	Retinoic Acid-Inducible Gene-I
RLRs	RIG-Like Receptors
RNA	Ribonucleic acid
RNAi	RNA interference
RT	Reverse Transcription
RT-PCR	Reverse transcription- polymerase chain reaction
RT-qPCR	Reverse transcription- <i>quantitative</i> polymerase chain reaction
SARM	Sterile- α and Armadillo Motif Containing Protein

SDS	Sodium dodecyl sulfate
siRNA	Small Interfering RNAs
SLC	Secondary Lymphoid-Tissue Chemokine
SLO	Streptolysin-O
SM	Sec1/Munc18-related proteins
SNAP	Soluble NSF attachment proteins
SNAP 23	Synaptosomal-associated protein 23
SNARE	Soluble-N-ethylmaleimide-sensitive-factor-accessory-protein receptor
SPF	Specific Pathogen Free
ss	Single-stranded
STX	Syntaxin
TBS	Tris Buffered Saline
TCR	T-Cell Receptor
TEMED	N,M,N'N'-Tetramethylethylenediamine
TGN	Tran Golgi Network
Th	T-helper
TIR	Toll-IL-1 Receptor
TLR	Toll-like receptor
TMB	3,3',5,5'-tetramethyl-benzidine
TNF- α	Tumour necrosis factor alpha
TRAM	Trif-related Adaptor Molecule
T _{REG}	T Regulatory
TRIF	TIR-domain-containing adaptor-inducing interferon- β
TTP	Thymidine Triphosphate
UV	Ultraviolet
VAMP	Vesicle associated membrane protein
WT	Wild Type

ACKNOWLEDGEMENTS

I would firstly like to thank Dr Christine Loscher. Thank you for being a fantastic supervisor. Your guidance and enthusiasm have been unending. Your work ethic and dedication have inspired me thought-out my PhD and are attributes I aim to emulate in my own career. Christine, thank you for always believing in me and helping me believe in my own ability.

The Loscher Lab. You have been the most amazing group of friends I have had the pleasure of making. The old lab, Ciara and Mary, you have been an inspiration of how to do a PhD. Mary you have been a constant support in every way, I am honoured to call you a friend. I can't wait for "Doctors on Tour". The T3ers, Fiona, Maja and Joey, little did they know what the fab five and the twelve apostles would become. I will always look back on our conference trips with wonderful memories (if not a fear for delayed or diverted flights and trains). The younger lab, although I've known you guys the least amount of time it feels like you have always been there. Mark, Iza, Kathy, Catherine and Niamh your support has been fantastic. It is a pleasure to go to work in the morning. Iza I'm FINALLY free for a coffee again and I can't wait!

To my wonderful friends outside of the PhD bubble, Louise, I've known you since playschool, thank you for always being there and having such great navigation skills. Liann, Brad, Emma and Dara thanks for reminding me there was a world outside science.

Keith. To have had someone at my side that understood the process so completely has been fantastic. This journey would have been impossible without you and to have had you there I am so unbelievably grateful. Thank you for doing everything in your ability make me believe it would all work out perfectly. Now lets book that holiday!

Last but most important, my phenomenal Mum, Yvonne. To you I dedicate this thesis. You have been a never-ending support to me from the moment I was born down to the last sentence written in this thesis. Thank you for being a fantastic support for the highs and lows this PhD has brought. I hope I have made you proud and it somewhat repays you for everything you have done for me.

“People cannot foresee the future well enough to predict what's going to develop from basic research. If we only did applied research, we would still be making better spears.”

2006 Physics Nobel Laureate, Dr. George Smoot

PUBLICATIONS

Mary Canavan, Ciara McCarthy, Nadia Ben Larbi, Jennifer Dowling, Laura Collins, Finbarr O'Sullivan, Grainne Hurley, Carola Murphy, Aoife Quinlan, Gerry Moloney, Trevor Darby, John MacSharry, Hiroyuki Kagechika, Paul Moynagh, Silvia Melgar and Christine E Loscher (2013)

Activation of Liver X Receptor Suppresses the Production of the IL-12 Family of Cytokines by Blocking Nuclear Translocation of NF- κ B

Innate Immunity published online 17 September 2013

Laura E Collins, Mark Lynch, Izabela Marszalowska, Maja Kristek, Keith Rochfort, Mary O'Connell, Henry Windle, Dermot Kelleher and Christine E Loscher (2013)

Surface Layer Proteins Isolated from *Clostridium difficile* Induce Clearance Responses in Macrophages

Re-Submitted with corrections to *Microbes and Infection*

Maja Kristek, Laura E. Collins, Joseph DeCoursey, Fiona A. McEvoy, Christine E. Loscher

Soluble factors from colonic epithelial cells contribute to gut homeostasis by modulating macrophage phenotype

To be re-submitted with corrections to *Innate Immunity*

Eimear Kennedy, Ciaran J. Mooney, Chris Greene, Roya Hakimjavadi, Emma Fitzpatrick, Shaunta Guha, Laura E. Collins, Christine Loscher, David Morrow, Eileen M. Redmond and Paul A. Cahill

Vascular Smooth Muscle Cells in Culture – Derivation from Multipotent Vascular Stem Cells?

To be re-submitted with corrections to the Journal of Vascular Research

Eimear Kennedy, Chris Greene, Roya Hakimjavadi, Ciaran J. Mooney, Emma Fitzpatrick, Laura E. Collins, Christine Loscher, Shaunta Guha, David Morrow, Eileen M Redmond and Paul A. Cahill

Embryonic rat vascular smooth muscle cells revisited – a model for neonatal, NeointimalvSMC or differentiated vascular stem cells?

To be re-submitted with corrections to Vascular Cell

Laura E Collins, Joseph DeCoursey and Christine E. Loscher

Cytokines and Chemokines Secretion by Dendritic Cells

Review Article - Accepted Invited Abstract to Journal Frontiers in Immunology

Laura E Collins, Joseph DeCoursey, Silvia Melgar and Christine E. Loscher

The Role of STX-3 in Dendritic Cell Secretion

Manuscript in preparation

Laura E Collins, Joseph De'Coursey, Udo ZurStadt, Silvia Bulfone-Paus and Christine E. Loscher

STX-11 Negatively regulates IFN- γ production from BMDCs

Manuscript in preparation

CHAPTER 1

GENERAL

INTRODUCTION

1.0 THE IMMUNE SYSTEM

The immune system is composed of a network of lymphoid organs, cells, humoral factors and cytokines which can be divided into the innate and the adaptive immune response. The innate, how we sense infection and the adaptive, how we eradicate infection. Although separate, these “arms” of the immune system act interdependently.

1.1 OVERVIEW OF INNATE AND ADAPTIVE IMMUNITY

The innate immune response is our first line of defence against pathogens. It is a non-specific response and does not give long lasting immunity. It includes physical, chemical and microbiological barriers and also provides immediate host defence by way of neutrophils, monocytes, macrophages, complement, cytokines and acute phase proteins. It is a rapid but non specific response and can sometimes cause tissue damage as a result. It is a highly conserved response and can be seen in the simplest of animals confirming its importance for host survival (Parkin and Cohen 2001).

The adaptive immune system is controlled and assisted by the innate immune system .It is a characteristic of higher animals and is extremely specific and precise and can take several days to weeks to mount a response. This response is mediated by antigen-specific lymphocytes, in particular, T cells which express a vast array of recombinant receptors. These receptors are capable of recognising every pathogen that a host may encounter. Cells with the appropriate receptor required for the scenario, proliferate, in a process called clonal expansion or are eliminated to induce tolerance through the process called clonal elimination (Kimbrell and Beutler 2001).

1.2 LINKING THE INNATE AND ADAPTIVE: THE DENDRITIC CELL

Dendritic cells (DCs), were first described by Ralph Steinman and Zanvil Cohn, as a rare murine spleen cell which had dendrite like protrusions with phagocytic ability (Steinman and Cohn 1973). Since then, technological advances have progressed cellular immunology research, coupled with the fact that dendritic cells can now be readily obtained in sufficient quantities, has allowed the role of DCs in immunity to be understood.

DCs are cells of the hematopoietic immune system and are referred to as immature cells before they undergo maturation. Immature DCs, present in the peripheral tissues, are characterised by a high capacity for antigen capture and processing by phagocytosis, chemokine receptor expression, chemokine responsiveness and low T cell stimulatory capability (Banchereau and Steinman 1998b).

The ability of DCs to regulate immunity is dependant on DC maturation. During maturation, which is induced by the interaction of a variety of factors such as pathogens, which are converted into immunogens and subsequently presented to T cells, DCs express molecules such as cytokines, chemokines and co-stimulatory molecules.

1.3 ENGAGEMENT OF PATHOGEN RECOGNITION RECEPTORS (PRRS) IN DCS IS A CRITICAL STEP IN THE INDUCTION OF THE ADAPTIVE IMMUNE RESPONSE.

Cells of the innate immune system, in particular DCs, are activated when pathogen-associated molecular patterns (PAMPs) or endogenous damage-associated molecular patterns (DAMPs) engage pattern recognition receptors (PPRs). These PPRs can be divided into Toll-like receptors (TLRs), nucleotide-binding domain and leucine-rich repeat containing receptors (NLRs) and retinoic acid-inducible gene-I (RIG)-like receptors (RLRs) (Creagh and O'Neill 2006). Once these PRRs are engaged, it results in the activation of signalling cascades that induce the production of pro-inflammatory cytokines. These signalling cascades include nuclear factor κ -light-chain-enhancer of activated B cells (NF κ B), interferon (IFN) response factors (IRFs), activator protein-1 (AP-1) and mitogen-activated protein kinases (MAPK) (Rakoff-Nahoum et al. 2004).

1.3.1 Toll-like Receptors (TLRs)

Toll-like receptors (TLRs) have emerged over the past decade as the crucial sensors of PAMPs from microorganisms or DAMPs from damaged tissue. The TLR family consists of at least 10 members in human and 13 in mice (Kawai and Akira 2006). TLR proteins are type 1 transmembrane receptors that are composed of a ligand binding domain of leucine rich repeats and a signalling Toll-IL-1 receptor (TIR) domain that interacts with TIR domain containing adaptor molecules, of which there are five: myeloid differentiation primary response 88 (MyD88), MyD88-adaptor-like (Mal), TIR-domain-containing adaptor-inducing interferon- β (TRIF), TRIF-related adaptor molecule (TRAM) and sterile- α and Armadillo motif containing protein (SARM) (McGettrick and O'Neill 2004). Engagement of these different adaptors is

dependent on the TLR utilising them and results in the induction of the aforementioned signalling cascades to ultimately produce pro-inflammatory mediators, cytokines and chemokines, see Figure 1.1 (Kenny and O'Neill 2008).

1.3.2 TLR location – Critical to their Function

The TLRs are located on the cell surface, recognise markers on the surface of pathogens. These include TLR1, 2, 4, 5 and 6, present on the surface of the cell, which recognise lipid structures and in the case of TLR5, the protein Flagellin. TLRs located within the cell are classed as endosomal. These include TLR3, 7, 8 and 9 and reside intracellularly to be able to recognise nucleic acids derived from the genome of viruses and bacteria (Lavelle et al. 2010).

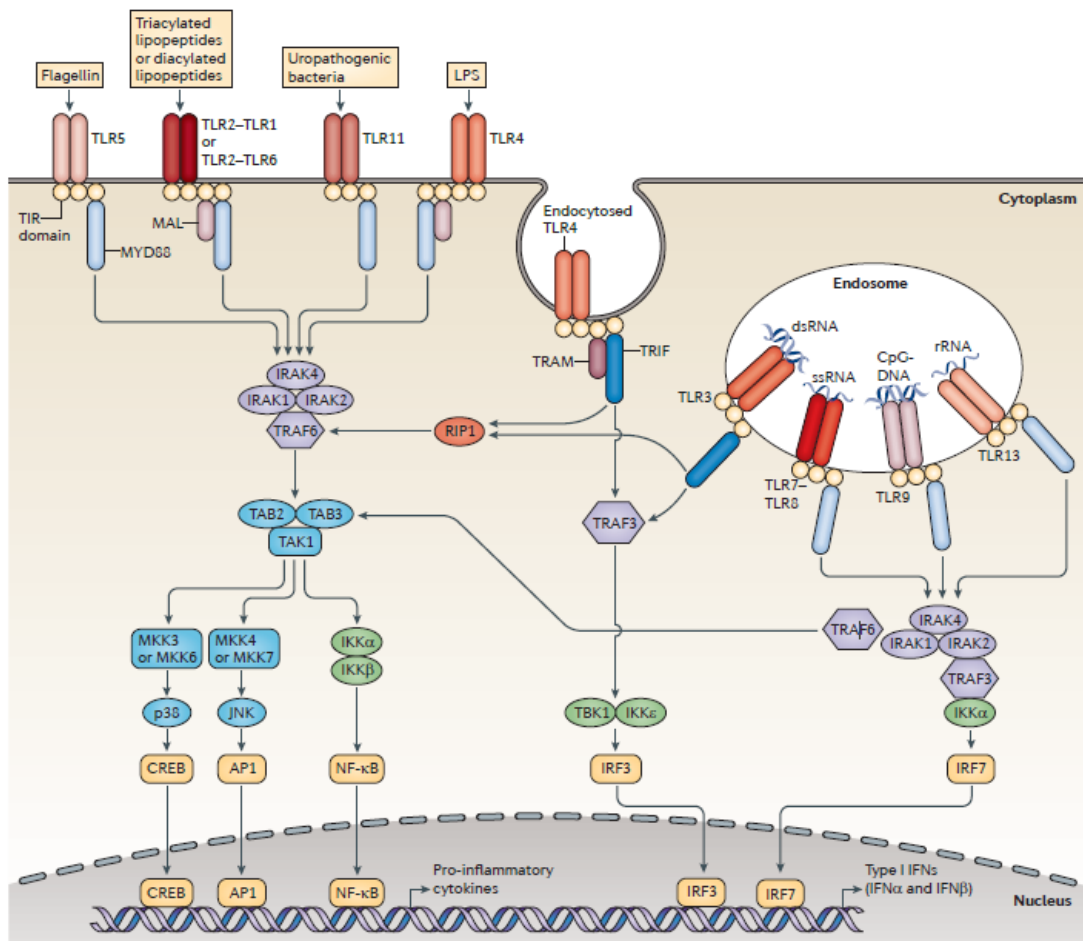


Figure 1.1: A detailed overview of the mammalian TLR signalling pathways.

This includes the location of TLRs, surface or endosomal, the structure of the TIR domain containing the adaptor molecules which induce signalling cascades which ultimately produce pro-inflammatory mediators, cytokines and chemokines (O'Neill, Golenbock and Bowie 2013).

1.4 MATURE DCS – POTENT INDUCERS OF EFFECTOR T CELL RESPONSES

Following PRR ligation and subsequent DC maturation, the DC becomes an antigen presenting cell (APC) that migrate to secondary lymphoid tissue selecting antigen-specific lymphocytes to which they present the processed antigen initiating clonal immunity.

1.4.1 Migration to Lymphoid Organs – A Role for Chemokines

Migration to areas of inflammation and subsequently to lymphoid organs from the peripheral tissues is an important function of DCs. Essential components of migration are chemokines and their subsequent receptors. Immature DCs express chemokine receptors C-C chemokine receptor-1 (CCR1), CCR2, CCR5, CCR6 and CXCR1 and are attracted to inflamed areas by Macrophage Inflammatory Protein (MIP)-3 α (Hartgers, Figdor and Adema 2000). Following maturation DCs lose responsiveness to MIP-3 α and lose their cell surface expression of CCR1 CCR5 and CCR6 (Sallusto et al. 1999). The mature DC becomes responsive to chemokines such as MIP-3 β and secondary lymphoid-tissue chemokine (SLC). SLC attracts DC and T cells which aids in their colocalisation (Chan et al. 1999). With the arrival of the DC at the lymphoid organs the mature DC primes a naive T cell to become an effector T cell. To do this three signals are required, antigen presentation, up-

regulation of co-stimulatory markers and secretion of cytokines, **Figure 1.2.**

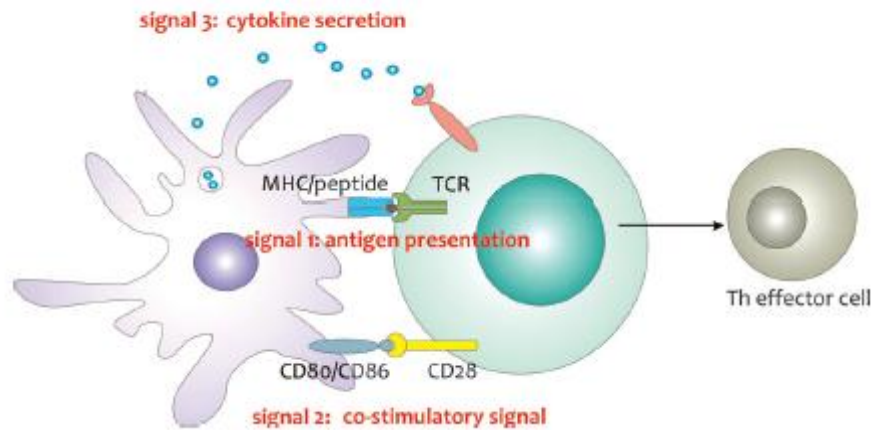


Figure 1.2: Overview of the Three Signals Required to Polarise Naive T-Cells.

Signal 1 is delivered by MHC/peptide complex stimulation of the TCR, signal 2 is the co-stimulatory surface expression on the APC and CD28 on the T cell and signal 3 involves secretion of the cytokines that polarise T cells into the different T cell subsets (De Koker et al. 2011).

1.4.2 Signal 1 - Antigen Presentation - MHC Class I and II

DCs are potent T cell activators and this is related to the constitutive expression of both major histocompatibility complex (MHC) class I/II. To prime a naive T cell to become an effector T cell, T helper (Th) or a cytotoxic T lymphocyte (CTL), the antigen needs to be presented via the MHC molecule by the APC, to the cognate T-cell receptor (TCR) (Ni and O'Neill 1997).

Antigen presentation via MHCI to Cluster of Differentiation 8 (CD8) T cells enables them to recognise and kill transformed and virally infected cells. The MHCI pathway

is present in almost all cell types. Peptides that have originated from proteins degraded in the cytosol by the proteasome which have been transported to the ER are loaded on the MHCI molecule (Villadangos and Schnorrer 2007). However MHCII presents antigen to CD4 T cells and is only present in professional APCs such as B-cells, macrophages, basophils and DCs. MHCII presents peptides from endocytosed antigens also via the ER and transported to the cell surface (De Koker et al. 2011).

1.4.3 Signal 2 – Co-Stimulation molecules CD80/CD86

Surface molecules CD80 and CD86 on APCs, such as DCs, mediate co-stimulation through interaction with the CD28 receptor on T cells. Maturation of the DC results in up-regulation of these surface molecules and immature DCs generally have low expression, making them weak APCs. However, these immature DCs can undergo a functional maturation which induces migration to lymphoid organs, presentation of self antigen and expression of these co-stimulatory markers. Instead of an immune response, it results in important mechanisms of tolerance to self antigens by the means of T cell anergy, clonal deletion or development of immunosuppressive T regulatory (T_{REG}) (Luckashenak et al. 2008).

1.4.4 Signal 3 – Cytokine polarisation

Cytokines are classified into interleukins (IL), colony-stimulating factors, interferons (IFNs). Different cytokines secreted from DCs can polarise the naïve T cells into different subsets of T cells. These differential cytokine secretion patterns are dependant on the PRR activation and as a result this shapes the Th response.

Subsequently certain pathogens have associated Th subsets in immune activation against them (Pulendran 2004). Secretion of IL-12 from DCs is triggered by generally by intracellular bacteria and viruses and drives T helper 1 (Th1) cell differentiation. Following activation of the DC with a helminth, secretion of IL-4 is triggered which induces Th2 phenotype. IL-6 and IL-23 are associated with Th17 differentiation following PRR recognition of bacteria and fungi and IL-10 secretion promotes T_{REG} response, see **Figure 1.3** (Mills 2011).

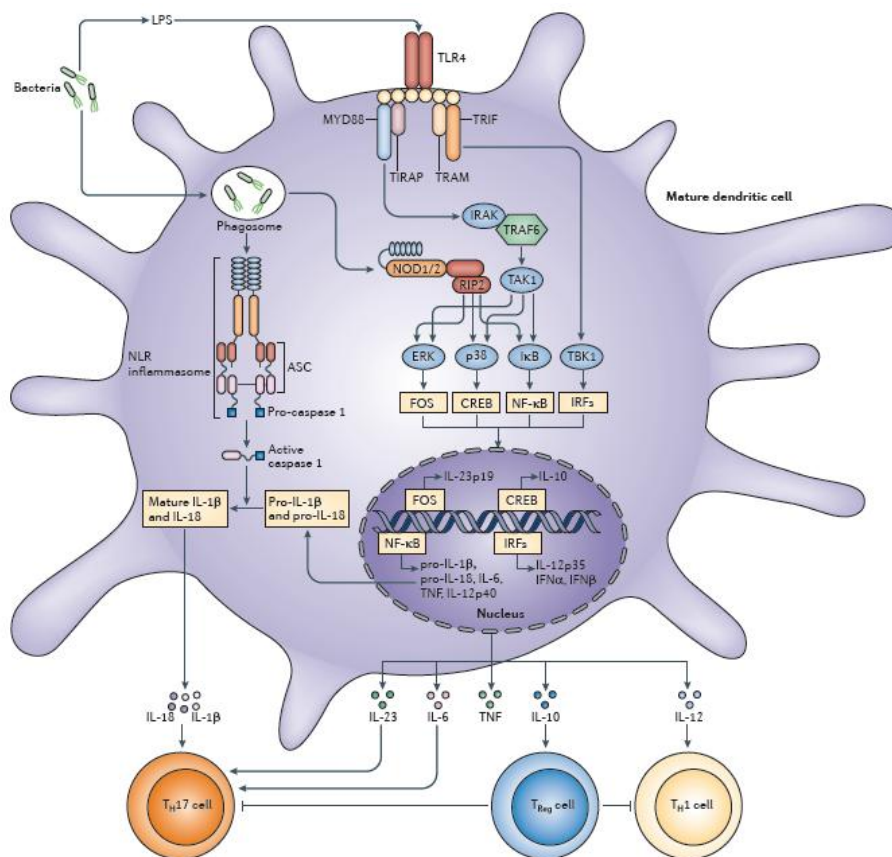


Figure 1.3: TLR4 stimulation of a dendritic cell leads to cytokine production that promotes the activation of T-cells (Mills 2011).

1.5 CYTOKINES AND CHEMOKINES AS TARGETS IN INFLAMMATORY DISEASE

Cytokines have been implicated in inflammatory diseases as critical mediators either through production and/or as maturation stimuli of cells such as DCs which then can become APCs which can select autoreactive lymphocytes (Blanco et al. 2008). This makes their secretion an attractive option to study to possibly target blocking their secretion in inflammatory diseases. The advantages of this include inhibition of the “critical cytokine” which is acting as a master regulator and so there is the possibility to switch off inflammation without any detrimental side effects (Macdonald 2011). For example, IL-23, a cytokine important for the development of Th17 polarisation, has been shown to be important in the pathogenesis of experimental autoimmune encephalitis (EAE), collagen-induced arthritis (CIA) and inflammatory bowel disease (IBD). This has been established through the inhibition of disease using IL-23 knockout mouse models or subjecting wild-type mice to anti-IL-23 treatment (Cua et al. 2003, Murphy et al. 2003, Hue et al. 2006). Blockade of IL-6, another cytokine important in driving the Th17 subset, has been shown to be successful in autoimmune diseases and the use of a humanized anti-IL-6 receptor antibody in patients with RA and systemic-onset juvenile chronic arthritis (JCA) was demonstrated to have remarkable clinical effects (Yoshizaki 2009). These are just some of the numerous studies that demonstrate the benefits of blocking cytokines in disease and provide a solid rationale for us attempting to uncover which SNARE proteins control the secretion of such cytokines in DCs.

1.6 PROTEIN TRAFFICKING

The presence of biochemically distinct intracellular compartments is an outstanding feature of eukaryotic cells. Membrane carriers, often vesicles, mediate trafficking between these compartments to and from the cell surface. Budding, target selection and fusion of these carriers require a large array of proteins (Stow and Murray 2013)

1.6.1 Cytokine Secretion

While the functions of cytokines and chemokine are well documented, how these immune mediators are secreted is not as well understood. There are several secretory pathways reported in eukaryotic cells (Stow et al. 2009). Firstly newly synthesised protein precursors are loaded onto the endoplasmic reticulum (ER). They are then folded, checked for quality and glycosylated and loaded into vesicles for transport to the Golgi complex for post-translational processing and further glycosylation. The final step in the Golgi complex is the trans Golgi network (TGN) and beyond this the secretory pathways differ and diverge in their routes, vesicles and organelles (Farquhar and Palade 1998). These can be broadly divided into constitutive, regulated and unconventional. Constitutive secretion is present in nearly all cells, regulated secretion, is required in specialized cells to secrete a large dose of stored cytokine in response to a specific stimulus and unconventional, in which a number of immune mediators are synthesized in the cytoplasm, are released from the cell without passing through the ER and Golgi complex (Stow and Murray 2013). It seems that cytokines can employ any of these pathways for secretion across the various cells of the immune system. However how these cytokines are released through these secretion pathways is relatively unknown. We do know there is an integral family of proteins that are involved in this trafficking. These proteins are

called members of the soluble N-ethylmaleimide-sensitive-factor attachment protein receptor (SNARE) family (Hay 2001).

1.7 SNARES

Since SNAREs were identified almost two decades ago they have since been identified as key elements in membrane fusion. The significance of SNARE discovery was recognised in 2013 as the Nobel Prize was awarded to instrumental researchers in the trafficking field, James Rothman, Randy Schekman and Thomas Südhof.

Their research has led to the characterisation of key elements and mechanisms of eukaryotic cell trafficking which in turn can contribute to many diseases, including those of the immune system. These researchers Nobel Prize winning work was ignited when Schekman discovered a set of genes involved in secretion in yeast and mammalian cells, while at the same time Rothman purified two soluble proteins with these that developed an *in vitro* trafficking assay which reconstituted efficient transport (Schekman and Orci 1996, Balchet al. 1984). These proteins were later identified to be N-ethylmaleimide sensitive factor (NSF) and an adaptor protein called soluble NSF attachment protein (SNAP), which act in many intracellular pathways (Block et al. 1988, Clary, Griff and Rothman 1990). Subsequently the NSF attachment protein receptor; SNARE hypothesis was born. Südhof identified key regulators of SNARE membrane fusion such as the mammalian uncoordinated (MUNC) protein, which enforce precise timing and coordination that is required to fuse membranes. This group also identified targets for SNARE inactivation in the form of bacterial toxins derived from tetanus and botulinum (Sudhof 1995).

1.7.1 SNARE Structure

There are currently 38 identified members of the SNARE family. SNARE proteins have a simple structure, which is characterised by the presence of a SNARE motif approximately 60-70 amino acids in length, arranged in heptad repeats (Stow and Murray 2013, Weimbs et al. 1997). The SNARE motif is also found in all SNAREs and contains the crucial 16 residues and polar layer. Most SNAREs contain a single SNARE motif which is connected by a short linker to the transmembrane domain located at the C-terminal end. The SNARE N-terminal domain is not as conserved as SNARE motifs or C-terminals, however they provide variation which allows for distinction between subsets of SNAREs, see **Figure 1.4**. The SNARE family are classed into R-SNAREs (generally on vesicles) and Qa-, Qb-, Qc-, Qb,c- (usually at the target membrane). This classification is based on whether the central functional residue in the motif is arginine (R) or glutamine (Q) and sub-classification of Q-SNAREs is based on where their SNARE domains would sit in an assembled trans-SNARE complex (Jahn and Scheller 2006).

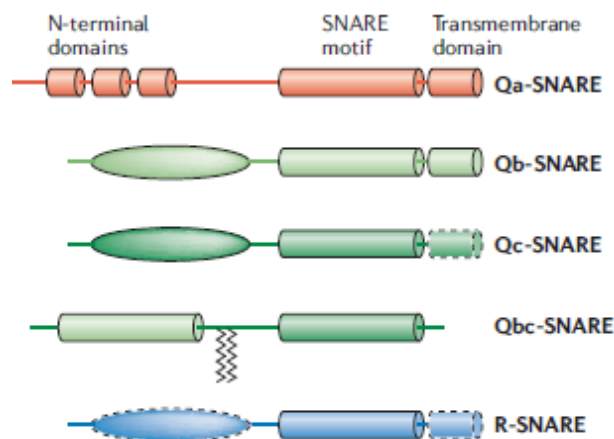


Figure 1.4: The Domain Structure and Classification of SNAREs Proteins:The distinguishing feature of SNARE protein is the SNARE motif. However most also

contain a transmembrane domain and a N-terminal domain and are classified into R-SNARES and Q-SNAREs according to whether the central functional residue in the motif is arginine (R) or glutamine (Q) [Taken with adaptations from (Jahn and Scheller 2006)].

1.7.2 SNARE Functions

SNARE proteins are present on opposing membranes that drive fusion using the free energy which is released from the formation of a central coiled coil SNARE motifs. The crystal structure of this “coiled coil” SNARE complex was first solved by Sutton *et al.*, who analysed a complex involved during the process of exocytosis. This was measured to a resolution of 2.4Å and from this discovered that the SNARE complex assumes a 4 α -helix bundle structure with a cylindrical shape. The complex is 120Å in length with a circular cross section with all four helices arranging themselves so that their C-termini are at the anchor end while the rest of the protein is available for a two-helix interaction. The high stability of these bonds within the SNARE complex makes them resistant to treatments with detergents such as Sodium dodecyl sulphate (SDS) (Sutton et al. 1998). Thus fusion of the two membranes generally requires four SNAREs, an R-SNARE, for example a vesicle associated membrane protein (VAMP), and three Q-SNAREs, such as Syntaxin (STX) or synaptosome-associated protein of 23 (SNAP-23). Firstly Q-SNAREs assemble with the aid of SM (Sec1/Munc18-related proteins) which R-SNAREs interact with through the N-terminal end of the SNARE motifs forming the four-helical trans-complex. This results in a *trans*-SNARE complex, which forms to pull the vesicle and target membranes together. Once this has happened the *trans* complex converts to a *cis* complex allowing all the SNAREs associate in the same membrane allowing for transport of the contents from the vesicle, see **Figure 1.5**. Specialized chaperone machinery is in place for the disassembly of *cis*-SNARE complexes due to its extreme kinetic and thermodynamic stability. These chaperones, previously mentioned NSF and SNAP, utilise Adenosine Triphosphate (ATP) hydrolysis to disassemble *cis*-SNARE complexes releasing SNAREs for *trans*-SNARE complex

assembly and allowing recycling of these previously used SNAREs for another round of membrane fusion (Ungar and Hughson 2003).

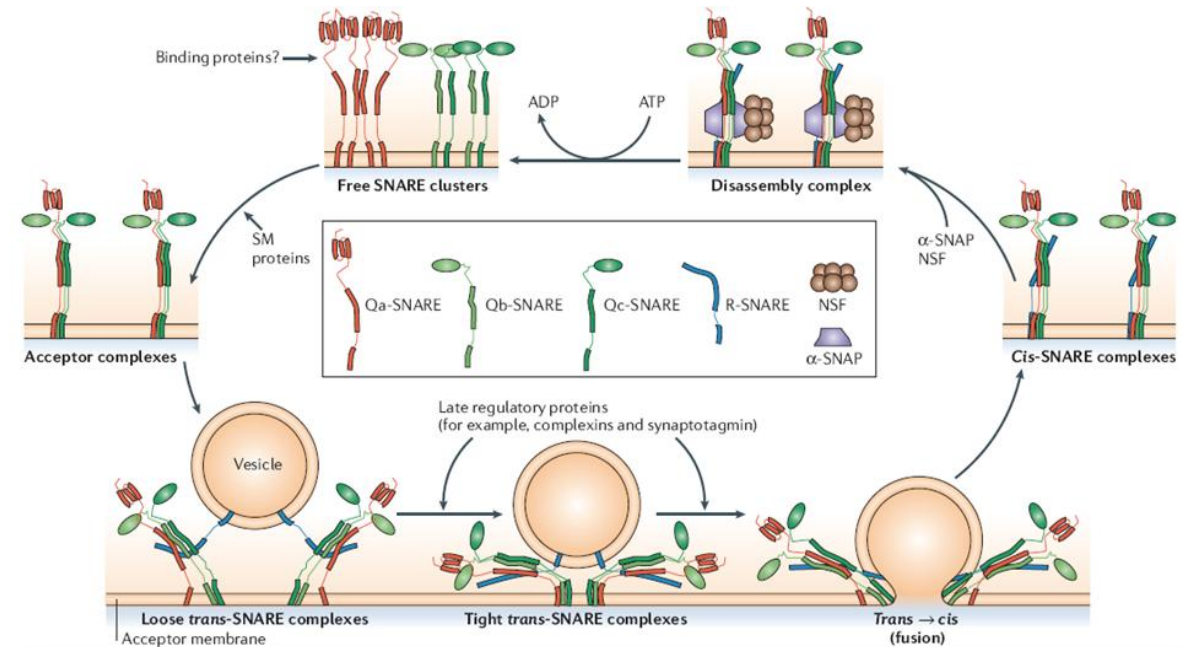


Figure 1.5 SNARE Mediated Fusion: This mechanism is identical in all cells but SNARE partners differ. Generally there are three Q-SNAREs on the acceptor membrane and one R-SNARE on the vesicle. Assembly of the acceptor complexes is composed by clusters of Q-SNAREs with the possible aid of SM proteins. R-SNAREs interact with the acceptor complex through the N-terminal end of the SNARE motifs forming the four-helical trans-complex. The transition from a loose trans-complex to a tight trans-complex is due to the “zippering” of just one N-terminal portion of the SNARE motifs to where this is almost completed. When the strained trans-complex relaxes into a cis-complex, a fusion pore develops. Chaperone NSF and co-chaperone SNAP disassemble the cis-complex with the energy of ATP hydrolysis allowing for the recycling of SNAREs they have already performed a membrane fusion [Taken from (Jahn and Scheller 2006)].

1.8 SNARES AND THEIR ROLE IN DISEASE

SNAREs have been implicated in many human diseases which have defective membrane fusion, such as familial hemophagocytic lymphohistiocytosis type-4 (FHL-4), Hermansky-Pudlak syndrome, Griscelli syndrome, Chediak-Higashi syndrome and Early-onset myocardial infarction (zur Stadt et al. 2005, Huizing, Anikster and Gahl 2000, Shirakawa et al. 2004, Tchernev et al. 2002, Shiffman et al. 2006). Genetic mutations in SNARE proteins can result in these diseases and symptoms include high levels of pro-inflammatory cytokines in serum levels of patients (IFN- γ , IL-6, Tumour necrosis factor alpha (TNF- α)) or impaired leukocyte degranulation (Offenhaeuser et al. 2011, Stow, Manderson and Murray 2006b). Therefore it indicates the importance of regulation of SNAREs during immune activation.

1.9 SNARES IN IMMUNE CELLS

As the immune system is composed of a large quantity of cell types all with different specific functions, the mechanism of trafficking is extremely important for secretion of immune mediators, such as cytokines and chemokines.

1.9.1. NEUTROPHILS

Neutrophils are critical cells of the innate immune system and make up the majority of circulating lymphocytes (40-80% in healthy individuals). Post their speedy recruitment to sites of inflammation; they exert protective or pathogenic effects depending on the inflammatory signal (Lacy 2006). Neutrophils store a wide range of immune mediators (including cytokines such as TNF- α and IL-12) and factors

(such as antimicrobial products) in pre-formed granules (Beil et al., 1995, Denkers et al., 2003). There are four different types of these granules: primary (azurophilic), secondary (specific), tertiary (gelatinase) and secretory vesicles with each granule having an associated set of SNARE proteins (Stow, Manderson and Murray 2006a). mRNA levels of STX1a, 3, 4, 5, 6, 7, 9, 11 and 16 have been identified by Reverse transcription- polymerase chain reaction (RT-PCR) in human neutrophils and a neutrophil-differentiated cell line (HL-60). Subsequently STX4 was identified as a functional SNARE in two trans complexes, STX4-SNAP-23-VAMP-2 and STX4-SNAP-23-VAMP-1, that are involved in the secretion of specific and gelatinase granules (Martin-Martin et al. 1999, Mollinedo et al. 2006). STX11 has been described to be highly expressed in human neutrophils, which is interesting given the role for STX11 in FHL-4 (Xie et al. 2009). Recently a role for STX11 has been indicated in activated neutrophils. Degranulation of activated neutrophils from STX11 deficient mice was impaired, indicating that STX11 controls neutrophil degranulation (D'Orlando et al. 2013).

1.9.1 MAST CELLS

Like DCs, mast cells are also cells of the hematopoietic-immune system. They are critical effector cells in allergic disorders and when activated can secrete a large array of biologically active products, such as cytokines and chemokines that can facilitate in the development of the adaptive immune system (Galli et al. 2005). These inflammatory mediators are stored in secretory granules and secretory vesicles and their release is initiated by mast cell stimulation with IgE through the FcεRI receptor, through compound exocytosis. A cascade of granule-to granule fusion, commences with the primary fusion of a granule to the cell surface. This exocytosis

is mediated through R-SNAREs and Q-SNAREs present on the primary granule and cell membrane, but they are also present on the deeper lying granules within the cell to trigger secondary fusion of the granule-to-granule (Pickett and Edwardson 2006). Mast cells have been reported to express a large number of SNARE proteins, including SNAP-23, STX2, 3, 4, and 6 and VAMP2, 3, 4, 7 and 8, however SNARE functionality in these cells has only been somewhat explored (Lorentz et al. 2012). SNAREs were first indicated in mast cell degranulation in 1998, where SNAP-23 was shown to be essential for exocytosis (Guo, Turner and Castle 1998). Subsequently STX4 was reported to have a role in degranulation. siRNA of STX4 inhibited exocytosis and following stimulation with IgE, STX4 and SNAP23 were shown to localise at the mast cell membrane (Woska and Gillespie 2011, Wong et al. 1998). These Q-SNAREs STX-4-SNAP23 complex with R-SNAREs VAMP2, VAMP3 and VAMP8 to form at least three trans-SNARE complexes (Puri et al. 2003). In 2011, Frank *et al*, found that antibodies blocking STX3 and SNAP23 but not STX2 or VAMP3 inhibited release from all chemokines tested, although these Q-SNAREs were previously indicated to form SNARE complexes with VAMP2, VAMP3 and VAMP8, it appeared that only VAMP8 was involved in the release of chemokines IL-8 (Frank et al. 2011).

1.9.2 NATURAL KILLER CELLS

Natural Killer Cells (NK cells) are a cytotoxic lymphocyte which secrete cytolytic granules to kill virally infected or transformed cells and cytokines which have immunostimulatory effects, antimicrobial and antiviral effects (Hamerman, Ogasawara and Lanier 2005). The role of SNAREs has not yet been very well defined in these cells however SNAP23, STX4, STX6 and VAMP7 have all been

reported to be expressed at the mRNA level in a natural killer cell line and it has been elucidated that VAMP7 is essential for targeting cell killing (Marcet-Palacios et al. 2008). Recently STX11 has been implicated in the secretion of IFN- γ from NK cells, however more work is required to fully understand this (D'Orlando et al. 2013).

1.9.3 MACROPHAGE

TNF- α secretion from macrophage is one of the best researched and most understood pathways of cytokine secretion. These cells of the innate immune system are highly reliant on trafficking due to a large array of functions including sampling their environment and secretion of immune mediators, thus indicating a requirement for SNAREs to regulate this trafficking (Murray et al. 2005a). Resting macrophage, like most cells, sustain low levels of constitutive secretion to sustain “housekeeping” levels of protein transport. However upon macrophage activation cytokine secretion is up-regulated and subsequently so are SNARE proteins (Murray et al. 2005b). Stow and colleagues exploited these trends of up-regulation in the mRNA and/or protein levels of R- and Q- SNAREs following activation with Lipopolysaccharide (LPS) to correlate them with cytokine secretion. With this method they first identified STX4 as a regulator of TNF- α secretion which they confirmed by the cell-surface localisation of STX4 and the ability of a mutant variant of STX4 to block TNF- α surface delivery and secretion. STX4 forms part of the Q SNARE complex with SNAP23 at the cell surface (Pagan et al. 2003). STX6-STX7-Vti1b Q-SNARE complex was also identified in this manner and facilitates transport of TNF from the trans-golgi-network (TGN) (Murray et al. 2005a). The R-SNARE required for fusion of these two Q-SNAREs was identified as VAMP3, which was present on the

recycling endosome (RE), which implies a possible role for a two step TNF secretion pathway (Murray et al. 2005b). The role of the RE in this secretion was later shown to be related to the membrane contribution from the RE to the plasma membrane to aid in phagocytosis and subsequently TNF- α secretion is linked to phagocytosis (Stow, Manderson and Murray 2006a). This pathway is overview in Figure 1.6.

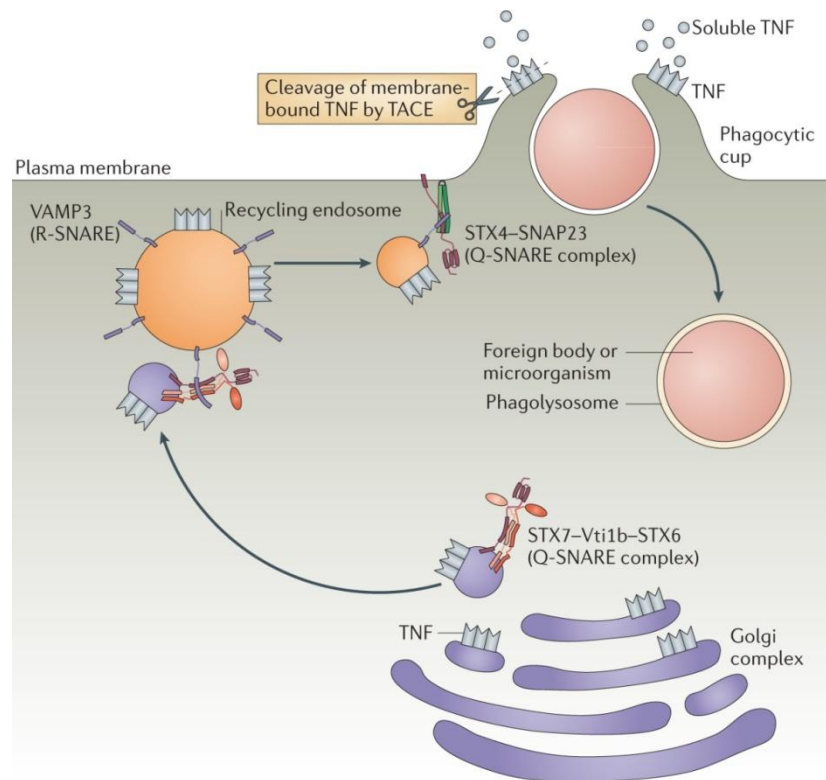


Figure 1.6-Overview of Macrophage SNARE-mediated pathway for TNF- α secretion: Newly synthesized TNF- α is transported from the Golgi complex in vesicles containing the Q-SNARE complex STX7-Vti1b-STX6. The vesicle then interacts with RE bearing the R-SNARE, VAMP3 which fuses the two vesicles together. The RE also contains the Q-SNARE complex STX4-SNAP23, which then translocates to the phagocytic cup. Interaction with VAMP3 results the membranes fusing and TNF- α being displayed on the cell surface. Once on the surface, TNF- α is

cleaved by TNF-converting enzyme (TACE) and released (Stow, Manderson and Murray 2006b).

1.9.4. Dendritic Cell

As described in section 1.4, DCs are APCs that are capable of linking innate and adaptive immunity (Banchereau and Steinman 1998a). SNARE profiles in DCs are possibly one of the most neglected areas of SNARE research. VAMP8 has been reported to be involved in phagocytosis in dendritic cells. Over-expression of VAMP8 resulted in significant inhibition of phagocytosis and use of *VAMP8*^{-/-} DCs significantly increased phagocytic ability. This was a study on a SNARE protein reported to functionally inhibit phagocytosis from phagocytic cells (Ho et al. 2008). Cai *et al.*, reported that SNARE expression of Vti1a, Vti1b, VAMP3, VAMP8 and STX8 in DCs are up-regulated in response to acetylsalicylic acid (ASA), the main ingredient in aspirin. This study stated that Vti1a and Vti1b localised to the phagosomes and that up-regulated expression of these SNAREs inhibited phagocytosis in DCs. As the cellular targets of aspirin are poorly understood this provides new insight to both immunopharmacology of aspirin and role of SNAREs in DCs (Cai et al. 2011).

1.10 PROJECT AIMS AND OBJECTIVES

Although there are numerous reports of SNARE function in immune cells there are relatively few in DCs and none in DC secretion. This project aims to identify SNARE proteins involved in cytokine or chemokine secretion in these important immune cells. Our overall objectives were as follows:

- To characterise BMDCs and JAWSII DCs in response to TLR stimulation, with respect to surface marker expression and cytokine/chemokine secretion and from this establish a cytokine/chemokine model of secretion from DCs

- To assess if SNAREs have a role *in vitro* following TLR stimulation in DCs and *in vivo* in colitis models of disease and if so identify possible candidate SNAREs that play a role in DC secretion

- To determine the functional roles of SNAREs, STX3 and STX11 in DC secretion

Defining the role of SNAREs in secretion of cytokines and chemokines provides an exciting new opportunity to target inflammatory mediators in disease even before they are secreted.

CHAPTER 2

MATERIALS AND

METHODS

2.1 MATERIALS

2.1.1 Cell Culture Materials and Reagents

TABLE 2.1: Tissue culture materials and reagents used including suppliers.

Materials	Source
Tissue culture flasks T-25/T-75/T-175cm²	Nunc [™]
Sterile Petri Dishes	Nunc [™]
6, 24, 96-well tissue culture plates	Nunc [™]
96 round bottom plates	Sarstedt
Dimethyl sulphoxide (DMSO)	Sigma [®]
rGM-CSF	Sigma [®]
Trypan blue (0.4% v/v)	Sigma [®]
CellTiter 96[®] Aqueous One Solution	Pierce
α-MEM	Invitrogen [™]
Foetal Bovine Serum (FBS)	Invitrogen [™]
Penicillin Streptomycin	Invitrogen [™]
Gentomycin	Invitrogen [™]
CpG	Invitrogen [™]
Flagellin	Invitrogen [™]
LPS (<i>E. Coli</i> serotype R515)	Enzo Life Sciences
PamC₃S₄	Invitrogen [™]
PGN	Invitrogen [™]
Poly:IC	Invitrogen [™]
Zyosan	Invitrogen [™]

2.1.2 Enzyme Linked ImmunoSorbent Assay Reagents

TABLE 2.2: Materials and reagents used for ELISAs including suppliers.

Materials	Source
96-well microtitre plate	Nunc™
3,3',5,5'-tetramethyl-benzidine (TMB)	BD OptEIA™
Tween® 20	Sigma®
Bovine serum albumin (BSA)	Sigma®
DuoSet ELISA kits	R&D Systems®
1X PBS	Invitrogen™

2.1.3 Flow Cytometry Reagents

TABLE 2.3: Antibody concentrations, suppliers and controls used for cell surface staining

Antibody	Fluorochrome	Source	Stock Concentration	Isotype Control	Working Concentration
TLR4-MD-2	PE	eBio	0.2mg/ml	RatIgG2a κ	0.5 µg
MHCII	FITC	BD	0.5mg/ml	Rat IgG2a κ	0.5 µg
CD80	PE	BD	0.2mg/ml	HamsterIgG κ	0.5 µg
CD86	FITC	BD	0.5mg/ml	Rat IgG2aκ	0.5 µg
CD40	PE	BD	0.2mg/ml	Rat IgG2aκ	0.5 µg
CD14	FITC	eBio	0.5mg/ml	Rat IgG2aκ	0.5 µg
CCR5	PE	BD	0.2mg/ml	Rat IgG2cκ	0.5 µg
TLR2	FITC	eBio	0.5mg/ml	Rat IgG2aκ	0.5 µg
CD11c	APC	BD	0.2mg/ml	Hamster IgG1	0.5 µg

2.1.4 FACS Aria Reagents

TABLE 2.4: Reagents required for FACS Aria and corresponding suppliers

Materials	Source
FACS Clean	BD
FACS Flow	BD
FACS Rinse	BD

2.1.5 RNA Isolation and cDNA synthesis Reagents

TABLE 2.6: Antibodies used for FACs analysis of cell surface markers; suppliers and concentrations used.

Materials	Source
Nucleospin RNA II Columns	Machinery Nagel
2-Mercaptoethanol	Sigma
DEPC H ₂ O	Invitrogen
High Capacity cDNA Reverse Transcription Kit	Applied Biosciences

2.1.6 Polymerase Reaction Chain Reaction Reagents

TABLE 2.7: Reagents used for RT-PCR and qRT-PCR and corresponding supplier

Material	Source
GoTaq ® DNA polymerase Ladder	Promega
Fast Start Universal Sybr Green	Roche
MicroAmp Optical 96-well Plate	Applied Biosystems
MicroAmp Optical Adhesive Film	Applied Biosystems

2.1.7 Quantitative Reverse Transcriptase Polymerase Chain Primers

TABLE 2.8: Primers used for PCR and their sequences.

Gene	Ref Seq ID	Forward [5' to 3']	Reverse [5' to 3']
SNAP-23	NM_009222	GTTCTTGCTCAGGCTTCC	CCAACCAACCAATACCAATAATG
STX-2	NM_007941	GGTGGCAAAGGTGATGTT	CAGGTATGGTCGGAGTCA
STX-3	NM_001025307	CCACAACCACTAGCATCATAA	CTCAAGAGATATCCGCCTTAA
STX-4	NM_009294	GGTGTC AAGTGTGAGAGAG	AACCTCATCTTCATCGTCTG
STX-5	NM_001167799.1	GCAAGTCCCTCTTTGATGAT	TTCAGATTCTCAGTCCTCACT
STX-6	NM_021433	CAAGGATTGTTTCAGAGATGGA	CCTGACAATTTGCCGAGTA
STX-7	NM_016797	CACAACGCATCTCCTCTAAC	TAATCGGCTTTTCTGTATCTTTCTC
STX-11	NM_001163591.1	ATCACGGCAAATGAAGGA	GGTCGGTCTCGAACACTA
STX-12	NM_133887	CGCAAGAAGATGTGTATCCT	CTCTGAGGCAAGCACTTC
STX-16	NM_001102432.1	GAGCAGTACCAGAAGAAGAAC	CAAGTCCTATACCAATAATCCA
Vti1a	NM_016862	GAATGTATAGCAACAGGATGAGA	CCGTGTTATCCAGCAGATG
Vti1b	NM_016862	TACCTTGGAGAACGAGCAT	TGGACATTGAGCGAAGAATC
VAMP-1	NM_001080557	CCCTCTGTTTGCTTTCTCA	CGTTGTCTTCGGGTAGTG
VAMP-2	NM_009497	CTCCTTCCCTTGGATTTAACC	TGAAACAGACAGCGTATGC
VAMP-3	NM_009498	TTGTTCTTGTGTATATCACTCCTAA	GGCTCGCTCTCACAGTAT
VAMP-4	NM_016796	GTATGCCTCCCAAGTTCAAG	TGTAGTTCATCCAGCCTCTC
VAMP-7	NM_011515	GATGGAGACTCAAGCACAAAG	GACACAATGATATAGATGAACACAAT
VAMP-8	NM_016794	GGCGAAGTTCTGCTTTGA	CTTGACTCCCTCCACCTC
Mip-1α/CCL3	NM_011337	CCTTGCTGTTCTTCTCTGTACC-	CGATGAATTGGCGTGGAATC
MIP-2/CXCL2	NM_009140	CAGAAGTCATAGCCACTCTCAAG	CTTTCCAGGTCAGTTAGCCTT -
MCP/CCL2	NM_011333	CATCCACGTGTTGGCTCA	AACTACAGCTTCTTTGGGACA-
TNF-α	NM_013693	AGA CCCTCA CACTCA GAT CA	TCT TTG AGATCC ATG CCGTTG
IL-6	NM_031168	AGC CAG AGT CCT TCA GAG A	TCC TTA GCC ACT CCT TCT GT
IFN-γ	NM_008337.3	ATGAACGCACACACTGCATC	CCATCCTTTTGCCAGTTCTC
S18	NM_011296	CTGAGAAGTTCCAGCACATT	GCTTTCCTCAACACCACAT

2.1.8 Protein Purification Reagents

TABLE 2.9: Reagents used for protein purification and corresponding suppliers.

Material	Source
Ammonium Persulphate (APS)	Sigma®
BCA Assay	Pierce®
Bis-Acrylamide 30% (w/v)	Sigma®
Complete Protease Inhibitor	Roche
Dithiothreitol (DTT)	Sigma®
Luminata HRP Solution	Millipore
N,N,N',N'-Tetramethylethylenediamine (TEMED)	Sigma®
Nitrocellulose membranes, iBlot	Invitrogen®
PageRuler™ Prestained Protein Ladder Plus	Fermentas
Complete Phosphatase Inhibitor	Sigma®
Potassium Chloride (KCl)	Sigma®
Potassium Phosphate (KH ₂ PO ₄)	Sigma®
Propan-2-ol (isopropanol)	VWR International Ltd.
Protease Inhibitor	Sigma®
Re-Blot Plus Solution (10X)	Millipore
Sodium dodecylsulphate (SDS)	Sigma®
Sodium Phosphate Dibasic (Na ₂ PHO)	Sigma®
Trizma Base	Sigma®
Tween ® 20	Sigma®

2.1.9 Antibodies used for Western and Immunofluorescence

TABLE 2.10: Antibodies used for western blotting and immunofluorescence corresponding suppliers.

Antibody	Source	Species
Anti-STX3	Abcam®	Rabbit
Anti-β actin	Sigma®	Mouse

2.1.10 Immunofluorescence Reagents

TABLE 2.11: Reagents used for immunofluorescence and corresponding suppliers.

Material	Source
0.13-0.16mm Coverslips (RA 1.5)	Harley and Davidson
Paraformaldehyde	Fisher Scientific
Ammonium Chloride	Sigma
Saponin	Sigma
Fish Gelatin	Sigma
Sodium Azide	Sigma
Propidium Iodide	Miltenyi Biotec
DAKO	Invivogen

2.1.11 Immunofluorescence Secondary antibodies

TABLE 2.12: Reagents used for immunofluorescence straining and corresponding suppliers.

Dye	Absorption max. (nm)	Emission max.(nm)	Species	Reactivity	Isotype	Source
AlexaFluro 488	496	519	Donkey	Anti-rat	IgG	Invivogen®
AlexaFluro 488	496	519	Donkey	Anti Goat	IgG	Invivogen®
AlexaFluro 488	496	519	Donkey	Anti Mouse	IgG	Invivogen®
AlexaFluro 488	496	519	Donkey	Anti Rabbit	IgG	Invivogen®
AlexaFluro 546	556	573	Donkey	Anti Mouse	IgG	Invivogen®
AlexaFluro 546	556	573	Donkey	Anti Rabbit	IgG	Invivogen®
AlexaFluro 633	632	647	Donkey	Anti Goat	IgG	Invivogen®
AlexaFluro 633	632	647	Goat	Anti Rat	IgG	Invivogen®
Strep Alexa 488	496	519	Goat	Anti Mouse	IgG	Invivogen®

2.2 METHODS

2.2.1 Stock Solutions and Buffers

TABLE 2.13: Stock Solutions and recipes.

Buffer	Composition
10 X Phosphate Buffered Saline (10 X PBS)	8 mM Na ₂ HPO ₄ , 1.5 M KH ₂ PO ₄ , 137 mM NaCl, 2.7 mM KCL, pH 7.4
PBS-Tween (PBS-T)	1 X PBS with 0.05% Tween [®] 20
10 X Tris Buffered Saline (10 X TBS)	20 mM Trizma, 150 mM NaCl pH 7.2 – 7.4
TBS-Tween (TBS-T)	1 X TBS with 0.05% Tween [®] 20
TAE Buffer (50X)	40mM Tris, 20mM acetic acid, 1mM EDTA pH 8.4

2.3 CELL CULTURE TECHNIQUES

All cell culturing techniques were carried out using aseptic technique in a class II laminar airflow unit (Holten 2010- ThermoElectron Corporation, USA). Cells were maintained in a 37°C incubator with 5% CO₂ and 95% humidified air (Model 381 – ThermoElectron Corporation USA). Cells were cultured in α -Minimum Essential Medium (α -MEM) supplemented with 20% Non-heat inactivated fetal bovine serum (FBS), 100 μ g/ml/100 μ g/ml penicillin/streptomycin, 50 μ g/ml gentamycin and 50 μ g/ml murine recombinant GMCSF and visualised with an inverted microscope (Olympus CKX31, Olympus Corporation, Toyko, Japan).

2.3.1 CELL ENUMERATION AND VIABILITY ASSESSMENT

Counts and viability were assessed using a haemocytometer and trypan blue exclusion test. This test is based on the principle that viable cells with intact membranes are able to actively exclude the dye whereas dead cells are unable and appear blue when viewed under the microscope. A glass coverslip was mounted onto the moistened shoulders of a haemocytometer until the phenomenon of Newton's rings was observed ensuring the coverslip had adhered and the depth of the chamber was correct. 100 µl of gentle agitated cell suspension was added to 150 µl of PBS and 250 µl of trypan blue solution (0.4% (v/v)). After ~2 minutes cells were gently applied to a Brightline™ Neubauer haemocytometer (Sigma) and drawn out into the chamber by capillary action. Cells were counted under a 10X magnification using phase contrast microscope in one set of the 16 squares (equates to number of cells x10⁴/ml)[Figure 2.1], this was repeated four times and averaged.

Cells per ml

$$= N (\text{Average Cell Number}) \times 5 (\text{dilution factor}) \times 10^4 (\text{constant})$$

To assess cell viability, total cell number, (i.e. dead plus alive cells) is expressed as a fraction of alive cells as follows.

% Viability

$$= \left(\frac{N(\text{Average } \mathbf{Alive} \text{ Cell Number}) \times 5 (\text{dilution factor}) \times 10^4 (\text{constant})}{N(\text{Average } \mathbf{Total} \text{ Cell Number}) \times 5 (\text{dilution factor}) \times 10^4 (\text{constant})} \right) \times 100$$

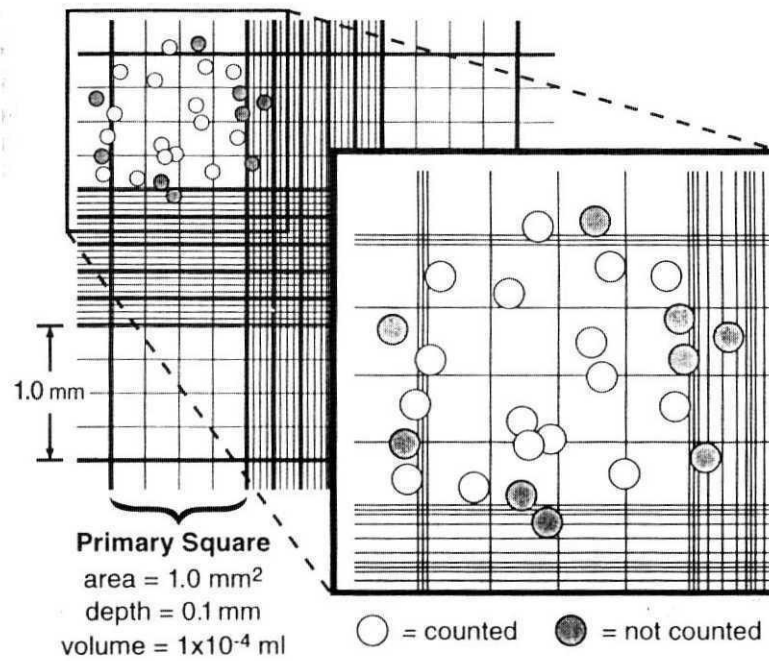


FIGURE 2.1: Cell enumeration and viability assessment using the Neubauer haemocytometer. Inset indicating the 16 squares where viable (colourless) and non-viable (blue stained) cells were counted. Cells touching the left or top boundary are counted however those that touch the lower or right hand boundary are not counted.

[Adapted

from

<http://www.cf.ac.uk/biosi/staffinfo/kille/Methods/Cellculture/HAEMO.html>]

2.3.2 JAWS II DENDRITIC CELL LINE

The murine dendritic cell line JAWS II (CRL-11904) was used extensively in this study and is referred to as JAWS II DCs throughout. The cell line was bought from ATCC and maintained in fully supplemented α -MEM [see **Appendix**] in T75cm² flasks. JAWS II DCs are an immature dendritic cell line derived from a p53 growth suppressor gene deficient C57BL/6 mice, which have been reported to be induced to become an activated dendritic cell line with the ability to stimulate T cells to proliferate (MacKay and Moore, 1997). JAWS II DCs are a mixed culture of attached and suspension cells thus for subculture, after seven days of growth, suspension cells were transferred to a 50ml falcon before adherent cells being washed with PBS and 0.25% trypsin-0.53mM EDTA being added. All cells were pooled, centrifuged at 1000 rpm for 10 minutes and subcultured at a 1:5 ratio and incubated at 37°C and 5% CO₂.

2.3.3 ISOLATION AND CULTURE OF BONE MARROW-DERIVED DENDRITIC CELLS

2.3.3.1 Day 1 – Bone Marrow Harvest

Isolation of bone marrow-derived dendritic cells (BMDCs) was adapted from Lutz *et al.*, 1999 (Lutz et al. 1999) Bone marrow was isolated aseptically from the tibiae and femurs of C57BL/6 mice (Charles River) aged 6-12 weeks which were housed in a Specific Pathogen Free (SPF) unit. This was done by flushing α -MEM through the cut bones using a 27.5g needle and syringe into a sterile 50ml falcon. Bone marrow,

still intact, was then gently broken up with a 19.5g needle and syringe. Cells were then centrifuged for five minutes at 1200 rpm, supernatant removed, pellet resuspended in α -MEM to allow for 1ml of cells per Petri dish required. To ensure an adequate number of viable cells had been harvested a cell count using the trypan blue exclusion method was performed. 9ml of α -MEM supplemented with 50 ng/ml rGMCSF and 1ml of cells were added to each Petri dish and incubated at 37°C and 5% CO₂.

2.3.3.2 Day 4 – Feeding Cells

To visualise the monolayer of adherent cells, the Petri dish was tipped forward and using a transfer pipette ~6mls of media was gently removed without disturbing the cells. 10 mls of pre-warmed α -MEM with r-GMCSF was added to the Petri dish and incubated at 37°C and 5% CO₂.

2.3.3.4 Day 7 – Counting and Plating Cells

To remove the semi-adherent, i.e. the immature DCs, a transfer pipette with media was repeatedly pipetted onto the Petri dish surface before being collected in a 50ml falcon tube. Petri dishes were then examined under the microscope to ensure the majority of the cells were removed. Cells were centrifuged at 1200rpm for 5 minutes, resuspended and counted using trypan blue exclusion method. The cell concentration was adjusted with α -MEM and generally cells were plated at 1×10^6 /ml.

2.3.4 Cryogenic Preservation of Cell Stocks

To maintain reserves of cells, JAWS II DCs were cryogenically preserved in liquid nitrogen. JAWS II DCs were grown to a state of sub-confluency, counted and resuspended at 10×10^6 cells/ml of complete α -MEM with 5% (v/v) DMSO. 1ml

aliquots were transferred to labelled and dated cryovials (Nalgene®) and placed in a Mr Frosty® in a -80°C freezer. Mr Frosty provides a 1°C/min cooling rate which is required for successful cryopreservation of cells. After three hours the cryovials were then transferred for storage to the liquid nitrogen vessel.

2.3.5 Revival of Frozen Stocks

A cryovial was removed from liquid nitrogen, thawed rapidly (~2 minutes) by gentle agitation in a 37°C water bath. As soon as contents were thawed, the vial was sprayed with 70% ethanol and the contents were removed under aseptic conditions and transferred into 9 ml complete α -MEM. Cells were centrifuged for 5 minutes at 1000rpm. The pellet was resuspended in 10 ml complete α -MEM and placed in a pre-warmed T25cm² culture flask incubated at 37°C and 5% CO₂.

2.3.6 Toll-Like Receptor Activation

Cells were activated with TLR ligands outlined in the **Table 2.14**, and incubated for a period of time ranging from 1-24 hours before being used for the relevant experimental set up outlined.

TABLE 2.14: Concentrations of TLR ligands used for the maturation of dendritic cells.

TLR	Ligand	Stock Concentration	Working Concentration
2	PGN	200µg/ml	5µg/ml
2/1	Pam3CSK4	1mg/ml	1µg/ml
3	Poly IC HMW	1mg/ml	10µg/ml
4	Rough LPS	1mg/ml	100ng/ml
5	Flagellin	100µg/ml	5µg/ml
7	Loxoribine	10mM	1mM
9	CpG	500µM	2µM

2.3.7 Cytotoxicity Assay

To measure cytotoxicity a CellTiter 96[®]AQ_{ueous}One Solution Proliferation Assay (Promega) was employed. This reagent contains a novel tetrazolium compound [3-(4,5-dimethylthiazol-2-yl)-5-(3-carboxymethoxyphenyl)-2-(4-sulfophenyl)-2H-tetrazolium, inner salt; MTS] and an electron coupling reagent (phenazineethosulfate; PES). This is a colourimetric method for determining the number of viable cells in proliferation as the MTS is bio-reduced by cells into a soluble coloured formazan product (figure 2.2). The quantity of formazan produced is measured at an absorbance of 490nm and is directly proportional to the number of living cells in culture.

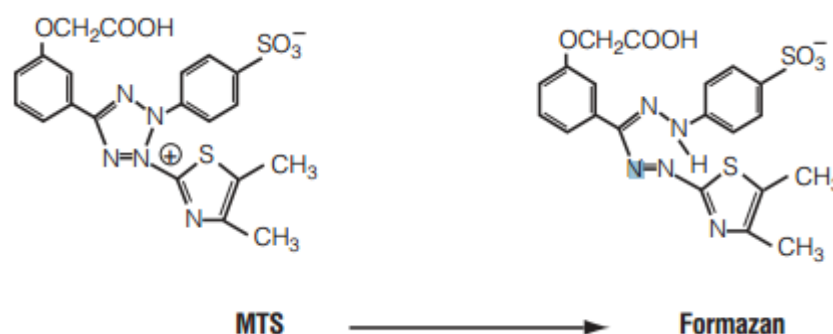


FIGURE 2.2: MTS tetrazolium structure and its formazan product [adapted from <http://worldwide.promega.com/resources/protocols/technical-bulletins/0/celltiter-96-aqueous-one-solution-cell-proliferation-assay-system-protocol/>].

JAWSII DCs were trypsinized, counted and plated at $0.1 \times 10^6 / 100 \mu\text{l}$ of complete α -MEM in tissue culture treated 96-well plates and left to rest overnight. The following day cells were stimulated with TLR ligands (as outlined in section 2.3.6) for 24 hours. A volume of $20 \mu\text{l}$ of CellTiter 96[®]AQ_{ueous}One Solution was added to each

well, incubated for two hours at 37°C in 5% CO₂ after which absorbance was read at 490nm by plate reader. The cell viability of each sample was expressed as a percentage of the control cells (absorbance of control treated at 100%).

2.4 ENZYME LINKED IMMUNOSORBANT ASSAY (ELISA)

A sandwich ELISA can measure the amount of antigen, in this case cytokine or chemokine, between a capture and detection antibody, as indicated in figure 2.3. The antigen contains at least two antigenic sites for the capture and detection antibodies to bind to. Sandwich ELISAs offer higher sensitivity to that of direct or indirect ELISAs as samples do not have to be purified before analysis.

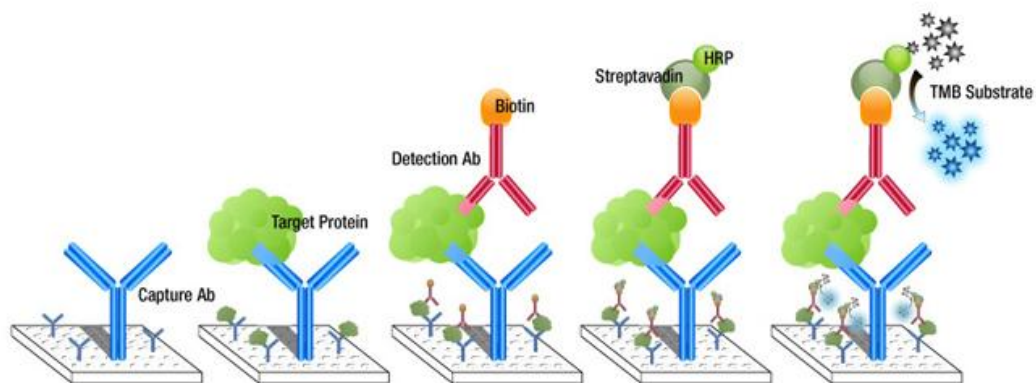


FIGURE 2.3: Illustration of the principles behind the sandwich ELISA [taken with adaptations from <http://www.epitomics.com>].

An overview; using the ELISA DuoSet from R&D Systems, a 96 well plate was coated with specific (to the target antigen) capture antibody diluted in buffer such as PBS. The plate was sealed and incubated overnight at RT. The following day blocking buffer such as 5% BSA/PBS was added to block any remaining protein

binding sites on the plate. A two-fold serial dilution of the top standard was prepared, along with the samples (containing unknown concentrations of antigen) were added to the plate and incubated overnight at 4°C to allow antigen to bind to the capture antibody. On day three the detection antibody specific to the target antigen, which is biotinylated, was added to the plate. Streptavidin-Horseradish peroxidase (HRP) was then added to the plate for 20 minutes at room temperature. Streptavidin binds to biotin with high affinity. The substrate 3, 3', 5, 5' - Tetramethylbenzidine (TMB) was added. HRP catalyzes TMB to form a coloured blue compound. The intensity of the blue colour formed is proportional to the concentration of antigen present in the sample or standard. The reaction was stopped with 2N H₂SO₄, which changes the blue colour to a yellow colour which was then read at 450nm on a spectrophotometer.

2.4.1 DETECTION OF CYTOKINES, IL-6, IL-10, TNF-ALPHA, IL-12P40, IL-12-70, IL-23 AND IL-27P28

The cytokines IL-6, IL-10, TNF- α , IL-12p40, IL-12p70, IL-23 and IL-27p28 were quantified according to manufactures recommendations. 1% (w/v) BSA/PBS was used for blocking buffer and reagent diluent. Washing buffer consisted of 0.05% Tween-20 in PBS.

2.4.2 DETECTION OF CYTOKINES, IL-1BETA AND IFN-GAMMA

The cytokines IL-1 β and IFN- γ were quantified according to manufacturer's recommendations. 1% (w/v) BSA/PBS was used for blocking buffer and 0.1% (w/v)

BSA/TBS +0.05% (v/v) Tween-20 was used for reagent diluent. Washing buffer consisted of 0.05% Tween-20 in PBS.

2.4.3 DETECTION OF CHEMOKINES, MIP-1 AND MIP-2

Cytokines MIP-1 α and MIP-2 were quantified according to manufacturer's recommendations. 1% (w/v) BSA/PBS was used for the blocking buffer and reagent diluent. Washing buffer consisted of 0.05% Tween-20 in PBS.

2.5 FLOW CYTOMETRY

Flow cytometry is a powerful technique for the analysis of multiple parameters of cells within a heterogeneous cell population. These include inherent cell characteristics such as size, shape, granularity and expression of cell surface markers and intracellular molecules. The flow cytometer does this by passing the cell suspension into a hydrodynamically focused, sheath fluid through a 100 μm nozzle, which allows one cells at a time past a laser light, see figure 2.4, (a). The light scattered and the fluorescence emitted (from positively stained cells) are read by detectors. The detector in front of the laser beam is called the Forward Scatter which determines cell size and the detectors to the side such as the Side Scatter determines the granularity. When a cell has been stained by a fluorochrome, it will emit light at a certain wavelength when excited by a laser at the corresponding excitation. The emitted light is detected by detectors called a photomultiplier tubes (PMTs) which convert the energy of a photon into an electrical signal called a voltage, see figure

2.4 b. Each voltage pulse equates to an “event” and 100,000 of these are recorded on average.

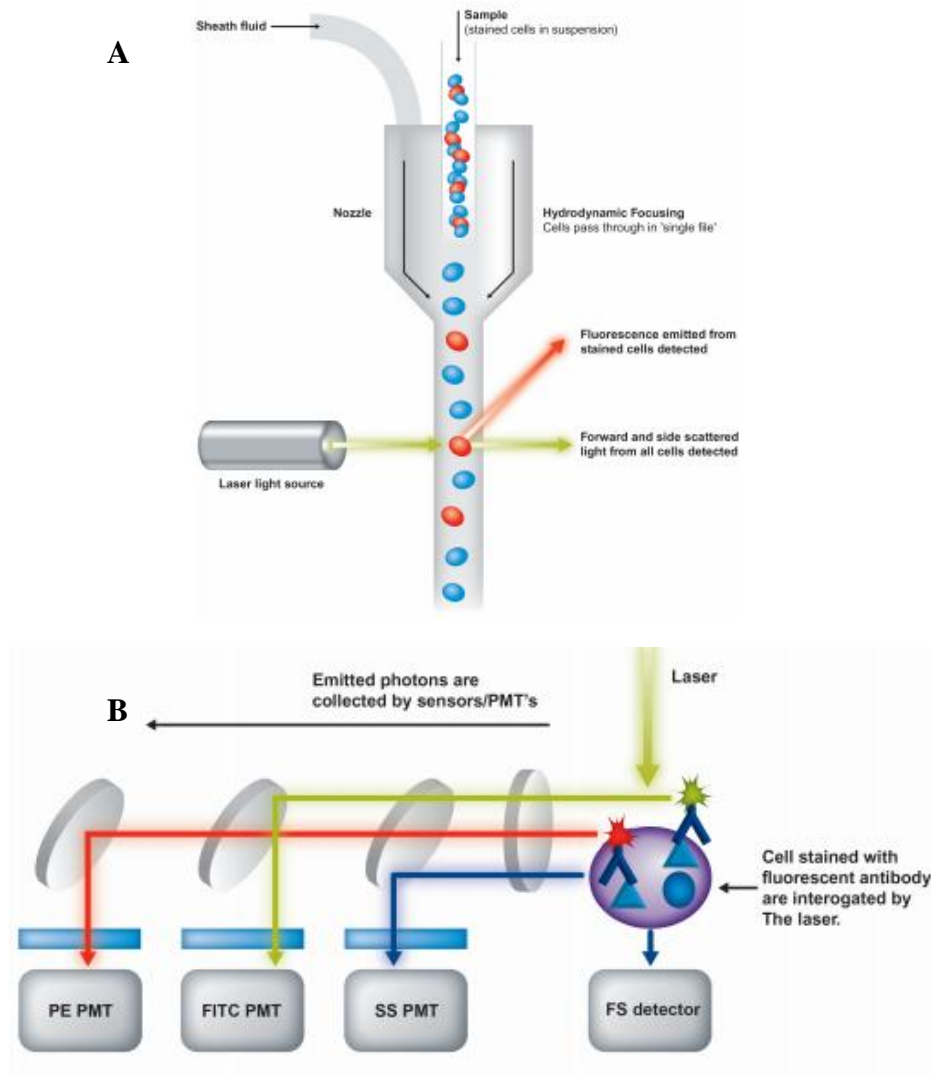


FIGURE 2.4: (a) “single file” cells being passed through the nozzle (100 μm on the FACS Aria I) under hydrodynamic focusing into the path of the laser and (b) measurement of scattered light and fluorescence by PMTs. Take with amendments from <http://www.abcam.com>].

In order to investigate an antigen on the surface of a cell, the cell is incubated with a fluorescently labelled monoclonal antibody specific to the antigen of interest. These fluorochromes are excited by a laser and emit light at specific wavelengths. In this study we used three-colour polychromatic flow cytometry with Fluorescein isothiocyanate (FITC), excited at 495nm, emits at 520nm, Phycoerythrin (PE) 465nm, emits at 578nm and Allophycocyanin(APC) excites at 635nm, emits at 660nm the fluorophores used through-out the study. See figure 2.5.

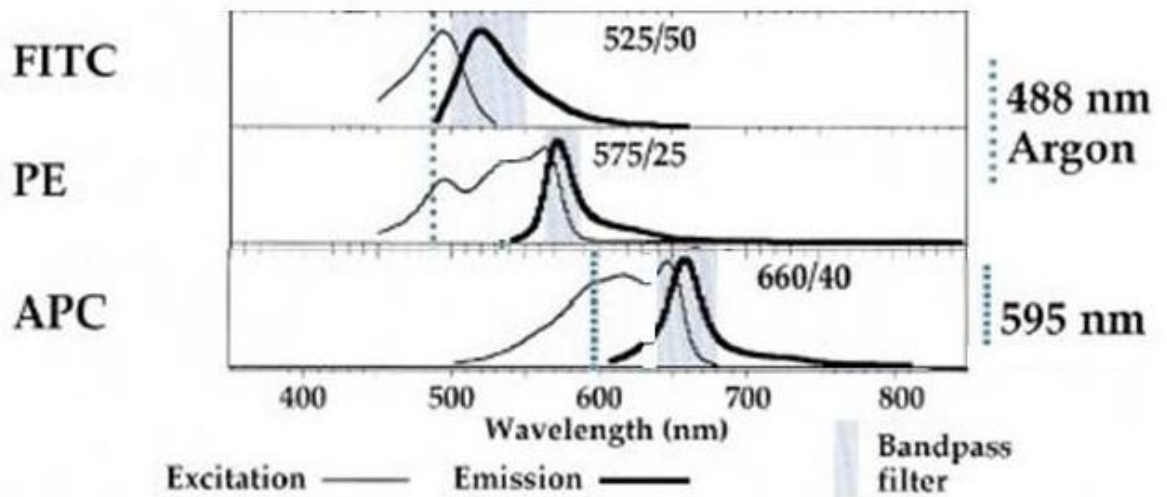


Figure 2.5: Excitations, emissions, laser and bandpass filter used for FITC, PE and APC staining, taken with adaptations from (Baumgarth and Roederer 2000).

2.5.1 CELL SURFACE STAINING

Cells, either JAWS II DCs or BMDCs were trypsinized or scraped, counted and plated at 2×10^6 cells per well on a six well plate, in a total of 2ml of media and left to rest overnight. Cells were then stimulated for the indicated period of time, generally 24 hours with an appropriate ligand (see section 2.3.6). Cells were then

scraped in media, transferred to a falcon tube with an equal amount of FCS, to block non specific binding, for 15 minutes. Following this, cells were centrifuged at 1200 rpm for 5 minutes. The resulting pellet was resuspended in 1 ml of FACS buffer. 200 μ l of cells (~400,000 cells) were added per well of a 96-well round bottomed plate, spun at 1200 rpm for 5 minutes and stained with antibody (see Table 2.3) including separate wells for corresponding isotype matched controls. These plates were left in the dark at 4°C for 30 minutes, following which; cells were spun at 2000 rpm for 5 minutes at 4°C and washed by being resuspended in 200 μ l FACS buffer three times. Cells were then transferred to labelled FACS tubes and the volume was brought up to 500 μ l with FACS buffer. Samples were then acquired immediately on the Becton Dickinson (BD) FACSAria™ I Cell Sorter and analysed using FlowJo software (Tree Star) with cells gated on CD11⁺ cells.

2.5.2 CELL VIABILITY

To measure cell viability we employed the use of propidium iodide (PI), which serves as a dead cell indicator. It does this as PI is membrane impermeant, thus it does not enter viable cells with intact membranes. When cells are dead their membrane is compromised, PI can enter and intercalate with nucleic acids, see figure 2.6. Fluorescence is then enhanced 20-30 fold, shifting its fluorescence excitation maximum ~30-40 nm to 535 nm and emission maximum is shifted ~15nm to 617nm. Cells were prepared as in 2.5.X, with two exceptions. Only antibodies that do not emit in the PI spectra were used for analysis of other surface markers in the incubation step and PI is added at the last step at a concentration of 1 μ g/ml for 15 minutes and read immediately. All FACS experiments included viability testing to ensure populations were comparable.

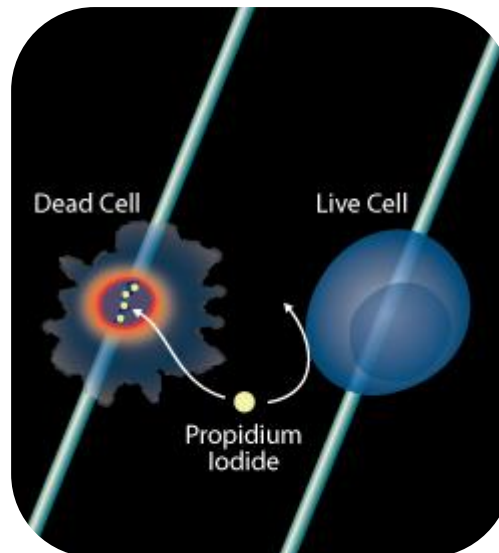


Figure 2.6: PI is a membrane impermeant that is generally excluded from viable cells. However when the membrane is compromised it binds to double stranded DNA by intercalating between base pairs, which is then excited at 488nm and emits at 617nm [Taken from <http://www.rndsystems.com>].

2.6 QUANTITATIVE POLYMERASE CHAIN REACTION (QPCR)

2.6.1 RNase Free Working Environment

To ensure the quality of RNA, work was conducted in a ribonuclease (RNase) free environment. RNase is an enzyme that catalyzes the degradation of RNA into smaller compounds. They are found in both prokaryotes and eukaryotes. The human body uses RNases to defend against microorganisms hence they are present in flaked skin and hair that could fall into the bench destroying RNA samples. A dedicated RNase free bench was set up in the lab at which gloves were worn at all times and exchanged for fresh ones after touch any area outside of this. A dedicated set of pipettes were left in the RNase free area and only used with filter inserted RNase-

free pipette tips. Diethylpyrocarbonate (DEPC) treated- H₂O was used at all times as DEPC inactivates enzymatic activity of potential RNases in H₂O.

2.6.2 RNA Isolation

Cells, either JAWS II DCs or BMDCs were trypsinized or scraped, counted and plated at 2×10^6 cells per well on a six well plate, in a total of 2ml and left to rest overnight. Cells were then stimulated with appropriate ligand with for the indicated period of time, between 1 and 12 hours with the appropriate ligand (see table 2.14). RNA was then extracted by NucleoSpin[®] RNA kit (Machinney Nagel) spin columns. Cells were lysed in a solution containing chaotropic ions, which inactivate RNases and create appropriate binding conditions for absorption of the RNA to the silica membrane on the spin column. rDNase was added to the silica membrane to remove contaminating DNA which may also have bound. Two different buffers were used for washing steps which remove salts, metabolites and macromolecular cellular components. RNA was eluted under low ionic strength conditions with RNase free H₂O. All RNA was stored at -80°C.

2.6.3 RNA Integrity Analysis and Quantification by Spectrometry

The NanoDrop Spectrophotometer reads the absorbance spectra from 230nm to 600 nm. As little as 1µl of sample, in this case nucleic acid, can give quantitative assessment and purity information. RNA should have a A_{260}/A_{280} ratio of 2 (due to the absorbance of uracil to thymidine).

Historically the A_{260}/A_{280} ratio has been the primary measure of purity, however examining the entire absorbance spectra, including the A_{260}/A_{230} can help you

identify problems such as contaminants. For example, phenol absorbance will lower the samples A_{260}/A_{230} which should be around 1.8-2.2, see **Figure 2.7**.

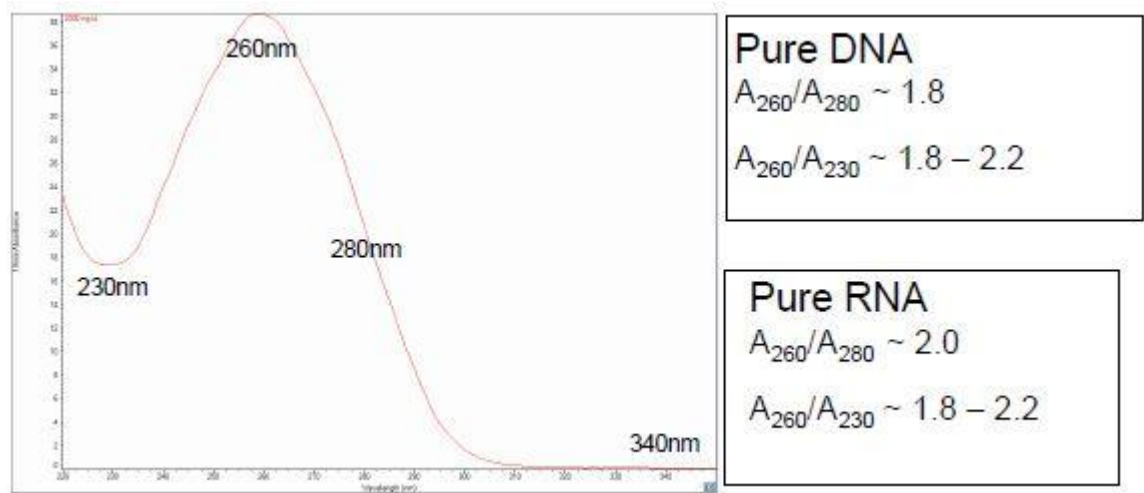


Figure 2.7:Readout from a Nanodrop and the corresponding ratios of pure RNA.

2.6.4 RNA Integrity Analysis by Gel Electrophoresis

To assess the integrity of the RNA, 1 μg of all RNA samples were made up in sample buffer containing formamide, heated to 65°C for 10 minutes and run on a denaturing agarose gel at 100V for 45 minutes. The gel was then visualised using the G-Box Gel Imagine System (Syngene). Intact total RNA will have two clear ribosomal RNA bands at 28S and 18S. The 28S rRNA band should be 2:1 the intensity as the 18S rRNA. This indicates the RNA is completely intact.

2.6.5 Reverse Transcription (RT) – complementary DNA (cDNA) Synthesis

cDNA was generated using the High Capacity cDNA Reverse Transcription kit (Applied Biosystems). In an RT reaction single-stranded RNA is reversely

transcribed into cDNA by using, in this case, total RNA, a reverse transcriptase enzyme, random primers, dNTPs and an RNase inhibitor. 1µg of mRNA was converted to cDNA as follows.

TABLE 2.15: cDNA Reaction Components.

Components	Total
10X RT Buffer	2µl
10X Random Primers	2µl
25X dNTP Mix (100mM)	0.8µl
Reverse Transcriptase (50U/µl)	1µl
Nuclease Free H ₂ O/RNA mix	14.2µl
Total per reaction	20µl

Samples were mixed and spun before being placed in a Thermocycler and set according to Table 2.16. cDNA was at -20°C until further use.

TABLE 2.16:cDNA Cycling Settings.

Steps	Temperature	Duration
1	25°C	10 minutes
2	37°C	120 minutes
3	85°C	5 minutes
4	4°C	∞

2.6.6 Reverse Transcriptase Polymerase Chain Reaction (RT-PCR)

RT-PCR is a two step process, in the first step, RNA is transcribed into cDNA using a reverse transcriptase (“RT”) and this has been described in section 2.6.5. This cDNA is the template for subsequent PCR reactions using specific primers for one or more genes. Go-Taq[®] Green (Promega) was used as the master mix and 500 ng of cDNA was amplified as outlined in **Table 2.17** and PCR products run out on a 1% agarose gel and visualised then visualised using the G-Box Gel Imagine System (Syngene).

TABLE 2.17: Constituents used for the 25 μ l RT-PCR reaction mixture.

2X GoTaq[®] Green Master Mix	12.5 μ l
10μM Forward Primer	1 μ l
10μM Reverse Primer	1 μ l
H₂O/cDNA Template	10.5 μ l

Samples were mixed and spun before being placed in a Thermoocycler and amplified using the conditions as outlines in **Table 2.18**.

TABLE 2.18: The conditions used for amplification of the cDNA.

Steps	Temperature	Duration
1	95°C	5 minutes
2	95°C	15 seconds
3	55-65°C	30 seconds
4	72°C	15 seconds
5	Steps 2-4 were repeated 60 times	
6	72°C	5 minutes
7	4°C	∞

2.6.7 Temperature Gradients

Primers (Sigma and IDT) were supplied with theoretical annealing temperatures. This temperature is generally calculated on the number of G's, C's, A's and T's in the primers sequence as follows;

$$T_m = 4^{\circ}C \times (\text{numbers and G's and C's in the primer sequence}) \\ + 2^{\circ}C \times (\text{numbers of A's and T's in the primer sequence})$$

As too low an annealing temperature can produce non-specific products and too high a temperature the PCR yield can be low product, annealing temperature optimisation was carried out. A thermacyler with a block gradient feature was used [**Figure 2.8**]. RT-PCR was performed as in section 2.6.6 with a temperature gradient between 55°C

and 65°C. PCR products run out on a 1% agarose gel and then visualised using the G-Box Gel Imagine System (Syngene) [See Appendix].

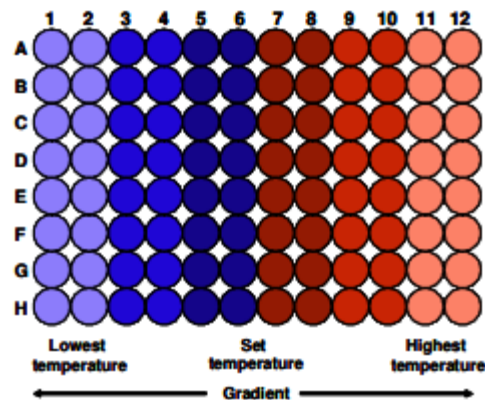


FIGURE 2.8: Schematic representation of the thermocyclers temperature gradient across the 96-well block [taken from <http://www.techne.com>].

2.6.8 Primer Efficiency Curves

To move on to quantitative PCR (qPCR) the assay efficiency had to be determined as it is critical to accurate data interpretation. A serial dilution of neat cDNA was generated; a standard curve plotting the log of the dilution factor against the Ct value obtained from the cDNA and the target of interest. The equation of the line was generated and the slope was used to calculate the efficiency based on the following equation;

$$Efficiency = 10 \left(\frac{-1}{Slope} \right) - 1$$

Ideally the efficiency of the assay should be 100%, indicating that PCR product is doubling during the logarithmic phase of the reaction. This means that the slope value would have to be -3.32, however slopes in the range of -3.60 to -3.10, equating

to efficiencies of 90% to 110% are considered acceptable. R^2 value of the line was also taken into account and values of >0.950 were deemed acceptable.

2.6.9 Quantitative Reverse Transcriptase Polymerase Chain Reaction (qRT-PCR)

As all points of the PCR reaction were optimised qRT-PCR could then be carried out. The technology used for quantification. For this SYBR-Green based detection was employed. This method was chosen over probe-based detection as it is high throughput and we were taking a screening approach with the data. SYBR Green dye binds to double stranded DNA produced during PCR reactions. SYBR Green has an excitation of 494 nm and emission maxima of 521 nm.

An overview; in step one, denaturation, double-stranded DNA is heated to 94°C - 98°C , melting the DNA helix into two separate strands (step two). To anneal the single stranded DNA, step three, primers bind to the single stranded DNA template, the reaction is cooled to 45°C - 65°C . Complimentary nucleotides, dATP, dCTP, dGTP and TTP are incorporated into the primed template with the aid of DNA polymerases. A slight raise in temperature during this extension cycle (65°C - 75°C) as the optimal temperature of Taq DNA polymerase is 72°C , yields a double-stranded DNA complex. As SYBR green is a double stranded DNA binding dye, it binds to newly synthesized double-stranded DNA helixes and fluoresces. The level of intensity of fluorescence of SYBR Green that is greater than background is measured and the amount of newly generated DNA strands is directly proportional to the amount of SYBR green fluorescence accumulated at the end of the PCR cycle.

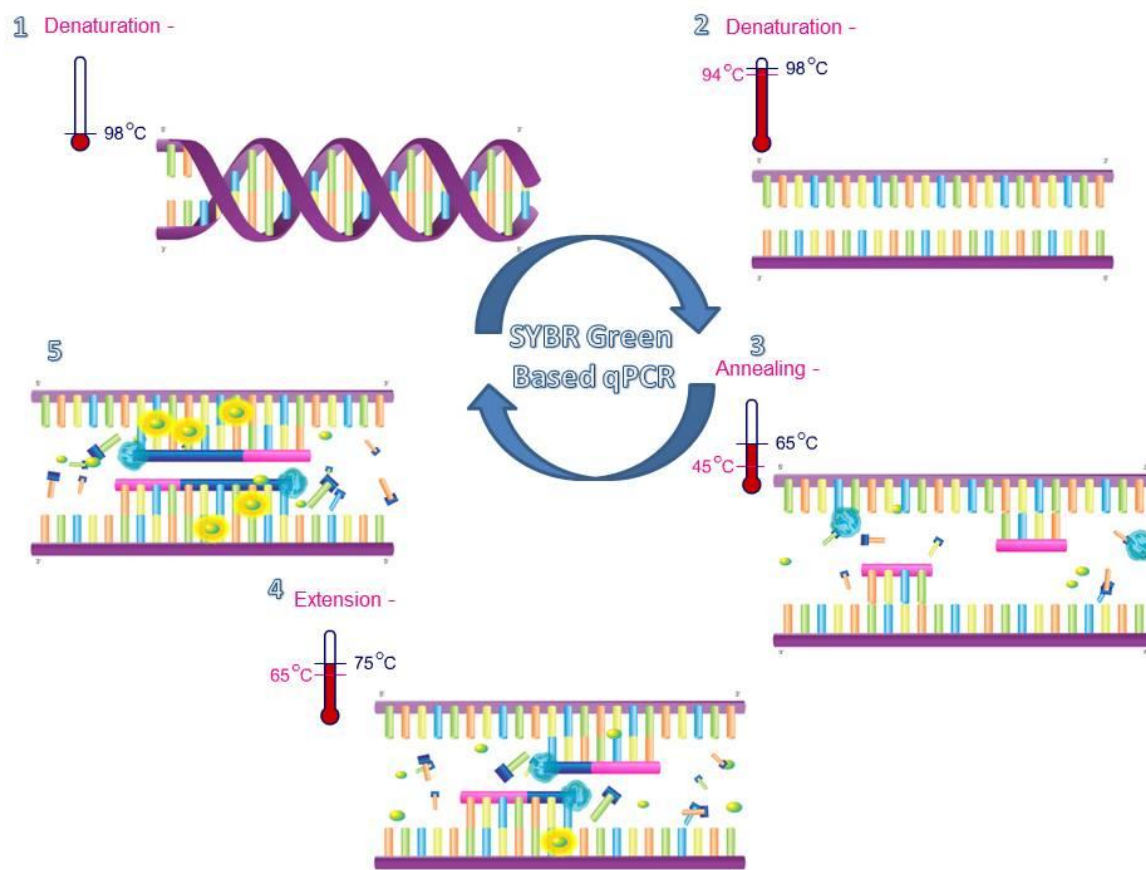


FIGURE 2.9: Schematic representation of the steps involved in SYBR Green I based qPCR. Step 1&2 Denaturation; double-stranded complex denatures, target primers and complimentary nucleotides anneal with the aid of DNA polymerases resulting in Step 3; Extension of the new double-stranding DNA complex to which SYBR green binds and fluoresces [Taken with adaptations from <http://www.sigmaldrich.com>].

TABLE 2.19: Constituents used for the 25µl qRT-PCR reaction mixture.

Component	Total
2X SYBR Green I® Green Master Mix	12.5µl
300nM Forward Primer	1µl
300nM Reverse Primer	1µl
H ₂ O/cDNA Template	10.5µl

TABLE 2.20: The conditions used for amplification of the cDNA in qRT-PCR.

Steps	Temperature	Duration
1	95°C	10 minutes
2	95°C	15 seconds
3	55-65°C	60 seconds
4	72°C	15 seconds
5	Steps 2-4 were repeated 50 times	
6	72°C	5 minutes
7	4°C	∞

2.7 WESTERN BLOTTING

2.7.1 Isolation of Whole cell Lysates

JAWS II DCs were seeded at 1×10^6 cell/ml in a 24-well plate and left overnight to rest. Cells were then transfected for 24 hours. Cells were washed with PBS and scraped in 200 μ l of NP-40 lysing buffer [see **Appendix**]. Protease and phosphatase inhibitor cocktails were added just before use. Cells were scraped into pre-chilled tubes and inverted at 4°C for 30 minutes. Lysates were then centrifuged at 12,000 x g for 10min at 4°C and supernatants were transferred to new pre-chilled tubes. The protein concentration of the supernatants were then determined using the BCA assay and aliquots containing equal amounts of protein were mixed with 4X SDS sample buffer, boiled at 100°C for 10 min and separated using SDS denaturing polyacrylamide gel electrophoresis.

2.7.3 SDS Denaturing Polyacrylamide Gel Electrophoresis

Sodium Dodecylsulphate-Polyacrylamide Electrophoresis (SDS-PAGE) resolution of protein lysates was carried out. Acrylamide gels (12 % (w/v)) [see **Appendix**] were cast between a pair of 10*100mm glass plates and affixed to the electrophoresis

unit using spring clamps. Running buffer [see **Appendix**] was added to the electrophoresis tank and 10 μ l (10 μ g) of protein lysate were loaded into the wells. A molecular weight protein ladder (Fermentas) ranging from 10-250kDa was added to lanes either side of the protein lysates. Gels were run at 30mA per gel for ~45 minutes.

2.74. Protein Transfer

Transfer of the proteins from the gel onto a nitrocellulose membrane was done using the iBlot Dry Blotting System (Invitrogen™) [**Figure 2.10**]. The iBlot has a patented gel matrix technology that allows for transfer of the proteins from the gel onto the membrane in only seven minutes. It does this due to shortened distance between the electrodes, high field strength and high currents.

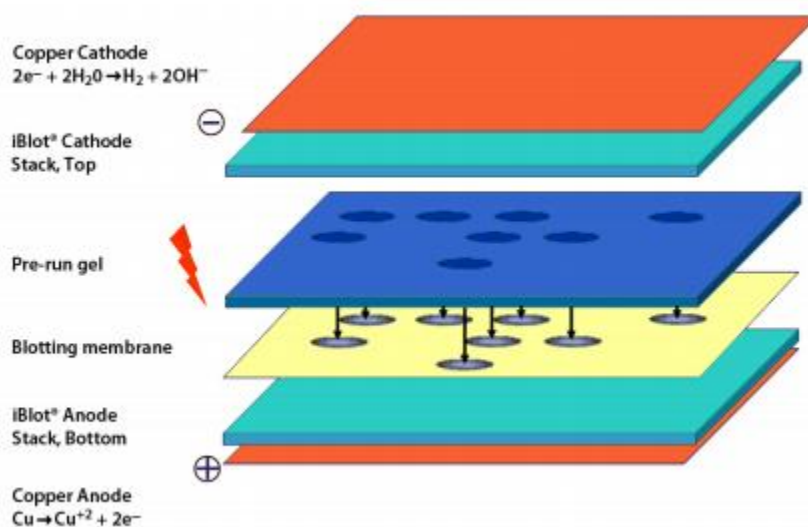


FIGURE 2.10: Schematic of the transfer stack of the iBlot showing the flow of current which results in shortened transfer time. Taken from lifetechnologies.com.

2.7.6 Immunoblotting and Detection

Post transfer, the membranes were incubated with 5 % (w/v) BSA/TBS-T for 1 hour on a rocker at RT to block non-specific protein binding. Membranes were then washed x 3 with TBS-T (wash buffer) for 5 minutes and incubated with the appropriate primary antibody in [see **Table 2.1.8**] 5 % (w/v) BSA/TBS-T overnight at 4°C. Following overnight incubation, membranes were washed three times for 5 minutes in wash buffer. Membranes were then incubated with the appropriate Horse Radish Peroxidase (HRP)-conjugated secondary antibody [see **Table 2.1.8**] in 5% (w/v) BSA/TBS-T with gentle rocking at room temperature for 2 hours. The blots were then washed three times for 5 minutes in wash buffer. Luminata chemiluminescence substrate was then added to the membranes to detect HRP-labelled antibody complexes. The intensity of signals was detected by the G-Box fluorescence gel analysis system (Syngene NJ USA) and exposed for a range of different times depending on the concentration of protein.

2.8 INHIBITION OF INTRACELLULAR PROTEIN STX-3

The STX-3 antibody [see **Table 2.1.8**] used in this study recognises the cytoplasmic NH₂-terminal region required for SNARE binding. Bacterial-derived Streptolysin-O (SLO) toxin (Sigma) temporarily permeabilises cells to allow for delivery of the neutralising antibody which inhibits STX-3 activity.

0.5×10^6 JAWSII DCs were washed and resuspended with Hanks Balanced salt solution (HBSS) containing 30 mM HEPES. 20 µg/ml Streptolysin-O (SLO) toxin and 20 µg/ml STX-3 antibody were added to the JAWS II DCs and were incubated

in a water bath for 15 minutes. Ice cold α -MEM was added (to allow pores in cells to close) for 1 hour on ice. Cells were centrifuged, resuspended in α -MEM and incubated for 4 hours at 37°C in 5% CO₂. Supernatants were removed and analysed for the levels of IL-1 β , IL-6, TNF- α and MIP-1 α .

2.9 RNAI

RNAi is a biological process where gene expression is inhibited by RNA molecules which cause the destruction of specific mRNA molecules. We exploited this pathway to study the gene function of STX-3 in JAWS II DCs.

2.9.1 siRNA

Small interfering (siRNAs) are a double-stranded RNA molecule, usually 20-25 base pairs in length. In this study we used a specific siRNA to STX-3 to interfere with the expression of this gene. We also used a scrambled RNA as a negative control and assessed transfection efficiency using fluorescently labelled CyTM3 labelled Glyceraldehyde 3-phosphate dehydrogenase (GAPDH) (InvitrogenTM) [**See Appendix**]. Genesilencer (Genelantis) is a cationic lipid formulation designed for delivery of siRNAs into cells.

JAWSII DCs were plated at 1x 10⁶/ml on a 24-well plate and left to rest overnight. Genesilencer reagent and serum free media were added to one tube and siRNA diluent, specific siRNA (1nM) and serum free media were added to another tube and left to incubate at RT for 5 minutes. The two tubes were then mixed together and incubated for 10 minutes. This mixture was then added directly to the plate and left for 24 hours. Medium was then removed, replenished with fresh media and left

another 4 hours. Supernatants were removed and analysed for the levels of IL-1 β , IL-6, TNF- α and MIP-1 α .

2.10 *IN VIVO* MOUSE MODELS OF DISEASE

2.10.1 DSS Model of Colitis

In this model of colitis mice receive a chemical compound, dextran sulphate sodium (DSS) which, when given orally in the drinking water of mice, results in acute and chronic colitis resembling UC. During the acute phase, the mice develop colonic mucosal inflammation with ulcerations, loss to their body weight and bloody diarrhoea. In the chronic stages of disease the mice develop severe infiltration of mononuclear cells and regenerative changes in the epithelium (Melgar et al., 2005).

The DSS colitis model was carried out in collaboration with Silvia Melgar in the Alimentary Pharmabiotic Centre, University College Cork. Isolation of the lamina propria, tissue sectioning and immunohistochemistry was performed by Maja Kristek and Dr Joseph DeCoursey.

On arrival at the Biological Services Unit (BSU) at UCC 25 C57BL/6 female mice were weighed (18-20g). The mice were then split into one control group which contained 6 mice and 4 test groups with 6-8 mice. 3% DSS (Sigma) was prepared fresh daily and added to the drinking water of the mice for 5 days. Early acute, late acute and chronic mice were culled at 7, 12 and 26 days respectively post DSS

treatment for 5 days. Sections of the distal colon were homogenised and total RNA was extracted as described in **Section 2.6.2**.

2.10.2 *CITROBACTER RODENTIUM* Model

Citrobacter rodentium is a gram negative murine specific bacterium that causes a similar pathology in mice to that caused by enteropathogenic *Escherichia coli* in humans. This rare model offers the opportunity for understanding chronic inflammatory responses seen in genetically susceptible IBD patients following abnormal exposure to enteric bacteria of the intestinal mucosal immune system (Bhinder et al. 2013).

The *C. rodentium* colitis model was also carried out in collaboration with Silvia Melgar in the Alimentary Pharmabiotic Centre, University College Cork. On arrival at the Biological Services Unit (BSU) at UCC 25 C57BL/6 female mice were divided into 5 groups of 6-8, one control and 4 infected groups. Mice were inoculated orally by a 200µl gavage of approximately 200×10^9 CFU *C. rodentium*. Mice were culled at 9, 14, 21 and 28 days post infection for tissue processing. Post removal and washing, colons were weighed and measured as an indication of gut inflammation. Sections of the distal colon were homogenised and total RNA was extracted as described in **Section 2.6.2**.

2.11 IMMUNOFLUORESCENCE

In order to investigate the sub-cellular location of STX-3 in JAWSII DCs we employed the use of confocal microscopy. Confocal microscopy has several advantages over conventional optical microscopy, including depth of field control,

elimination of out of focus light and collection of several optical sections to construct a 3-D image. Confocal microscopy is able to achieve this by its arrangement pinholes (at the source of the laser light and at the detection point) to exclude out of focus light not allowing it to reach the photomultiplier (PMT) detector [Figure 2.11].

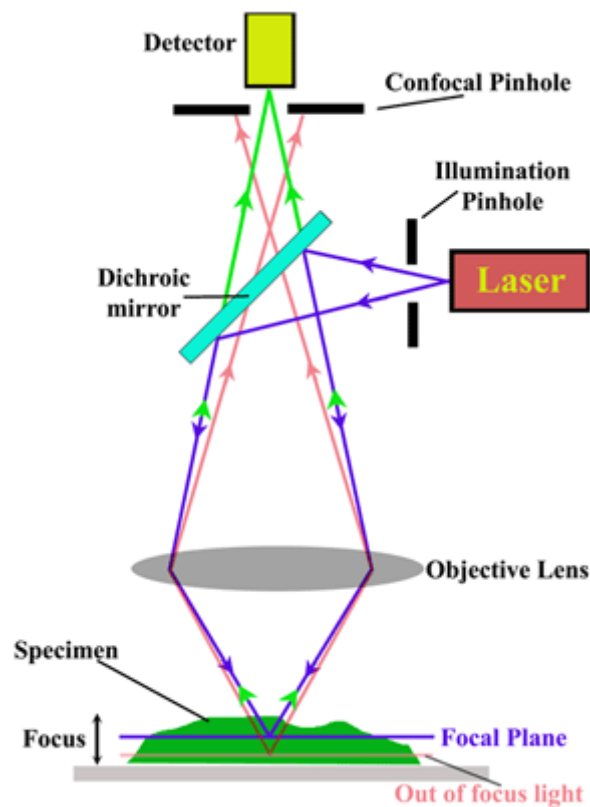


Figure 2.11: Schematic representation of the components of a confocal microscope.

[Taken from www.jic.ac.uk].

2.11.1 Coverslips

0.13-0.16 mm thick coverslips (Harly and Davidson) with a refractive index of 1.5 were placed in 100%EtOH and sterilized through a Bunsen flame. These coverslips were then placed in a 6-well plate and exposed to Ultra-Violet (UV) light for 30minutes. 0.5×10^5 JAWSII DCs were added to the 6-well plate and left over-night

to adhere. Cells were then stimulated with the appropriate TLR ligand for 1 hour. Media was removed and coverslips were washed with 0.2 μ M filtered PBS.

2.11.2 Fixation

1 ml of 3% Paraformaldehyde (PAF) [See Appendix] was added to each well containing coverslips and left on ice for 20minutes. This reaction was then quenched with 50 mM Ammonium Chloride for 5 minutes. Cells were then permeabilised with “perm-block” solution [See Appendix] for 20 minutes.

2.11.3 Intracellular SNARE Staining

The STX3 primary antibody was added to the coverslips and incubated overnight at 4°C. Coverslips were then washed with perm-block solution 3 times and corresponding fluorescently conjugated secondary antibody [Table 2.12] was added to the coverslips and incubated for 1 hour at room temperature. Coverslips were then washed 3 times with perm-block and nucleus stained with PI for 10minutes. Coverslips were then washed again and DAKO (an anti-fading medium) was applied, coverslips inverted onto a slide, left at 4°C for 5 minutes and sealed with nail varnish to avoid drying out. Slides were then viewed using a Zeiss 710 confocal microscope and analysed using LSM software.

2.12 STX11^{-/-} *IN VITRO* STUDY

Wild Type (WT) and STX11^{-/-} mice on a C57BL/6 background were provided by Department of Immunology and Cell Biology, Research Centre Borstel, Germany in collaboration with Silvia Bulfone-Paus and Udo ZurStadt. Mice were used between

10-12 weeks old and maintained in specific pathogen-free conditions at University Medical Centre Hamburg Eppendorf animal facility. BMDCs were generated from WT and STX-11^{-/-} mice as previously described in section 2.3.2. Absence of STX-11 gene from these mice was proven by RT-qPCR [See Appendix].

2.13 STX11^{-/-} BMDC T-CELL CO-CULTURE

2.13.1 Isolation of Splenocytes

Spleens were removed aseptically from female C57BL/6 mice (Charles River) aged 6-12 weeks which were housed in a Specific Pathogen Free (SPF) unit and collected in cRPMI [See Appendix] on ice. The spleens were pressed through a 40 µm cell strainer to achieve a single cell suspension.

2.13.2 CD4⁺ T-Cell Magnetic Particle Isolation

CD4⁺ T cells were isolated according to Stemcell technologies – Easysep[®] Mouse CD4⁺ T-cell isolation (19765) protocol. Splenocytes were prepared at a concentration of 1x10⁶ cells/ml and placed into a 5ml polystyrene falcon tube. 50µl/ml of rat serum and 50µl/ml of antibody cocktail (Easysep[™] mouse CD4⁺ T-cell enrichment cocktail) was added to the splenocytes, mixed and left to incubate at RT for 10 minutes. This cocktail of antibodies target cell surface markers of all the cells excluding T-cells. To isolate CD4⁺ the antibody cocktail consisted of CD8, CD11b, CD11c, CD19, CD24, CD24, CD45r, CD49B, TCRγ/δ and TER119. Easysep[™] streptavidin rapidospheres[™] were vortexed for 30 seconds to ensure they were in a uniform suspension, added to the cell suspension at concentration of 75

$\mu\text{l/ml}$, mixed and left at RT for 2.5 minutes. The total cell suspension was mixed, brought up to 2.5 ml with cRPMI, capped and placed in the Easysep™ magnet for 2.5 minutes at RT. In one sweeping motion the CD4^+ T cells were poured off from the magnet and set aside for **Section 2.13.3**.

2.13.3 Proliferation Analysis using CFSE Dye

To assess T-cell proliferation non-fluorescent carboxyfluorescein diacetate succinimidyl ester (CFDE-SE) was added to the T-cells. This compound contains acetate groups, which are highly permeable and toxic, however when it is added to cells it enters the cytoplasm of the cells and is highly stable. It loses the acetate groups and becomes the fluorescent molecule CFSE, which has an excitation at 494 nm and an emission at 521 nm. When the cell divides, so does the CFSE fluorescence allowing proliferation to be monitored up to 8 generations. CFSE-SE was added at a concentration of $5\mu\text{M}$ in a 5% FBS/PBS solution to buffer the toxic effects of the CD4^+ T cells. Cells were incubated for 5 minutes, then washed twice with 5% FBS/PBS solution and resuspended in cRPMI.

2.13.4 BMDC T-Cell Co-Culture

CD4^+ T-cells were isolated in **section 2.13.2**. $\text{STX11}^{-/-}$ BMDCs were previously isolated [**Section 2.12**] from STX11 deficient mice which were obtained from Silvia Bulfone-Paus group in the Borstel Research Institute, Hamburg Germany. WT and $\text{STX11}^{-/-}$ BMDCs were stimulated with LPS (100 ng/ml) for 4 hours, washed and added to the CD4^+ T-cells (CFSE stained, **Section 2.13.3**) at a 1:100 dilution

respectively onto a α -CD3 coated plate for 72 hours. Cells were scraped and analysed on FACS Aria while supernatants were removed and analysed for the levels of IFN γ , IL-2, IL-4 and TNF $-\alpha$.

2.14 STATISICAL ANALYSIS

The parametric student's T-test was used to determine significant differences between two samples. The level of statistical significance was indicated by * $p \leq 0.05$, ** $p \leq 0.01$ *** $p \leq 0.001$.

One-way analysis of variance (ANOVA) was used to determine significant differences between more than two samples. When this indicated significance ($p \leq 0.05$), post-hoc Student-Newmann-Keul test was used to determine which conditions were significantly different from each other. The level of statistical significance was indicated by * $p \leq 0.05$, ** $p \leq 0.01$ *** $p \leq 0.001$.

Parametric statistical test's were used throughout this study. Sample size was not large enough to test distribution and thus it was assumed the data was normally distributed.

CHAPTER 3

CHARACTERISATION

OF JAWS II

DENDRITIC CELLS

3.1 INTRODUCTION

DCs are innate immune cells, originally identified by Steinman and Cohn which play a critical role in the initiation of the adaptive immune response (Steinman and Cohn 1973). Maturation of DCs, which are antigen presenting cells, by immunogenic agents such as microbes, triggers an immune response. These microbes contain PAMPs which signal through a variety of PRRs, such as toll like receptors TLRs, allowing the DC to present antigen (Blanco et al. 2008). These DCs then activate T cells by presenting the processed antigen to naïve T cells in an immunogenic form. The subsequent activation of these naïve T cells not only requires antigen presentation but also the secretion of immune mediators called cytokines. Different cytokines polarise the naïve T cells into different subsets of T cells. IL-12 drives T helper 1 (T_H1) cell differentiation, IL-4 drives T_H2 phenotype, IL-10 promotes a T regulatory (T_{REG}) and IL-1, IL-6 and IL-23 are associated with T_H17 differentiation (Mills 2011).

These cytokines and others have also been shown to play a role in the pathogenesis of many inflammatory and autoimmune diseases (Taylor and Feldmann 2009). Blockade of TNF- α has been clinically successful in a number of immune mediated pathologies such as rheumatoid arthritis, Crohn's disease and psoriasis, however it is not successful in all patients or autoimmune diseases (Williams, Paleolog and Feldmann 2007). Abolishment of IL-23 by either utilising IL-23 knockout mouse models or subjecting wild-type mice to anti-IL-23 treatment has been shown to render mice resistant to certain inflammatory and autoimmune diseases such as experimental autoimmune encephalitis (EAE), collagen-induced arthritis (CIA) and

inflammatory bowel disease (IBD) (Cua et al. 2003, Murphy et al. 2003, Hue et al. 2006). As DCs act as a link between innate and adaptive immunity and secrete cytokines which are important in inflammatory diseases, investigating how DCs secrete these cytokines may provide us with new therapeutic targets in these diseases.

Mechanisms that control the release of cytokines from different cell have not been well studied in comparison to the numerous studies describing the detailed signalling pathways induced by cytokines. However SNARE family members have been implicated at each step of membrane fusion in intracellular trafficking pathway including that of cytokine release (Stow, Manderson and Murray 2006a). Indeed a novel SNARE complex, STX6 and Vti1b, has been reported to be involved in the secretion of TNF- α in macrophage. STX6 and Vti1b were shown to be up-regulated in parallel with increasing cytokine secretion and have been shown to have rate limiting roles in TNF- α trafficking and secretion. This study indicates the specific role for SNAREs in intracellular trafficking of cytokines secretion (Murray et al. 2005a). Therefore we wanted to examine the role of these proteins in DCs.

In order to investigate the role of SNAREs in DCs we first determined whether we could use a DC cell line. Research in DC biology most commonly uses primary derived DCs, however a cell line would have significant advantages, including the provision of a pure population to study the expression of SNARE proteins in DCs, which could be later validated in primary DCs. There are two types of DC cell lines available; an immortalised DC cell line and a growth factor-dependent DC line (Pinchuk, Lee and Filipov 2007). A DC cell line that closely mimics behaviour *in vivo* is preferred and which can also be easily matured *in vitro*. (Girolomoni et al.

1995) Thus in this study we chose JAWS II, a C57BL/6 immature DC line, derived from p53^{-/-} mice, which is grown in the presence of the differentiating factor GM-CSF. JAWSII DCs have previously been reported to be able to be matured and subsequently have T-cell stimulatory abilities (MacKay and Moore, 1997).

JAWS II, a C57BL/6 murine DC line, was used in this study. Previously JAWS II DCs have been used for immunobiological studies of *Chlamydia muridarum* (Jiang et al. 2008), to examine the expression of nicotinic acetylcholine receptor during cell maturation (Kondo et al. 2010), to assess the role of CD40 in activation of naïve T cells (Haase, Michelsen and Jorgensen 2004), to assess the transduction of IL-12 genes (Pajtasz-Piasecka et al. 2007) and the genetic modification to express immunomodulatory molecule CTLA4Ig to prolong antigen-specific skin graft survival (Ierino et al. 2010). The latter studies indicate this cell line as an attractive option for *in vitro* studies of intracellular pathways through RNA interference (RNAi).

The objective of this chapter was to examine the cytokine and chemokine profile of the JAWS II DC in response to a panel of TLR ligands in order to characterise the cell line.

3.2 RESULTS

3.2.1 THE DOSES OF THE TLR LIGANDS USED ON JAWSII DCS HAVE NO SIGNIFICANT EFFECT ON CELL VIABILITY

To compare the cytokine production and surface marker expression from JAWS II DCs following stimulation with a panel of TLR ligands, we firstly had to examine the potential toxicity of the ligands to the cells by exposing them to the JAWS II DCs. Following stimulation with 5 µg/ml peptidoglycan (PGN), 10 µg/ml Polyinosinic-polycytidylic acid (Poly (I:C)), 100 ng/ml Lipopolysaccharide (LPS) (*E. coli* serotype R515), 5 µg/ml Flagellin, 10 µg/ml Zymozan, 1 mM Loxoribine or 2 µM CpG oligodeoxynucleotides (CpG ODN) for 24 h, the cell viability was assessed using Cell Titer 96 Aqueous One Solution (Promega, WI, USA) according to the manufacturer's instructions. These doses did not exhibit any significant cytotoxic effect on JAWS II DCs *in vitro* and thus were used at these concentrations for all subsequent experiments [Figure 3.1].

3.2.2 JAWSII DCS TIME DEPENDENTLY SECRETE PRO-INFLAMMATORY CYTOKINES IN RESPONSE TO THE TLR4 LIGAND, LIPOPOLYSACCHARIDE (LPS)

JAWS II DCs were cultured for seven days in the presence of murine recombinant GM-CSF (r-GM-CSF) (Sigma ®) and plated at 1×10^6 cell/ml. Cells were then stimulated with 100 ng/ml LPS (*E. coli* serotype R515) for 1 h, 2 h, 4 h, 6 h, 12 h and 24 h time-points. Supernatants were removed and analysed for the levels of IL-

1 β , IL-6, TNF- α and IL-27p28 [Figure 3.2] using specific immunoassays. A time dependent secretion of the pro-inflammatory cytokines IL-1 β , IL-6, TNF- α and IL-27p28 was observed [Figure 3.2]. All the cytokines examined were secreted at significant levels at 24 h ($p \leq 0.01$, $p \leq 0.001$), this was the time point used for subsequent experiments.

3.2.3 COMPARISON OF CYTOKINE AND CHEMOKINE SECRETION FROM JAWSII DCS AND BMDCS FOLLOWING ACTIVATION WITH THE TLR2 LIGAND, PEPTIDOGLYCAN (PGN)

In order to characterise JAWS II DCs we compared them to well characterised Bone Marrow Dendritic Cells (BMDCs) following activation with a panel of TLR ligands. BMDCs harvested from C57BL/6 mice and JAWS II DCs were cultured for seven days in the presence of r-GM-CSF (Sigma ®) and plated at 1×10^6 cell/ml. Cells were then stimulated with 5 μ g/ml PGN for 24h. Supernatants were removed and analysed for the levels of, IL-12p40, IL-12p70, IL-23, IL-27p28 [Figure 3.3], IL-1 β , IL-6, IL-10, TNF- α [Figure 3.4], Macrophage inflammatory protein- α (MIP-1 α) and MIP-2 [Figure 3.5] using specific immunoassays.

Activation of BMDCs with PGN resulted in significant levels of IL-12p40 ($p \leq 0.01$) and high levels of IL-12p40, IL-23 and IL-27 (not statistically significant), however these cytokines were not secreted by JAWS II DCs when stimulated with PGN [Figure 3.3]. BMDCs significantly increased secretion of IL-6 and TNF- α ($p \leq 0.05$, $p \leq 0.01$) and produced high levels of IL-1 β and IL-10 (not statistically significant) in response to PGN. JAWSII DCs also significantly increased secretion of IL-6 and TNF- α ($p \leq 0.01$, $p \leq 0.001$) and high levels of IL-10 in response to PGN (not

statistically significant) however the levels were lower than BMDCs [Figure 3.4]. PGN stimulation induced significant secretion of MIP-2 from both BMDCs and JAWSII DCs ($p \leq 0.01$) and induced significant secretion of MIP-1 α from JAWSII DCs ($p \leq 0.01$) with small levels from BMDCs [Figure 3.5].

3.2.4 COMPARISON OF CYTOKINE AND CHEMOKINE SECRETION FROM JAWSII DCS AND BMDCS FOLLOWING ACTIVATION WITH THE TLR3 LIGAND, POLYINOSINIC-POLYCYTIDYLIC ACID (POLY (I:C))

BMDCs harvested from C57BL/6 mice and JAWS II DCs were cultured for seven days in the presence of r-GM-CSF (Sigma ®) and plated at 1×10^6 cell/ml. Cells were then stimulated with 10 μ g/ml Poly (I:C) for 24h. Supernatants were removed and analysed for the levels of, IL-12p40, IL-12p70, IL-23, IL-27p28 [Figure 3.6], IL-1 β , IL-6, IL-10, TNF- α [Figure 3.7], MIP-1 α and MIP-2 [Figure 3.8] using specific immunoassays.

As with TLR2 stimulation, TLR3 stimulation did not induce any secretion of IL-12p40, IL-12p70 or IL-23 from JAWS II DCs with only a low level of significant IL-27 secretion ($p \leq 0.001$) whereas BMDCs in response to TLR3 stimulation secreted significant levels IL-12p40 and IL-27p28 ($p \leq 0.05$, $p \leq 0.001$) and high levels of IL-12p70 and IL-23 [Figure 3.6]. Poly (I:C) stimulation induced significant levels of IL-6 and TNF- α ($p \leq 0.01$, $p \leq 0.05$, $p \leq 0.001$) high levels of IL-10 compared to control from both JAWSII DCs and BMDCs, IL-1 β was secreted at low levels in response to PGN in BMDCs and was not induced in JAWSII DCs [Figure

3.7]. MIP-1 α and MIP-2 were significantly secreted from JAWSII DCs in response to PGN ($p \leq 0.05$). There was significant secretion of MIP-1 α ($p \leq 0.05$) and a higher amount of MIP-2 (not statistically significant) in BMDCs in response to PGN however levels were much lower than JAWSII DCs [**Figure 3.8**].

3.2.5 COMPARISON OF CYTOKINE AND CHEMOKINE SECRETION FROM JAWSII DCS AND BMDCS FOLLOWING ACTIVATION WITH THE TLR4 LIGAND, LIPOPOLYSACCHARIDE (LPS)

BMDCs harvested from C57BL/6 mice and JAWS II DCs were cultured for seven days in the presence of r-GM-CSF (Sigma ®) and plated at 1×10^6 cell/ml. Cells were then stimulated with 100 ng/ml LPS (*E. coli* serotype R515) for 24h. Supernatants were removed and analysed for the levels of, IL-12p40, IL-12p70, IL-23, IL-27p28 [**Figure 3.9**], IL-1 β , IL-6, IL-10, TNF- α [**Figure 3.10**], MIP-1 α and MIP-2 [**Figure 3.11**] using specific immunoassays.

BMDCs secreted significant levels of IL-12p40, IL-23 and IL-27p28 ($p \leq 0.001$, $p \leq 0.01$) and high levels of IL-12p70 in response to LPS stimulation compared to undetectable secretion levels of IL-12p40, IL-12p70 or IL-23 and only low levels of IL-27p28 ($p \leq 0.001$) from JAWS II DCs [**Figure 3.9**].

IL-1 β was significantly secreted by JAWS II DCs and BMDCs following LPS stimulation ($p \leq 0.05$, $p \leq 0.01$) however at higher levels from JAWSII DCs. IL-6, IL-10 and TNF- α were all significantly secreted by JAWS II DCs and BMDCs

following LPS stimulation at comparable levels ($p \leq 0.001$, $p \leq 0.05$, $p \leq 0.01$) [Figure 3.10]. TLR4 activation promoted significant secretion of MIP-1 α and MIP-2 from JAWS II DCs and BMDCs however at higher levels from JAWSII DCs ($p \leq 0.001$) [Figure 3.11].

3.2.6 COMPARISON OF CYTOKINE AND CHEMOKINE SECRETION FROM JAWSII DCS AND BMDCS FOLLOWING ACTIVATION WITH THE TLR5 LIGAND, FLAGELLIN

BMDCs harvested from C57BL/6 mice and JAWS II DCs were cultured for seven days in the presence of r-GM-CSF (Sigma ®) and plated at 1×10^6 cell/ml. Cells were then stimulated with 5 μ g/ml of Flagellin for 24h. Supernatants were removed and analysed for the levels of, IL-12p40, IL-12p70, IL-23, IL-27p28 [Figure 3.12], IL-1 β , IL-6, TNF- α , IL-27p28 [Figure 3.13], MIP-1 α and MIP-2 [Figure 3.14] using specific immunoassays.

Stimulation with the TLR5 agonist resulted in a low level of significant secretion of IL-27p28 by JAWS II DCs but no secretion of IL-12p40, IL-12p70 or IL-23 ($p \leq 0.01$). BMDCs secreted significant levels IL-12p40 ($p \leq 0.01$) and high levels of IL-12p70 (not statistically significant) and not IL-23 and IL-27p28 in response to Flagellin [Figure 3.12]. BMDCs produced low levels of IL-1 β , IL-6, IL-10 and TNF- α , however secretion was not up-regulated in response to Flagellin. JAWSII DCs however did significantly secrete IL-10 and TNF- α ($p \leq 0.05$) and high levels of IL-6 (not statistically significant) in response to TLR5 activation [Figure 3.13]. MIP-1 α secretion was only detected in TLR5 stimulated JAWS II DCs. Although

MIP-2 secretion was higher in JAWS II DCs than BMDCs it was not induced by Flagellin stimulation whereas it was significantly secreted from BMDCs ($p \leq 0.01$) [Figure 3.14].

3.2.7 COMPARISON OF CYTOKINE AND CHEMOKINE SECRETION FROM JAWSII DCS AND BMDCS FOLLOWING ACTIVATION WITH THE TLR7 LIGAND, LOXORIBINE

BMDCs harvested from C57BL/6 mice and JAWS II DCs were cultured for seven days in the presence of r-GM-CSF (Sigma ®) and plated at 1×10^6 cell/ml. Cells were then stimulated with 1 mM Loxoribine for 24 h. Supernatants were removed and analysed for the levels of, IL-12p40, IL-12p70, IL-23, IL-27p28 [Figure 3.15], IL-1 β , IL-6, IL-10, TNF- α [Figure 3.16], MIP-1 α and MIP-2 [Figure 3.17] using specific immunoassays.

Stimulation using the TLR7 ligand resulted in no secretion of IL-12p70 and IL-23 and low significant levels of IL-12p40 and IL-27 in JAWS II DCs ($p \leq 0.001$). BMDCs secreted significant levels of IL-12p40 and IL-27 but not IL-23 ($p \leq 0.05$, $p \leq 0.01$) in response to Loxoribine. IL-12p70 was secreted by BMDCs but not induced following TLR activation [Figure 3.15]. IL-1 β , IL-6, IL-10 and TNF- α secretion was significantly secreted from both JAWS II DCs and BMDCs following Loxoribine stimulation ($p \leq 0.05$, $p \leq 0.01$, $p \leq 0.001$), however at higher levels in the JAWS II DCs [Figure 3.16]. There was significant secretion of MIP-1 α and MIP-2 in response to Loxoribine from JAWSII DCs and BMDCs with higher levels from JAWS II DCs compared to BMDCs ($p \leq 0.001$, $p \leq 0.01$) [Figure 3.17].

3.2.8 COMPARISON OF CYTOKINE AND CHEMOKINE SECRETION FROM JAWSII DCS AND BMDCS FOLLOWING ACTIVATION WITH THE TLR9 LIGAND, CPG OLIGODEOXYNUCLEOTIDES (CPG ODN)

BMDCs harvested from C57BL/6 mice and JAWS II DCs were cultured for seven days in the presence of r-GM-CSF (Sigma ®) and plated at 1×10^6 cell/ml. Cells were then stimulated with 2 μ M CpG oligodeoxynucleotides (CpG ODN) for 24h. Supernatants were removed and analysed for the levels of, IL-12p40, IL-12p70, IL-23, IL-27p28 [Figure 3.18], IL-1 β , IL-6, IL-10, TNF- α [Figure 3.19] MIP-1 α and MIP-2 [Figure 3.20] using specific immunoassays.

BMDCs secreted significant levels of IL-12p40, IL-23 and IL-27 ($p \leq 0.01$, $p \leq 0.001$) with high levels of IL-12p70 (not statistically significant) in response to CpG stimulation. JAWSII DCs also secreted significant levels of IL-12p40 and IL-27p28 ($p \leq 0.01$) in response to CpG but at much lower amounts compared to BMDCS and did not secrete any IL-12p70 or IL-23 [Figure 3.18]. IL-6, IL-10 and TNF- α were all significantly secreted from BMDCs in response to CpG stimulation ($p \leq 0.05$, $p \leq 0.001$, $p \leq 0.01$) however at smaller levels from JAWSII DCs. IL-1 β was secreted from JAWSII DCs and BMDCs however its expression was not induced upon CpG stimulation [Figure 3.19]. Secretion of MIP-1 α and MIP-2 was significantly secreted from BMDCs following CpG stimulation ($p \leq 0.001$, $p \leq 0.01$). MIP-1 α was not secreted from JAWSII DC and MIP-2 was secreted however was not induced by CpG stimulation [Figure 3.20].

3.2.9 COMPARISON OF CELL SURFACE MARKER EXPRESSION ON JAWSII DCS AND BMDCs FOLLOWING ACTIVATION WITH THE TLR2 LIGAND, PEPTIDOGLYCAN (PGN)

BMDCs harvested from C57BL/6 mice and JAWS II DCs were cultured for seven days in the presence of r-GM-CSF (Sigma ®) and plated at 1×10^6 cell/ml. Cells were then stimulated with $5\mu\text{g/ml}$ PGN for 24h. Cells were subsequently washed and stained with fluorochrome-labelled monoclonal antibodies to the cell surface markers, TLR-4-MD-2, TLR-2, CD14 [Figure 3.21], CD40, CD80, CD86, and MHC II [Figure 3.22] in preparation for cytometric analysis by flow cytometry. MFI values are shown stimulated versus control cells.

Activation of TLR2 resulted in small increases of expression of TLR4-MD-2 (MFI JAWS 238 v 196, MFI BMDCs 3430 v 3416), TLR2 (MFI JAWS 586 v 534, MFI BMDCs 3340 v 2596) and CD14 (MFI JAWS 808 v 582, MFI BMDCs 17100 v 3970), in both JAWS II DCs and BMDCs [Figure 3.21]. Expression of CD80 (MFI JAWS 662 v 612, MFI BMDCs 16900 v 10900) and MHC II (MFI JAWS 424 v 365, MFI BMDCs 48500 v 37600), were up-regulated in both JAWS II DCs and BMDCs but at smaller levels in JAWSII DCs [Figure 3.22]. CD40 (MFI BMDCs 7311 v 2121) and CD86 (MFI BMDCs 16900 v 10900), were up-regulated in BMDCs in response to TLR2 stimulation but not present in JAWSII DCs [Figure 3.22]. Summarised in Table 3.1 and Table 3.2.

3.2.10 COMPARISON OF CELL SURFACE MARKER EXPRESSION ON JAWSII DCS AND BMDCs FOLLOWING ACTIVATION WITH THE TLR3 LIGAND, POLYINOSINIC-POLYCYTIDYLIC (POLY (I:C))

BMDCs harvested from C57BL/6 mice and JAWS II DCs were cultured for seven days in the presence of r-GM-CSF (Sigma ®) and plated at 1×10^6 cell/ml. Cells were then stimulated with 10 µg/ml Poly (I:C) for 24 hours. Cells were subsequently washed and stained with fluorochrome-labelled monoclonal antibodies to the cell surface markers, TLR-4-MD-2, TLR-2, CD14, [Figure 3.23] CD40, CD80, CD86, and MHC II [Figure 3.24] in preparation for cytometric analysis by flow cytometry.

Expression of TLR-2 (MFI JAWS 768 v 534, MFI BMDCs 2980 v 2596) was slightly up-regulated in JAWS II DCs and BMDCs in response to the TLR3 ligand. TLR-4-MD-2 (MFI JAWS 269 v 196, MFI BMDCs 3338 v 3416) and CD14 (MFI JAWS 693 v 582, MFI BMDCs 3928 v 3970) were up-regulated in JAWS II DCs and down-regulated in BMDCs in response to PGN [Figure 3.23]. There was increased expression of MHC II in JAWS II DCs and BMDCs. CD40 (MFI BMDCs 5103 v 2121), CD80 (MFI BMDCs 15500 v 10900) and CD86 (MFI BMDCs 4452 v 3504), remained unchanged in JAWS II DCs however was up-regulated in BMDCs following PGN stimulation. [Figure 3.24]. Summarised in Table 3.1 and Table 3.2.

3.2.11 COMPARISON OF CELL SURFACE MARKER EXPRESSION ON JAWSII DCS AND BMDCs FOLLOWING ACTIVATION WITH THE TLR4 LIGAND, LIPOPOLYSACCHARIDE (LPS)

BMDCs harvested from C57BL/6 mice and JAWS II DCs were cultured for seven days in the presence of r-GM-CSF (Sigma ®) and plated at 1×10^6 cell/ml. Cells were then stimulated with 100 ng/ml LPS (*E.coli* serotype R515) for 24h. Cells were subsequently washed and stained with fluorochrome-labelled monoclonal antibodies to the cell surface markers, TLR-4-MD-2, TLR-2, CD14 [Figure 3.25], CD40, CD80, CD86, and MHC II [Figure 3.26] in preparation for cytometric analysis by flow cytometry.

Ligation of the TLR4 agonist LPS resulted in up-regulation of TLR2 (MFI JAWS 1016 v 511, MFI BMDCs 3313 v 3040) and CD14 (MFI JAWS 1511 v 724, MFI BMDCs 12000 v 4930) expression in JAWS II DCs and BMDCs. TLR-4-MD-2 (MFI JAWS 254 v 509, MFI BMDCs 1603 v 1285) was down-regulated in JAWS II DCs and an up-regulation in BMDCs following LPS stimulation [Figure 3.25]. CD40 (MFI BMDCs 10400 v 1276), CD80 (MFI JAWS 766 v 655, MFI BMDCs 18900 v 8270), CD86 (MFI JAWS 187 v 121, MFI BMDCs 4282 v 1891) and MHC II (MFI JAWS 727 v 343, MFI BMDCs 23800 v 15500) expression were all highly up-regulated in BMDCs however this was seen to a lesser extent in JAWS II DCs, with again no expression of CD40 in response to LPS [Figure 3.26]. Summarised in Table 3.1 and Table 3.2.

3.2.12 COMPARISON OF CELL SURFACE MARKER EXPRESSION ON JAWSII DCS AND BMDCS FOLLOWING ACTIVATION WITH THE TLR5 LIGAND, FLAGELLIN

BMDCs harvested from C57BL/6 mice and JAWS II DCs were cultured for seven days in the presence of r-GM-CSF (Sigma ®) and plated at 1×10^6 cell/ml. Cells were then stimulated with 5 µg/ml of Flagellin for 24 h. Cells were subsequently washed and stained with fluorochrome-labelled monoclonal antibodies to the cell surface markers, TLR-4-MD-2, TLR-2, CD14, [Figure 3.27] CD40, CD80, CD86, and MHC II [Figure 3.28] in preparation for cytometric analysis by flow cytometry.

Activation of TLR5 in JAWS II DCs resulted in no change of expression of TLR2, CD14 and a small up-regulation in TLR4 (MFI JAWS 263 v 196) however in BMDCs there was an up-regulation of TLR2 (MFI BMDC 4472 v 3040), CD14 (MFI BMDC 10700 v 4930) and TLR4 (MFI BMDC 1481 v 1285) following Flagellin stimulation [Figure 3.27]. There was no change in expression of CD80, CD86 and MHC II following activation of TLR5 in JAWS II DCs and once again there was no expression of CD40. Expression of CD80 (MFI BMDC 13500 v 8270), CD86 (MFI BMDC 2665 v 1891), MHC II (MFI BMDC 20200 v 15500) and CD40 (MFI BMDC 3042 v 1276) were all up-regulated in BMDCs. [Figure 3.28]. Summarised in Table 3.1 and Table 3.2.

3.2.13 COMPARISON OF CELL SURFACE MARKER EXPRESSION ON JAWSII DCS AND BMDCS FOLLOWING ACTIVATION WITH THE TLR7 LIGAND, LOXORIBINE

BMDCs harvested from C57BL/6 mice and JAWS II DCs were cultured for seven days in the presence of r-GM-CSF (Sigma ®) and plated at 1×10^6 cell/ml. Cells were then stimulated with 1 mM Loxoribine for 24 h. Cells were subsequently washed and stained with fluorochrome-labelled monoclonal antibodies to the cell surface markers, TLR-4-MD-2, TLR-2, CD14 [Figure 3.29], CD40, CD80, CD86, and MHC II [Figure 3.30] in preparation for cytometric analysis by flow cytometry.

Activation of TLR7 resulted in a similar response in JAWS II DCs and BMDCs with the up-regulation TLR-4-MD-2 (MFI JAWS 265 v 196, MFI BMDCs 3069 v 1174), TLR-2 (MFI JAWS 708 v 534, MFI BMDCs 6185 v 3040) and CD14 (MFI JAWS 2286 v 582, MFI BMDCs 28500 v 4930) [Figure 3.29]. Expression of CD80 (MFI JAWS 985 v 612, MFI BMDCs 16900 v 8270) and MHC II (MFI JAWS 814 v 365, MFI BMDCs 27400 v 3040) were also up-regulated JAWSII DCs and BMDCs following Loxoribine stimulation. There was an upregulation of the markers CD40 (MFI BMDCs 11200 v 1276) and CD86 (MFI BMDCs 3625 v 1891) in BMDCs but not in JAWSII DCs. [Figure 3.30]. Summarised in Table 3.1 and Table 3.2.

3.2.14 COMPARISON OF CELL SURFACE MARKER EXPRESSION ON JAWSII DCS AND BMDCS FOLLOWING ACTIVATION WITH THE TLR9 LIGAND, CPG OLOGODEOXYNUCLEOTIDES (CPG ODN)

BMDCs harvested from C57BL/6 mice and JAWS II DCs were cultured for seven days in the presence of r-GM-CSF (Sigma ®) and plated at 1×10^6 cell/ml. Cells were then stimulated with 2 μ M of CpG oligodeoxynucleotides for 24 h. Cells were

subsequently washed and stained with fluorochrome-labelled monoclonal antibodies to the cell surface markers, TLR-4-MD-2, TLR-2, CD14 [Figure 3.31], CD40, CD80, CD86, and MHC II [Figure 3.32] in preparation for cytometric analysis by flow cytometry.

Stimulation with CpG in BMDCs resulted in the up-regulation of the surface marker expression of TLR-4-MD-2 (MFI BMDCs 3720 v 3416), TLR2 (MFI BMDCs 2709 v 2596) and CD14 (MFI BMDCs 6620 v 3971) however there was no up-regulation of these markers in JAWSII DCs [Figure 3.31]. Expression in BMDCs of CD40 (MFI BMDCs 7544 v 2121), CD80 (MFI BMDCs 7544 v 2121), CD86 (MFI BMDCs 4294 v 3504) and MHC II (MFI BMDCs 34300 v 16800) were all upregulated in response to CpG stimulation. JAWS II DCs did not upregulate CD80 and MHC II following CpG stimulation and there was no expression of CD40 or CD86 in control or CpG stimulated JAWSII DCs. [Figure 3.32]. Summarised in Table 3.1 and Table 3.2.

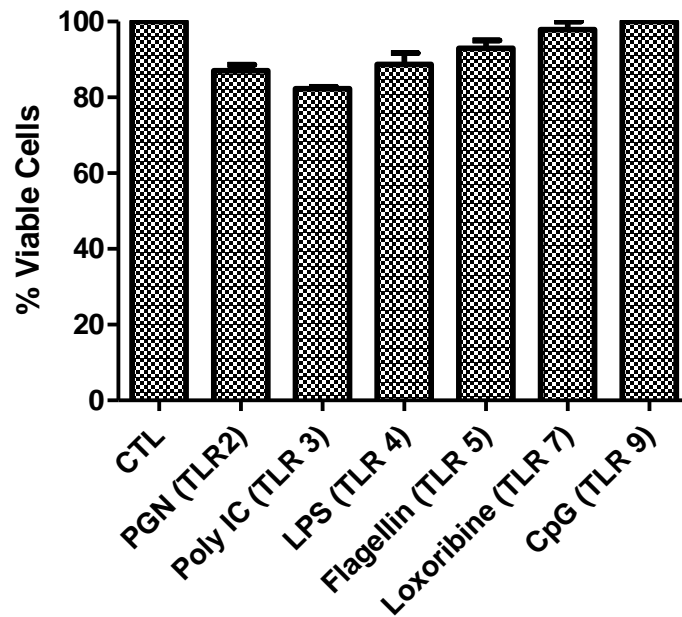


FIGURE 3.1: The concentrations of TLR ligands do not significantly affect the viability JAWS II DCs. JAWS II DCs were plated at 1×10^5 cells/well overnight and then treated $5 \mu\text{g/ml}$ peptidoglycan (PGN), $10 \mu\text{g/ml}$ Polyinosinic-polycytidylic acid (Poly (I:C)), 100ng/ml Lipopolysaccharide (LPS) (*E. coli* serotype R515), $5 \mu\text{g/ml}$ Flagellin, 1mM Loxoribine or $2 \mu\text{M}$ CpG oligodeoxynucleotides (CpG ODN). Following 24 hr treatment cellular viability was assessed using an [3-(4,5-dimethylthiazol-2-yl)-5-(3-carboxymethoxyphenyl)-2-(4-sulfophenyl)-2H-tetrazolium inner salt (MTS) assay (Cell Titer 96 Aqueous One Solution – Promega, WI, USA). Results are expressed as a percentage of untreated cells. Results are mean \pm SEM of quadruplicate assays and represent three independent experiments.

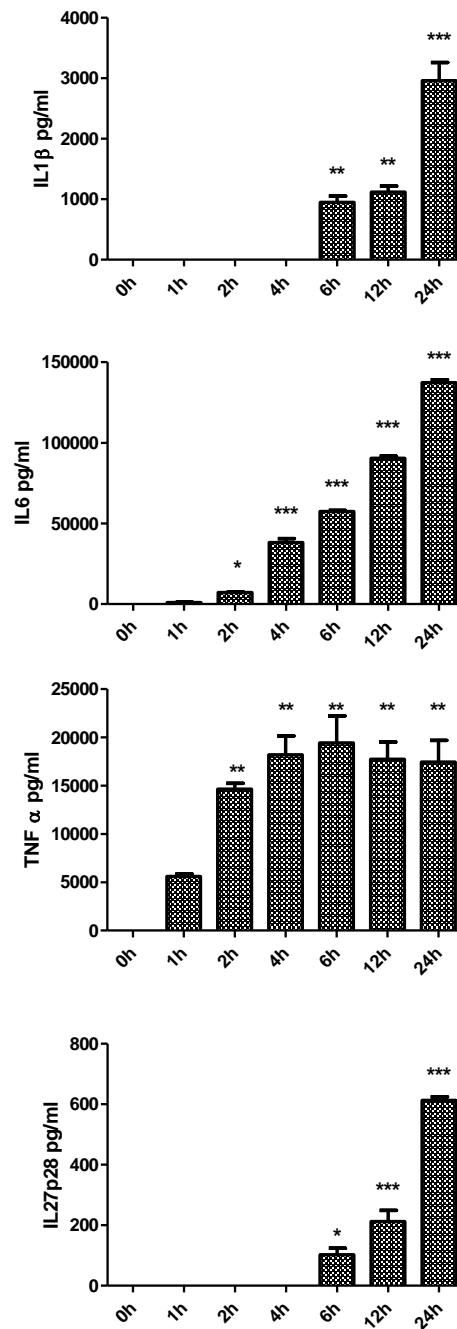


FIGURE 3.2: The secretion of pro-inflammatory cytokines (IL-1 β , IL-6, TNF- α and IL-27p28) from JAWS II DCs in response to a time course of LPS. DCs were cultured in r-GM-CSF for seven days. Cells were plated at (1×10^6 cells/ml) and left to rest overnight. Cells were then stimulated *in vitro* with LPS (100 ng/ml) and supernatants recovered after 24h. Levels of pro-inflammatory cytokines were measured using specific immunoassays. Results are mean \pm SEM of quadruplicate assays and represent three independent experiments. *** $p \leq 0.001$, ** $p \leq 0.01$, * $p \leq 0.05$ comparing CTL vs 1 h, 2 h, 4 h, 6 h, 12 h and 24 h groups as determined by one-way ANOVA test.

TLR 2

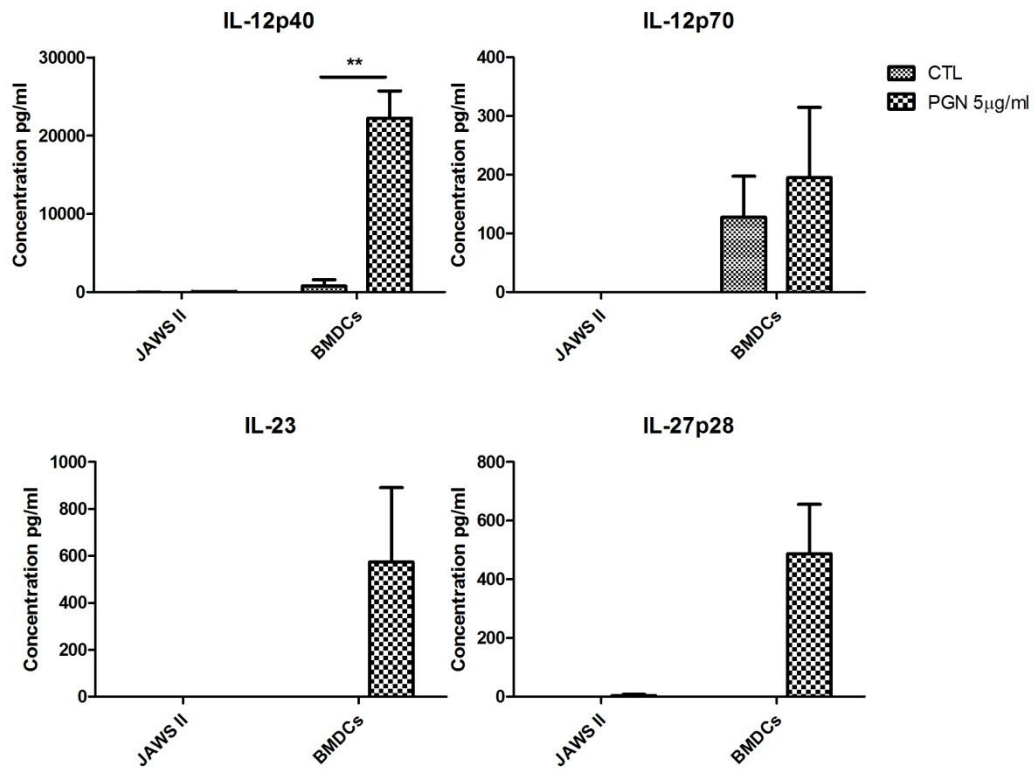


FIGURE 3.3: Comparison of cytokine secretion from JAWS II DCs and BMDCs following TLR2 activation. DCs were cultured in r-GM-CSF for seven days and subsequently were plated (1×10^6 cells/ml) and left to rest overnight. Cells were then stimulated with 5 µg/ml PGN and supernatants were recovered after 24 h and assessed for levels of cytokines using specific immunoassays. Results are \pm SEM of quadruplicate assays and represent three independent experiments. $**p \leq 0.01$ comparing control versus 5µg/ml PGN stimulated JAWSII DCs or BMDCs as determined by a two-tailed t-test.

TLR 2

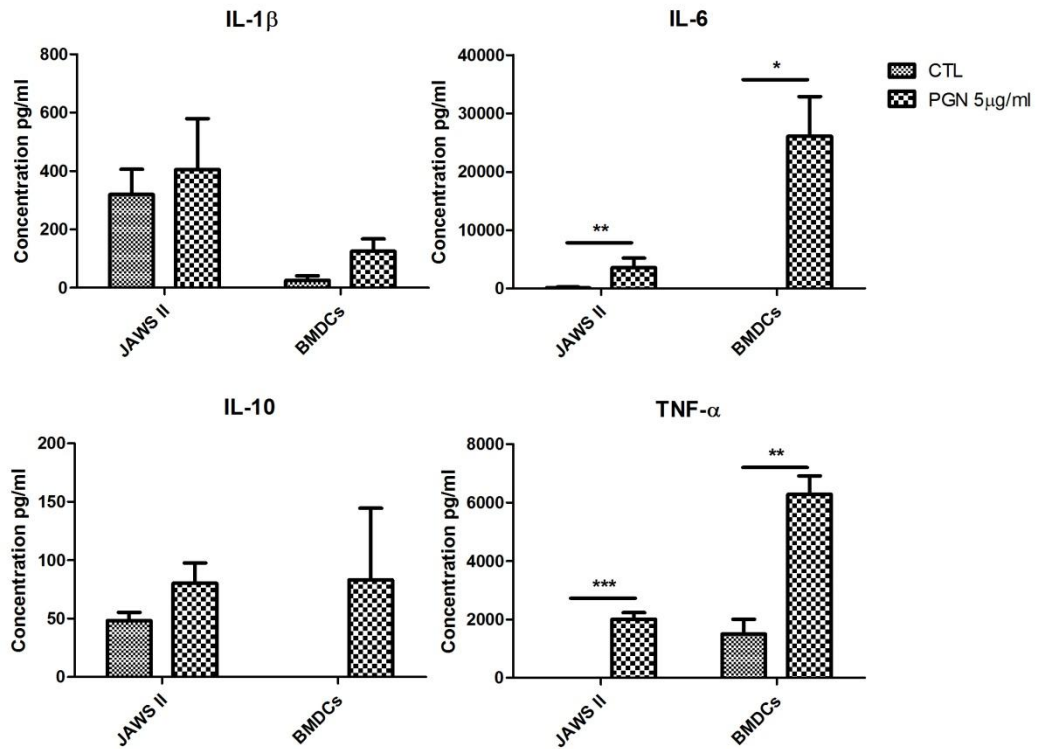


FIGURE 3.4: Comparison of cytokine secretion from JAWS II DCs and BMDCs following TLR2 activation. DCs were cultured in r-GM-CSF for seven days and subsequently were plated (1×10^6 cells/ml) and left to rest overnight. Cells were then stimulated with 5 μ g/ml PGN and supernatants were recovered after 24 h and assessed for levels of cytokines using specific immunoassays. Results are \pm SEM of quadruplicate assays and represent three independent experiments. * $p \leq 0.05$, ** $p \leq 0.01$ and *** $p \leq 0.001$ comparing control versus 5 μ g/ml PGN stimulated JAWSII DCs or BMDCs as determined by a two-tailed t-test.

TLR 2

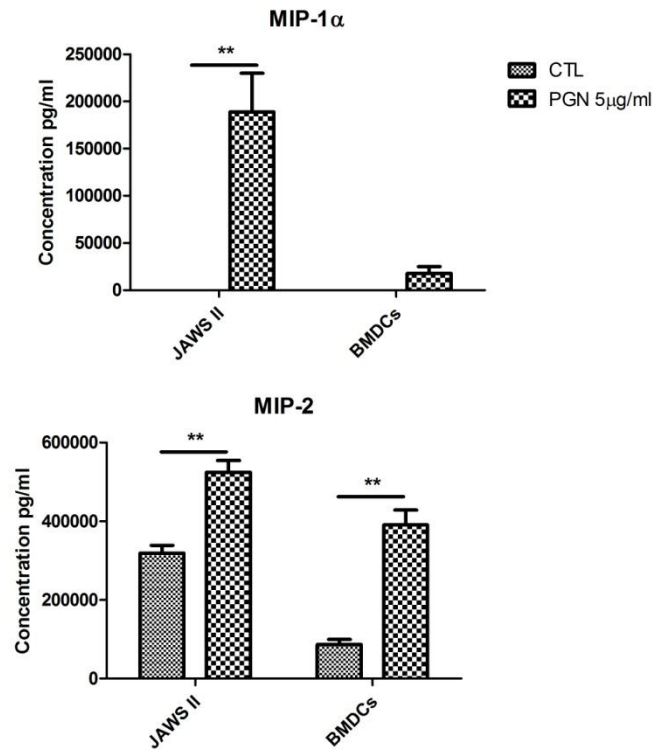


FIGURE 3.5: Comparison of chemokine secretion from JAWS II DCs and BMDCs following TLR2 activation. DCs were cultured in r-GM-CSF for seven days and subsequently were plated (1×10^6 cells/ml) and left to rest overnight. Cells were then stimulated with 5 $\mu\text{g/ml}$ PGN and supernatants were recovered after 24 h and assessed for levels of chemokines using specific immunoassays. Results are \pm SEM of quadruplicate assays and represent three independent experiments. $**p \leq 0.01$ comparing control versus 5 $\mu\text{g/ml}$ PGN stimulated JAWSII DCs or BMDCs as determined by a two-tailed t-test.

TLR3

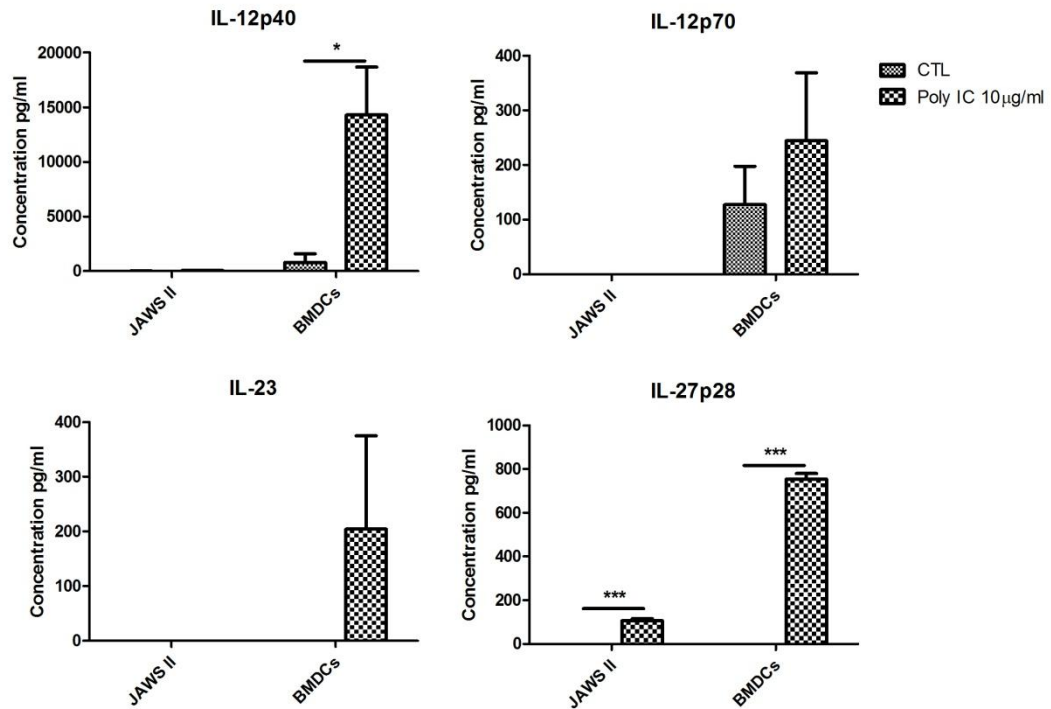


FIGURE 3.6: Comparison of cytokine secretion from JAWS II DCs and BMDCs following TLR3 activation. DCs were cultured in r-GM-CSF for seven days and subsequently were plated (1×10^6 cells/ml) and left to rest overnight. Cells were then stimulated with 10 µg/ml Poly (I:C) and supernatants were recovered after 24 h and assessed for levels of cytokines using specific immunoassays. Results are \pm SEM of quadruplicate assays and represent three independent experiments. * $p \leq 0.05$, and *** $p \leq 0.001$ comparing control versus 10 µg/ml Poly IC stimulated JAWSII DCs or BMDCs as determined by a two-tailed t-test.

TLR3

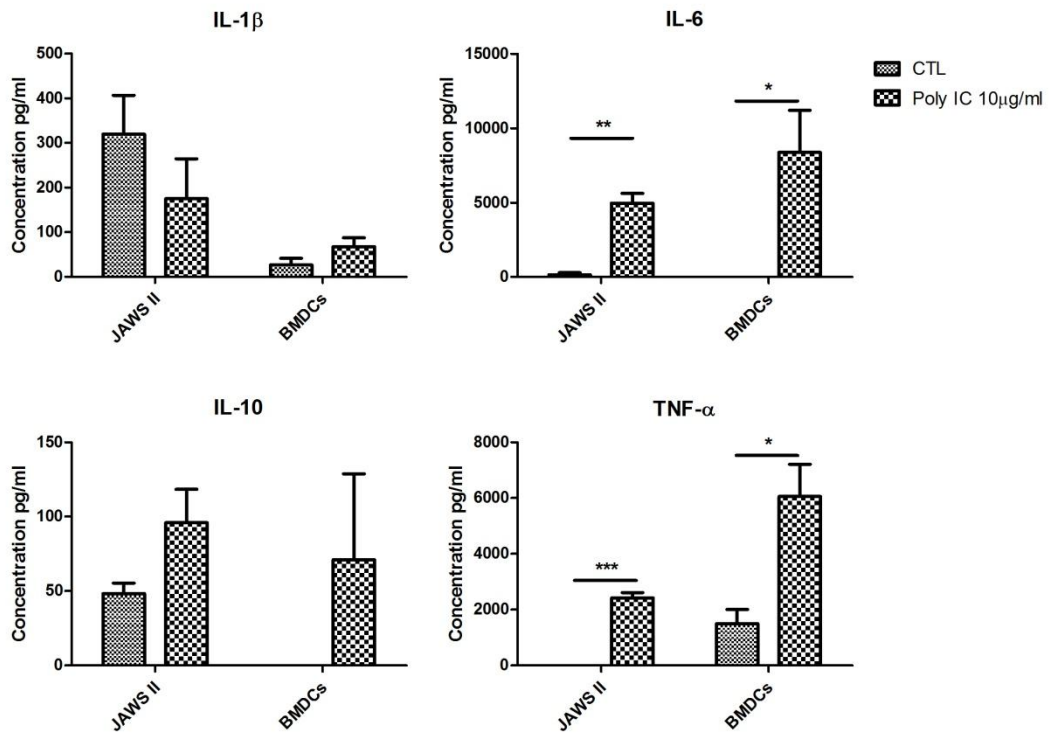


FIGURE 3.7: Comparison of cytokine secretion from JAWS II DCs and BMDCs following TLR3 activation. DCs were cultured in r-GM-CSF for seven days and subsequently were plated (1×10^6 cells/ml) and left to rest overnight. Cells were then stimulated with 10 μ g/ml Poly (I:C) and supernatants were recovered after 24 h and assessed for levels of cytokines using specific immunoassays. Results are \pm SEM of quadruplicate assays and represent three independent experiments. * $p \leq 0.05$, ** $p \leq 0.01$ and *** $p \leq 0.001$ comparing control versus 10 μ g/ml Poly IC stimulated JAWSII DCs or BMDCs as determined by a two-tailed t-test.

TLR3

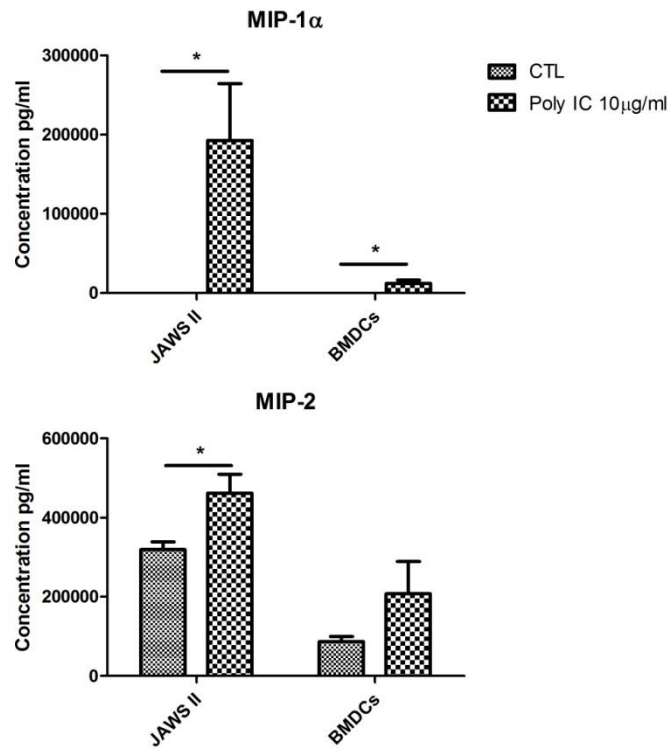


FIGURE 3.8: Comparison of chemokine secretion from JAWS II DCs and BMDCs following TLR3 activation. DCs were cultured in r-GM-CSF for seven days and subsequently were plated (1×10^6 cells/ml) and left to rest overnight. Cells were then stimulated with 10 μ g/ml Poly (I:C) and supernatants were recovered after 24 h and assessed for levels of chemokines using specific immunoassays. Results are \pm SEM of quadruplicate assays and represent three independent experiments. * $p \leq 0.05$ comparing control versus 10 μ g/ml PGN stimulated JAWSII DCs or BMDCs as determined by a two-tailed t-test.

TLR4

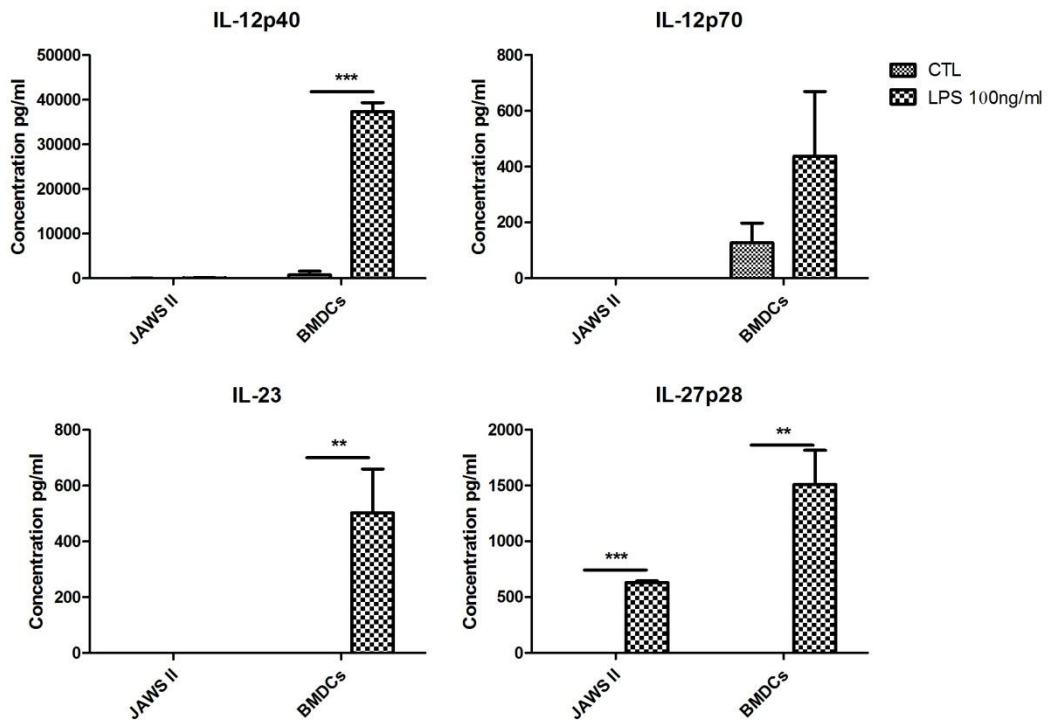


FIGURE 3.9: Comparison of cytokine secretion from JAWS II DCs and BMDCs following TLR4 activation. DCs were cultured in r-GM-CSF for seven days and subsequently were plated (1×10^6 cells/ml) and left to rest overnight. Cells were then stimulated with 100 ng/ml LPS and supernatants were recovered after 24 h and assessed for levels of cytokines using specific immunoassays. Results are \pm SEM of quadruplicate assays and represent three independent experiments. ** $p \leq 0.01$ and *** $p \leq 0.001$ comparing control versus 100ng/ml LPS stimulated JAWSII DCs or BMDCs as determined by a two-tailed t-test.

TLR4

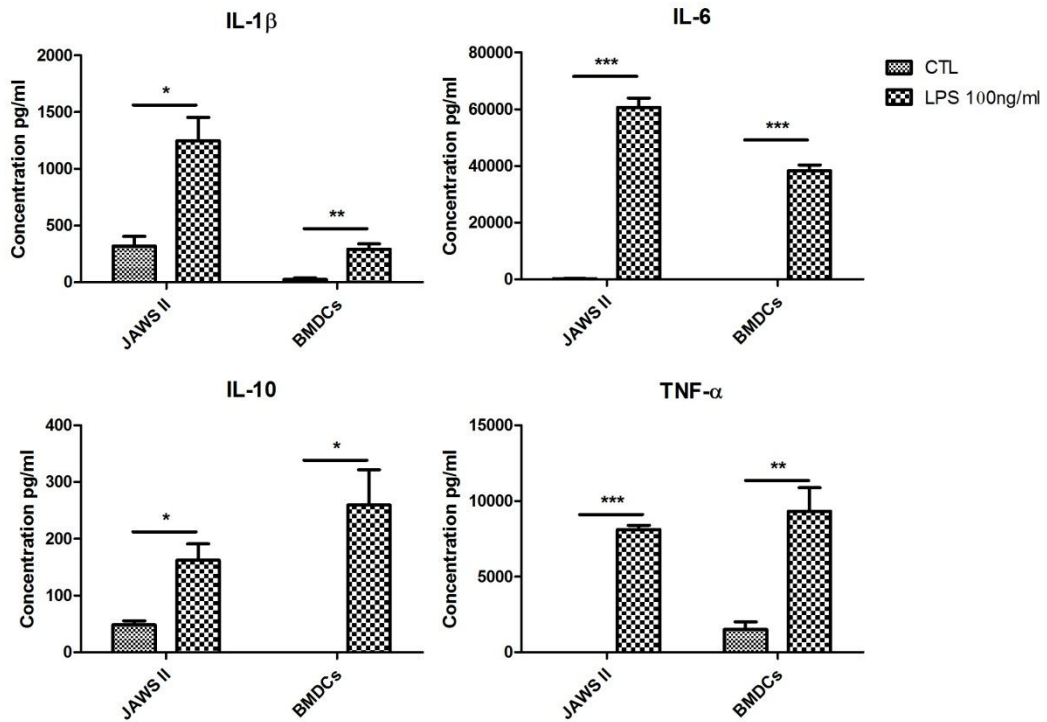


FIGURE 3.10: Comparison of cytokine secretion from JAWS II DCs and BMDCs following TLR4 activation. DCs were cultured in r-GM-CSF for seven days and subsequently were plated (1×10^6 cells/ml) and left to rest overnight. Cells were then stimulated with 100 ng/ml LPS and supernatants were recovered after 24 h and assessed for levels of cytokines using specific immunoassays. Results are \pm SEM of quadruplicate assays and represent three independent experiments. * $p \leq 0.05$, ** $p \leq 0.01$ and *** $p \leq 0.001$ comparing control versus 100ng/ml LPS stimulated JAWSII DCs or BMDCs as determined by a two-tailed t-test.

TLR4

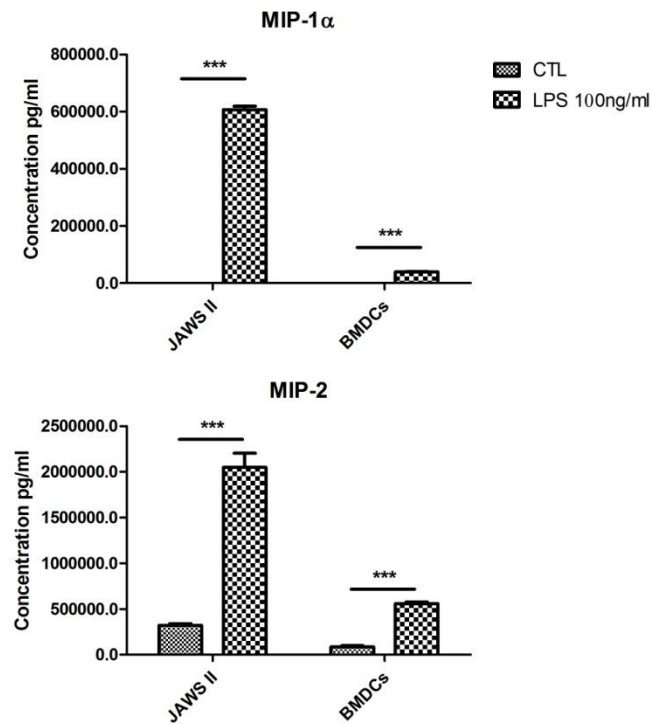


FIGURE 3.11: Comparison of chemokine secretion from JAWS II DCs and BMDCs following TLR4 activation. DCs were cultured in r-GM-CSF for seven days and subsequently were plated (1×10^6 cells/ml) and left to rest overnight. Cells were then stimulated with 100 ng/ml LPS and supernatants were recovered after 24 h and assessed for levels of chemokines using specific immunoassays. Results are \pm SEM of quadruplicate assays and represent three independent experiments. *** $p \leq 0.001$ comparing control versus 100 ng/ml LPS stimulated JAWSII DCs or BMDCs as determined by a two-tailed t-test.

TLR5

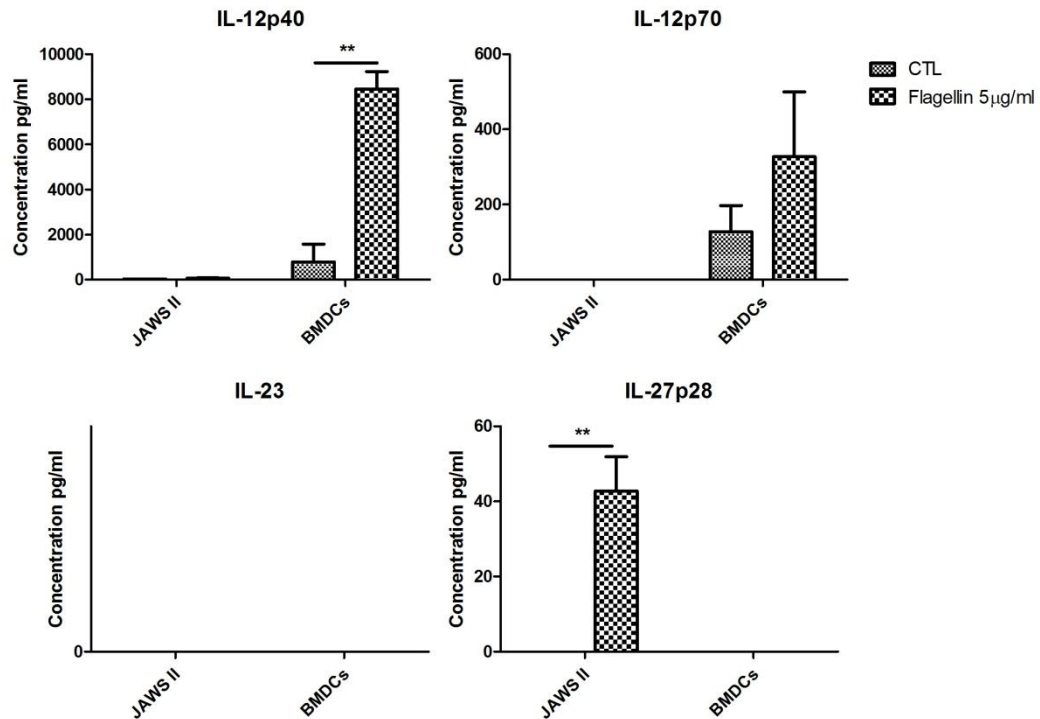


FIGURE 3.12: Comparison of cytokine secretion from JAWS II DCs and BMDCs following TLR5 activation. DCs were cultured in r-GM-CSF for seven days and subsequently were plated (1×10^6 cells/ml) and left to rest overnight. Cells were then stimulated with 5 µg/ml Flagellin and supernatants were recovered after 24 h and assessed for levels of cytokines using specific immunoassays. Results are \pm SEM of quadruplicate assays and represent three independent experiments. ** $p \leq 0.01$ comparing control versus 5 µg/ml Flagellin stimulated JAWSII DCs or BMDCs as determined by a two-tailed t-test.

TLR5

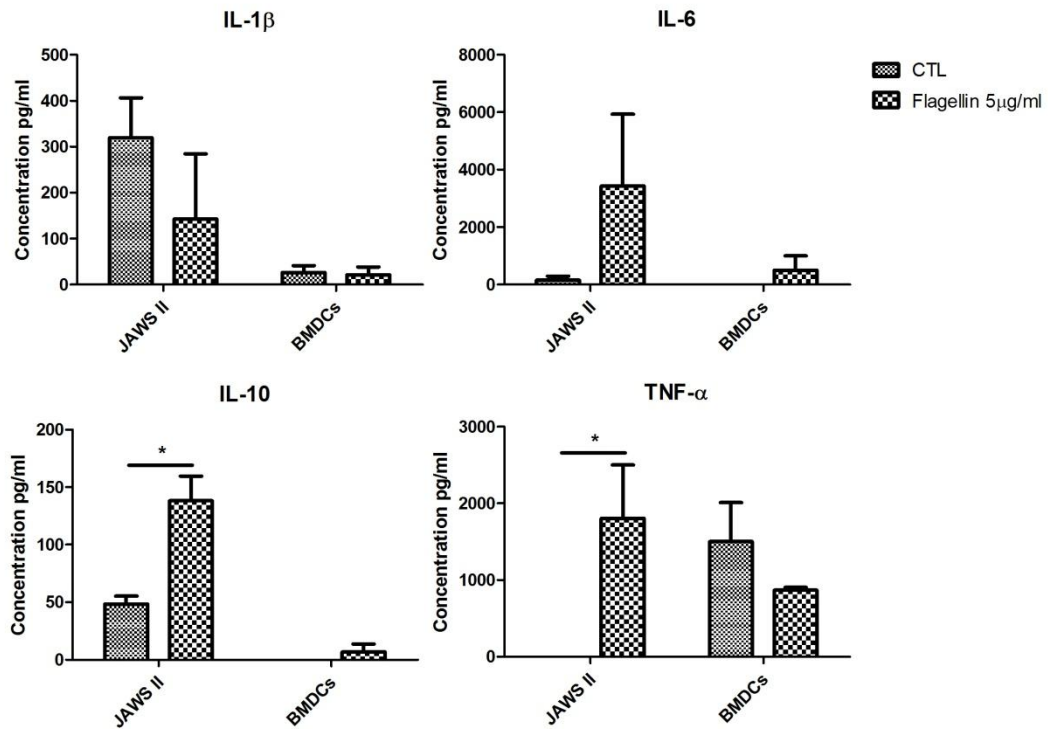


FIGURE 3.13: Comparison of cytokine secretion from JAWS II DCs and BMDCs following TLR5 activation. DCs were cultured in r-GM-CSF for seven days and subsequently were plated (1×10^6 cells/ml) and left to rest overnight. Cells were then stimulated with 5 μ g/ml Flagellin and supernatants were recovered after 24 h and assessed for levels of cytokines using specific immunoassays. Results are \pm SEM of quadruplicate assays and represent three independent experiments. * $p \leq 0.05$, comparing control versus 5 μ g/ml Flagellin stimulated JAWSII DCs or BMDCs as determined by a two-tailed t-test.

TLR5

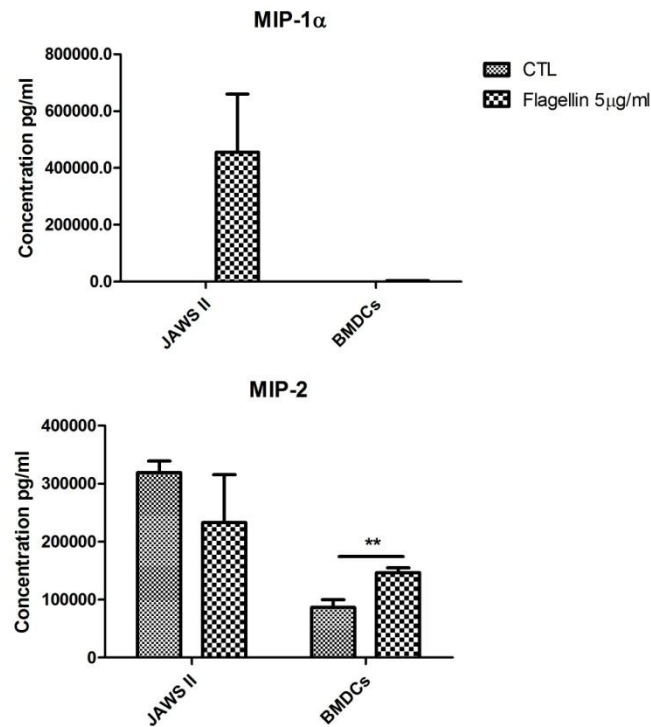


FIGURE 3.14: Comparison of chemokine secretion from JAWS II DCs and BMDCs following TLR5 activation. DCs were cultured in r-GM-CSF for seven days and subsequently were plated (1×10^6 cells/ml) and left to rest overnight. Cells were then stimulated 5 $\mu\text{g/ml}$ Flagellin and supernatants were recovered after 24 h and assessed for levels of chemokines using specific immunoassays. Results are \pm SEM of quadruplicate assays and represent three independent experiments. $**p \leq 0.01$ comparing control versus 5 $\mu\text{g/ml}$ Flagellin stimulated JAWSII DCs or BMDCs as determined by a two-tailed t-test.

TLR7

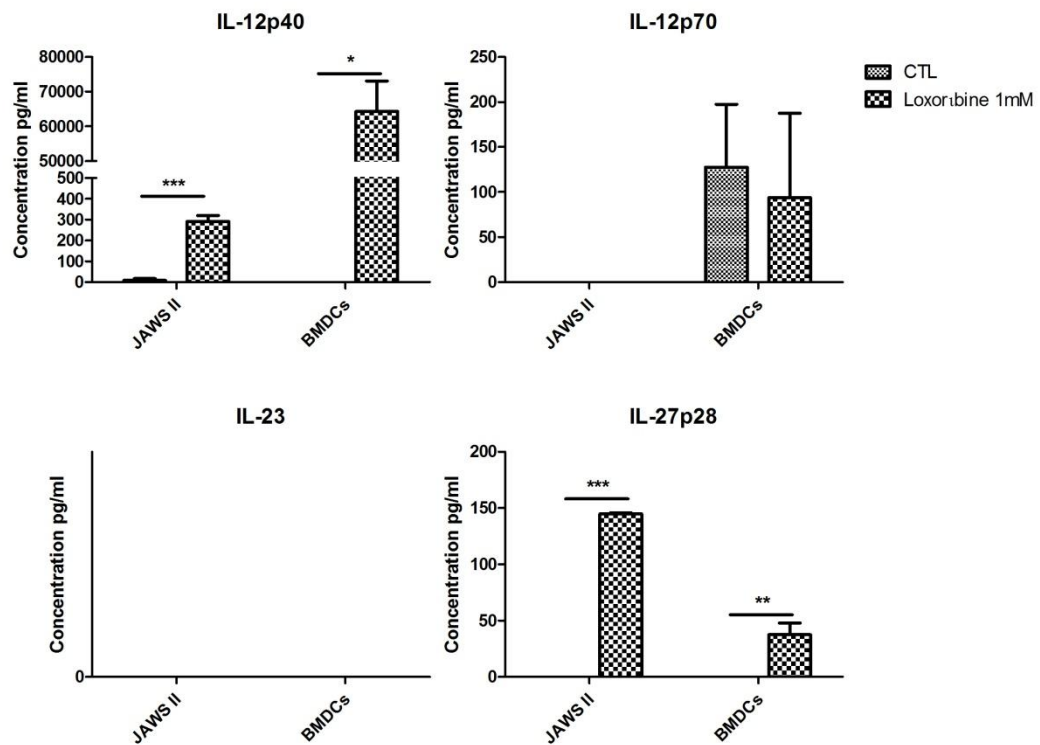


FIGURE 3.15: Comparison of cytokine secretion from JAWS II DCs and BMDCs following TLR7 activation. DCs were cultured in r-GM-CSF for seven days and subsequently were plated (1×10^6 cells/ml) and left to rest overnight. Cells were then stimulated with 1 mM Loxoribine and supernatants were recovered after 24 h and assessed for levels of cytokines using specific immunoassays. Results are \pm SEM of quadruplicate assays and represent three independent experiments. * $p \leq 0.05$, ** $p \leq 0.01$ and *** $p \leq 0.001$ comparing control versus 1 mM Loxoribine stimulated JAWSII DCs or BMDCs as determined by a two-tailed t-test.

TLR7

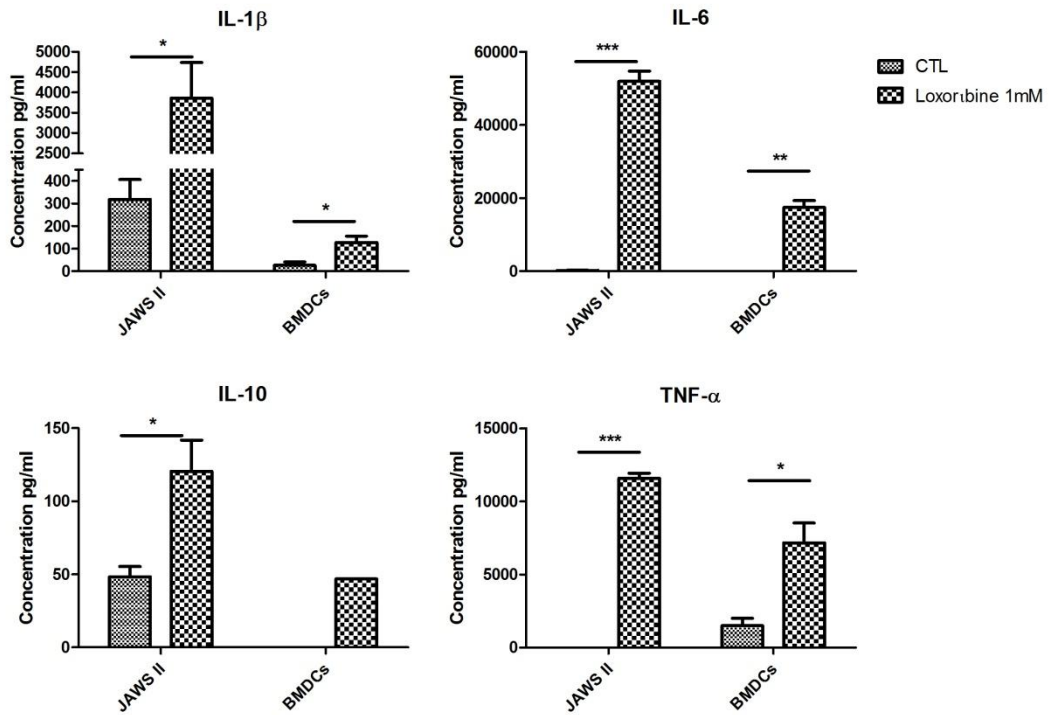


FIGURE 3.16: Comparison of cytokine secretion from JAWS II DCs and BMDCs following TLR7 activation. DCs were cultured in r-GM-CSF for seven days and subsequently were plated (1×10^6 cells/ml) and left to rest overnight. Cells were then stimulated with 1 mM Loxoribine and supernatants were recovered after 24 h and assessed for levels of cytokines using specific immunoassays. Results are \pm SEM of quadruplicate assays and represent three independent experiments. * $p \leq 0.05$, ** $p \leq 0.01$ and *** $p \leq 0.001$ comparing control versus 1 mM Loxoribine stimulated JAWSII DCs or BMDCs as determined by a two-tailed t-test.

TLR7

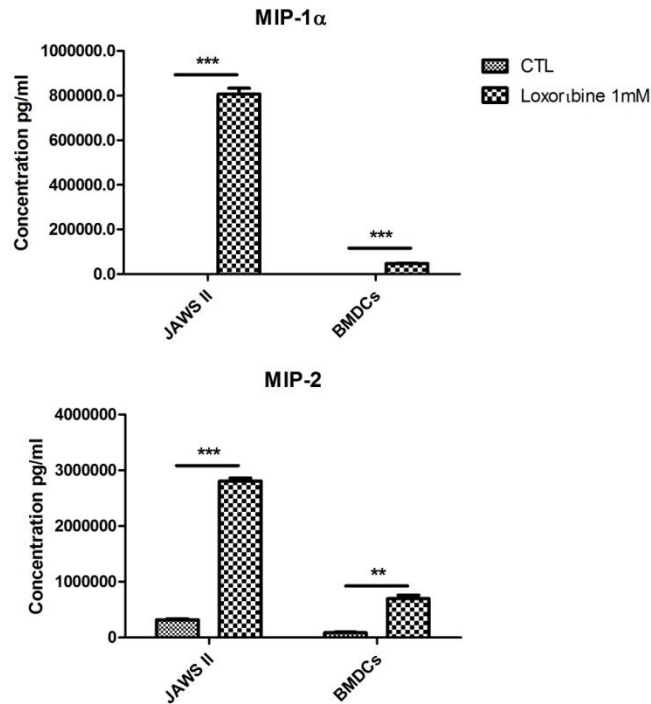


FIGURE 3.17: Comparison of chemokine secretion from JAWS II DCs and BMDCs following TLR7 activation. DCs were cultured in r-GM-CSF for seven days and subsequently were plated (1×10^6 cells/ml) and left to rest overnight. Cells were then stimulated with 1 mM Loxoribine and supernatants were recovered after 24 h and assessed for levels of chemokines using specific immunoassays. Results are \pm SEM of quadruplicate assays and represent three independent experiments. $**p \leq 0.01$ and $***p \leq 0.001$ comparing control versus 1 mM Loxoribine stimulated JAWSII DCs or BMDCs as determined by a two-tailed t-test.

TLR9

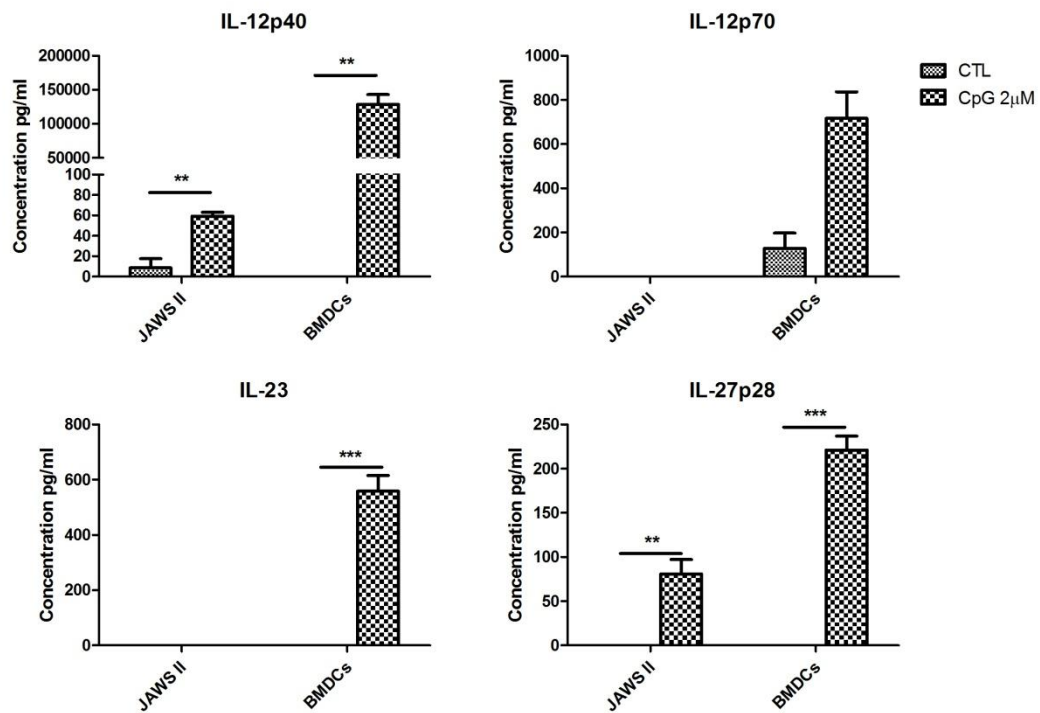


FIGURE 3.18: Comparison of cytokine secretion from JAWS II DCs and BMDCs following TLR9 activation. DCs were cultured in r-GM-CSF for seven days and subsequently were plated (1×10^6 cells/ml) and left to rest overnight. Cells were then stimulated with $2 \mu\text{M}$ CpG and supernatants were recovered after 24 h and assessed for levels of cytokines using specific immunoassays. Results are \pm SEM of quadruplicate assays and represent three independent experiments. ** $p \leq 0.01$ and *** $p \leq 0.001$ comparing control versus $2 \mu\text{M}$ CpG stimulated JAWSII DCs or BMDCs as determined by a two-tailed t-test.

TLR9

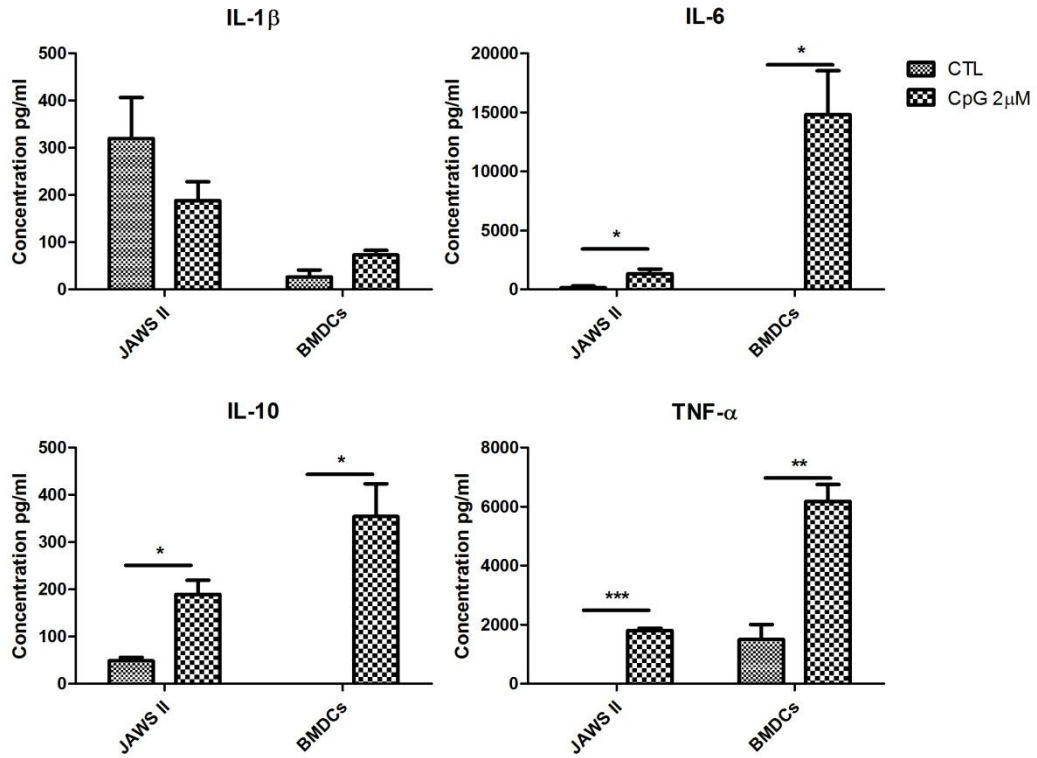


FIGURE 3.19: Comparison of cytokine secretion from JAWS II DCs and BMDCs following TLR9 activation. DCs were cultured in r-GM-CSF for seven days and subsequently were plated (1×10^6 cells/ml) and left to rest overnight. Cells were then stimulated with 2 μ M CpG and supernatants were recovered after 24 h and assessed for levels of cytokines using specific immunoassays. Results are \pm SEM of quadruplicate assays and represent three independent experiments. * $p \leq 0.05$, ** $p \leq 0.01$ and *** $p \leq 0.001$ comparing control versus 2 μ M CpG stimulated JAWSII DCs or BMDCs as determined by a two-tailed t-test.

TLR9

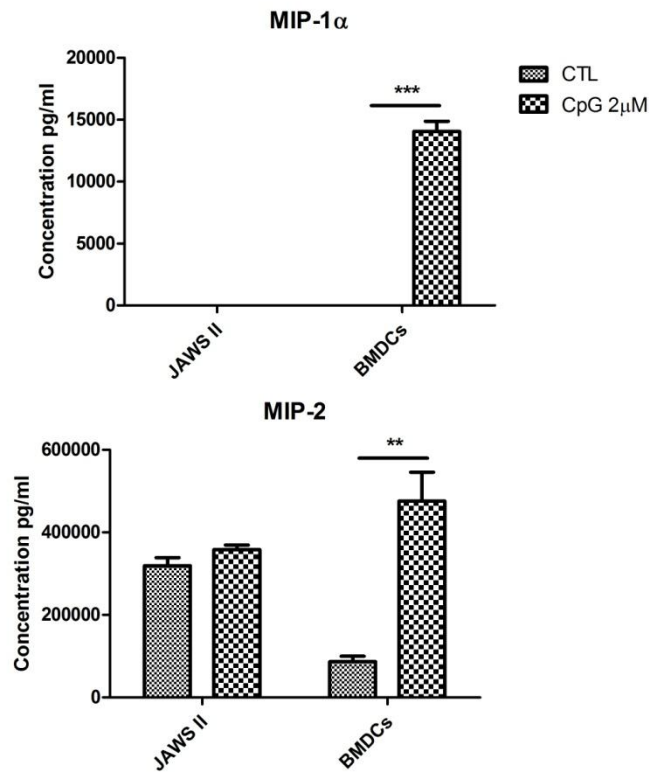


FIGURE 3.20: Comparison of chemokine secretion from JAWS II DCs and BMDCs following TLR9 activation. DCs were cultured in r-GM-CSF for seven days and subsequently were plated (1×10^6 cells/ml) and left to rest overnight. Cells were then stimulated with $2 \mu\text{M}$ CpG and supernatants were recovered after 24 h and assessed for levels of chemokines using specific immunoassays. Results are \pm SEM of quadruplicate assays and represent three independent experiments. ** $p \leq 0.01$ and *** $p \leq 0.001$ comparing control versus $2 \mu\text{M}$ CpG stimulated JAWSII DCs or BMDCs as determined by a two-tailed t-test.

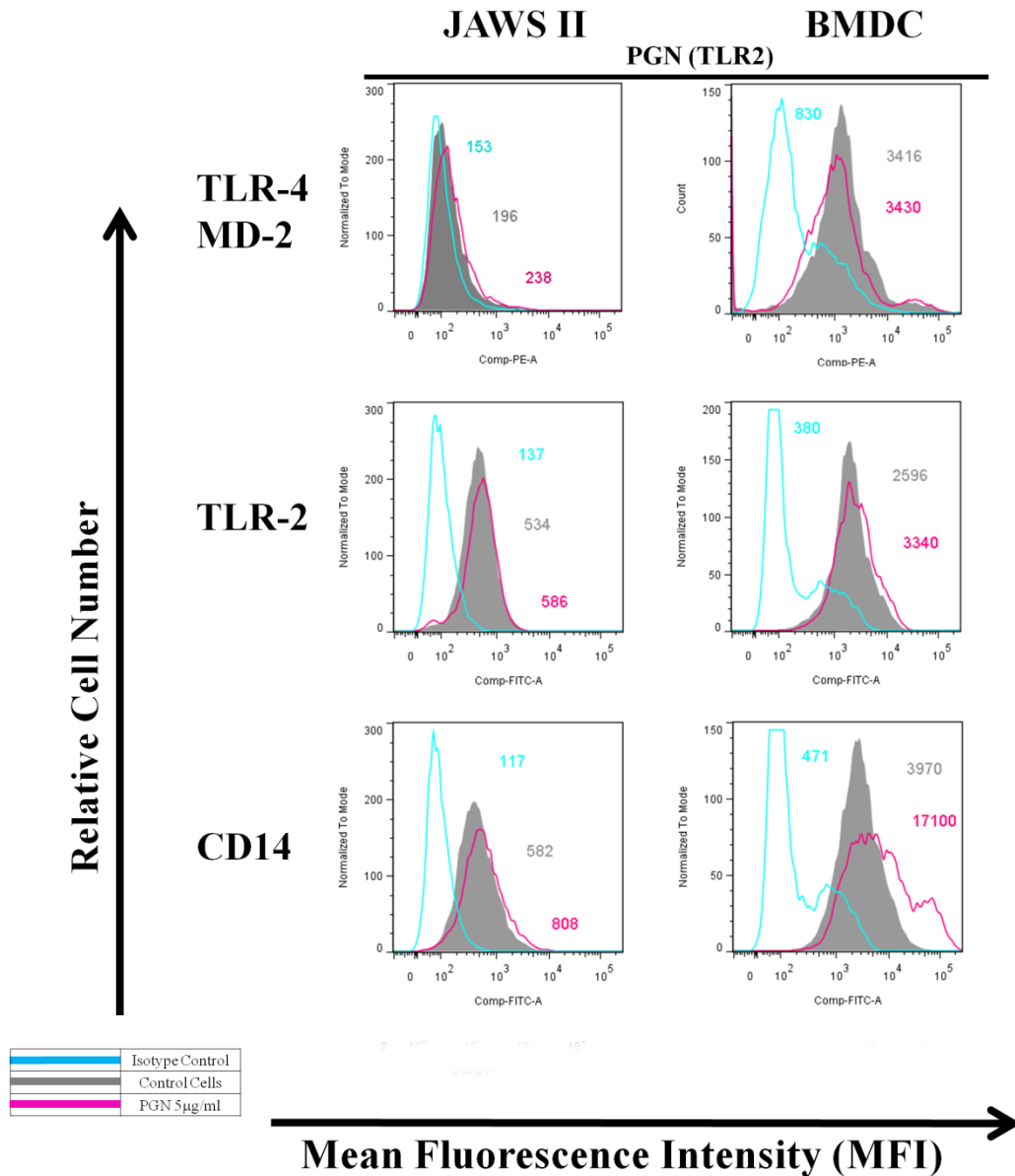


FIGURE 3.21: Comparison of surface marker expression on JAWS II and BMDCs following TLR2 activation. JAWS II and BMDC were differentiated in the presence of r-GMCSF for seven days and then stimulated with PGN (5 µg/ml) for 24 h. Subsequently, cells were washed and stained with specific antibodies or with an isotype matched control. Results of flow cytometric analysis and corresponding Mean Fluorescence Intensity (MFI) values are shown. Control DCs (grey filled histogram) vs PGN stimulated DCs (pink line) and isotype control (blue line). Profiles are shown for a single experiment and are representative of three experiments.

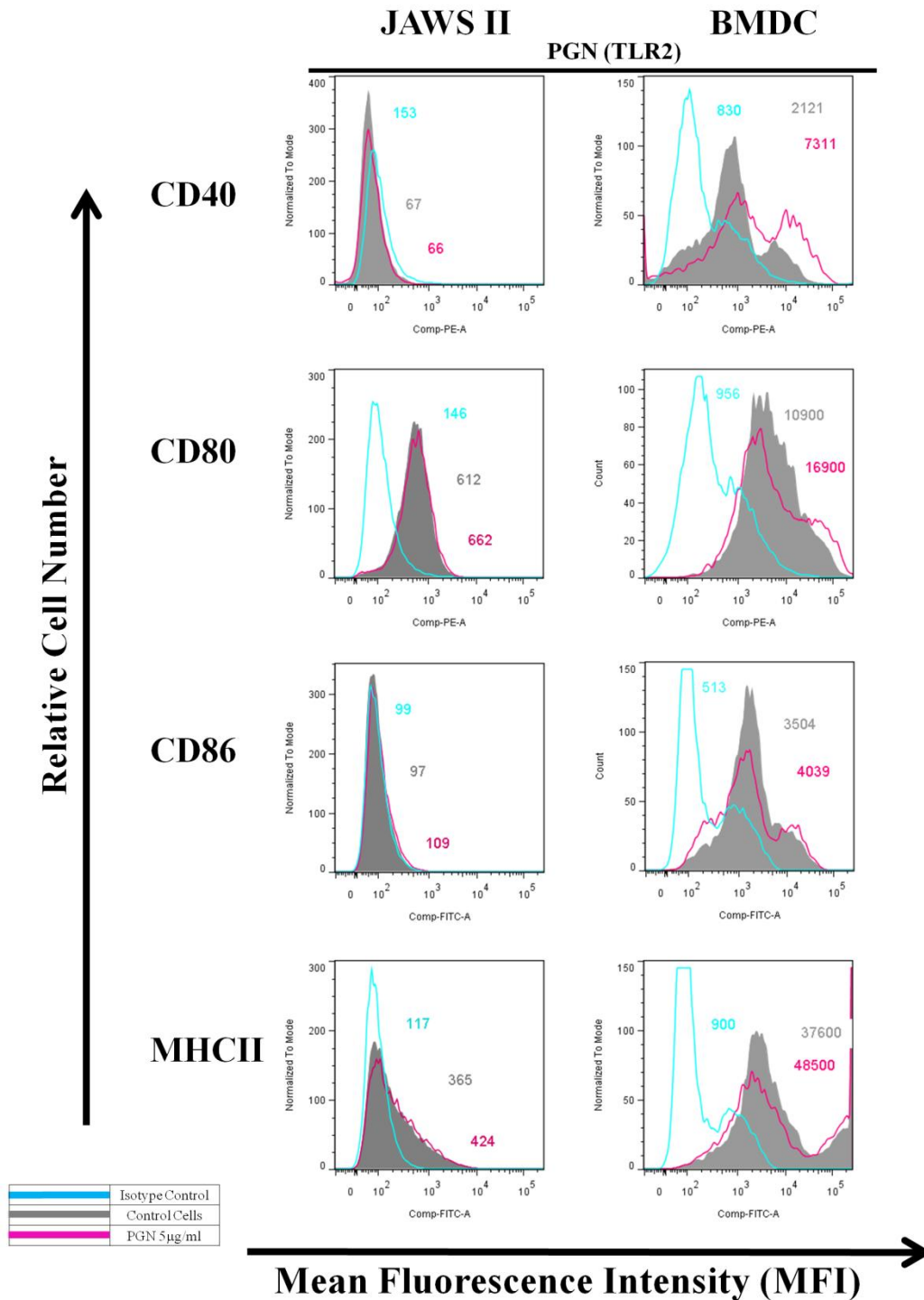


FIGURE 3.22: Comparison of surface marker expression on JAWS II and BMDCs following TLR2 activation. JAWS II and BMDC were differentiated in the presence of r-GMCSF for seven days and then stimulated with PGN (5 µg/ml) for 24 h. Subsequently, cells were washed and stained with specific antibodies or with an isotype matched control. Results of flow cytometric analysis and corresponding MFI values are shown. Control DCs (grey filled histogram) vs PGN stimulated DCs (pink line) and isotype control (blue line). Profiles are shown for a single experiment and are representative of three experiments.

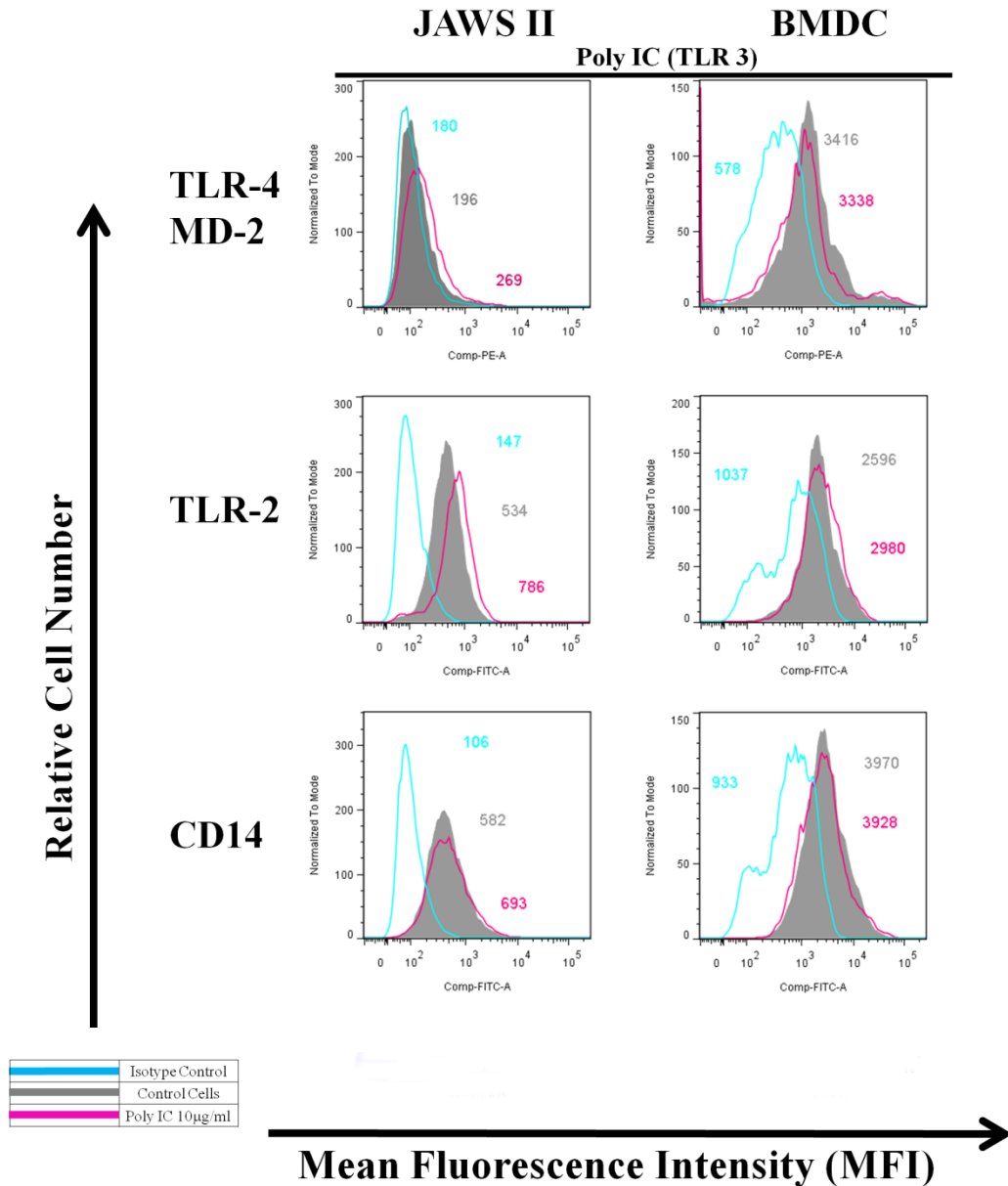


FIGURE 3.23: Comparison of surface marker expression on JAWS II and BMDCs following TLR3 activation. JAWS II and BMDC were differentiated in the presence of r-GMCSF for seven days and then stimulated with Poly (I:C) (10 µg/ml) for 24 h. Subsequently, cells were washed and stained with specific antibodies or with an isotype matched control. Results of flow cytometric analysis and corresponding MFI values are shown. Control DCs (grey filled histogram) vs Poly (I:C) stimulated DCs (pink line) and isotype control (blue line). Profiles are shown for a single experiment and are representative of three experiments.

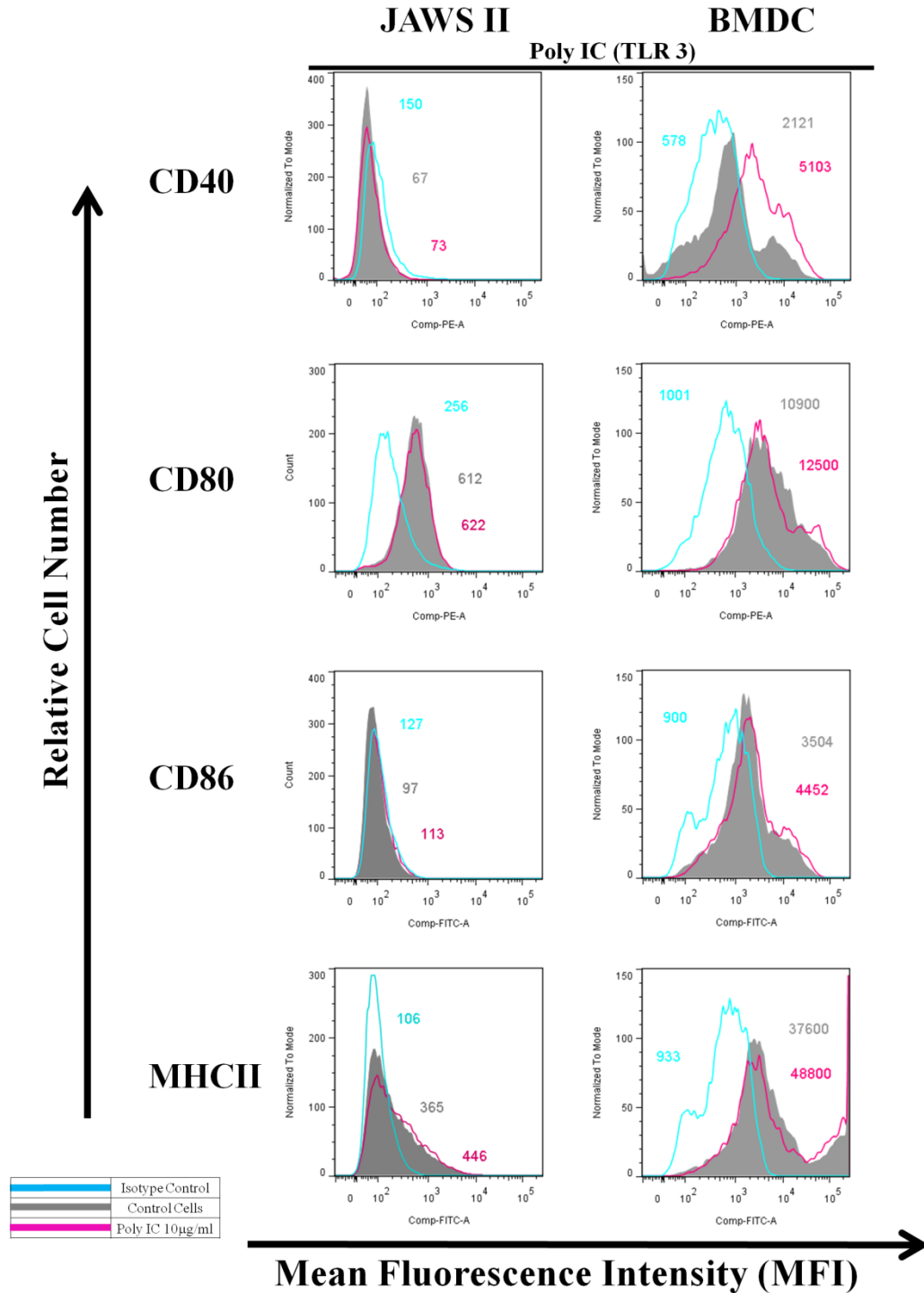


FIGURE 3.24: Comparison of surface marker expression on JAWS II and BMDCs following TLR3 activation. JAWS II and BMDC were differentiated in the presence of r-GMCSF for seven days and then stimulated with Poly (I:C) (10 µg/ml) for 24 h. Subsequently, cells were washed and stained with specific antibodies or with an isotype matched control. Results of flow cytometric analysis and corresponding MFI values are shown. Control DCs (grey filled histogram) vs Poly (I:C) stimulated DCs (pink line) and isotype control (blue line). Profiles are shown for a single experiment and are representative of three experiments.

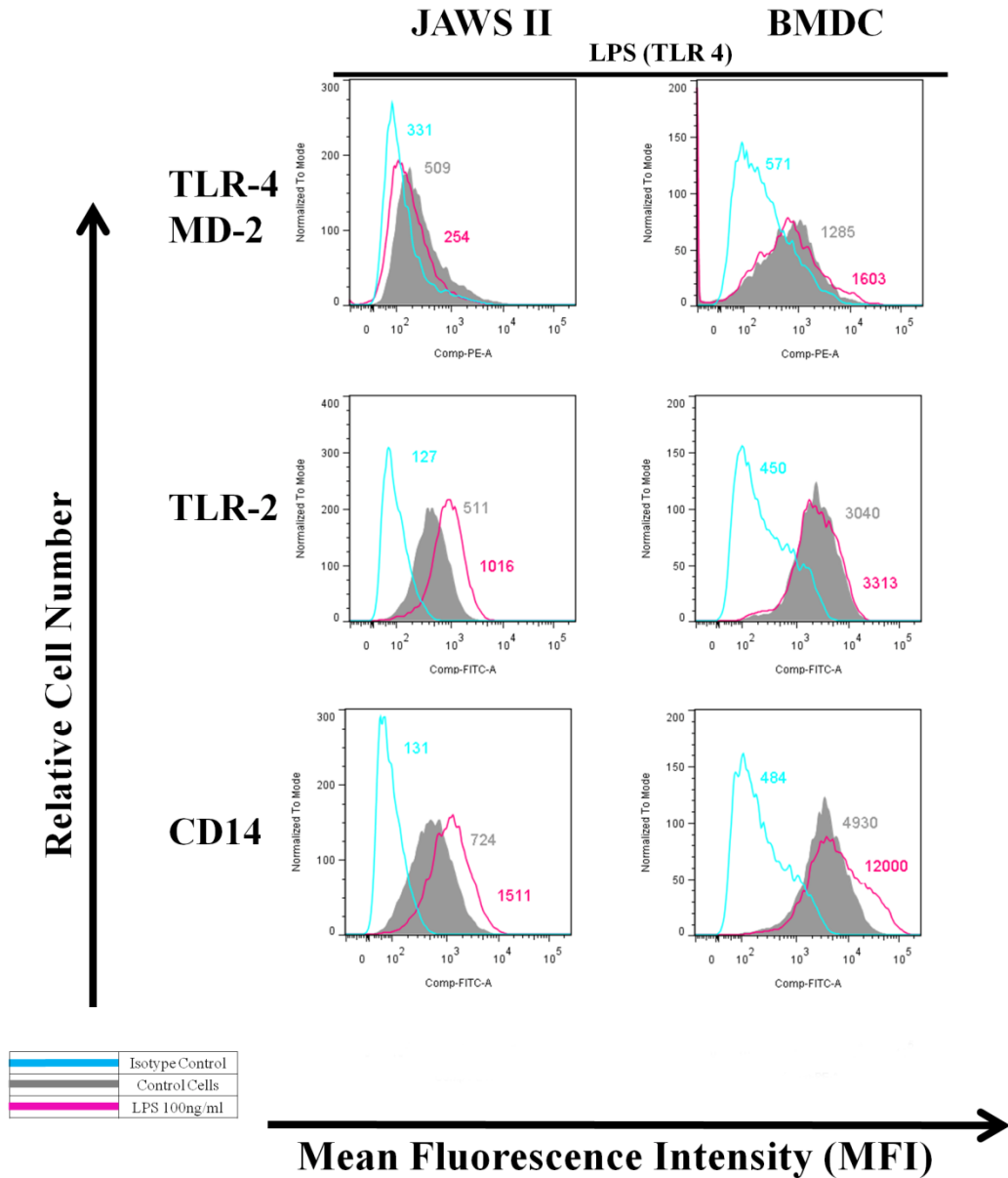


FIGURE 3.25: Comparison of surface marker expression on JAWS II and BMDCs following TLR4 activation. JAWS II and BMDC were differentiated in the presence of r-GMCSF for seven days and then stimulated with (LPS 100 ng/ml) for 24 h. Subsequently, cells were washed and stained with specific antibodies or with an isotype matched control. Results of flow cytometric analysis and corresponding MFI values are shown. Control DCs (grey filled histogram) vs LPS stimulated DCs (pink line) and isotype control (blue line). Profiles are shown for a single experiment and are representative of three experiments.

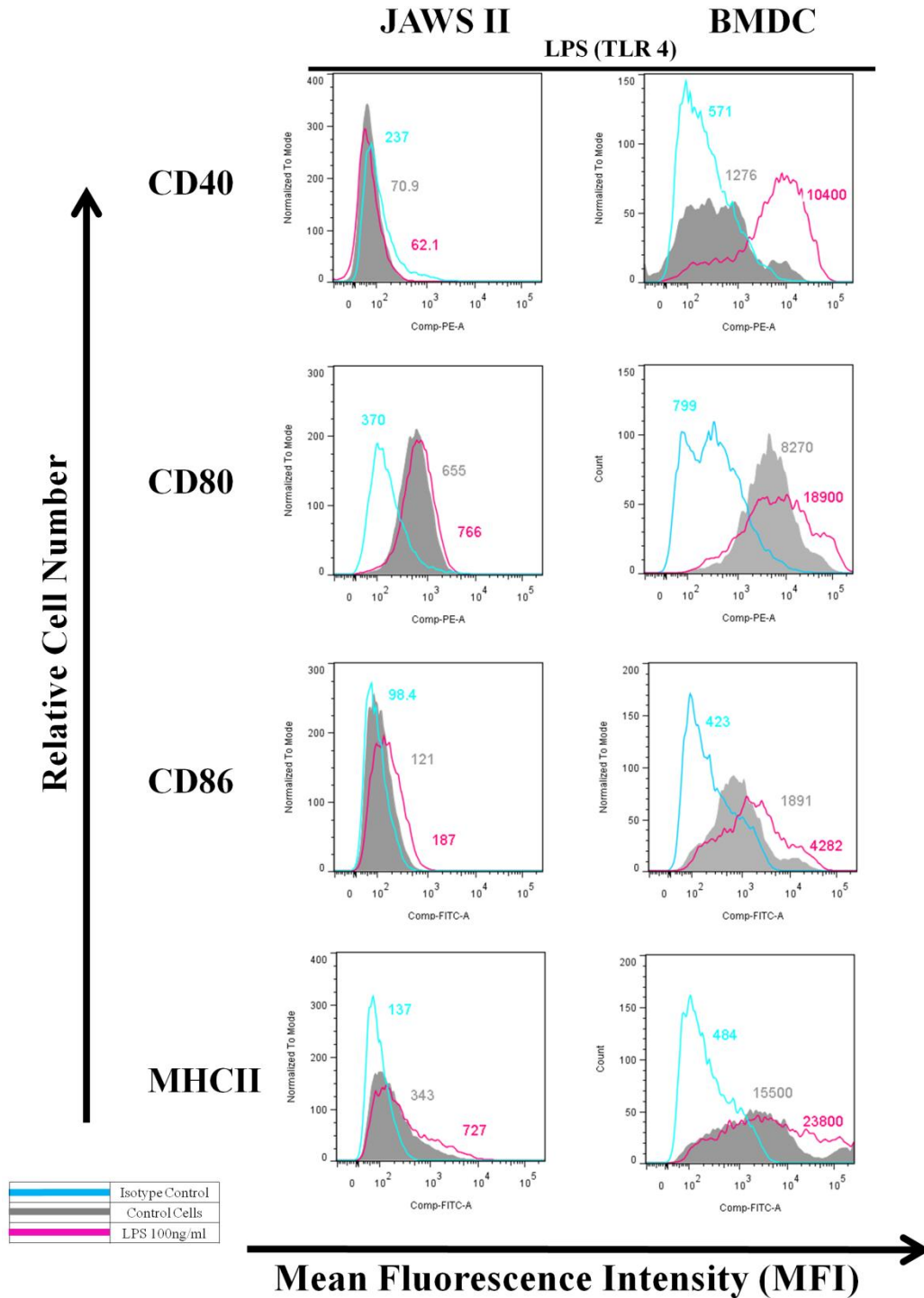


FIGURE 3.26: Comparison of surface marker expression on JAWS II and BMDCs following TLR4 activation. JAWS II and BMDC were differentiated in the presence of r-GMCSF for seven days and then stimulated with (LPS 100 ng/ml) for 24 h. Subsequently, cells were washed and stained with specific antibodies or with an isotype matched control. Results of flow cytometric analysis and corresponding MFI values are shown. Control DCs (grey filled histogram) vs LPS stimulated DCs (pink line) and isotype control (blue line). Profiles are shown for a single experiment and are representative of three experiments.

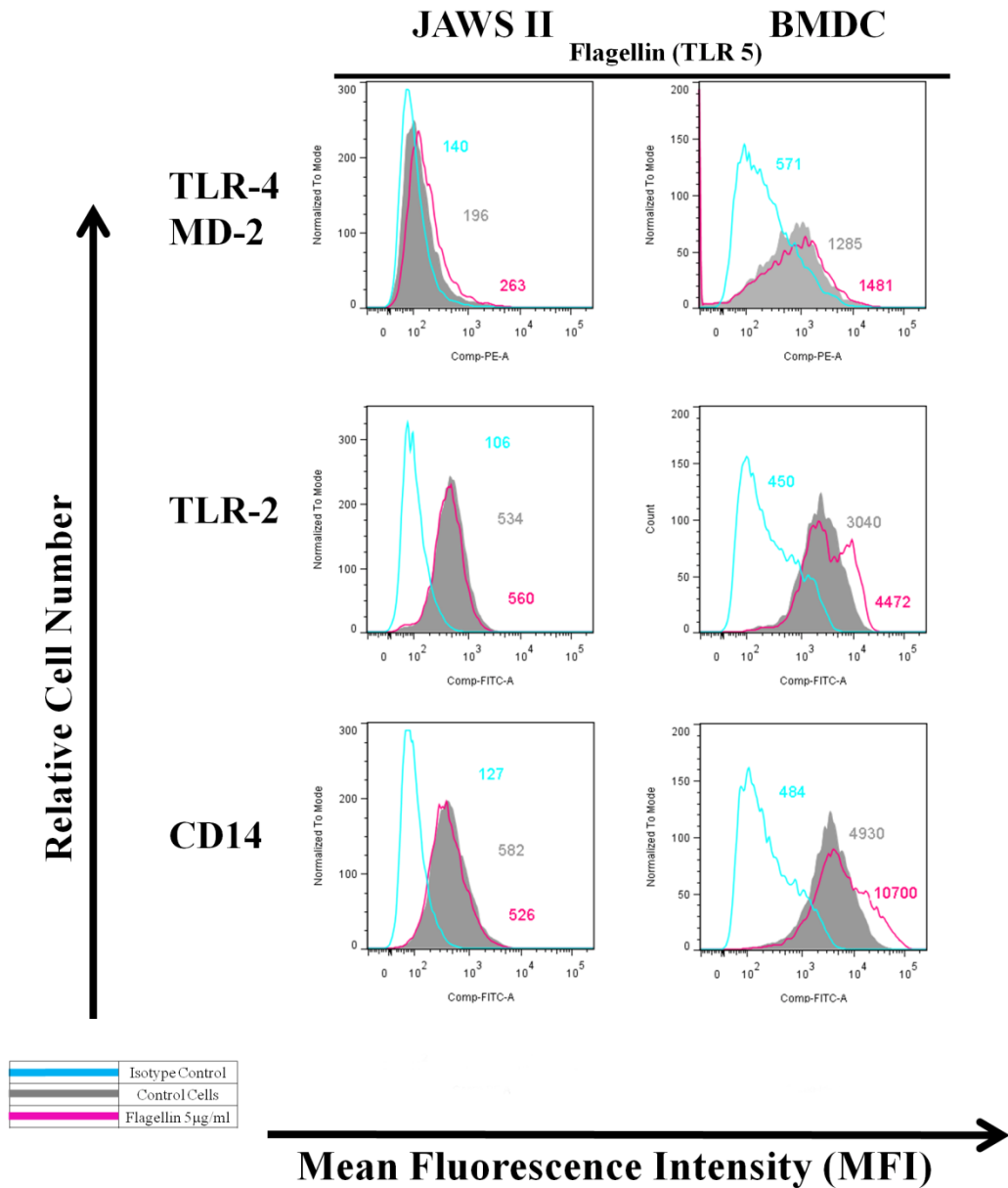


FIGURE 3.27: Comparison of surface marker expression on JAWS II and BMDCs following TLR5 activation. JAWS II and BMDC were differentiated in the presence of r-GMCSF for seven days and then stimulated with Flagellin (5 µg/ml) for 24 h. Subsequently, cells were washed and stained with specific antibodies or with an isotype matched control. Results of flow cytometric analysis and corresponding MFI values are shown. Control DCs (grey filled histogram) vs flagellin stimulated DCs (pink line) and isotype control (blue line). Profiles are shown for a single experiment and are representative of three experiments.

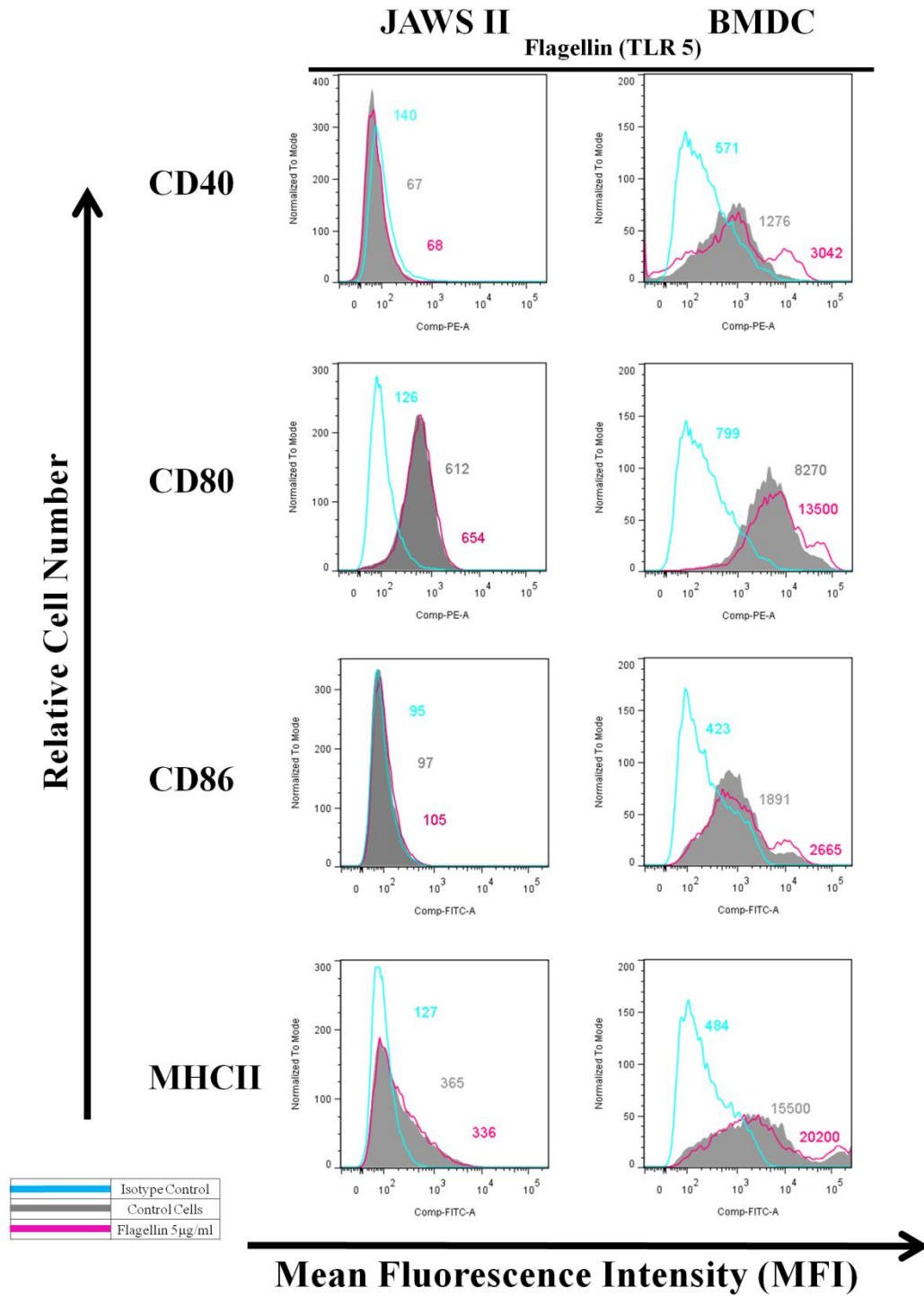


FIGURE 3.28: Comparison of surface marker expression on JAWS II and BMDCs following TLR5 activation. JAWS II and BMDC were differentiated in the presence of r-GMCSF for seven days and then stimulated with Flagellin (5 µg/ml) for 24 h. Subsequently, cells were washed and stained with specific antibodies or with an isotype matched control. Results of flow cytometric analysis and corresponding MFI values are shown. Control DCs (grey filled histogram) vs flagellin stimulated DCs (pink line) and isotype control (blue line). Profiles are shown for a single experiment and are representative of three experiments.

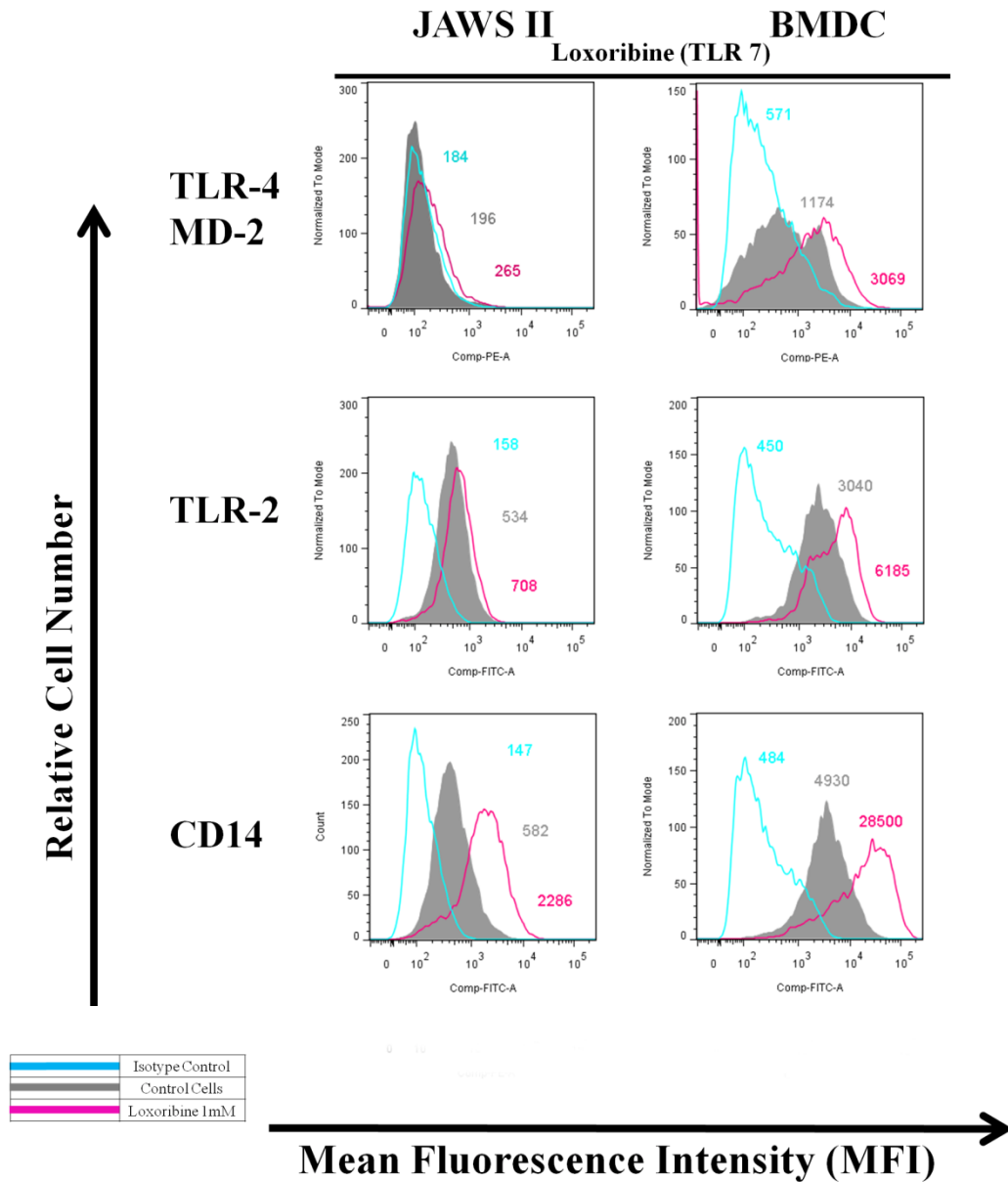


FIGURE 3.29: Comparison of surface marker expression on JAWS II and BMDCs following TLR7 activation. JAWS II and BMDC were differentiated in the presence of r-GMCSF for seven days and then stimulated with Loxoribine (1 mM) for 24 h. Subsequently, cells were washed and stained with specific antibodies or with an isotype matched control. Results of flow cytometric analysis and corresponding MFI values are shown. Control DCs (grey filled histogram) vs Loxoribine stimulated DCs (pink line) and isotype control (blue line). Profiles are shown for a single experiment and are representative of three experiments.

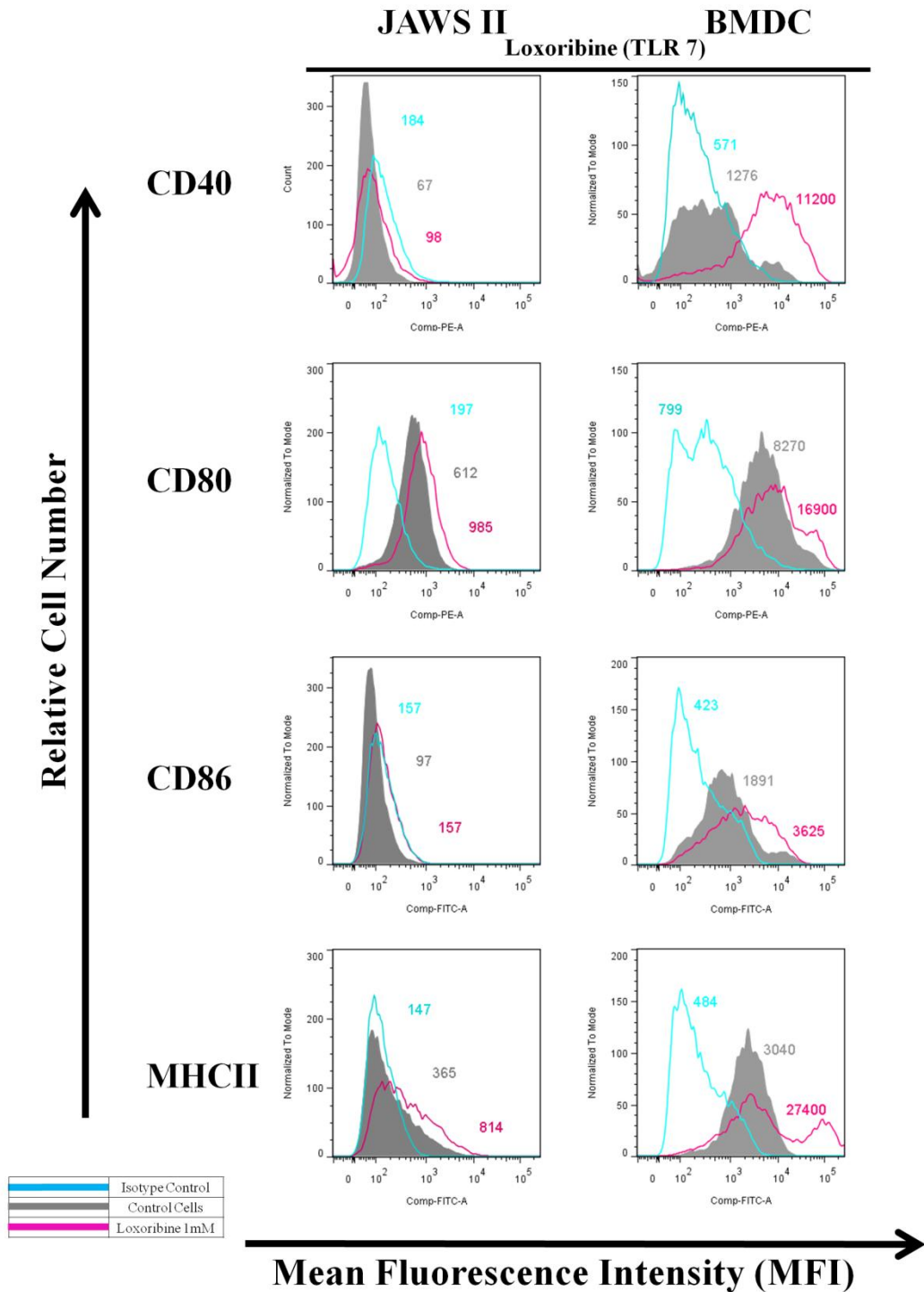


FIGURE 3.30: Comparison of surface marker expression on JAWS II and BMDCs following TLR7 activation. JAWS II and BMDC were differentiated in the presence of r-GMCSF for seven days and then stimulated with Loxoribine (1 mM) for 24 h. Subsequently, cells were washed and stained with specific antibodies or with an isotype matched control. Results of flow cytometric analysis and corresponding MFI values are shown. Control DCs (grey filled histogram) vs Loxoribine stimulated DCs (pink line) and isotype control (blue line). Profiles are shown for a single experiment and are representative of three experiments.

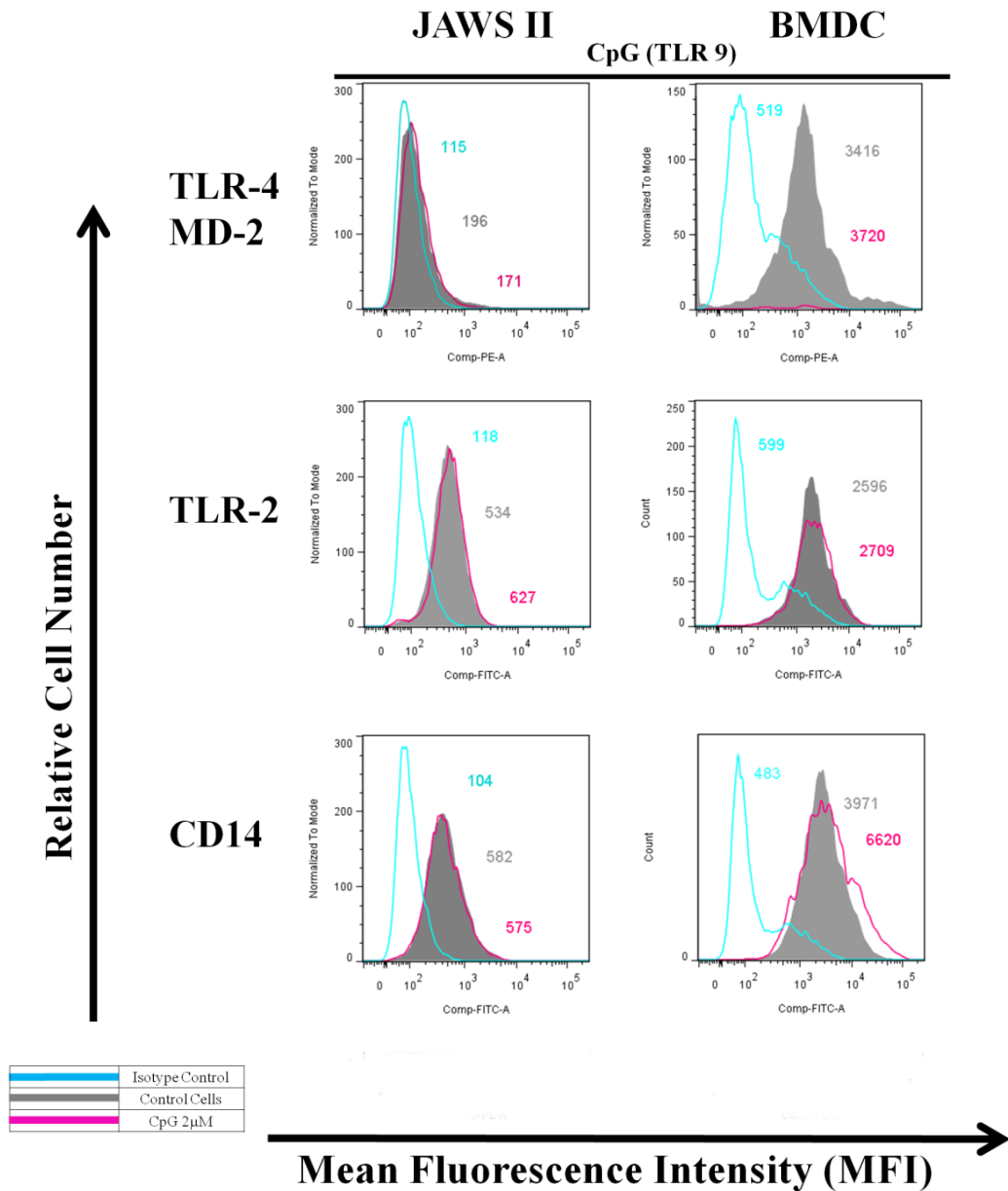


FIGURE 3.31: Comparison of surface marker expression on JAWS II and BMDCs following TLR9 activation. JAWS II and BMDC were differentiated in the presence of r-GMCSF for seven days and then stimulated with CpG (2 µM) for 24 h. Subsequently, cells were washed and stained with specific antibodies or with an isotype matched control. Results of flow cytometric analysis and corresponding MFI values are shown. Control DCs (grey filled histogram) vs CpG stimulated DCs (pink line) and isotype control (blue line). Profiles are shown for a single experiment and are representative of three experiments.

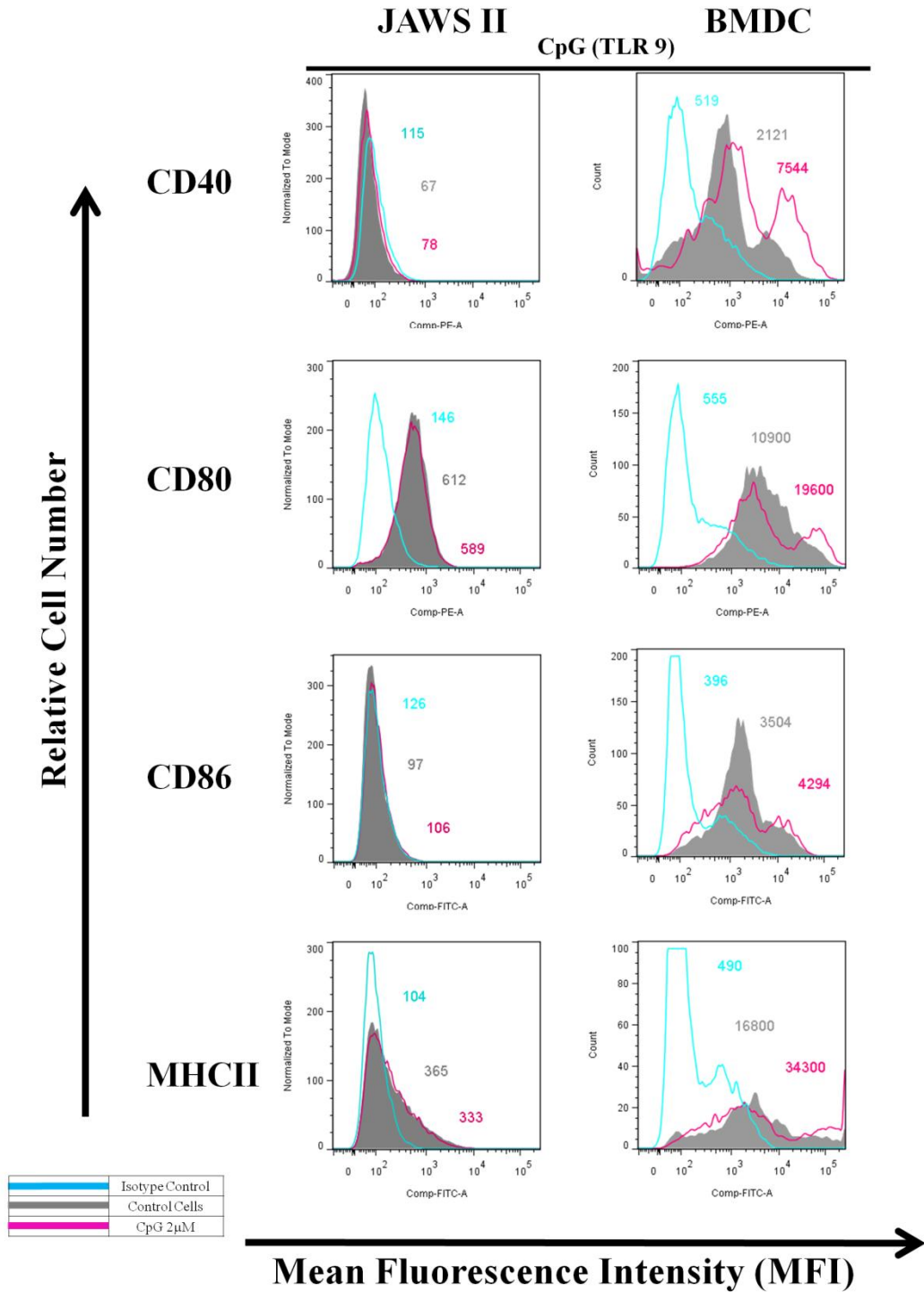


FIGURE 3.32: Comparison of surface marker expression on JAWS II and BMDCs following TLR9 activation. JAWS II and BMDC were differentiated in the presence of r-GMCSF for seven days and then stimulated with CpG (2 µM) for 24 h. Subsequently, cells were washed and stained with specific antibodies or with an isotype matched control. Results of flow cytometric analysis and corresponding MFI values are shown. Control DCs (grey filled histogram) vs CpG stimulated DCs (pink line) and isotype control (blue line). Profiles are shown for a single experiment and are representative of three experiments.

TABLE 3.1

	TLR4		TLR 2		CD14	
	JAWS II	BMDC	JAWS II	BMDC	JAWS II	BMDC
PGN (TLR 2)	↑	↑	↑	↑	↑	↑
Poly (I:C) (TLR3)	↑	↓	↑	↑	↑	↔
LPS (TLR4)	↓	↑	↑	↑	↑	↑
Flagellin (TLR5)	↑	↑	↔	↑	↔	↑
Loxoribine (TLR7)	↑	↑	↑	↑	↑	↑
CpG (TLR9)	↔	↑	↔	↑	↔	↑

TABLE 3.2

	CD40		CD80		CD86		MHC II	
	JAWSII	BMDC	JAWSII	BMDC	JAWSII	BMDC	JAWSII	BMDC
PGN (TLR 2)	NE	↑	↔	↑	↔	↑	↑	↑
Poly (I:C) (TLR3)	NE	↑	↔	↑	↔	↑	↑	↔
LPS (TLR4)	NE	↑	↑	↑	↑	↑	↑	↑
Flagellin (TLR5)	NE	↑	↔	↑	↔	↑	↔	↑
Loxoribine (TLR7)	NE	↑	↑	↑	↑	↑	↑	↑
CpG (TLR9)	NE	↑	↔	↑	↔	↑	↔	↑

TABLE 3.1 and 3.2: Summary of Surface Marker Expression on JAWS II DCs and BMDCs following stimulation with a panel of TLR ligands. JAWS II and BMDC were differentiated in the presence of r-GMCSF for seven days and then stimulated with 5 µg/ml peptidoglycan (PGN), 10 µg/ml Polyinosinic-polycytidylic acid (Poly (I:C)), 100 ng/ml Lipopolysaccharide (LPS) (*E. coli* serotype R515), 5 µg/ml Flagellin, 1 mM Loxoribine or 2 µM CpG oligodeoxynucleotides (CpG ODN) for 24h. NE = Not Expressed. Subsequently, cells were washed and stained with the specific antibodies or with an isotype matched control.

3.3 DISCUSSION

The characterisation of DCs began less than thirty years ago yet in that time have proven to be essential for the generation of a functional immune response. They do so by the capture and processing of antigens, expression of surface co-stimulatory molecules, migration to lymphoid organs and secretion of cytokines and chemokine (Steinman 1998). Understanding these actions, such as their ability to drive T helper cell responses makes the DC a powerful tool for manipulating the immune system. In this study our key objective was to compare the JAWS II DCs cell line to the BMDCs in order to determine whether they would be a suitable model for characterising SNARE function in DCs. In order to do this we assessed their response to a panel of TLR ligands. The parameters assessed included cytokine and chemokine secretion and expression of co-stimulatory molecules.

To date 13 murine TLR ligands have been described and can be divided into two groups, those expressed on the surface of the cell or those which reside intracellularly. In this study we examined the effect of stimulation of BMDCs and JAWS II DCs with six TLR ligands. TLR 2, 4 and 5 are surface TLRs which recognise markers from the exterior of a pathogen and intracellular TLRs, TLR3, 7 and 9 which recognise nucleic acids (McGettrick and O'Neill 2010). TLR4, the best characterised cell surface TLR, is responsible for the recognition of LPS, a glycolipid component of the outer wall of gram-negative bacteria. Activation of BMDCs and their cytokine, chemokine and surface marker expression has been well characterised in the literature and our findings on the effects of LPS on BMDCs concur with this.

Dowling *et al.*, showed similar levels of secretion of the cytokines, IL-6, IL-10, IL-12p40, IL-12p70 and TNF- α from BMDCs following LPS stimulation. Surface marker expression of CD40, CD80 and CD86 were also up-regulated similar to the profile we observed in BMDCs (Dowling, Hamilton and O'Neill 2008). Secretion of IL-1 β and MIP-1 α and up-regulation of MHC II in response to LPS has also been reported by Dearman *et al.*, 2008 consistent with our data (Dearman *et al.* 2009).

Flagellin, a structural protein subunit of the flagellum from gram-negative bacteria, mediates DC activation through TLR5 activation. It has been shown to evoke the production of low levels of pro-inflammatory cytokines, minimal levels of chemokines, such as MIP-1 α and up-regulation of the surface markers CD40, CD80, CD86 and MHC II (Dearman *et al.* 2009, Didierlaurent *et al.* 2004). BMDCs in this study responded in a similar manner consistent with this published data. This low level of response compared to other ligands may also be caused genetically. Indeed it has been reported there is a lack of expression of TLR5 mRNA in BMDCs isolated from C57BL6 mice (Means *et al.* 2003). PGN from gram-positive bacteria is reported to be a potent activator of NF κ B and TNF- α through another surface TLR, TLR2. PGN also has several other recognition molecules including CD14, a family of peptidoglycan recognition proteins (PGRPs), Nod1 and Nod2, and PGN-lytic enzymes (lysozyme and amidases) (Dziarski 2003). PGN is a component of a bacterial cell wall covalently attached to other polymers such as lipoproteins and lipoteichoic acid. It has been reported that PGN induces the up-regulation of CD86 and MHC II during DC maturation and stimulates the secretion of IL-6, TNF α , IL-12 and MIP-2, which correlates well with our findings (Michelsen *et al.* 2001).

Intracellular TLRs play an important role in detecting and combating both bacterial and viral infections. TLR3, TLR7 and TLR9 recognise double-stranded (ds)RNA, single-stranded(ss)RNA and un-methylated CpG motifs respectively (Akira and Hemmi 2003). The presence of dsRNA in a cell is due to viral replication which can stimulate immune cells via TLR3. This dsRNA binds and activates the dsRNA activated protein kinase, PKR, initiating down-stream signalling that inhibits viral replication and secretion of pro-inflammatory cytokines (Akira and Hemmi 2003). Dowling *et al.*, reported secretion of moderate levels of IL-6 and IL-12p40 with negligible levels of TNF- α from BMDCs stimulated with Poly (I:C) which correlates well with our data presented in this chapter. Surface marker levels of CD40, CD80 and CD86 were all up-regulated which were comparable with our results. A plethora of natural and synthetic agonists for TLR7 have been identified. Guanosine analogue, Loxoribine (7-Allyl-8-oxo-G), activates NF- κ B through TLR7. Activation induces production of pro-inflammatory cytokines and chemokines such as TNF- α , IL-12 and MIP-1 α (Gorden et al. 2005, Lee et al. 2003). We noted similar responses although information on specific BMDCs response to Loxoribine as an agonist to TLR7 is not well reported. Unmethylated CpG-dinucleotide-containing sequences (CpG ODNs) act as a TLR9 agonist in immune cells. These sequences are found much more frequently in bacterial genomes than in vertebrate genomes which are also usually methylated (Akira and Hemmi 2003). Treatment of BMDCs with CpG has been reported to be associated with a preferential type 1 cytokine and chemokine profile, similar to response of LPS stimulation. In agreement with this, CpG stimulation evoked secretion of high levels of IL-12. High levels of chemokine secretion in response to CpG has also been reported which we demonstrated with MIP-1 α and MIP-2 (Dearman et al. 2009). Furthermore CD40, CD80 and CD86

expression were all up-regulated, in agreement with previously published work (Dowling, Hamilton and O'Neill 2008).

In summary, we have demonstrated that the BMDCs in this study display a distinct pattern of TLR responsiveness consistent with the published literature. Different TLR ligation provoked selective cytokine and chemokine secretion along with surface marker expression. In order to determine if we could use JAWS II DCs as a model to examine the role of SNAREs in DCs we wanted to compare their response to TLR ligands to the response we observed with BMDCs. When we compared between primary BMDCs and the JAWS II DC cell line there were some differences in these parameters.

The IL-12 cytokine family is composed of IL-12, IL-23, IL-27 and the recently identified IL-35. The ability of DCs to release IL-12 in response to microbial stimuli is considered pivotal for the induction of a T_H1 response (Collison et al. 2007). We demonstrated BMDCs secreted IL-12 in response to most TLR ligation. In comparison JAWS DCs secreted negligible levels of IL-12p40 and IL-27p28, IL-12p70 and IL-23. IL-12 is composed of p35 and p40 subunits, which when they come together form the bioactive IL-12p70. IL-23 is also composed of the IL-12p40 subunit and IL-23p19 (Gee et al. 2009). The lack of IL-12p70 and IL-23 expression seen in this study may be accounted for by the low levels of IL-12p40 secreted from the JAWS II DCs. IL-27p28 subunit which makes up IL-27 when combined with Epstein-Barr virus induced gene 3 (EBI3) subunit is also expressed at low levels possibly indicating a redundancy in the IL-12 family in JAWS II DCs. There are conflicting reports in the literature regarding the secretion of IL-12 from JAWS II DCs. Jiang *et al.*, reported similar levels of IL-12 secretion from JAWS II and

BMDCs when stimulated with LPS and *Chlamydia* (Jiang et al. 2008) however Jørgensen *et al.*, also reported lack of IL-12 production along with Zapala *et al* (Jorgensen, Haase and Michelsen 2002, Zapala et al. 2011) Indeed Pajtasz-Piasecka *et al.*, had to transduce JAWS II DCs with IL-12 genes to generate an anti tumor response in immunotherapy of C57BL/6 mice bearing transplantable murine colon carcinoma (MC38) which strongly supports our findings (Pajtasz-Piasecka et al. 2007).

Other cytokines have been reported to be secreted in large amounts, such as, IL-1, IL-6 and TNF- α from JAWS II DCs in response to LPS (Jorgensen, Haase and Michelsen 2002), and Poly (I:C) (Zapala et al. 2011). This correlated with our results but to a lesser degree with Poly (I.C.). These discrepancies can be somewhat explained by the time-points used in our study, which was 24 hours and the published studies which used 48 hours. We also reported novel data regarding the secretion of these cytokines which were only slightly up-regulated in response to TLR2 and TLR5 stimulation and not with TLR9 agonist. Loxoribine stimulation resulted in a similar pattern of secretion to TLR4 stimulation.

Basal expression of IL-10, can be seen in JAWSII DCs. This could be indicative of picogram levels of endotoxin. FCS used in the fully supplemented media has been reported to contain this contaminating endotoxin (Rinehart et al., 1997). However the IL-10 levels are at such low amount and co-stimulatory markers are not up-regulated it would suggest that the JAWS DCs have not been matured due to the presence of an endotoxin.

Chemokine production has been reported on to a much lesser extent however Zapala *et al.*, report that monocyte chemotactic protein-1 (MCP-1) is secreted in response to LPS and Poly (I:C) stimulation and MIP-2 expression was seen at high levels when stimulated with TLR4 and TLR7 but not induced in response to TLR2, TLR3, TLR5 and TLR9 from JAWS II DCs (Zapala et al. 2011). This MIP-2 expression correlated well with our data. BMDCs secrete a wide range of chemokines upon stimulation so would need to be assessed further in JAWS II DCs. We show novel chemokine data of high-levels of MIP-1 α when stimulated with TLR4 and TLR7 and smaller amounts with TLR2, TLR3 and TLR5. There was no secretion following stimulation with TLR9. Previously reported data on the lack of TLR9 expression on DCs may be responsible for the lack of responsiveness to CpG stimulation (Zapala et al. 2011).

High levels of expression of MHC II have previously been reported in JAWS II DCs in response to LPS (Jorgensen, Haase and Michelsen 2002) which is in agreement with our results. We also noted expression of MHC II in response to TLR2, TLR3, TLR7 stimulation but not with TLR5 or TLR9. Co-stimulatory molecules such as CD80 and CD86 were up-regulated in response to a TLR4 agonist, as was CD14 expression post TLR4 activation, which is in agreement with previously published work (Jorgensen, Haase and Michelsen 2002). CD14 expression was also up-regulated in response to TLR2, TLR3 and TLR7, which to our knowledge is novel data as was Loxoribine being the only other TLR ligand to stimulate any expression of CD80 or CD86.

Zapala *et al.*, showed LPS, Poly (I:C) and CpG induced the expression of TLR2 JAWS II DCs (Zapala et al. 2011). This is in agreement with our data and we also

showed that TLR2 expression was up-regulated in response to PGN and Loxoribine stimulation. TLR4 expression has been reported to be “moderately” expressed on control JAWSII DCs and show little to no change following activation with TLR3, TLR4 or TLR9 ligands (Zapala et al. 2011), however we report that TLR4 expression was induced by TLR2, TLR3, and TLR7 activation but not TLR9 and TLR4.

Another important finding was that, JAWS II DCs appear not to have expression of the cell surface marker CD40 even after stimulation of with the TLR ligands. Jørgensen *et al.* also noted this with LPS stimulation (Jorgensen, Haase and Michelsen 2002). CD40 is a co-stimulatory molecule reported necessary for activation of naïve T cells. Interestingly Haase *et al.*, used the fact that JAWS II DCs do not express this marker to investigate its function and concluded that CD40 is necessary for activation of naïve T cells *in vivo* but not *in vitro* (Haase, Michelsen and Jorgensen 2004) .

Overall JAWS II DCs expressed markers of maturation and secreted immune mediators similar to BMDCs in response to a panel of TLR ligands. However two key differences included lack of CD40 expression and significantly reduced IL-12 secretion. Given that the purpose of the model will be to examine the role of SNAREs in DCs, the fact they do not secrete certain cytokines or chemokines in response to particular TLR ligands may provide us with a useful model to study its secretion by comparing SNARE expression in BMDCs versus JAWS II DCs.

CHAPTER 4

SNARE EXPRESSION

DURING IMMUNE

ACTIVATION

4.1 INTRODUCTION

Since the 1980s when SNARE proteins were first discovered there has been much work to characterise their function. In the 1990s Sudof *et al.*, was one of the first to look at SNARE proteins in membrane fusion. They did this with *in vivo* experiments which showed that membrane fusion could not occur when SNARE proteins were destroyed with neurotoxins. This study indicated an essential role for SNAREs in the trafficking of molecules and membranes within cells (Sudhof 1995). To date there are 38 members of the SNARE family, the subcellular locations and differential combinations of SNARE proteins differ between cell types. The pairing of SNARE proteins is selective, this limits trafficking and membrane fusion between intracellular organelles or membrane fusion (Stow, Manderson and Murray 2006a). Studies into expression of individual SNAREs and their subcellular locations has led to the mapping intracellular pathways. More advanced work has begun to assign functions to SNAREs in specific cellular immune responses such as the role of STX6 and Vti1b in the secretion of TNF from activated macrophage (Murray et al. 2005b).

In the previous chapter we confirmed the value of using the JAWS II DC cell line to examine the role of SNAREs in DCs. Given the important role of cytokine secretion from DCs in inflammatory disease we were particularly interested in exploring the SNAREs necessary for secretion of these key cytokines and chemokines.

In order to examine the role of SNAREs in DCs we used reverse transcriptase-polymerase chain reaction (RT-PCR) and reverse transcriptase *quantitative* polymerase chain reaction (RT-qPCR). Since 2009 and the publication of the Minimum Information for Publication of Quantitative Real Time PCR Experiments (MIQE) guidelines the procedures for PCR have become more stringent. These

guidelines are helping to create credible, consistent and reliable data which allow results be reproducible from lab to lab and allow for more reliable publications (Bustin et al. 2009). These guidelines and requirements have formed the basis of the protocols used in this chapter and are shown in the preliminary experiments at the start of this chapter. For example RNA integrity was investigated for each individual experiment; all details on qPCR target information such as gene symbol, sequence accession number and amplicon length are provided. Identification of a robust endogenous control was undertaken and primers have been validated by means of calibration curves.

The differential cytokine and chemokine secretion between BMDCs and JAWS II DCs and within the JAWS II DCs itself to TLR ligands, provides the opportunity to identify SNARE candidates which play key roles in specific cytokine or chemokine secretion. The objective of this chapter was to characterise the expression of SNARE proteins in JAWS II DCs following activation with TLR ligands. An up-regulation of SNARE expression in DCs following activation may indicate a role for them in cytokine or chemokine secretion. Furthermore identifying the expression and localization of SNARE proteins could provide us with potential therapeutic targets to modulate cytokine or chemokine secretion by DCs. Therefore we investigated the expression of SNARE mRNA in JAWS II DCs following activation with a number of TLR ligands.

We also wanted to determine the relevance of any up-regulated SNAREs in inflammatory disease. Therefore we examined their expression in two models of experimental IBD, the dextran sodium sulphate (DSS)-induced colitis mouse model and the *Citrobacter rodentium* infection model.

4.2 RESULTS

4.2.1 INSURANCE REMOVAL OF GENOMIC DNA

JAWS II DCs were cultured for seven days in the presence of murine recombinant GM-CSF (Sigma ®) and plated at 1×10^6 cell/ml. Cells were then stimulated with 100ng/ml LPS (*E. coli* serotype R515) for 24 hours. Total RNA was extracted from the cells using the Nucleospin™ RNA II extraction kit (Machinery Nagel, Dueren, Germany). RNA purity was checked by Nanodrop™ Spectrometer and RNA quality by electrophoresis on a denaturing agarose gel. Only intact RNA, which appeared as two sharp bands at 28S and 18S, was used for any experiment hereon [Figure 4.1A]. cDNA was synthesised using High Capacity Reverse Transcription Kit (Applied Biosystems™).

As can be seen from **Table 4.1** most of the primers target the non-coding mRNA. To prevent any amplification of this region, a DNase step was carried out to remove the genomic DNA in the RNA extraction. To ensure the removal of genomic DNA the use of an intron flanking primer was employed. PCR was performed using GoTaq® DNA polymerase (Promega, Southampton, UK) and the PCR products run out on an agarose gel [Figure 4.1B]. Presence of genomic DNA would result in two amplicons, one large amplicon containing the genomic DNA and one smaller containing the desired PCR product. All mRNA was checked by this means for genomic contamination, however none was detected.

4.2.2 EXPRESSION OF SNARE MRNA DURING LPS ACTIVATION

JAWS II DCs were cultured for seven days in the presence of murine recombinant GM-CSF (Sigma®) and plated at 1×10^6 cell/ml. Cells were then stimulated with 100ng/ml LPS (*E. coli* serotype R515) for 24 hours. Total RNA was extracted from the cells using the NucleoSpin RNA II extraction kit (Machinery Nagel, Dueren, Germany). cDNA was synthesised using High Capacity Reverse Transcription Kit (Applied Biosystems), PCR was performed using GoTaq® DNA polymerase (Promega, Southampton, UK) and the PCR products run out on an agarose gel [Figure 4.2].

Of the 38 known mammalian SNAREs, we screened 18 SNAREs for their presence in the JAWS II DCs. All eighteen SNAREs were expressed in the mRNA of the JAWS II DCs in response to LPS (100ng/ml) for 24 hours [Figure 4.2].

4.2.3 IDENTIFICATION OF ROBUST ENDOGENOUS CONTROL FOR RT-QPCR

JAWS II DCs were cultured for seven days in the presence of murine recombinant GM-CSF (Sigma ®) and plated at 1×10^6 cell/ml. Cells were then stimulated with 100ng/ml LPS (*E. coli* serotype R515) and 1mM Loxoribine for 24 hours. Total RNA was extracted and converted to cDNA and RT-qPCR was performed using 18S Ribosomal RNA (S18), β -actin and Glyceraldehyde 3-phosphate dehydrogenase (GAPDH) primers. Raw Cq's were plotted and S18 showed the smallest standard deviation between the technical replicates and the samples and thus was used for all subsequent experiments [Figure 4.3].

4.2.4 PRIMER OPTIMISATION

As PCR efficiency is highly dependant on the primers, PCR amplification efficiency was established by means of a calibration curve. JAWS II DCs were cultured for seven days in the presence of murine recombinant GM-CSF (Sigma ®) and plated at 1×10^6 cell/ml. Cells were then stimulated with 100 ng/ml LPS (*E. coli* serotype R515) for 24 hours. Total RNA was extracted and converted to cDNA. Using a series of ten-fold dilutions of this neat cDNA, absolute quantification RT-PCR was run. A calibration curve was prepared with the logarithm of the initial cDNA concentration plotted on the *x* axis and Cq on the *y* axis. From this the regression coefficient was calculated and the slope. PCR efficiency was calculated using the following formula:

$$PCR\ Efficiency = \left(10^{(-1/slope)} - 1\right) * 100\%$$

A good primer set should have an efficiency between 90% and 110% which corresponds to a slope of between -3.58 and -3.10. SNAP-23 achieved 99% [Figure 4.4] and the other 17 SNAREs and subsequent primers used in this thesis were also deemed to achieve efficiencies within the acceptable range [Table 4.1].

4.2.7 MRNA EXPRESSION OF SNARES IN JAWS DCS FOLLOWING TIME DEPENDENT ACTIVATION WITH A TLR LIGAND; TLR-2 PEPTIDOGLYCAN (PGN), TLR 4 LIPOPOLYSACCARIDE (LPS) AND TLR7 LOXORIBINE

JAWS II DCs were cultured for seven days in the presence of murine recombinant GM-CSF (Sigma ®) and plated at 1×10^6 cell/ml. Cells were then stimulated with $5\mu\text{g/ml}$ PGN, 100ng/ml LPS (*E. coli* serotype R515) or 1mM Loxoribine over a time-course. Total RNA was extracted, converted to cDNA, which was then subjected to quantitative real-time PCR. $2^{-\Delta\Delta Cq}$ formula of the delta-delta Cq method was used and a fold change in expression of SNARE genes was normalized against that of endogenous control S18. SNARE mRNA levels were determined relative to expression in the absence of TLR stimulation, which is given an arbitrary value of 1.

4.2.7.1 mRNA EXPRESSION OF Qa-SNAREs, STX2, STX3, STX4, STX5, STX7, STX11, STX12 AND STX16

Activation of JAWSII DCs with LPS and Loxoribine resulted in a significant decrease in STX2 mRNA expression at 4 hours (h) post stimulation compared to control cells ($p \leq 0.001$) [Figure 4.5]. However STX2 levels in response to PGN remained unchanged compared to control cells [Figure 4.5]. Expression of STX3 mRNA in JAWSII DCs significantly increased following activation with LPS and Loxoribine post 1h and 4h stimulation ($p \leq 0.01$ and $p \leq 0.05$) [Figure 4.6]. In contrast STX3 levels in response to PGN were decreased significantly at 1h, 4h and 12h ($p \leq 0.01$, $p \leq 0.05$ and $p \leq 0.05$) compared to control cells [Figure 4.6]. STX4 mRNA expression generally remained unchanged with LPS and PGN stimulation at 1h, 4h and 12h [Figure 4.7]. There was a significant decrease one hour post Loxoribine stimulation ($p \leq 0.05$) in STX4 mRNA expression compared to control cells [Figure 4.7]. No significant changes in STX5 mRNA were observed with LPS or Loxoribine stimulation at 1h, 4h or 12h [Figure 4.8], however PGN stimulation at 4h and 12h significantly increased STX5 mRNA expression compared to control cells ($p \leq 0.05$,

$p \leq 0.001$) [Figure 4.8]. Loxoribine stimulation for 12h significantly decreased STX7 mRNA expression in JAWS II DCs compared to control cells ($p > 0.05$) [Figure 4.9]. One hour stimulation of PGN significantly decreased mRNA expression of STX7 ($p \leq 0.05$) [Figure 4.9]. STX7 mRNA remained unchanged with LPS stimulation at 1h, 4h or 12h compared to control cells [Figure 4.9]. STX11 mRNA expression in JAWSII DCs increased significantly with LPS, Loxoribine and PGN at 1h and 4h compared to control cells ($p \leq 0.001$) [Figure 4.10]. 12h stimulation with LPS and Loxoribine also resulted in significantly up-regulated STX11 compared to control cells ($p \leq 0.001$) [Figure 4.10]. LPS stimulation of JAWSII DCs resulted in significant up-regulation of STX12 mRNA at 1h and 4 h compared to control cells ($p \leq 0.01$, $p \leq 0.001$) [Figure 4.11]. Loxoribine stimulation also significantly increased STX12 mRNA at 4h compared to control cells ($p \leq 0.001$) and PGN stimulation had no effect on STX12 mRNA levels compared to control cells [Figure 4.11]. There was significant up-regulation of STX16 mRNA in JAWSII DCs 4h and 12h post LPS stimulation in comparison to control cells ($p \leq 0.05$, $p \leq 0.001$) [Figure 4.12]. Loxoribine stimulation also resulted in significant up-regulation of STX16 compared to control cells at 12h ($p \leq 0.001$) and STX16 mRNA expression was significantly down-regulated at 1h ($p \leq 0.05$) and subsequently significantly up-regulated at 12h ($p \leq 0.05$) post PGN stimulation [Figure 4.12].

4.2.7.2 mRNA EXPRESSION OF Qbc SNARE SNAP23

SNAP-23 mRNA expression increased significantly post 12h stimulation with Loxoribine ($p \leq 0.001$) and PGN ($p \leq 0.05$) compared to control cells. SNAP-23 levels in response to LPS remained unchanged compared to control cells [Figure 4.13].

4.2.7.3 mRNA EXPRESSION OF Qb-SNAREs, VTI1a and VTI1b

There was a significant up-regulation of Vti1a mRNA at 4h and 12h post LPS and Loxoribine stimulation ($p \leq 0.01$, $p \leq 0.001$, $p \leq 0.01$) in comparison to control cells [Figure 4.14] Vti1a mRNA expression was significantly up-regulated following PGN at 1h and 4h ($p \leq 0.05$, $p \leq 0.01$) in comparison to control [Figure 4.14]. Vti1b mRNA expression was significantly down-regulated following stimulation with LPS and Loxoribine at 1h ($p \leq 0.05$) in comparison to control cells and in response to PGN stimulation was not significantly changed in response to PGN stimulation [Figure 4.15].

4.2.7.4 mRNA EXPRESSION OF Qc SNARE, STX6

STX6 mRNA remained unchanged with LPS stimulation at 1, 4 or 12 hour [Figure 4.16]. However Loxoribine and PGN stimulation at 12 hour resulted in significant increase of STX6 mRNA expression compared to control cells ($p \leq 0.001$, $p \leq 0.01$) [Figure 4.16].

4.2.7.5 mRNA EXPRESSION OF VAMP2, VAMP3, VAMP4, VAMP7 AND VAMP8

Following LPS, Loxoribine and PGN stimulation, VAMP1 expression was significantly down-regulated in JAWSII DCs at 1 h and 4 h ($p \leq 0.001$) in comparison to control cells and was also significantly down-regulated in response to Loxoribine and PGN at 12 h ($p \leq 0.001$, $p \leq 0.01$). [Figure 4.17]. There was significant up-regulation of VAMP2 mRNA expression at 12 h when stimulated with LPS,

Loxoribine and PGN ($p \leq 0.01$) compared to control cells [Figure 4.18]. Following LPS stimulation VAMP3 expression was significantly up-regulated after 1h compared to control cells ($p \leq 0.05$) however this expression was significantly down-regulated following 12 h of LPS stimulation ($p \leq 0.05$) [Figure 4.19]. Loxoribine significantly up-regulated VAMP3 expression after 4h ($p \leq 0.05$) compared to control cells and stimulation of PGN significantly down-regulated VAMP3 expression after 1 hour ($p \leq 0.05$) in comparison to control [Figure 4.19]. Loxoribine stimulation significantly down-regulated VAMP4 expression at 1 and 4 hour ($p \leq 0.05$, $p \leq 0.01$) in JAWS II DCs compared to control cells, however PGN stimulation resulted in an up-regulation at 12 hour ($p \leq 0.05$) compared to control cells. [Figure 4.20]. LPS stimulation did not have any significant effect on VAMP4 expression [Figure 4.20]. VAMP7 expression remained unchanged following stimulation with LPS and Loxoribine compared to control. However PGN stimulation resulted in significant down-regulation of VAMP7 after 1 hour ($p \leq 0.05$) compared to control cells [Figure 4.21]. Following Loxoribine stimulation VAMP8 expression was significantly down-regulated at 12 hour ($p \leq 0.05$) and up-regulated following PGN stimulation after 4h. LPS stimulation did not have any significant effect on VAMP8 expression [Figure 4.22].

The SNARE mRNA up-regulation from JAWSII DCs following TLR ligand stimulation data was tabulated along with JAWSII cytokine and chemokine to aid in identification of candidate SNAREs, see Table 4.2.

4.2.8 mRNA EXPRESSION OF PRO-INFLAMMATORY CYTOKINES AND CHEMOKINES IN THE COLON IN A OF DSS INDUCED COLITIS MODEL

Given that there were some significant changes in expression of SNAREs following activation of DCs with TLR ligands, in particular there were significant changes in STX3, STX11 and Vti1a (candidate SNAREs) with little changes in STX4, SNAP23 and VAMP4, we therefore wanted to assess whether they were regulated *in vivo* during inflammatory disease. For this we used the DSS model experimentally induced colitis. DSS is a negatively charged glucose polymer with engrafted sulphate groups, which, when delivered in drinking water of mice induces intestinal inflammation mimicking the clinical and histological features of IBDs that have characteristics of UC (Laroui et al. 2012).

This DSS colitis model was carried out in collaboration with Silvia Melgar in the Alimentary Pharmabiotic Centre, University College Cork. C57BL mice were split randomly into 5 groups. The control group contained 6 mice and the 4 test groups had 6-8 mice. DSS (Sigma) was prepared fresh daily and added to the drinking water of the mice at a final concentration of 3% for 5 days. Early acute, late acute and chronic mice were culled at 7, 12 and 26 days respectively. Mice were weighed and scored for daily disease activity (DDAI) every 3-4 days. DDAI was based on stool composition, fur texture and posture indicators of gut inflammation. The control group maintained a healthy weight and gained weight over the course of the study as expected. DSS treated groups lost weight immediately with the biggest loss in weight observed when the early acute mice were culled (day 7). Late acute and

chronic mice then began to recover and gain weight. Late acute mice (day 12) demonstrated a minor recovery in weight and when chronic mice (day 26) had recovered to their original weight with a slight gain [Figure 4.23(a)]. The DDAI clinical scoring showed a comparable pattern of disease with no disease observed in the control mice and a rapid increase in disease activity in all DSS-treated groups with some recovery in the chronic group at day 26 [Figure 4.23(b)]. The washed colons of each animal were removed, measured and weighed individually. Colon length and weight are indicators of gut inflammation as cell infiltration and inflammation increases the weight and shrinks the length of the colon. Colon length and weight from all DSS treated groups showed signs of gut inflammation with a significant increase in weight and significant decrease in colon length ($p \leq 0.01$, $p \leq 0.05$) [Figure 4.23(d),(e)]. Once the colons had been measured and weighted a small section of distal colon was removed for histology and homogenisation for total RNA isolation. The colon tissue was cast in optimal cutting temperature (OCT) compound and snap frozen in liquid nitrogen and stored at -80°C . Sections were then cut on a cryostat mounted onto slides and subjected to Hematoxylin and Eosin (H&E) staining for histological analysis. H&E staining demonstrated a healthy colon in the control group with good crypt formation and no infiltrating cells in the lower muscle layer of the gut. The early and late acute H&E staining shows a breakdown of crypt structures and infiltration of cells (purple spots) in the muscular layer with the worst infiltration evident in the late acute group. The chronic group shows some mild recovery with crypt structure evident and less infiltrating cells in the muscular layer consistent with the rest of the data [Figure 4.23(e)].

Total RNA was extracted from homogenised colonic tissue of mice at various stages of DSS colitis; early acute, late acute and chronic including controls, converted to

cDNA, which was then subjected to quantitative real-time PCR. $2^{-\Delta\Delta Cq}$ formula of the delta-delta Cq method was used and a fold change in expression of cytokine or chemokine genes was normalized against that of endogenous control S18. SNARE mRNA levels are relative to its expression in the absence of colitis, which is given an arbitrary value of 1.

This model is well characterised with increased cytokine and chemokine secretion during disease. Therefore we first confirmed disease in the colon by examining the level of pro-inflammatory cytokines and chemokines present. IL-6 mRNA expression was significantly up-regulated in early and late acute stages of DSS colitis ($p \leq 0.001$, $p \leq 0.05$) [Figure 4.24]. mRNA expression of TNF- α was significantly up-regulated in all stages of DSS colitis in comparison to healthy controls ($p \leq 0.001$, $p \leq 0.01$ and $p \leq 0.05$) [Figure 4.24]. Early acute stage of DSS colitis resulted in significant levels of IFN- γ mRNA expression compared to healthy controls ($p \leq 0.001$) [Figure 4.24]. MIP-1 α mRNA expression was significantly increased in the early acute, late acute and chronic stages of DSS colitis in comparison to healthy controls ($p \leq 0.001$ and $p \leq 0.01$) [Figure 4.24]. Early and late acute stages of disease resulted in significant increased levels of chemokine MIP-2 mRNA levels ($p \leq 0.001$ and $p \leq 0.05$) [Figure 4.24]. MCP mRNA expression was also up-regulated during early and late acute stages of disease along with chronic stage of DSS colitis in comparison to healthy controls ($p \leq 0.001$ and $p \leq 0.05$) [Figure 4.24].

4.2.9 mRNA EXPRESSION OF SNARES IN THE COLON FOLLOWING INDUCTION OF DSS INDUCED COLITIS MODEL

After confirming inflammation in the colon, we next examined expression of candidate SNAREs STX3, STX11 and Vti1a and unchanged SNARE, STX4, SNAP23 and VAMP4 post DC activation in DSS induced colitis.

Total RNA was extracted from colonic tissue of mice at various stages of DSS colitis; early acute, late acute and chronic including controls, converted to cDNA, which was then subjected to quantitative real-time PCR. $2^{-\Delta\Delta Cq}$ formula of the delta-delta Cq method was used and a fold change in expression of SNARE genes was normalized against that of endogenous control S18. SNARE mRNA levels are expressed relative to its expression in the absence of colitis, which is given an arbitrary value of 1.

STX11 and STX3 were the two SNAREs to be most significantly up-regulated in the DSS model. STX11 was significantly up-regulated in DSS induced colitis model with a ~30 fold change in early stages and a ~10 fold change in the late stages ($p \leq 0.001$, $p \leq 0.01$) [Figure 4.25]. STX3 mRNA expression was significantly increased with a ~3 fold change in the late acute stages of DSS colitis ($p \leq 0.01$). SNAP23 was also up-regulated significantly in late acute phase of stages of DSS colitis ($p \leq 0.01$) and STX4 mRNA expression was significantly increased in both the early and late acute stages of disease ($p \leq 0.05$) [Figure 4.25]. Early and late acute stages of DSS induced colitis have significantly up-regulated expression of Vti1a mRNA expression in comparison to healthy controls ($p \leq 0.01$, $p \leq 0.05$) [Figure 4.25]. Vamp4 was the only SNARE to be significantly decreased in expression during DSS colitis, which was during the early acute phase of disease ($p \leq 0.05$) [Figure 4.25].

4.2.10 mRNA EXPRESSION OF PRO-INFLAMMATORY CYTOKINES AND CHEMOKINES IN THE COLON FOLLOWING INFECTION WITH *CITROBACTER RODENTIUM*

We next wanted to examine the expression of the candidate SNAREs in another model of colitis, which is induced by *Citrobacter rodentium* infection. However we first had to assess the cytokine and chemokine production in the colons of the mice to confirm inflammation. *C. rodentium* is a gram negative murine specific bacterium that causes a similar pathology in mice to that caused by enteropathogenic *Escherichia coli* in humans. This rare model offers the opportunity for understanding chronic inflammatory responses seen in genetically susceptible IBD patients following abnormal exposure to enteric bacteria of the intestinal mucosal immune system (Bhinder et al. 2013).

The *C. rodentium* colitis model was also performed in collaboration with Silvia Melgar in the Alimentary Pharmabiotic Centre, University College Cork. C57BL mice in groups of 6-8 were inoculated orally by a 200 µl gavage of approximately 200×10^9 CFU *C. rodentium*. Mice were sacrificed at 9, 14, 21 and 28 days for tissue processing. Colons were removed, washed, measured and weighed to assess gut inflammation. There was a significant increase in colon weight at day 9 ($p \leq 0.001$) of infection which recovered at days 14, 21 and 28 [Figure 4.26]. The average colon length in the infected mice was also significantly decreased at day 9 ($p \leq 0.05$), with mild recovery at days 14, 21 and 28 [Figure 4.26]. These parameters indicate colitis like symptoms of inflammation in the *C. rodentium* infected mice.

In order to confirm disease total RNA was extracted from homogenised sections of the distal colon of mice infected with *Citrobacter rodentium* over a 21 day period, converted to cDNA, which was then subjected to quantitative real-time PCR. $2^{-\Delta\Delta Cq}$ formula of the delta-delta Cq method was used and a fold change in expression of cytokine or chemokine genes was normalized against that of endogenous control S18. Cytokine or chemokine mRNA levels are expressed relative to its expression in the absence of colitis, which is given an arbitrary value of 1.

IL-6, TNF- α and IFN- γ mRNA expression was significantly increased on day 9 of *C. rodentium* infection in comparison to healthy controls ($p \leq 0.05$, $p \leq 0.01$ and $p \leq 0.001$) [Figure 4.27]. There were no significant changes in MIP-1 α in comparison to healthy controls [Figure 4.27]. MIP-2 mRNA expression was significantly increased at day 3 and day 9 post infection with *C. rodentium* in comparison to healthy controls ($p \leq 0.05$ and $p \leq 0.01$) and MCP mRNA expression was significantly up-regulated at 9 and 21 days in comparison to healthy controls ($p \leq 0.001$ and $p \leq 0.01$) [Figure 4.27].

4.2.11 MRNA EXPRESSION OF SNARES IN THE COLON FOLLOWING INFECTION WITH *CITROBACTER RODENTIUM*

Total RNA was extracted from colonic tissue of mice infected with *C. rodentium* over a 21 day period, converted to cDNA, which was then subjected to quantitative real-time PCR. $2^{-\Delta\Delta Cq}$ formula of the delta-delta Cq method was used and a fold change in expression of SNARE genes was normalized against that of endogenous

control S18. SNARE mRNA levels are relative to its expression in the absence of infection, which is given an arbitrary value of 1.

There were little to no changes in SNAP23 or STX4 in *C. rodentium* infection with a small increase of expression at day 9 and day 3 respectively ($p \leq 0.01$, $p \leq 0.05$) [Figure 4.28]. Vamp4 mRNA expression was up-regulated at day 9 post infection with *C. rodentium* in comparison to healthy controls ($p \leq 0.01$) [Figure 4.28]. Interestingly STX3 was the only SNARE to be down-regulated during *C. rodentium* infection. It was significantly down-regulated at day 3 and day 21 post infection in comparison to healthy controls ($p \leq 0.001$ and $p \leq 0.01$) [Figure 4.28]. STX-11 was up-regulated but at day 9 and day 14 of *C. rodentium* infection in comparison to healthy controls ($p \leq 0.05$) [Figure 4.28]. Vti1a was up-regulated at day 3, day 9 and day 14 post infection in comparison to healthy controls ($p \leq 0.01$, $p \leq 0.001$ and $p \leq 0.05$) [Figure 4.28].

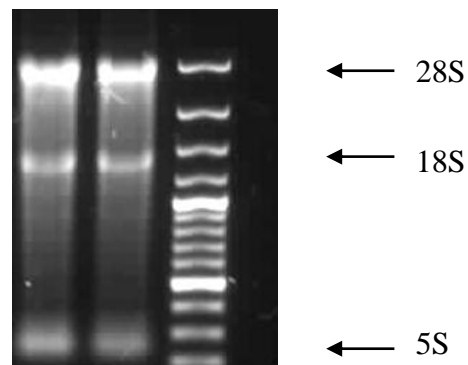
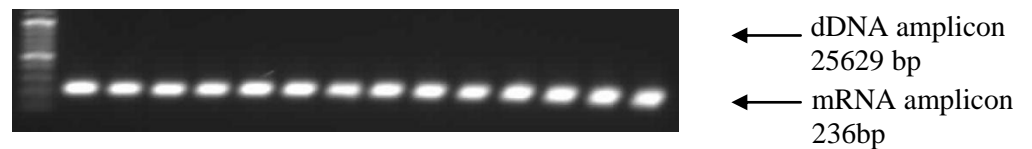
A**B**

FIGURE 4.1: mRNA quality and integrity. A: To assess the integrity of the mRNA post extraction an RNA gel electrophoresis was performed. The clear appearance of the 28S, the 18S and the 5S rRNA with no smearing indicates high quality of RNA. **B:** To ensure the removal of all genomic DNA during the mRNA extraction a PCR using of intron flanking primers, STX7, was conducted for every mRNA extraction. Presence of this contamination would have result in 1 large and 1 small amplicon when the PCR product was run out on a 1% agarose gel.

Table 4.1: Gene, Ref Seq ID, Primer sequences, amplicon length and location of amplicon within the genome.

Gene	Ref Seq ID	Forward [5' to 3']	Reverse [5' to 3']	Location of amplicon	Amplicon Length
SNAP-23	NM_009222	GTTCTTGCTCAGGCTTCC	CCAACCAACCAATACCAATAATG	3' UTR of transcripts 1, 2, and 3	184bp
STX2	NM_007941	GGTGGCAAAGGTGATGTT	CAGGTATGGTCGGAGTCA	3' UTR of transcripts 1	134bp
STX3	NM_001025307	CCACAACCACTAGCATCATAA	CTCAAGAGATATCCGCCTTAA	3' UTR of transcripts 1 and 2	157bp
STX4	NM_009294	GGTGTC AAGTGTGAGAGAG	AACCTCATCTTCATCGTCTG	5' UTR of transcripts 1	148bp
STX5	NM_001167799.1	GCAAGTCCCTCTTTGATGAT	TTCAGATTCTCAGTCCCTCACT	Intron Flanking Primer of transcript 1 and 2	244bp
STX6	NM_021433	CAAGGATTGTTTCAGAGATGGA	CCTGACAATTTGCCGAGTA	Intron Flanking Primer	237bp
STX7	NM_016797	CACAACGCATCTCCTCTAAC	TAATCGGTCTTTCTGTATCTTTCTC	Intron Flanking Primer of transcript 1	236bp
STX11	NM_001163591.1	ATCACGGCAAATGAAGGA	GGTCGGTCTCGAACACTA	3' UTR of transcripts 1	126bp
STX12	NM_133887	CGCAAGAAGATGTGTATCCT	CTCTGAGGCAAGCACTTC	3'UTR	100bp
STX-16	NM_001102432.1	GAGCAGTACCAGAAGAAGAAC	CAAGTCCTATACCAATAATCCA	Exon location 3	155bp
Vti1a	NM_016862	GAATGTATAGCAACAGGATGAGA	CCGTGTTATCCAGCAGATG	Exon Location 3 and 6 of transcript 201, 203, 201	165bp
Vti1b	NM_016862	TACCTTGGAGAACGAGCAT	TGGACATTGAGCGAAGAATC	Intron Flanking of transcript 1	254bp
VAMP1	NM_001080557	CCCTCTGTTTGCTTTCTCA	CGTTGTCTTCGGGTAGTG	3' UTR of transcripts 1 and 2	162bp
VAMP2	NM_009497	CTCCTTCCCTTGATTTAACC	TGAAACAGACAGCGTATGC	3' UTR of transcripts 1	246bp
VAMP3	NM_009498	TTGTTCTTGTTGTATATCACTCCTAA	GGCTCGCTCTCACAGTAT	3' UTR of transcripts 1	202bp
VAMP4	NM_016796	GTATGCCTCCAAGTTCAAG	TGTAGTTCATCCAGCCTCTC	5' UTR of all transcripts	256bp
VAMP7	NM_011515	GATGGAGACTCAAGCACAAAG	GACACAATGATATAGATGAACACAAT	Intron Flanking	242bp
VAMP8	NM_016794	GGCGAAGTTCTGCTTTGA	CTTGACTCCCTCCACCTC	5' UTR of transcript 1	111bp
Mip-1α/CCL3	NM_011337	CCTTGCTGTTCTTCTCTGTACC-	CGATGAATTGGCGTGAATC	Exon Location: 1 - 2	122bp
MIP-2/CXCL2	NM_009140	CAGAAGTCATAGCCACTCTCAAG	CTTCCAGGTCAGTTAGCCTT -	Exon Location: 2 - 4	1191bp
MCP/CCL2	NM_011333	CATCCACGTGTTGGCTCA	AACTACAGCTTCTTTGGGACA-	Exon Location: 1 - 3	142bp
TNF-α	NM_013693	AGA CCCTCA CACTCA GAT CA	TCT TTG AGATCC ATG CCGTTG	Exon Location: 2 - 4	145bp
IL-6	NM_031168	AGC CAG AGT CCT TCA GAG A	TCC TTA GCC ACT CCT TCT GT	Exon Location: 4 - 5	146bp
IFN-γ	NM_008337.3	ATGAACGCACACACTGCATC	CCATCCTTTTGCCAGTTCTC	Intron Flanking	137bp
S18	NM_011296	CTGAGAAGTTCCAGCACATT	GCTTTCCTCAACACCACAT	Intron Flanking Primer of transcript 1 and 2	126bp

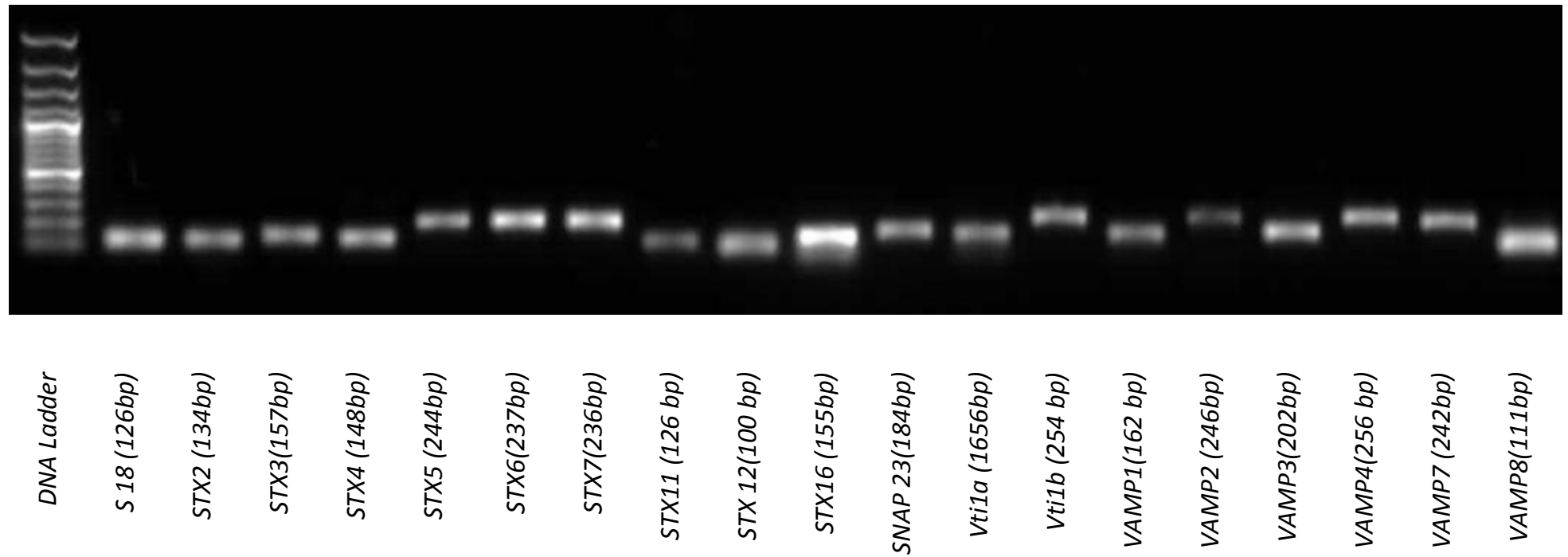


FIGURE 4.2: mRNA expression of SNAREs in JAWS II DCs. JAWSII DCs were plated at 1×10^6 /ml and stimulated with 100 ng/ml LPS for 24 hours. mRNA was extracted and RT-PCR was to detect all 18 SNAREs; STX2, STX3, STX4, STX5, STX6, STX7, STX11, STX12, STX16, SNAP23, Vti1a, Vti1b, VAMP1, VAMP2, VAMP3, VAMP4, VAMP7, VAMP8 and endogenous control S18. Expression of all targets was detected at their respective bp product size.

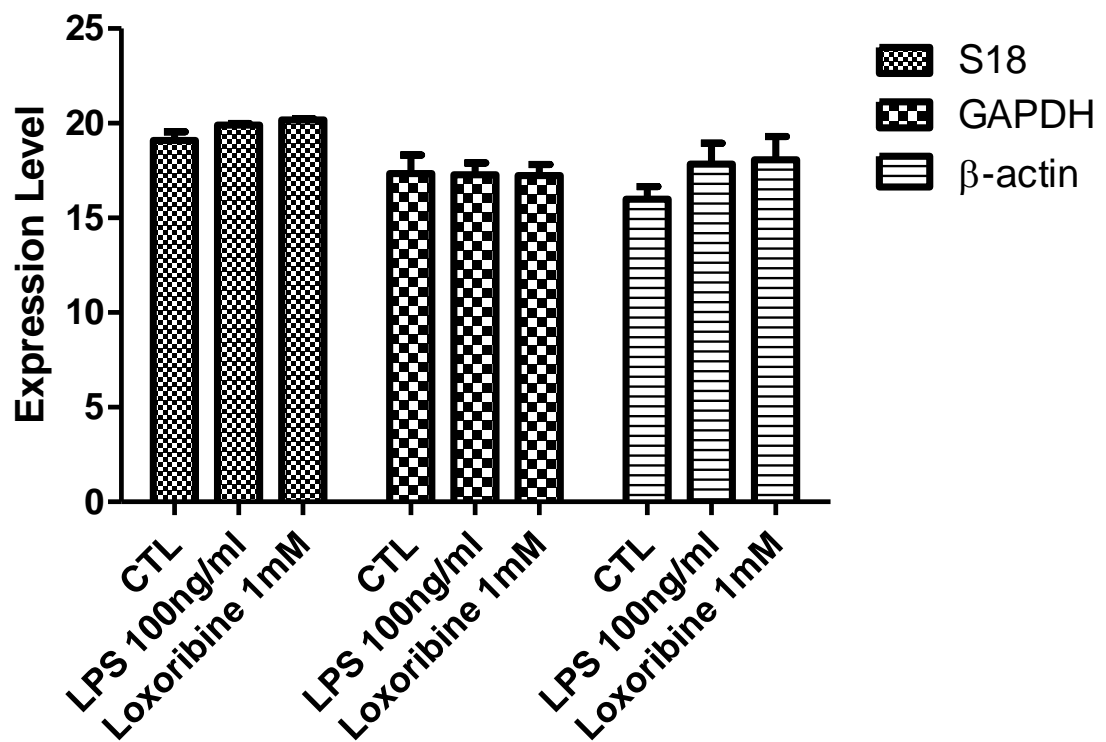


FIGURE 4.3: Identification of an endogenous control for JAWS II DCs. Cells were plated at 1×10^6 /ml and left to rest overnight. Cells were then stimulated with LPS 100 ng/ml and Loxoribine 1mM for 24hours. mRNA was then extracted and RT-qPCR was performed.

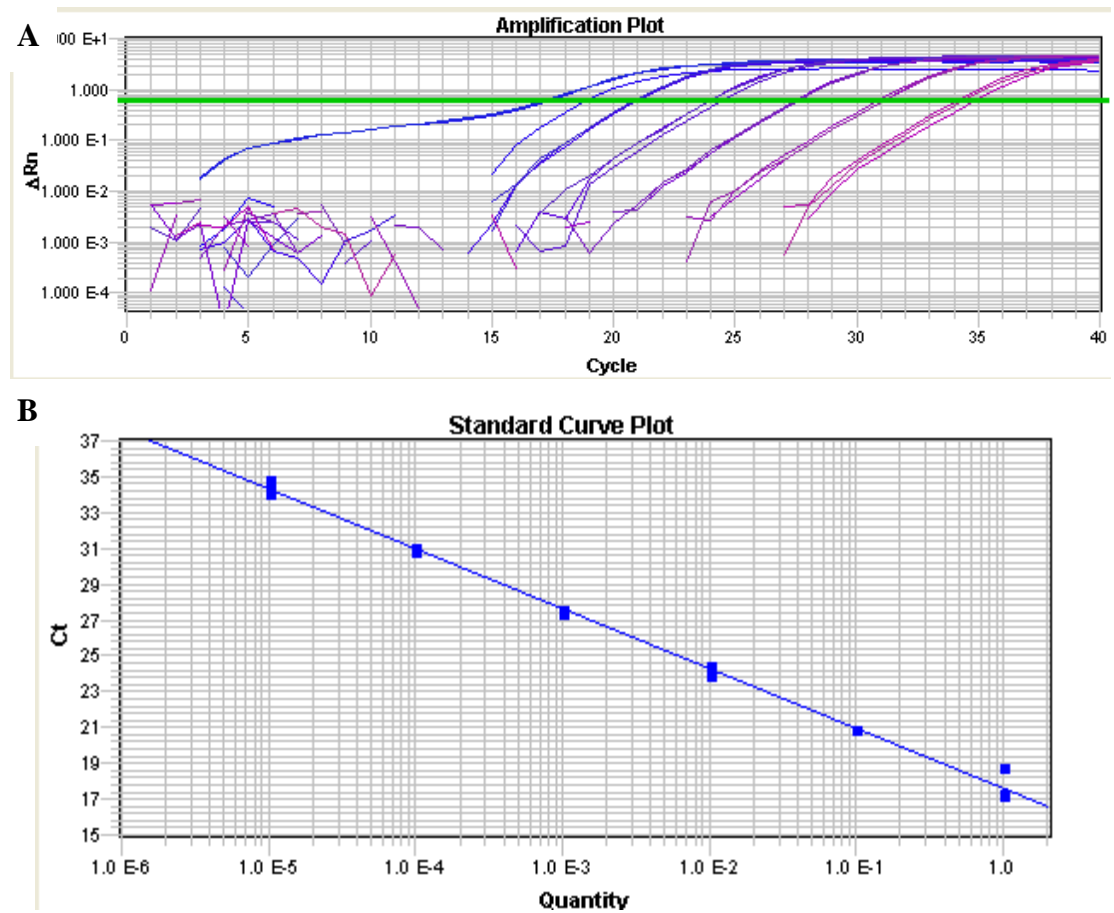


FIGURE 4.4: Assay Validation: Primer Efficiency Curve for SNAP23. RT-qPCR was performed using SNAP-23 primers. Six-fold dilution of neat cDNA of LPS 100 ng/ml JAWS II DCs was prepared. Every dilution was run in triplicate. **A:** Amplification plot of SNAP23. **B:** Standard Curve obtained from SNAP23. The efficiency was 99.37% and the regression squared value was 0.996.

Table 4.2: Assay Validation: Primer Efficiency Curves. RT-qPCR was performed. Six-fold dilution of neat cDNA of LPS 100 ng/ml JAWS II DCs was prepared. Every dilution was run in triplicate. From the standard curves obtained efficiency and the regression squared value were obtained.

Primer	R²	Efficiency
SNAP23	0.996	99%
STX2	0.971	102%
STX3	0.991	108%
STX4	0.992	91%
STX5	0.970	90%
STX6	0.999	90%
STX7	0.955	100%
STX11	0.996	96%
STX12	0.995	102%
STX16	0.991	98%
Vti1a	0.985	92%
Vti1b	0.995	90%
VAMP1	0.988	90%
VAMP2	0.989	120%
VAMP3	0.995	94%
VAMP4	0.999	86%
VAMP7	0.984	91%
VAMP8	0.999	98%
S18	0.988	93%

Table 4.3: Assay Validation: Primer Efficiency Curves. RT-qPCR was performed. Six-fold dilution of neat cDNA of colonic tissue was prepared. Every dilution was run in triplicate. From the standard curves obtained efficiency and the regression squared value were obtained.

Primer	R²	Efficiency
SNAP23	0.955	92%
STX3	0.997	110%
STX4	0.998	99%
STX11	0.955	109%
VAMP4	0.997	103%
S18	0.997	98%
TNF-α	0.997	100%
IFN-γ	0.998	110%

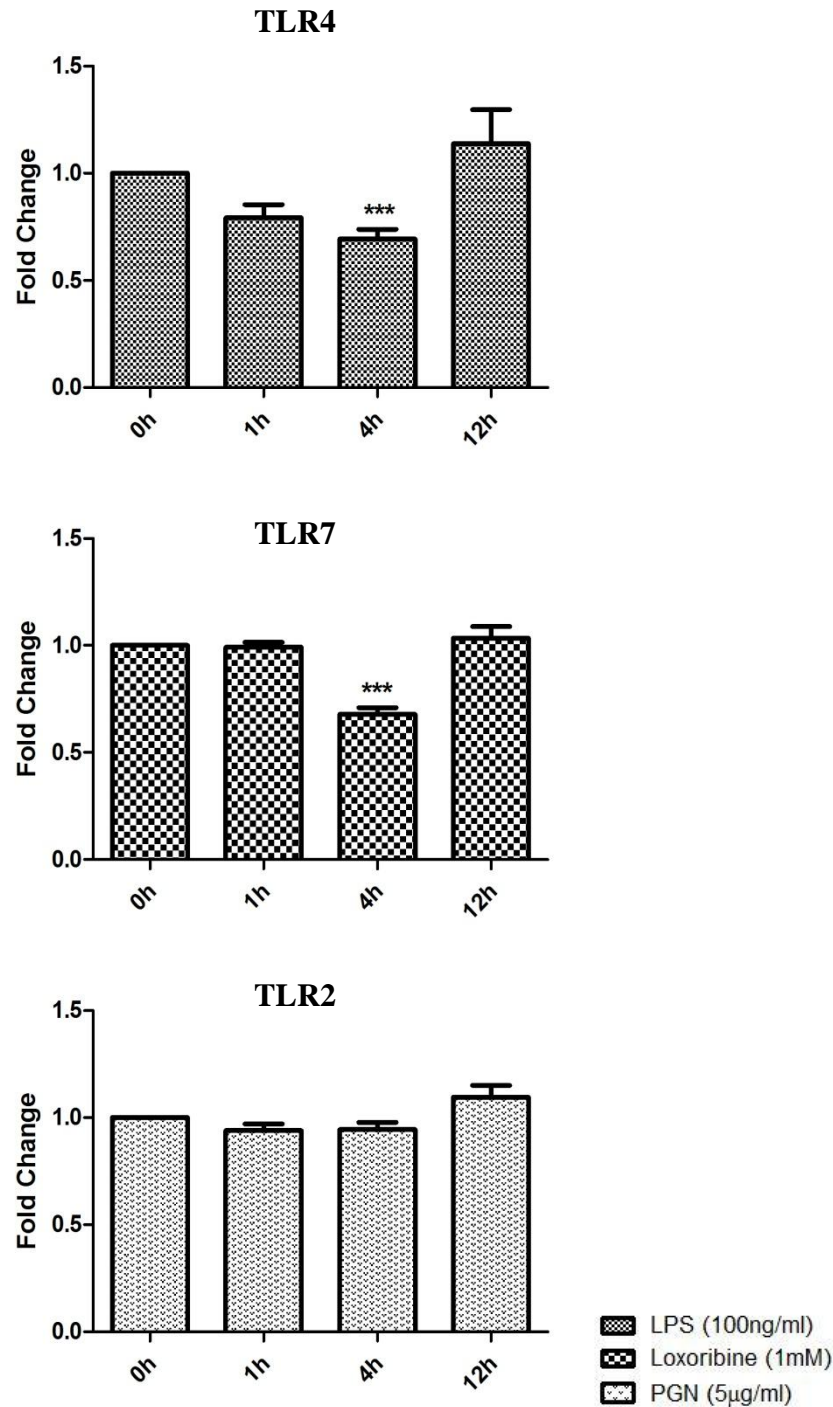


Figure 4.5: Effect of TLR ligand stimulation on STX2 mRNA expression in JAWS II DCs. JAWS II DCs was plated 1×10^6 /ml and stimulated with 100 ng/ml LPS, 1 mM Loxoribine or 5 µg/ml PGN at 1 h, 4 h, and 12 h. The amount of STX2 was quantified by reverse transcription followed by RT-qPCR using an ABI 7900 HT detection system. STX2 levels were assayed in triplicate (using SYBR green technology) and normalised with S18 levels. Fold differences were calculated relative to STX2 levels at time zero (assigned value of 1). Results are mean \pm SEM of quadruplicate assays. A two sample, two tailed student's t-test comparing Δ Cts of control and 1h, 4h, or 12h stimulated sample *** $p \leq 0.001$.

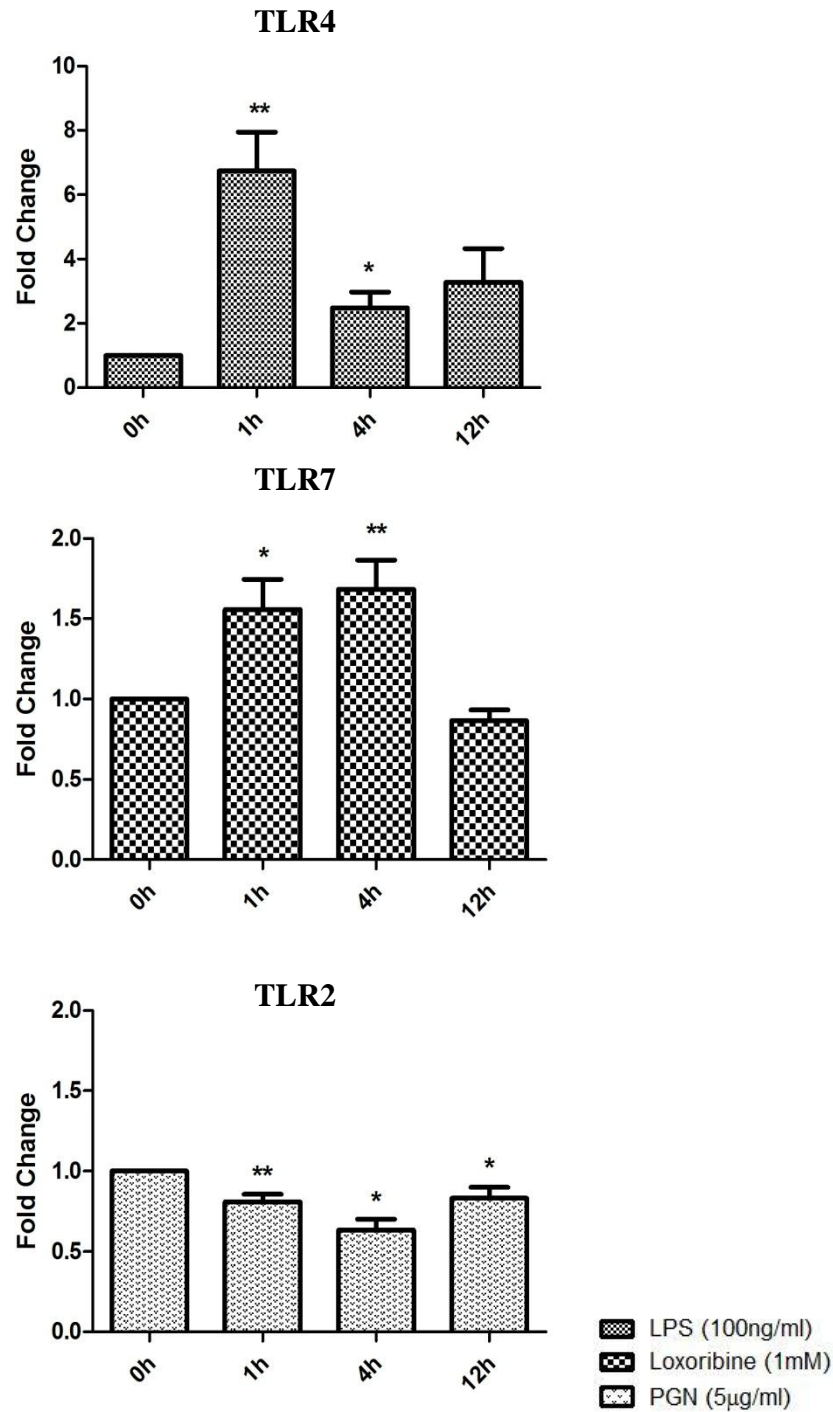


Figure 4.6: Effect of TLR ligand stimulation on STX3 mRNA expression in JAWS II DCs. JAWS II DCs was plated 1×10^6 /ml and stimulated with 100 ng/ml LPS, 1 mM Loxoribine or 5 µg/ml PGN at 1 h, 4 h, and 12 h. The amount of STX3 was quantified by reverse transcription followed by RT-qPCR using an ABI 7900 HT detection system. STX3 levels were assayed in triplicate (using SYBR green technology) and normalised with S18 levels. Fold differences were calculated relative to STX3 levels at time zero (assigned value of 1). Results are mean \pm SEM of quadruplicate assays. A two sample, two tailed student's t-test comparing Δ Cts of control and 1h, 4h, or 12h stimulated sample * $p \leq 0.05$, ** $p \leq 0.01$ *** $p \leq 0.001$.

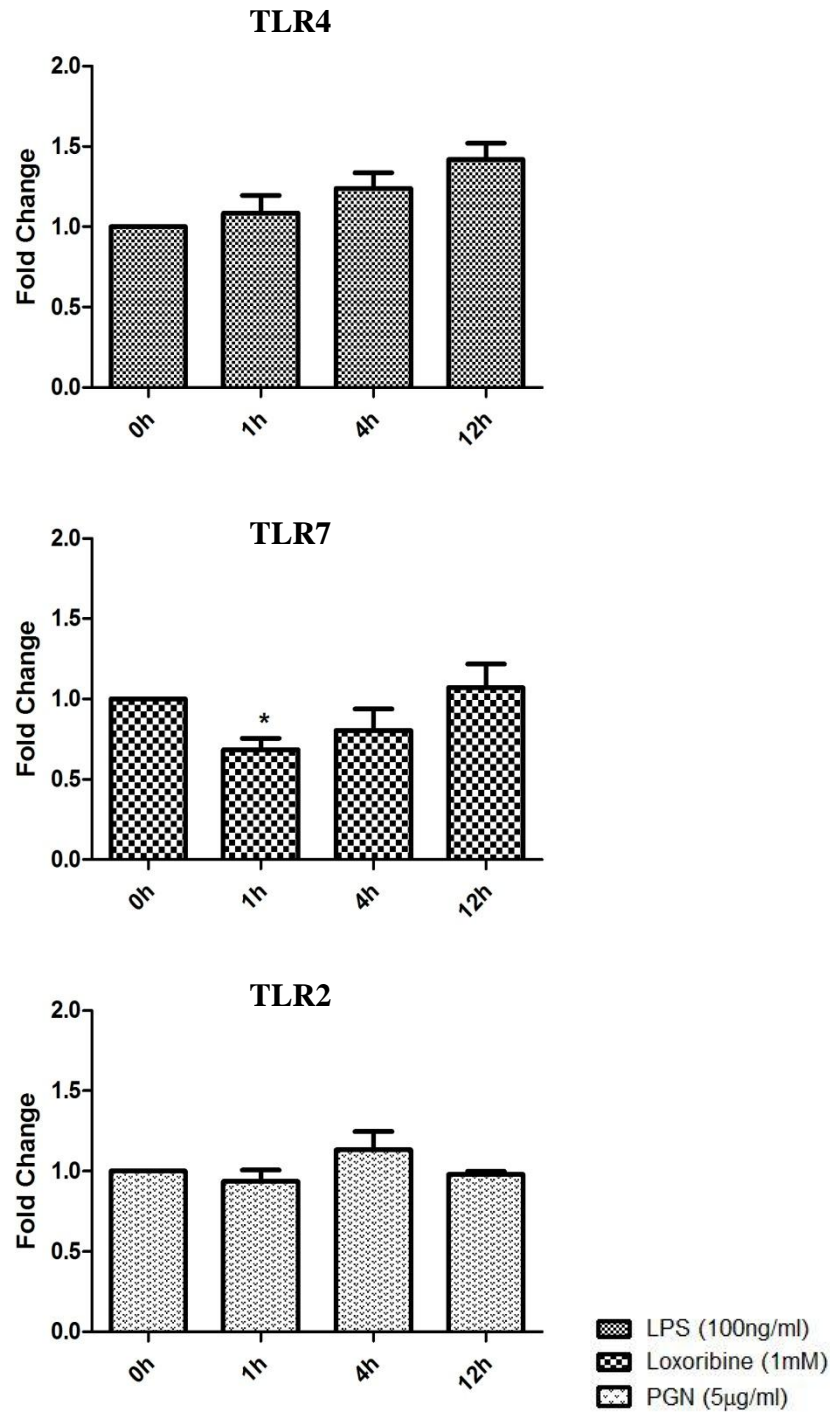


Figure 4.7: Effect of TLR ligand stimulation on STX4 mRNA expression in JAWS II DCs. JAWS II DCs was plated 1×10^6 /ml and stimulated with 100 ng/ml LPS, 1mM Loxoribine or 5µg/ml PGN at 1 h, 4 h, and 12 h. The amount of STX4 was quantified by reverse transcription followed by RT-qPCR using an ABI 7900 HT detection system. STX4 levels were assayed in triplicate (using SYBR green technology) and normalised with S18 levels. Fold differences were calculated relative to STX4 levels at time zero (assigned value of 1). Results are mean \pm SEM of quadruplicate assays. A two sample, two tailed student's t-test comparing Δ Cts of control and 1h, 4h, or 12h stimulated sample * $p \leq 0.05$.

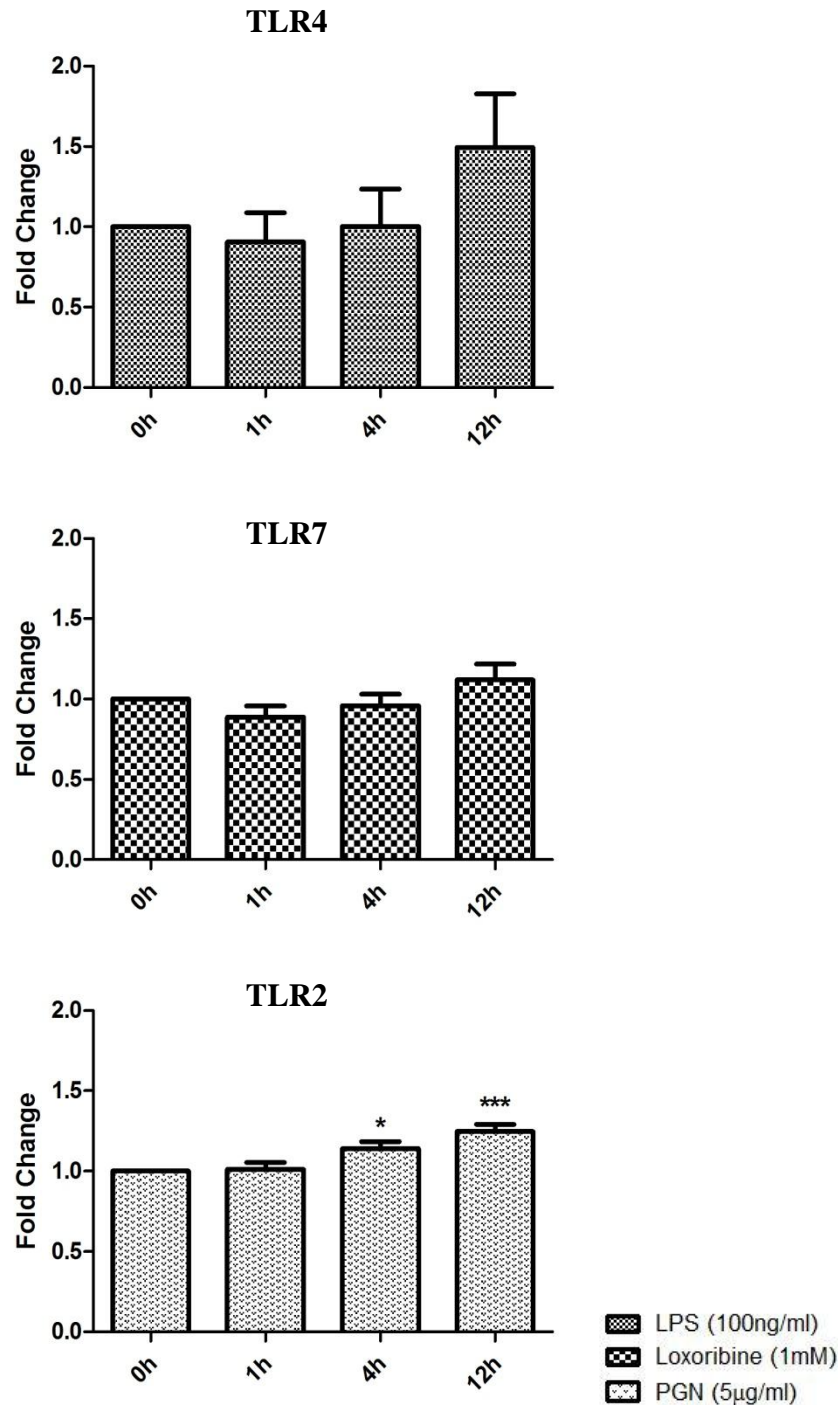


Figure 4.8: Effect of TLR ligand stimulation on STX5 mRNA expression in JAWS II DCs. JAWS II DCs was plated 1×10^6 /ml and stimulated with 100 ng/ml LPS, 1 mM Loxoribine or 5 µg/ml PGN at 1 h, 4 h, and 12 h. The amount of STX5 was quantified by reverse transcription followed by RT-qPCR using an ABI 7900 HT detection system. STX5 levels were assayed in triplicate (using SYBR green technology) and normalised with S18 levels. Fold differences were calculated relative to STX5 levels at time zero (assigned value of 1). Results are mean \pm SEM of quadruplicate assays. A two sample, two tailed student's t-test comparing Δ Cts of control and 1h, 4h, or 12h stimulated sample * $p \leq 0.05$, *** $p \leq 0.001$.

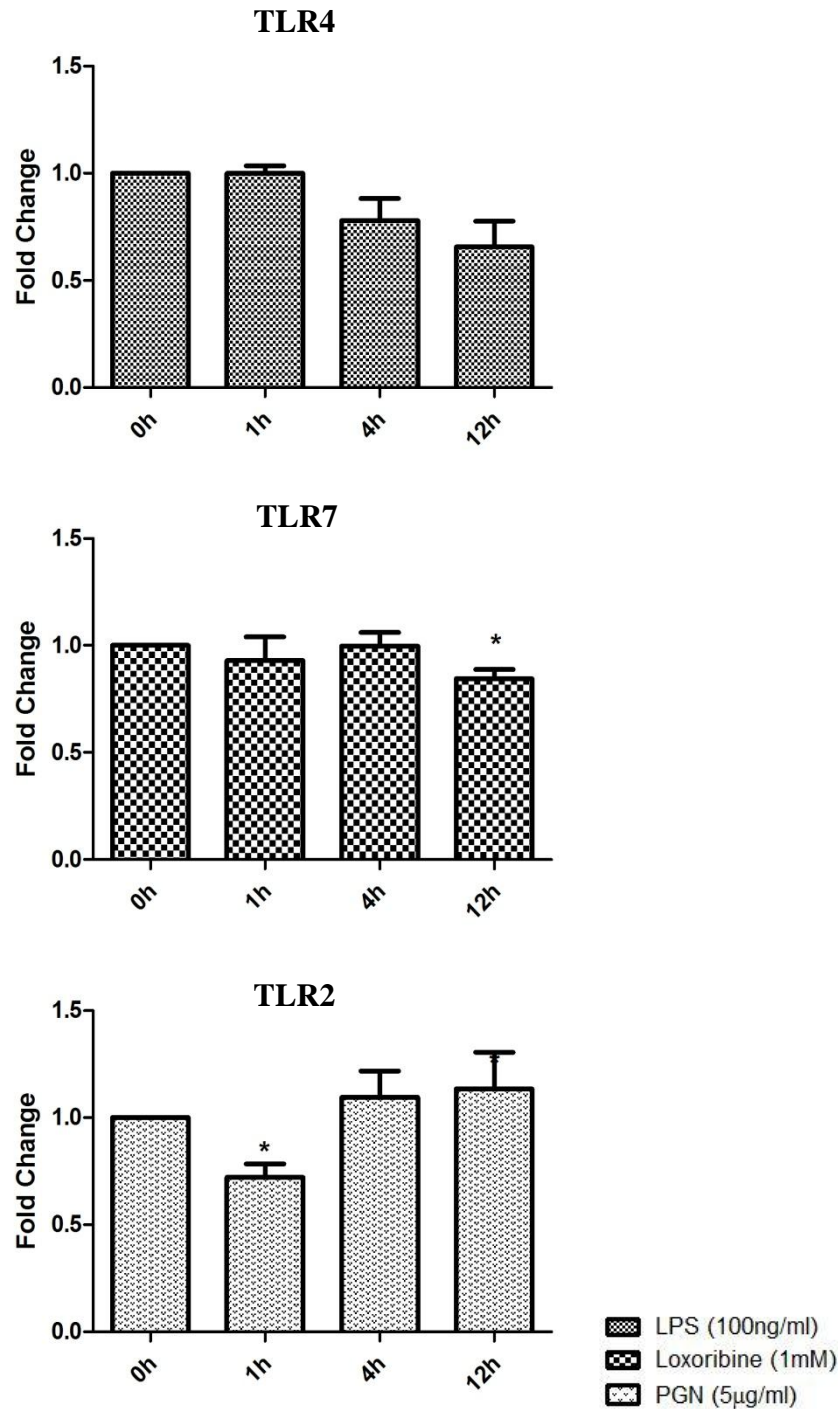


Figure 4.9: Effect of TLR ligand stimulation on STX7 mRNA expression in JAWS II DCs. JAWS II DCs was plated 1×10^6 ml and stimulated with 100 ng/ml LPS, 1 mM Loxoribine or 5 µg/ml PGN at 1 h, 4 h, and 12 h. The amount of STX7 was quantified by reverse transcription followed by RT-qPCR using an ABI 7900 HT detection system. STX7 levels were assayed in triplicate (using SYBR green technology) and normalised with S18 levels. Fold differences were calculated relative to STX7 levels at time zero (assigned value of 1). Results are mean \pm SEM of quadruplicate assays. A two sample, two tailed student's t-test comparing Δ Cts of control and 1h, 4h, or 12h stimulated sample * $p \leq 0.05$.

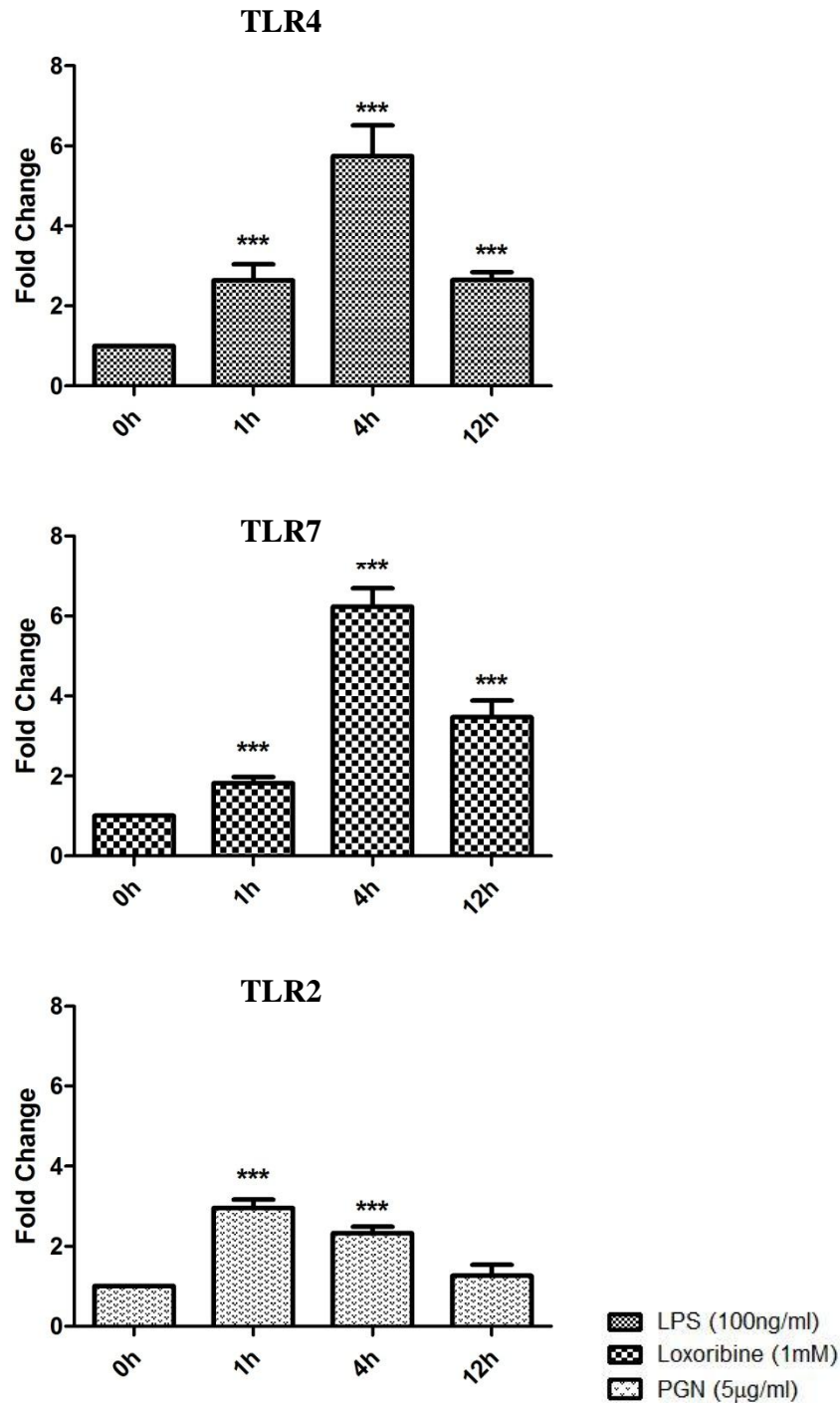


Figure 4.10: Effect of TLR ligand stimulation on STX11 mRNA expression in JAWS II DCs. JAWS II DCs was plated 1×10^6 /ml and stimulated with 100 ng/ml LPS, 1 mM Loxoribine or 5 µg/ml PGN at 1 h, 4 h, and 12 h. The amount of STX11 was quantified by reverse transcription followed by RT-qPCR using an ABI 7900 HT detection system. STX11 levels were assayed in triplicate (using SYBR green technology) and normalised with S18 levels. Fold differences were calculated relative to STX11 levels at time zero (assigned value of 1). Results are mean \pm SEM of quadruplicate assays. A two sample, two tailed student's t-test comparing Δ Cts of control and 1h, 4h, or 12h stimulated sample * $p \leq 0.05$, *** $p \leq 0.001$.

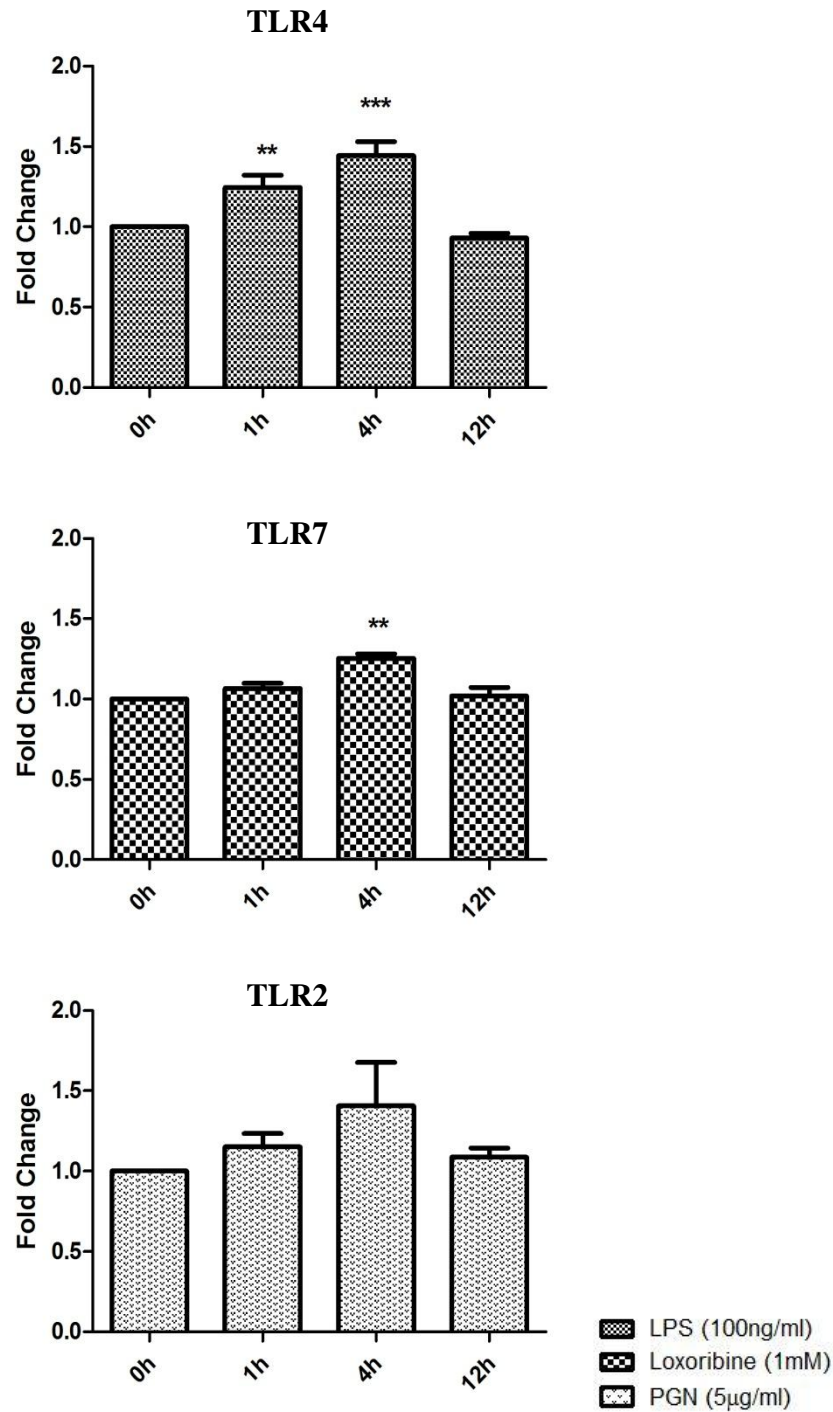


Figure 4.11: Effect of TLR ligand stimulation on STX12 mRNA expression in JAWS II DCs. JAWS II DCs was plated 1×10^6 /ml and stimulated with 100 ng/ml LPS, 1 mM Loxoribine or 5 µg/ml PGN at 1 h, 4 h, and 12 h. The amount of STX12 was quantified by reverse transcription followed by RT-qPCR using an ABI 7900 HT detection system. STX12 levels were assayed in triplicate (using SYBR green technology) and normalised with S18 levels. Fold differences were calculated relative to STX12 levels at time zero (assigned value of 1). Results are mean \pm SEM of quadruplicate assays. A two sample, two tailed student's t-test comparing Δ Cts of control and 1h, 4h, or 12h stimulated sample * $p \leq 0.05$, *** $p \leq 0.001$.

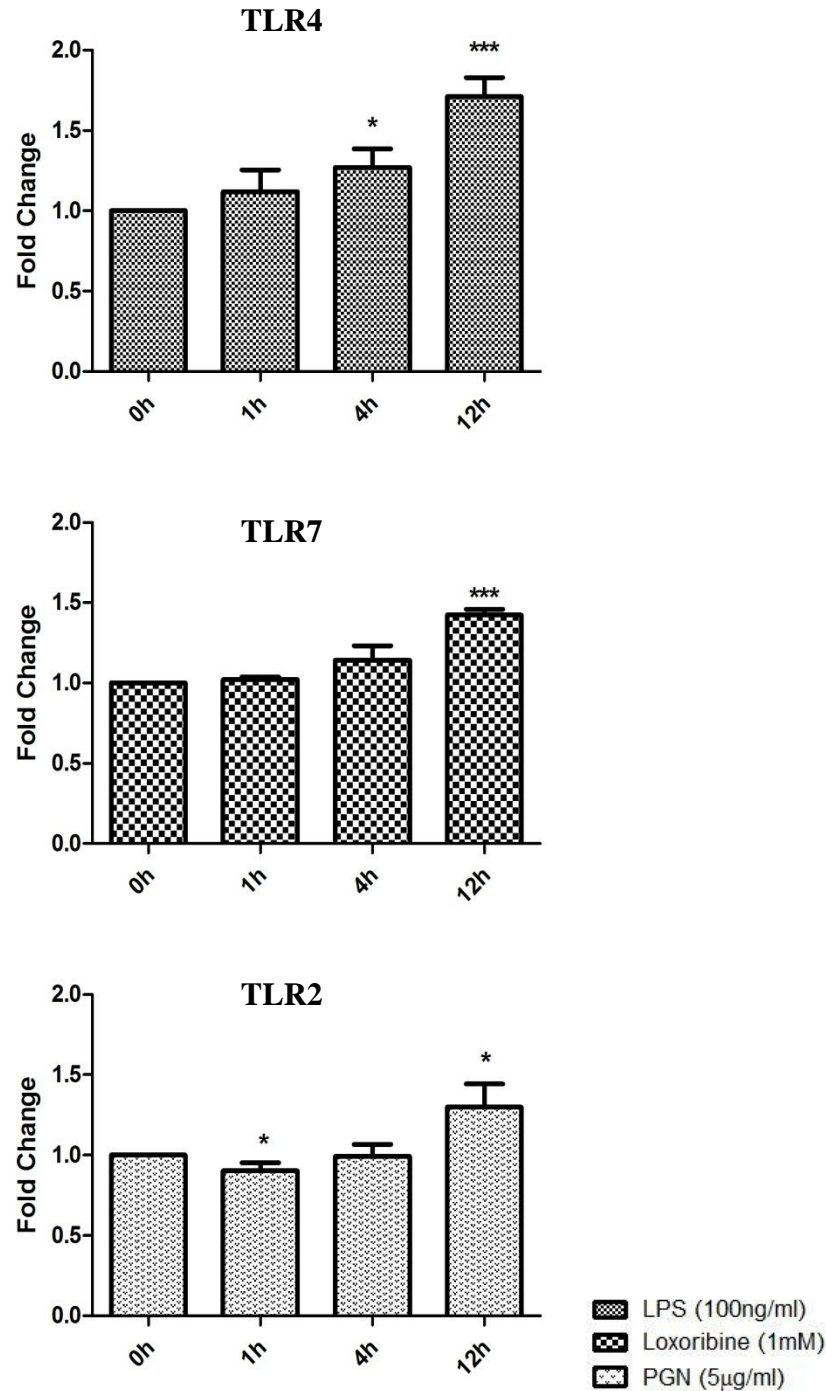


Figure 4.12: Effect of TLR ligand stimulation on STX16 mRNA expression in JAWS II DCs. JAWS II DCs was plated 1×10^6 ml and stimulated with 100 ng/ml LPS, 1 mM Loxoribine or 5 µg/ml PGN at 1 h, 4 h, and 12 h. The amount of STX16 was quantified by reverse transcription followed by RT-qPCR using an ABI 7900 HT detection system. STX16 levels were assayed in triplicate (using SYBR green technology) and normalised with S18 levels. Fold differences were calculated relative to STX16 levels at time zero (assigned value of 1). Results are mean \pm SEM of quadruplicate assays. A two sample, two tailed student's t-test comparing Δ Cts of control and 1h, 4h, or 12h stimulated sample * $p \leq 0.05$, *** $p \leq 0.001$.

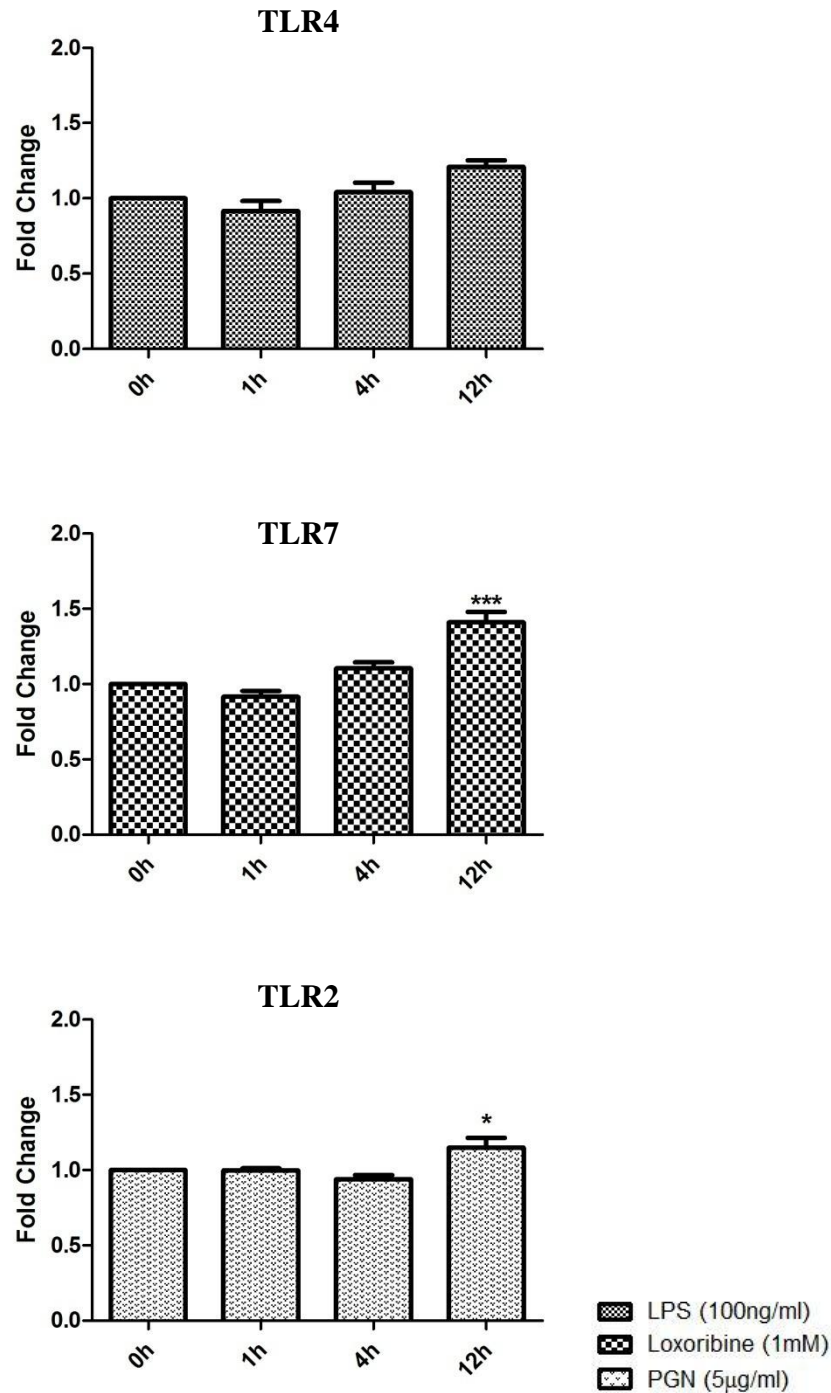


Figure 4.13: Effect of TLR ligand stimulation on SNAP23 mRNA expression in JAWS II DCs. JAWS II DCs was plated 1×10^6 /ml and stimulated with 100 ng/ml LPS, 1 mM Loxoribine or 5 µg/ml PGN at 1 h, 4 h, and 12 h. The amount of SNAP23 was quantified by reverse transcription followed by RT-qPCR using an ABI 7900 HT detection system. SNAP23 levels were assayed in triplicate (using SYBR green technology) and normalised with S18 levels. Fold differences were calculated relative to SNAP23 levels at time zero (assigned value of 1). Results are mean \pm SEM of quadruplicate assays. A two sample, two tailed student's t-test comparing Δ Cts of control and 1h, 4h, or 12h stimulated sample * $p \leq 0.05$ and *** $p \leq 0.001$.

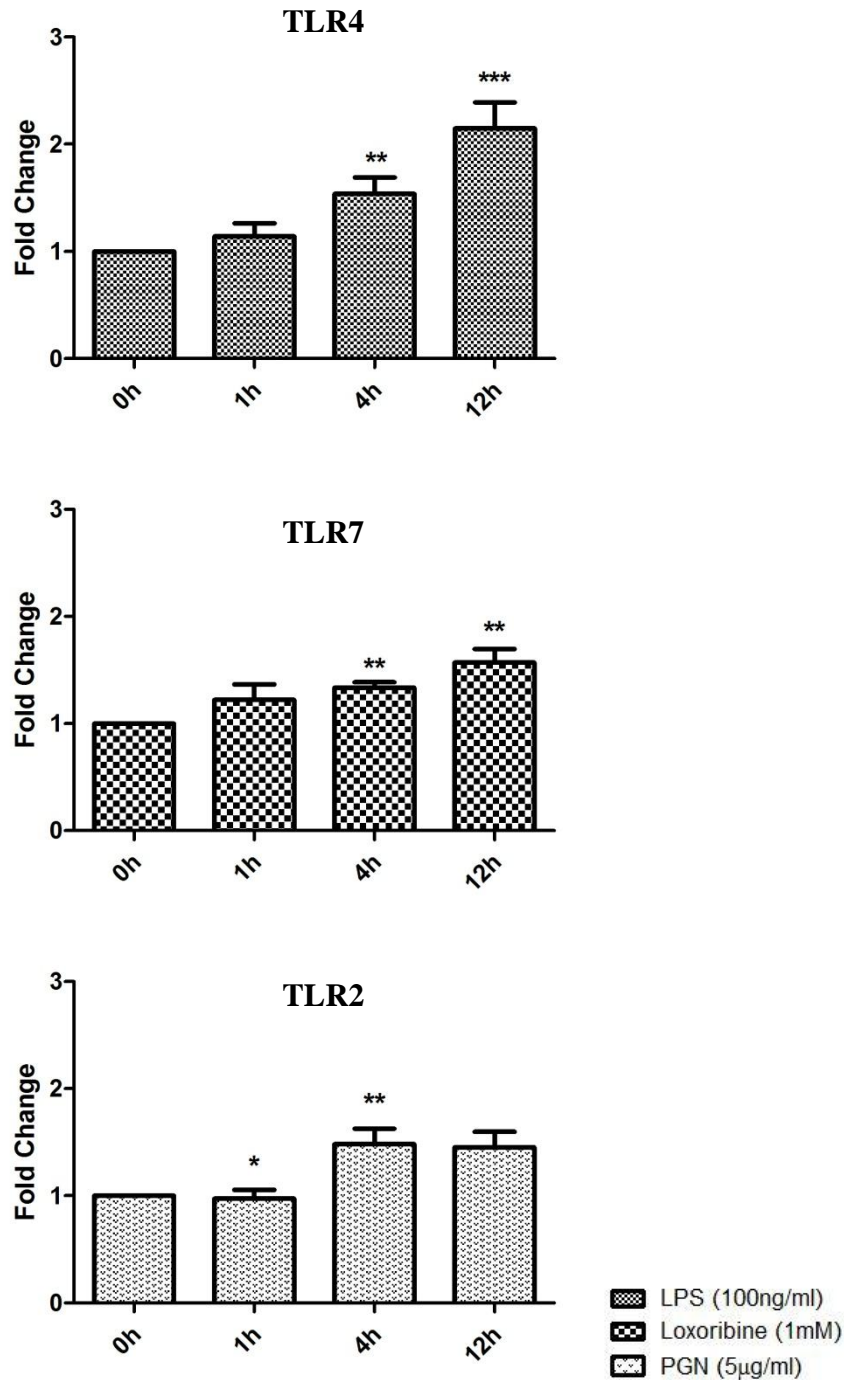


Figure 4.14: Effect of TLR ligand stimulation on Vt1a mRNA expression in JAWS II DCs. JAWS II DCs was plated 1×10^6 /ml and stimulated with 100 ng/ml LPS, 1 mM Loxoribine or 5 µg/ml PGN at 1 h, 4 h, and 12 h.. The amount of Vt1a was quantified by reverse transcription followed by RT-qPCR using an ABI 7900 HT detection system Vt1a levels were assayed in triplicate (using SYBR green technology) and normalised with S18 levels. Fold differences were calculated relative to Vt1a levels at time zero (assigned value of 1). Results are mean \pm SEM of quadruplicate assays. A two sample, two tailed student's t-test comparing Δ Cts of control and 1h, 4h, or 12h stimulated sample * $p \leq 0.05$, ** $p \leq 0.01$, *** $p \leq 0.001$.

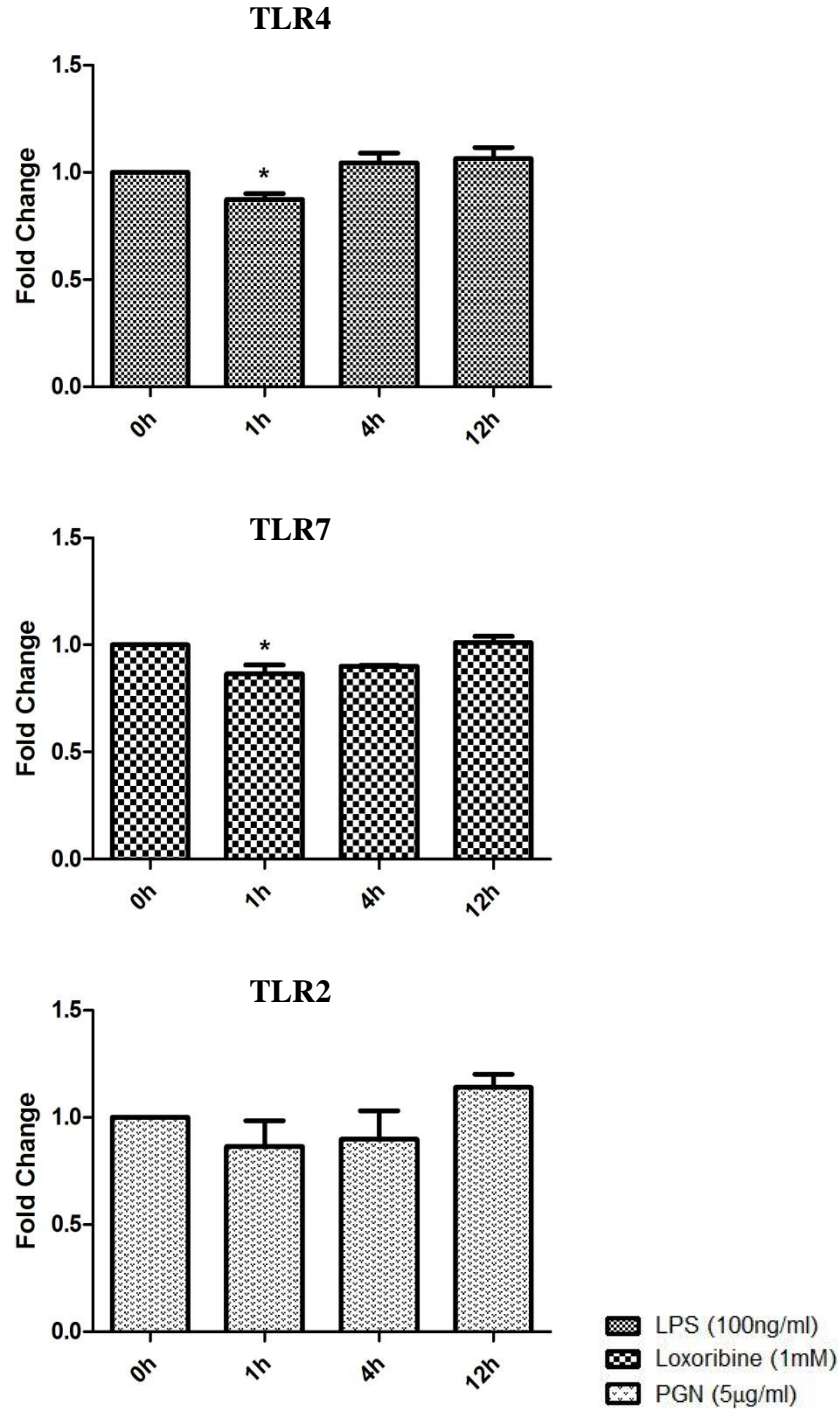


Figure 4.15: Effect of TLR ligand stimulation on Vti1b mRNA expression in JAWS II DCs. JAWS II DCs was plated 1×10^6 /ml and stimulated with 100 ng/ml LPS, 1 mM Loxoribine or 5 µg/ml PGN at 1 h, 4 h, and 12 h. The amount of Vti1b was quantified by reverse transcription followed by RT-qPCR using an ABI 7900 HT detection system Vti1b levels were assayed in triplicate (using SYBR green technology) and normalised with S18 levels. Fold differences were calculated relative to Vti1b levels at time zero (assigned value of 1). Results are mean \pm SEM of quadruplicate assays. A two sample, two tailed student's t-test comparing Δ Cts of control and 1h, 4h, or 12h stimulated sample * $p \leq 0.05$.

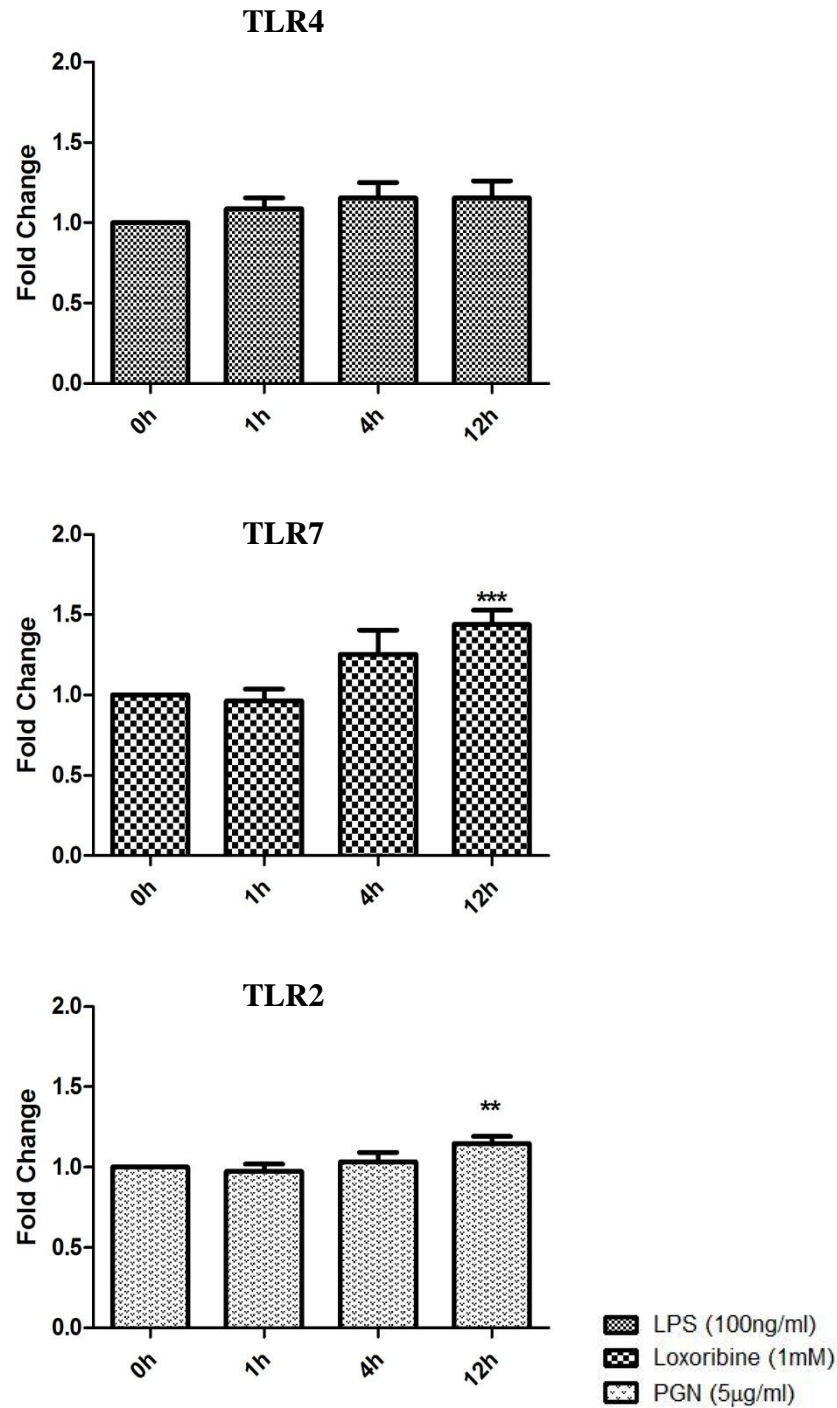


Figure 4.16: Effect of TLR ligand stimulation on STX6 mRNA expression in JAWS II DCs. JAWS II DCs was plated 1×10^6 /ml and stimulated with 100 ng/ml LPS, 1 mM Loxoribine or 5 µg/ml PGN at 1 h, 4 h, and 12 h. The amount of STX-6 was quantified by reverse transcription followed by RT-qPCR using an ABI 7900 HT detection system. STX6 levels were assayed in triplicate (using SYBR green technology) and normalised with S18 levels. Fold differences were calculated relative to STX6 levels at time zero (assigned value of 1). Results are mean \pm SEM of quadruplicate assays. A two sample, two tailed student's t-test comparing Δ Cts of control and 1h, 4h, or 12h stimulated sample * $p \leq 0.05$, *** $p \leq 0.001$

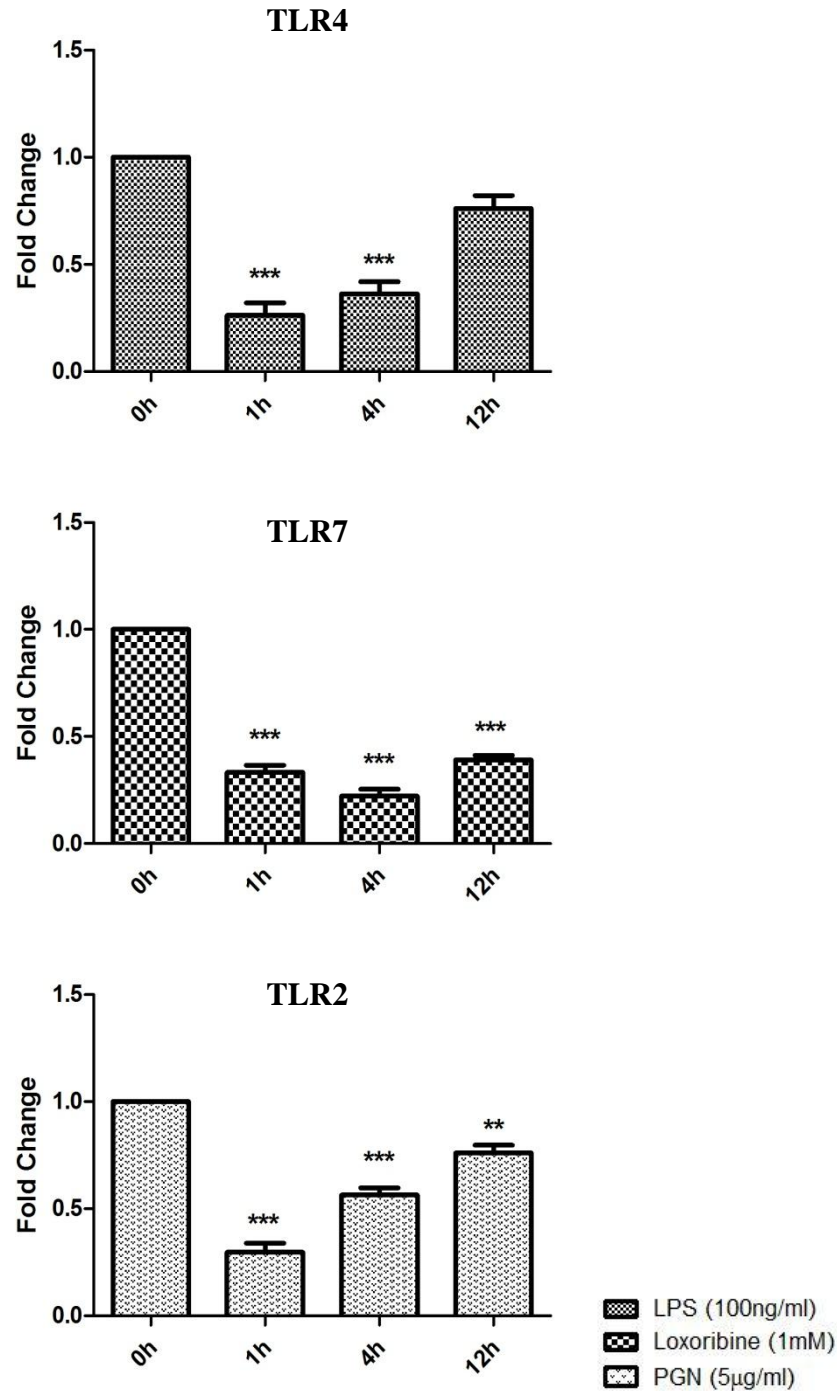


Figure 4.17: Effect of TLR ligand stimulation on VAMP1 mRNA expression in JAWS II DCs. JAWS II DCs was plated 1×10^6 /ml and stimulated with 100 ng/ml LPS, 1 mM Loxoribine or 5 µg/ml PGN at 1 h, 4 h, and 12 h. The amount of VAMP1 was quantified by reverse transcription followed by RT-qPCR using an ABI 7900 HT detection system. VAMP1 levels were assayed in triplicate (using SYBR green technology) and normalised with S18 levels. Fold differences were calculated relative to VAMP1 levels at time zero (assigned value of 1). Results are mean \pm SEM of quadruplicate assays. A two sample, two tailed student's t-test comparing Δ Cts of control and 1h, 4h, or 12h stimulated sample ** $p \leq 0.01$, *** $p \leq 0.001$.

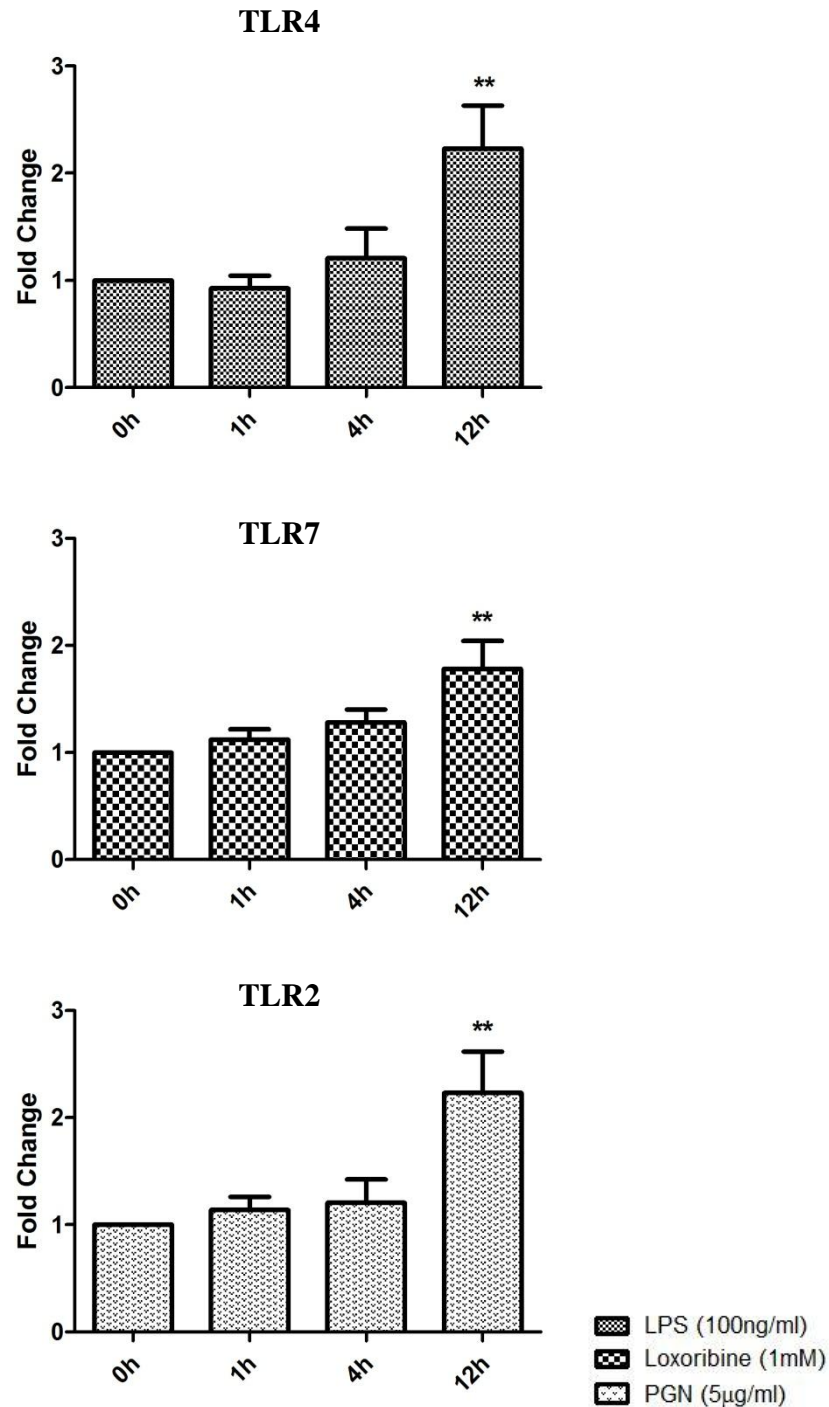


Figure 4.18: Effect of TLR ligand stimulation on VAMP2 mRNA expression in JAWS II DCs. JAWS II DCs was plated 1×10^6 ml and stimulated with 100 ng/ml LPS, 1 mM Loxoribine or 5 µg/ml PGN at 1 h, 4 h, and 12 h. The amount of VAMP2 was quantified by reverse transcription followed by RT-qPCR using an ABI 7900 HT detection system. VAMP2 levels were assayed in triplicate (using SYBR green technology) and normalised with S18 levels. Fold differences were calculated relative to VAMP2 levels at time zero (assigned value of 1). Results are mean \pm SEM of quadruplicate assays. A two sample, two tailed student's t-test comparing Δ Cts of control and 1h, 4h, or 12h stimulated sample $**p \leq 0.01$.

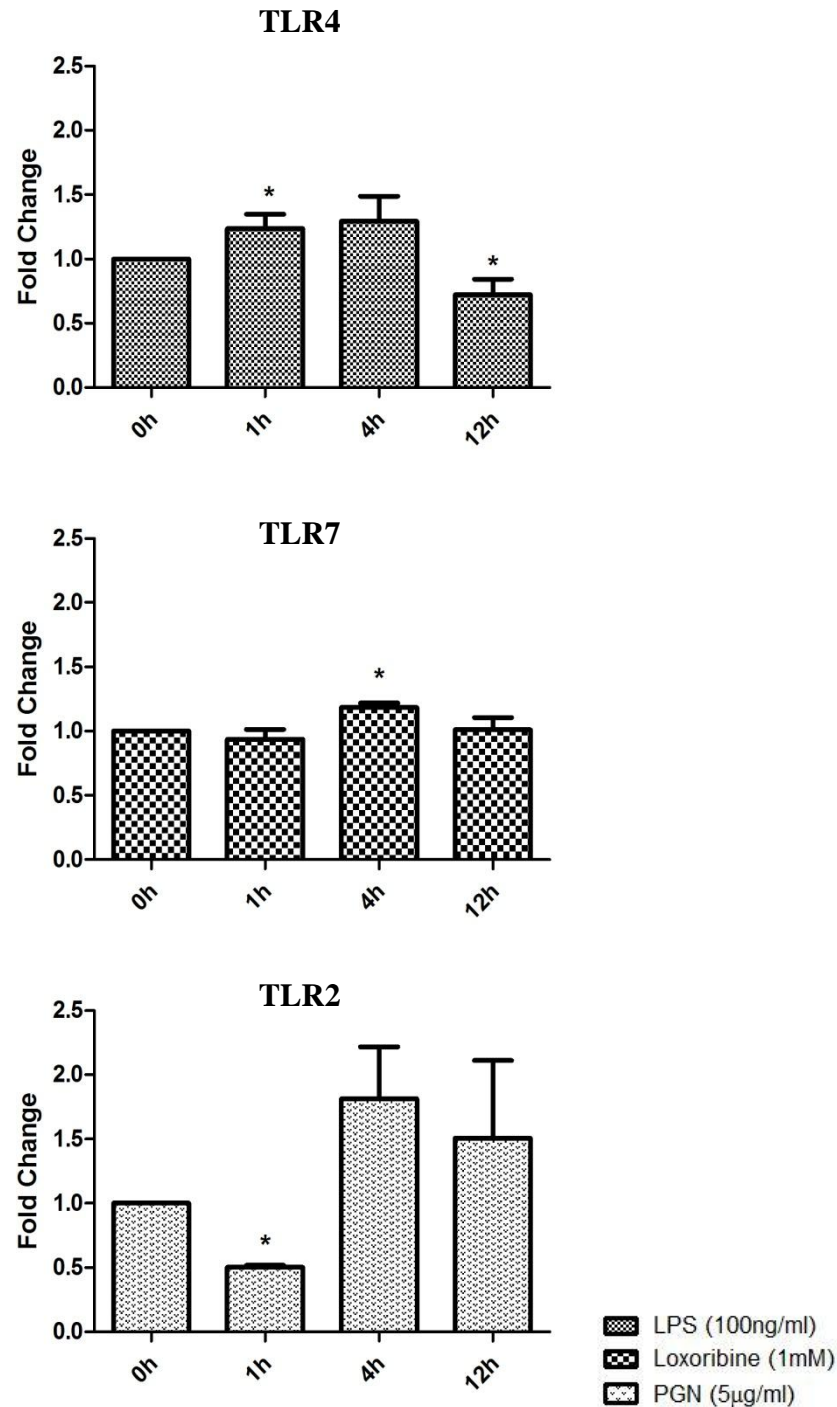


Figure 4.19: Effect of TLR ligand stimulation on VAMP3 mRNA expression in JAWS II DCs. JAWS II DCs was plated 1×10^6 /ml and stimulated with 100 ng/ml LPS, 1 mM Loxoribine or 5 µg/ml PGN at 1 h, 4 h, and 12 h. The amount of VAMP3 was quantified by reverse transcription followed by RT-qPCR using an ABI 7900 HT detection system. VAMP3 levels were assayed in triplicate (using SYBR green technology) and normalised with S18 levels. Fold differences were calculated relative to VAMP3 levels at time zero (assigned value of 1). Results are mean \pm SEM of quadruplicate assays. A two sample, two tailed student's t-test comparing Δ Cts of control and 1h, 4h, or 12h stimulated sample $*p \leq 0.05$.

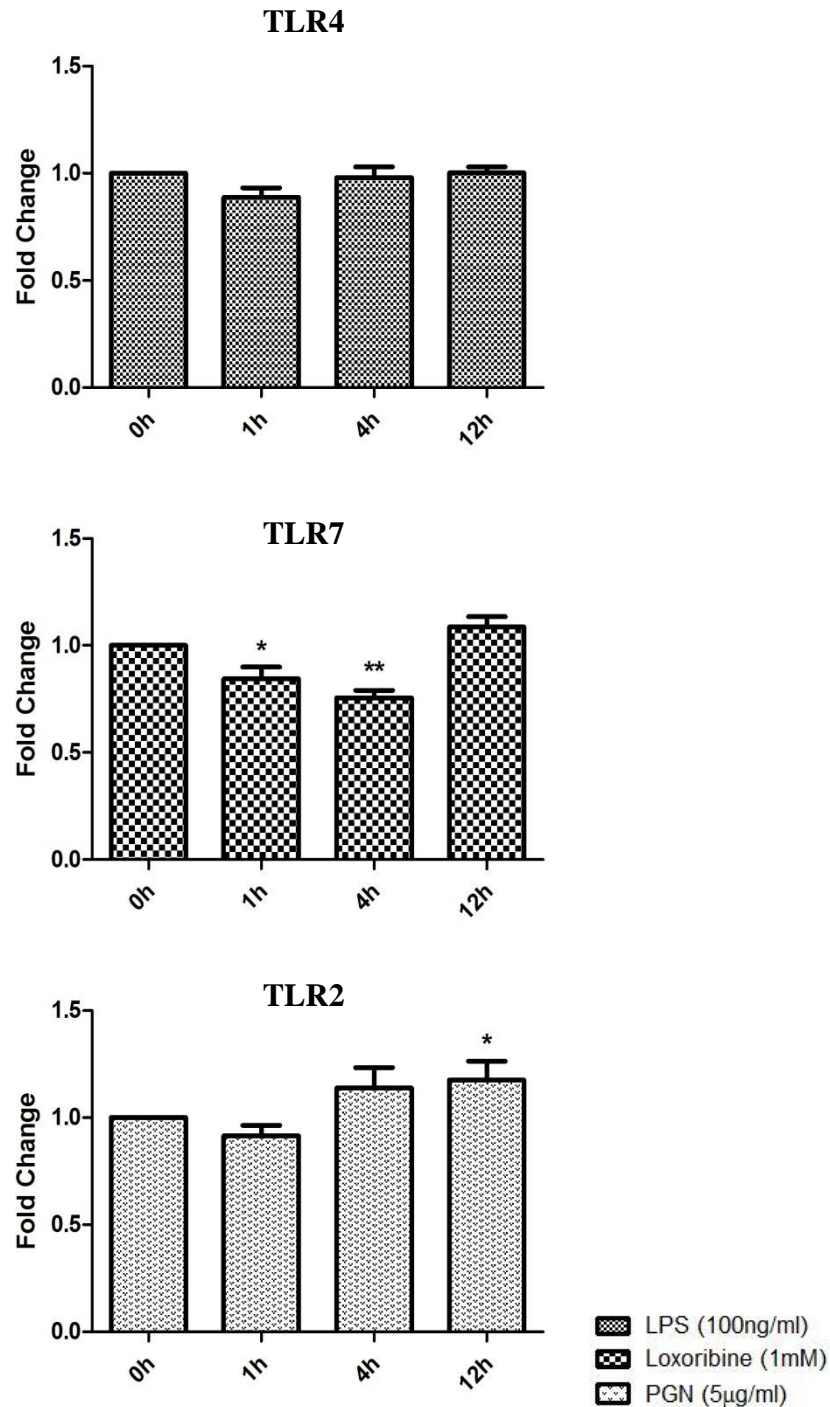


Figure 4.20: Effect of TLR ligand stimulation on VAMP4 mRNA expression in JAWS II DCs. JAWS II DCs was plated 1×10^6 ml and stimulated with 100 ng/ml LPS, 1 mM Loxoribine or 5 µg/ml PGN at 1 h, 4 h, and 12 h. The amount of VAMP4 was quantified by reverse transcription followed by RT-qPCR using an ABI 7900 HT detection system. VAMP4 levels were assayed in triplicate (using SYBR green technology) and normalised with S18 levels. Fold differences were calculated relative to VAMP4 levels at time zero (assigned value of 1). Results are mean \pm SEM of quadruplicate assays. A two sample, two tailed student's t-test comparing Δ Cts of control and 1h, 4h, or 12h stimulated sample * $p \leq 0.05$.

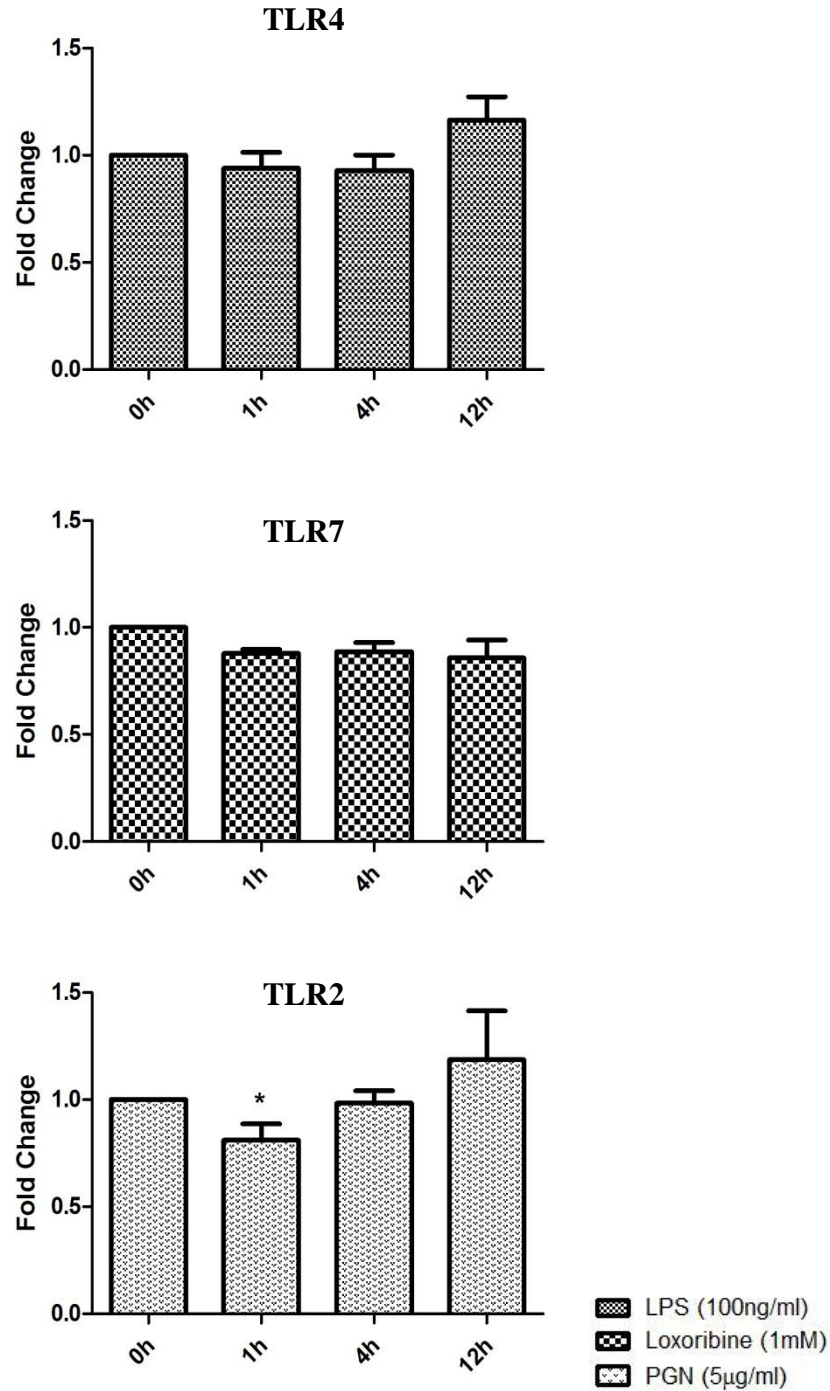


Figure 4.21: Effect of TLR ligand stimulation on VAMP7 mRNA expression in JAWS II DCs. JAWS II DCs was plated 1×10^6 /ml and stimulated with 100 ng/ml LPS, 1 mM Loxoribine or 5 µg/ml PGN at 1 h, 4 h, and 12 h. The amount of VAMP7 was quantified by reverse transcription followed by RT-qPCR using an ABI 7900 HT detection system. VAMP7 levels were assayed in triplicate (using SYBR green technology) and normalised with S18 levels. Fold differences were calculated relative to VAMP7 levels at time zero (assigned value of 1). Results are mean \pm SEM of quadruplicate assays. A two sample, two tailed student's t-test comparing Δ Cts of control and 1h, 4h, or 12h stimulated sample * $p \leq 0.05$.

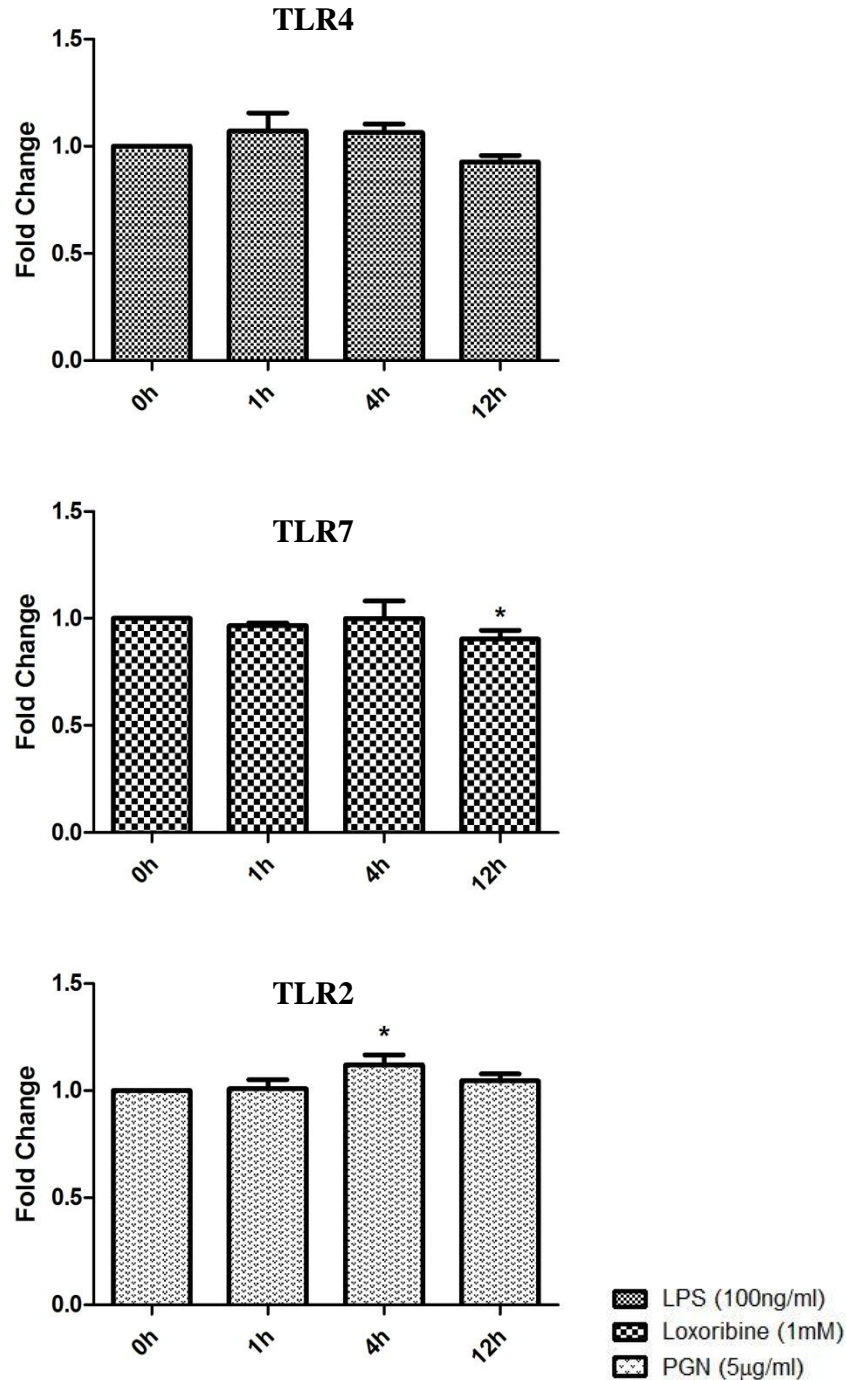


Figure 4.22: Effect of TLR ligand stimulation on VAMP8 mRNA expression in JAWS II DCs. JAWS II DCs was plated 1×10^6 /ml and stimulated with 100 ng/ml LPS, 1 mM Loxoribine or 5 µg/ml PGN at 1 h, 4 h, and 12 h. The amount of VAMP8 was quantified by reverse transcription followed by RT-qPCR using an ABI 7900 HT detection system. VAMP8 levels were assayed in triplicate (using SYBR green technology) and normalised with S18 levels. Fold differences were calculated relative to VAMP8 levels at time zero (assigned value of 1). Results are mean \pm SEM of quadruplicate assays. A two sample, two tailed student's t-test comparing Δ Cts of control and 1h, 4h, or 12h stimulated sample $*p \leq 0.05$.

Table 4.2 – Cytokine up-regulation correlated with mRNA up-regulation

	TLR2	TLR3	TLR4	TLR5	TLR7	TLR9
IL-1 β			↑		↑	
IL-6	↑	↑	↑		↑	↑
IL-10			↑	↑	↑	↑
TNF- α	↑	↑	↑	↑	↑	↑
IL-12p40					↑	↑
IL-12p70						
IL-23			↑			
IL-27p28		↑	↑	↑	↑	↑
MIP-1 α	↑	↑	↑		↑	↑
MIP-2	↑	↑	↑		↑	
SNAP 23	↑				↑	
STX2						
STX3			↑		↑	
STX4						
STX5	↑					
STX6	↑				↑	
STX7						
STX11	↑		↑		↑	
STX12			↑		↑	
STX16	↑		↑		↑	
VAMP1						
VAMP2	↑		↑		↑	
VAMP3			↑		↑	
VAMP4	↑					
VAMP7						
VAMP8	↑					
Vti1a	↑		↑		↑	
Vti1b						

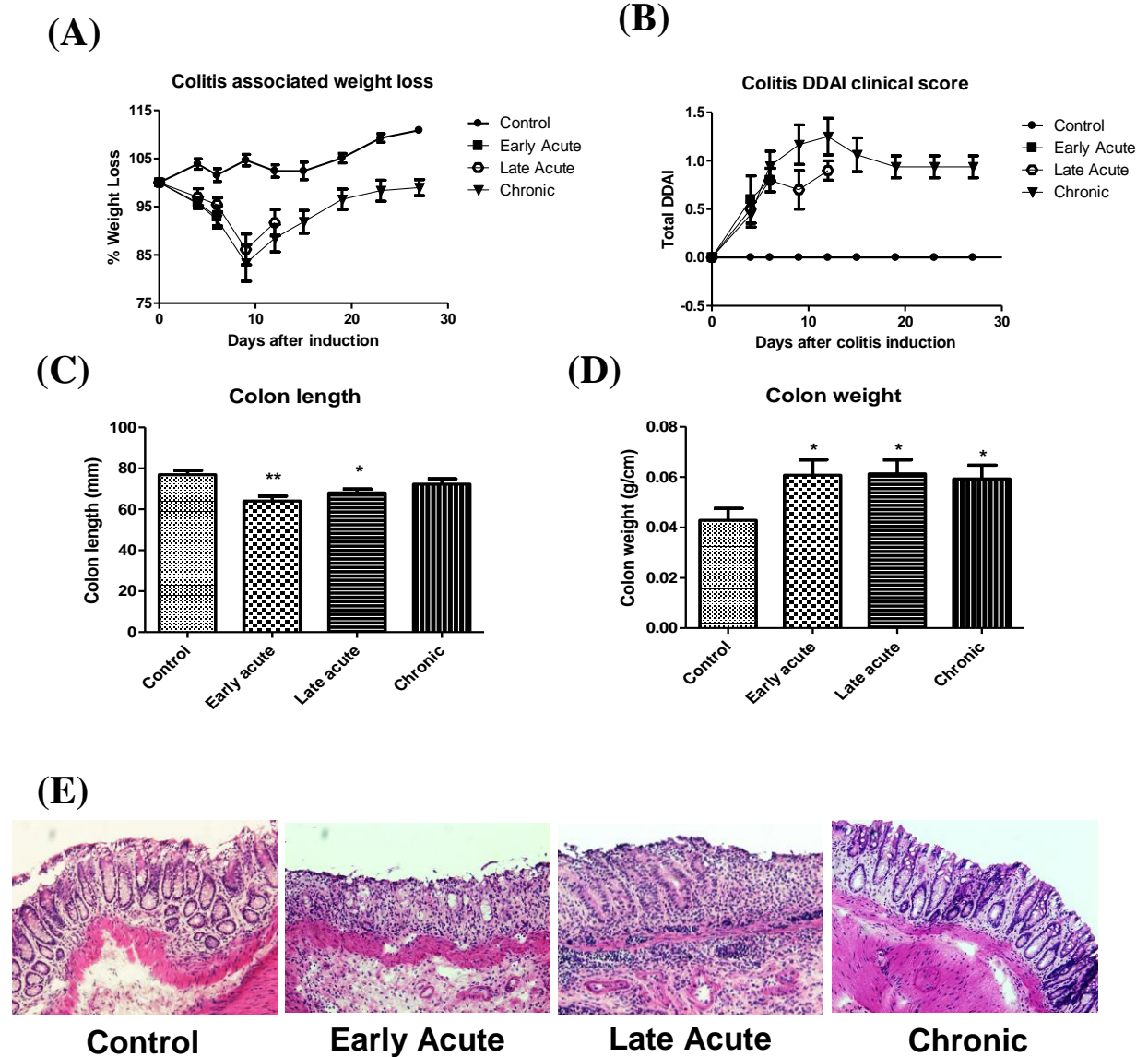


Figure 4.23 - Disease associated symptoms in the DSS colitis model – C57BL mice were grouped into a control group of 6 mice and 4 test groups. DSS was administered to mice in the drinking water for 5 days at a final concentration of 3%. Mice were weighed and disease scored based on fur texture/posture for a daily disease activity index (DDAI) every 3-4 days (A). The average % weight change of the 4 groups is plotted to the end point for each group. The starting weight on Day 0 is plotted as 100% of the weight with the rest of the weight relative to this value. Two control mice were culled at the end point for each test group. There is a drop in body weight for all test groups after day 0 and a healthy gain in weight for control mice (B). At the end point of each group the length (C) and weight (D) of each removed and washed colon was measured and used as an indication of inflammation in the colon. Sections of the distal colon were removed for histology and H&E staining in order to confirm inflammation. The control shows a healthy colon while infiltration and loss of crypt structure is evident in the acute slides with recovery in the chronic slides as expected (E). Results are means \pm SEM of at least 5 mice, a two sample, two tailed student's t-test was used to determine if differences between control and disease states were significant (* $p \leq 0.05$, ** $p \leq 0.01$).

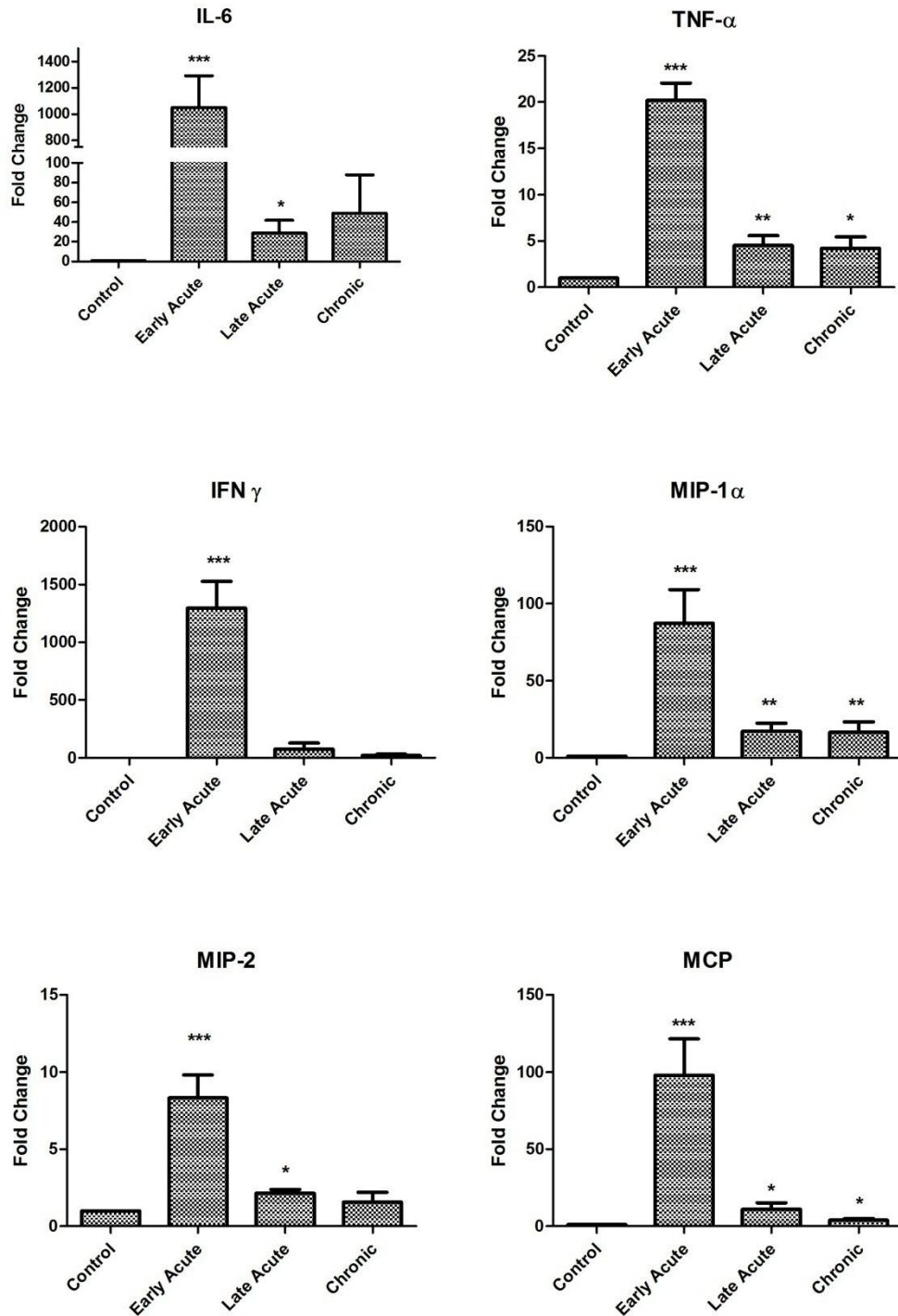


Figure 4.24: Cytokine and chemokine mRNA expression in DSS colitis mouse model. The amount of target mRNA at various stages of colitis post induction of colitis (early acute, late acute and chronic disease) were quantified by reverse transcription followed by RT-qPCR using an ABI 7900 HT detection system mRNA levels were assayed in triplicate (using SYBR green technology) and normalised with S18 levels. Fold differences were calculated relative to target mRNA levels at control (assigned value of 1). Results are means \pm SEM of at least 5 mice. A two sample, two tailed student's t-test comparing Δ Cts of control and disease groups. * $p \leq 0.05$, ** $p \leq 0.01$, *** $p \leq 0.001$.

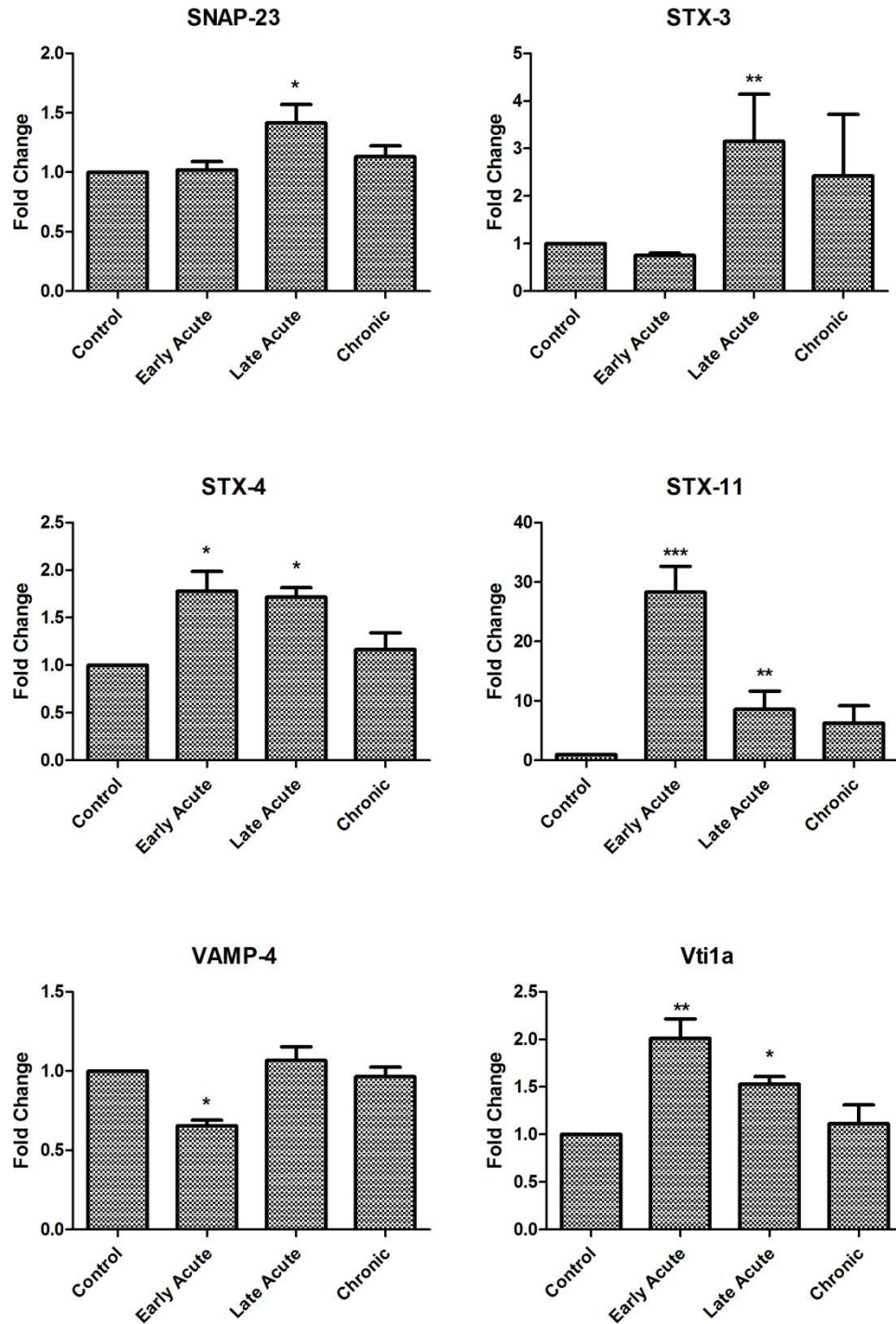


Figure 4.25: SNARE mRNA expression in DSS colitis mouse model. The amount of target mRNA at various stages of colitis post induction of colitis (early acute, late acute and chronic disease) were quantified by reverse transcription followed by RT-qPCR using an ABI 7900 HT detection system mRNA levels were assayed in triplicate (using SYBR green technology) and normalised with S18 levels. Fold differences were calculated relative to target mRNA levels at control (assigned value of 1). Results are means \pm SEM of at least 5 mice. A two sample, two tailed student's t-test comparing Δ Cts of control and disease groups. * $p \leq 0.05$, ** $p \leq 0.01$, *** $p \leq 0.001$.

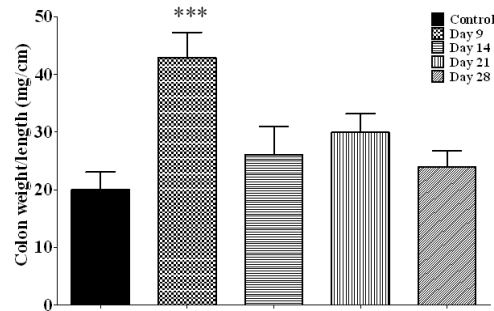
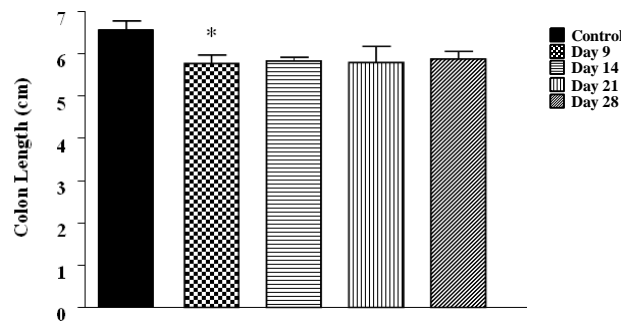
Colon Weight in *C. rodentium* infected mice**Colon Length in *C. rodentium* infected mice**

Figure 4.26 - Colon weight of mice infected with *Citrobacter rodentium* - C57BL mice were housed in groups of 6-8 mice and test mice were inoculated with *C.rodentium* orally by a 200 μ l gavage of approximately 200×10^9 CFU *C.rodentium*. Mice were sacrificed at 9, 14, 21 and 28 days. Colons were collected from mice and the contents carefully removed before washing and patting dry. At the end point of each group the length and weight of each colon was measured individually and used as an indication of colitis in the mouse model. There is a significant increase in colon weight at day 9 with a recovery in the later days. There is a significant decrease in colon length at day 9 with moderate recovery in the following days. Results are means \pm SEM of at least 5 mice, two tailed student's t-test was used to determine if differences between control and disease states were significant (* $p \leq 0.05$, *** $p \leq 0.001$).

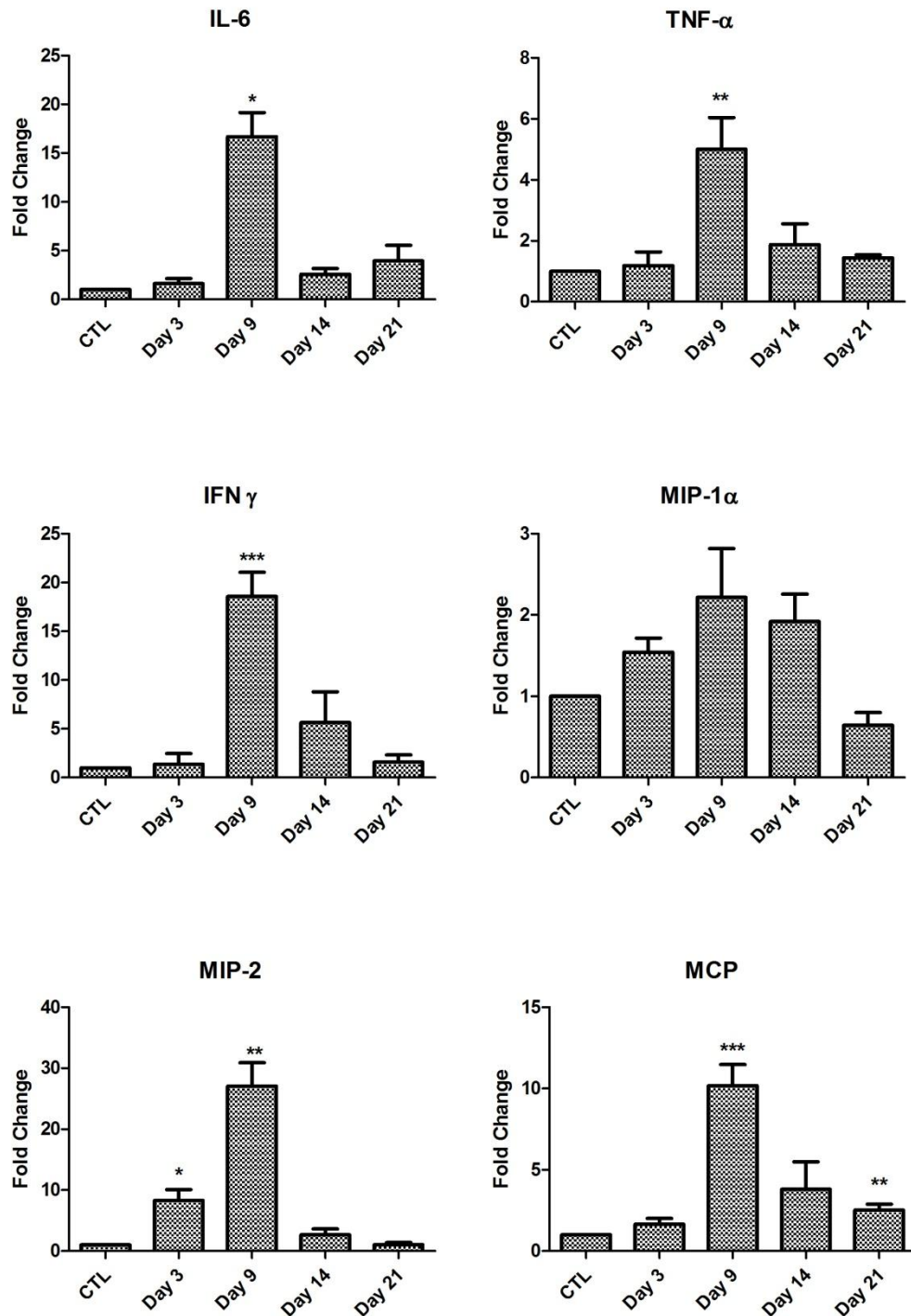


Figure 4.27: Cytokines and chemokine mRNA expression in *Citrobacter rodentium* infection. The amount of target mRNA in the colonic tissue of healthy and a time course of 21 days of *Citrobacter rodentium* infected mice was quantified by reverse transcription followed by RT-qPCR using an ABI 7900 HT detection system. mRNA levels were assayed in triplicate (using SYBR green technology) and normalised with S18 levels. Fold differences were calculated relative to target mRNA levels at control (assigned value of 1). Results are means \pm SEM of at least 5 mice. A two sample, two tailed student's t-test comparing Δ Cts of control and disease groups. * $p \leq 0.05$, ** $p \leq 0.01$, *** $p \leq 0.001$.

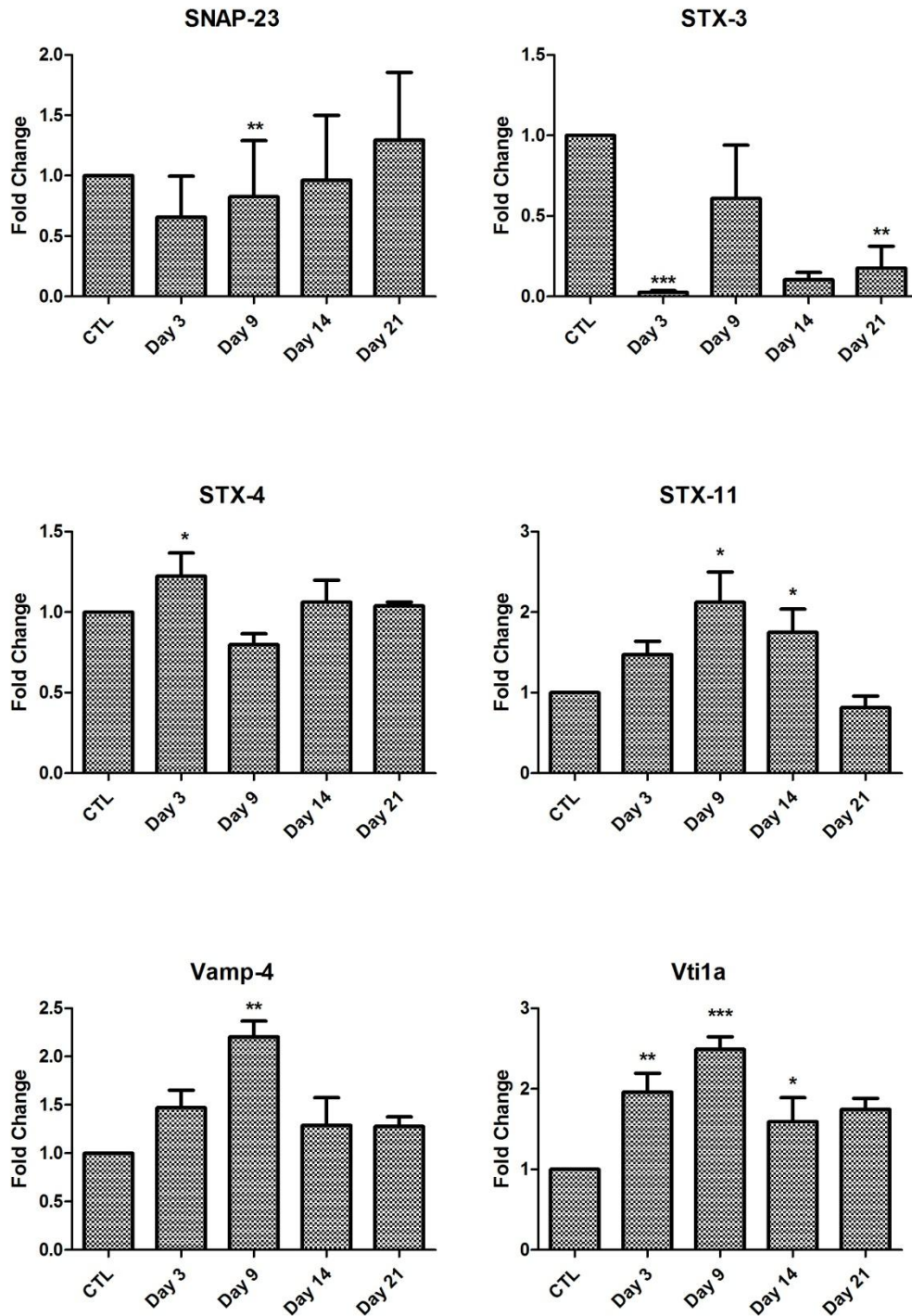


Figure 4.28: SNARE mRNA expression in *Citrobacter rodentium* infection. The amount of target mRNA in the colonic tissue of healthy and a time course of 21 days of *Citrobacter rodentium* infected mice was quantified by reverse transcription followed by RT-qPCR using an ABI 7900 HT detection system mRNA levels were assayed in triplicate (using SYBR green technology) and normalised with S18 levels. Fold differences were calculated relative to target mRNA levels at control (assigned value of 1). Results are means \pm SEM of at least 5 mice. A two sample, two tailed student's t-test comparing Δ Cts of control and disease groups. * $p \leq 0.05$, ** $p \leq 0.01$, *** $p \leq 0.001$.

4.3 DISCUSSION

Eukaryotic cells have the remarkable feature of transporting bio-chemically distinct intracellular vesicles to and from the cell surface. The specific mechanism for the secretion of immune mediators such as cytokines and chemokines has not been well studied however it is now known that SNARE proteins play a central role in this process (Stow, Manderson and Murray 2006a). Expression of SNAREs in immune cells, especially at mRNA level has not been well characterised. Investigating their expression in immune cells may provide valuable insight into their involvement in cytokine and/or chemokine secretion and provide potential targets for inhibition of cytokines and chemokines in inflammatory disease.

Real time-qPCR is often referred to as the gold standard and believed to be easy, however the emergence of new guideline has confirmed that this is not the case. RT-qPCR has a high level of variability and involves many steps involved in optimising the assay. To streamline this complex assay, MIQE was published to offer easy to follow guidelines (Bustin et al. 2009). The key issues highlighted by the guidelines include sample quality, reverse transcription, assay validation, PCR efficiency and normalisation. To follow these guidelines, at the start of all experiments purity and integrity of mRNA were checked and only used if at high enough standard. Secondly, primers had to be optimised. PCR amplification efficiency is highly dependant on the primers used and this was assessed using calibration curves. A serial dilution of the cDNA was used for each sample and the log was plotted on the *x* axis (independent variable).and corresponding C_q (dependant variable) on the *y* axis. Using the slope and the equation $10^{-1/\text{slope}} - 1$, a theoretical max of 1 or (100%)

would be expected as the Cq should double with each cycle. However efficiencies between 90%-110% are acceptable. All primer sets fell within this range. This successful validation means the assays are efficient, robust and sensitive. Only after these guidelines were followed could examination of the expression of SNAREs mRNA in JAWS II DCs begin.

We initially used RT-PCR to assess the expression of mRNA of eighteen SNARE proteins in JAWS II DCs following TLR4 stimulation. This proved evidence that all eighteen SNAREs were present in the JAWSII DCs. Subsequently we then examined the expression of these SNAREs using RT-qPCR following TLR2, TLR4 and TLR7 activation over a time course. Our data demonstrated that the expression of SNAREs following TLR ligation, differed dependently on the TLR ligand used. Furthermore there was huge variation in the level of expression of individual SNAREs in the DCs.

VAMP8 has been previously indicated to also be involved in dendritic cell function, phagocytosis. Ho *et al.*, reported that an over-expression of VAMP8 significantly inhibited phagocytosis suggesting that VAMP8 negatively regulates phagocytosis (Ho et al. 2008). Although we did not report any change in mRNA expression of VAMP8 in JAWS II DCs the same group in another study note that although they have indicated a role for VAMP8 in DCs, VAMP8 mRNA was not significantly elevated during DC maturation and accredited this to regulation at the mRNA level of VAMP8 by caspases (Ho et al. 2009). However VAMP8 mRNA has been shown to be up-regulated in over-reactive human platelets. There was a higher fold expression of 4.8 in hyper-reactive platelets compared to hypo-reactive platelets

(Kondkar et al. 2010). This highlights the role for caspases and other molecules involved in post transcriptional regulation of SNARE mRNA.

Several other SNAREs in this study also remained unchanged. This was of interest as some SNAREs have been well reported to play a role in other immune cells for example STX6 mRNA was up-regulated 2 hours post stimulation of LPS was reported in RAW 264.7 macrophage cells (Murray et al. 2005b) and SNAP23 mRNA from the skeletal muscle of patients with type II diabetes was up-regulated (Bostrom et al. 2010). As SNAREs are used up during the fusion reactions and are recycled for numerous rounds of transport (Malsam, Kreye and Soellner 2008), we propose that along with caspases, other post-transcriptional regulation and recycling of SNAREs may be another reason for the lack of changes of mRNA expression.

In a study by Stow *et al.*, there was up-regulation of STX4 protein levels at the same time-point as TNF secretion from macrophage following LPS stimulation prompted the investigation of the role of STX-4 (Murray et al. 2005b) (Stow, Manderson and Murray 2006a, Murray et al. 2005b). This study using the correlation of SNARE expression and cytokine expression concept may help us in the following chapter to elucidate the SNAREs involved in cytokines or chemokines secretion within our own data.

We demonstrated that there was a significant up-regulation of Vti1a mRNA at 4 and 12 hours post LPS and Loxoribine stimulation. It has previously been reported that up-regulation of Vti1a and Vti1b inhibits phagocytosis in DCs (Cai et al. 2011). As mature DCs are known to have reduced phagocytic ability (Ruedl and Hubele 1997)

it may suggest that Vti1a was up-regulated to inhibit phagocytosis as the DC matured.

One of most significant increases in mRNA expression over time was that of STX-3. Expression of STX3 mRNA in JAWSII DCs significantly increased following activation with LPS and Loxoribine 1 and 4 hour post stimulation and conversely was significantly down-regulated following PGN activation. A role for STX3 has been documented in mast cells and epithelial cells but not yet in DCs. STX3 and VAMP7 have been shown to be important for apical transport of trans-membrane and secretory proteins in epithelial cells (Carmosino et al. 2010). Interestingly a role for STX3 has been recently documented in the secretion of chemokines from mast cells. This study demonstrated that blocking STX3 activity with neutralising antibodies inhibited the secretion of chemokines following IgE stimulation. The chemokines inhibited included IL-8, MCP, MIP-1 α and MIP-1 β (Frank et al. 2011). As the JAWS II DCs secreted large amounts of MIP-1 α it may suggest that STX3 also has a role in chemokine secretion in DCs.

Another interesting finding was the significant up-regulation of STX11 mRNA expression in response to LPS Loxoribine and PGN compared to control cells. STX11 is highly expressed in cells of the immune system and interestingly has an already established role in an immune disease. Loss or mutation of the STX11 gene results in an autosomal recessive disorder known as, familial hemophagocytic lymphohistiocytosis type-4 (FHL-4), which causes immune dysregulation This disorder is characterised by high levels of inflammatory cytokines and defective function of T cells and natural killer cell (Offenhaeuser et al. 2011). STX11 has been

reported to be up-regulated in dendritic cells following LPS activation but *Stx11* deficiency did not appear to affect DC function (D'Orlando et al. 2013) STX11 has been indicated to regulate other cells of the immune system such as NK, CD8⁺ T cells, macrophage, platelets and in human blood neutrophils where up-regulation of STX11 mRNA expression during differentiation of has been reported (Offenhaeuser et al. 2011, Xie et al. 2009, D'Orlando et al. 2013).

It was clear from our findings that SNAREs are regulated in JAWS II DCs in response to TLR ligation and that their expression changed depending on the type of TLR ligand used to activate the cell. To further the work it would be advantageous to screen the SNARE expression in BMDCs. This would lead to a more comprehensive model of SNARE expression in DC following activation with TLR ligands that could be correlated with cytokine or chemokine expression.

Given the role SNAREs have during immune activation *in vitro*, we identified candidate which were significantly changes in DCs, STX3, STX11 and Vti1a and candidate SNAREs with little changes, STX4, SNAP23 and VAMP4. We therefore wanted to assess whether they were regulated *in vivo* during inflammatory disease, – in this case - two models of experimental IBD, the dextran sodium sulphate (DSS)-induced colitis mouse model and *Citrobacter rodentium* infection. Expression of a large number of cytokines and other soluble immune mediators have been previously reported to up-regulated or down-regulated during mouse models of colitis. The reason mice colitis models are an attractive way to study inflammatory disease owes to the fact a similar expression of cytokines in colitis mouse models has been described for the human homologues when measured in intestinal tissue obtained from IBD patients (Boismenu and Chen 2000).

We employed RT-qPCR to study specific pro-inflammatory cytokines and chemokines as that have been reported to play a role in chemically induced model of intestinal inflammation, the DSS model (Yan et al. 2009). DSS is a negatively charged glucose polymer with engrafted sulphate groups, when delivered in drinking water of mice induces intestinal inflammation mimicking the clinical and histological features of IBDs that have characteristics of UC (Laroui et al. 2012). During early acute inflammation there was significant increase in expression of all cytokines and chemokines; IL-6, TNF- α , IFN- γ , MIP-1 α , MIP-2 and MCP and associated decrease of these cytokines and chemokines in the chronic states. This trend of IL-6 and TNF- α expression was also observed by Alex *et al.*, up-regulation of IFN- γ mRNA in DSS colitis correlates with previously published data and Yan *et al.*, reported similar profile of cytokines IL-6 and TNF- α and the chemokine MIP-2 (Yan et al. 2009, Alex et al. 2009, Egger et al. 2000). In fact, MIP-2, which acts in a similar manner to IL-8 in humans, was reported to be expressed during DSS colitis in another study but also to enhance effects of DSS due to its presence (Ohtsuka and Sanderson 2003). Although colonic tissue consists of many cells which can secrete these cytokines and chemokines, DCs have been previously indicated in the development of acute DSS due to their production of TNF- α , MIP-1 α , MIP-2 and MCP-1 (Berndt et al. 2007). In parallel with the increases of IL-6, TNF- α , IFN- γ , MIP-1 α , MIP-2 and MCP during acute early inflammation there was a significant increase in expression of STX11 and Vti1a which persisted in the late acute phase of disease. Expression of STX11 and Vti1a were most significantly up-regulated with some of the highest fold changes during DSS colitis model. There was also a significant up-regulation in SNAP23 and STX3 in the late acute phase which correlates with increased levels of IL-6, TNF- α , MIP-1 α , MIP-2 and MCP. The

correlation between inflammatory cytokines and chemokines and the increase in expression of SNAREs such as STX3, STX11 and Vti1a points to a potential role for these SNAREs in the secretion of these cytokines during inflammation. Furthermore our data showing that these SNAREs are increased in DCs following activation further supports a role for them in cytokine and chemokine secretion.

As IBD is a multifactorial disease of unknown aetiology (Perse and Cerar 2012) we employed the use of a second colitis model – *C.rodentium* infection. *C.rodentium* can colonise the gut of mice with over 10^9 organisms within 7 to 14 days but is virtually cleared by day 21. *C.rodentium* is part of a group of enteric pathogens which is related to *E.coli* but as *E.coli* is poorly pathogenic in mice and *C.rodentium* is a natural mouse pathogen it provides us with an excellent *in vivo* model of infections of the lumen of the intestine (Mundy et al. 2005). Day 9 post *C.rodentium* infection cytokines and chemokine data was significantly up-regulated. Smith *et al*, also reported an increase in the mRNA of pro-inflammatory cytokines, IL-6, TNF- α , IFN- γ and the chemokine MCP-1 (Smith et al. 2011) Another study examining IFN- γ and TNF- α expression also correlated with our data (Higgins et al. 1999). Expression of SNAREs, SNAP-23, STX11, VAMP4 and Vti1a were also significantly up-regulated nine days post *C.rodentium* infection. Interestingly STX3 mRNA expression was significantly down-regulated 3 days post infection and remained down-regulated over the 21 days of the model.

The results in this chapter indicate that specific SNAREs are up-regulated *in vitro* and *in vivo* in two models of inflammatory disease. To the best of our knowledge

this is the first time the expression of SNAREs have been characterised in colitis models and hence implicated in inflammatory disease of the gastrointestinal tract. This data highlights the possibility of targeting SNAREs in inflammatory disease as a therapeutic measure. In the final chapter we will aim to elucidate the roles of the SNAREs, STX3 and STX11, as they have indicated *in vivo* and *in vitro* they might have a role in dendritic cells during immune activation.

CHAPTER 5

**FUNCTIONAL ROLES
FOR STX3 AND STX11**

5.1 INTRODUCTION

In the previous chapter, a number of SNAREs were identified, that may have a role in dendritic cell secretion. Following on from this, it was of interest to further elucidate the roles of the SNARE proteins, STX3 and STX11 as these SNAREs showed the most change *in vitro* and *in vivo*. This was achieved by means of RNAi and use of *Stx11*^{-/-} BMDCs.

In the last chapter, it was shown that STX3 was highly up-regulated following activation with TLR4 and TLR7 but not TLR2. This was correlated with the secretion of IL-6 from JAWSII DCs since IL-6 was secreted at high levels from JAWSII DCs when stimulated with TLR4 and TLR7 but not TLR2. STX3 was first identified in the plasma membrane by Bennett *et al.*, and subsequently, it was reported to be involved in trafficking exocytic vesicles from the TGN to the apical plasma membrane of polarized epithelial cells (Bennett et al. 1993, Low et al. 1996). STX3 has also been implicated in human cytomegalovirus (Cepeda et al., 2010). It has been suggested that STX3 is involved in late endosomes/lysosomes since RNAi inhibition of STX3 results in the reduced expression of lysosomal membrane glycoproteins (Cepeda et al., 2010). Recently, STX3 has been indicated as an essential requirement, partnered with SNAP23 for chemokine release of IL-8, MCP and MIP-1 α from mature human mast cells (Frank et al. 2011). However, missing from the literature is a role for STX3 in dendritic cells secretion.

Since it was shown that STX11 was significantly up-regulated in response to all 3 TLR ligands, highly expressed in experimental models of inflammatory disease and has been defined in familial hemophagocytic lymphohistiocytosis type-4 (FHL-4 hyper-inflammatory disease known it was of interest to investigate the possible role

of STX11 in dendritic cell secretion. STX11 is an atypical SNARE which was first identified in 1998. It was shown that patients with the hyper-inflammatory disease FHL-4 have a deletion or a mutation in STX11. As a result of this these patients possess high levels of pro-inflammatory cytokines (IFN- γ , IL-6, TNF- α and IL-18) and a higher number of activated macrophages. As a consequence, patients with FHL-4 have defective cytotoxic T lymphocytes (CTL) and natural killer (NK) cell activity. Furthermore, the high numbers of activated macrophages results in incorrect phagocytosis of cell from the hematopoietic lineage (D'Orlando et al. 2013, Marsh et al. 2010).

Recently, STX11 was examined in BMDCs and it was reported that although mRNA levels were up-regulated in BMDCs, STX11 deficiency did not affect BMDC activities or TLR-induced secretion of IL-12, IL-6 or TNF- α . This study went on to identify a role for STX11 in NK and CD8⁺ T-cell cytotoxicity and neutrophil degranulation and also noted that CTLs and NK cells produced abnormal levels of IFN- γ (D'Orlando et al. 2013). In order to further investigate the possible role of STX11 we assessed additional parameters of BMDC activation by examining secretion of more cytokines, including chemokines and investigate cell surface markers compared to the study by D'Orlando *et al.* (D'Orlando et al. 2013).

5.2 RESULTS

5.2.1 RE-CAP OF STX3 MRNA EXPRESSION AND JAWS II AND BMDC CYTOKINE AND CHEMOKINE SECRETION DATA

As previously reported in Chapter 4, STX3 expression was highly up-regulated in response to LPS and Loxoribine stimulation at 1 hour and 4 hour [Figure 5.1.A]. To identify patterns in cytokine and chemokine secretion that may correlate with the mRNA data we analysed the secretion of IL-6, TNF- α and MIP-1 α over the same time-course of 1, 4 and 12 hours [Figure 5.1.B].

JAWS II DCs were cultured for seven days in the presence of r-GM-CSF (Sigma ®) and plated at 1×10^6 cell/ml. Cells were then stimulated with 5 μ g/ml PGN, 100 ng/ml LPS and 1nM Loxoribine for 1, 4 and 12 h. Supernatants were removed and analysed for the levels of IL-6, TNF- α and MIP-1 α [Figure 5.1.B] using specific immunoassays. IL-6 secretion was significantly up-regulated from JAWSII DCs following LPS stimulation at 4 and 12 hours and Loxoribine at 12 hours ($p \leq 0.01$, $p \leq 0.001$) but remained unchanged following PGN stimulation. TNF secretion was significantly up-regulated at 4 and 12 hours following LPS, Loxoribine and PGN stimulation ($p \leq 0.001$, $p \leq 0.05$ and $p \leq 0.01$) and MIP-1 α secretion was significantly up-regulated following LPS stimulation at 4 and 12 hours ($p \leq 0.01$ and $p \leq 0.001$) and Loxoribine stimulation at 12 hours ($p \leq 0.001$) but not with PGN stimulation [Figure 5.1.B]. The trend of expression of IL-6 and TNF- α in response to LPS and Loxoribine stimulation at 4 and 12 hour and MIP-1 α at 4 hours post correlated with up-regulation of STX3 mRNA expression at 1 hour following LPS and Loxoribine stimulation but not PGN stimulation [Figure 5.1.A and Figure 5.1.B].

The data in chapter 3 was re-examined and it was identified that IL-6 was secreted by BMDCs when activated with all three TLR ligands (LPS, Loxoribine and PGN). However it was shown that IL-6 was only secreted significantly following stimulation with LPS and Loxoribine [**Figure 5.1.C**]. This was later drawn upon for subsequent experiments.

5.2.2 KNOCKDOWN OF STX3 SIGNIFICANTLY DECREASES THE SECRETION OF IL-6 AND MIP-1 ALPHA FROM JAWSII DCs

STX3 was knocked down by use of STX3 specific siRNAs (Invitrogen™). JAWS II DCs were cultured for seven days in the presence of r-GM-CSF (Sigma ®) and plated at 0.5×10^6 cell/ml overnight. The following day, cells were transfected with 1nM STX3 specific siRNA (Invitrogen™), 1nM scrambled non-silencing siRNA and 1nM of fluorescently labelled Cy™3 labelled GAPDH (Invitrogen™) [**See Appendix**], using GeneSilencer ® (Genelantis) according to manufacturer's instructions. Supernatants were removed after 24 hours and replaced with fresh media. Supernatants were subsequently removed 4 hours later and analysed for the levels of IL-1 β , IL-6, TNF- α and MIP-1 α [**Figure 5.2**]. In the absence of STX3, IL-6 and MIP-1 α are significantly decreased ($p \leq 0.05$ and $p \leq 0.01$) whereas IL-1 β is significantly increased ($p \leq 0.05$), with no significant changes in TNF- α secretion [**Figure 5.2**].

5.2.2 NEUTRALISATION OF STX3 WITH A STX3 SPECIFIC ANTIBODY SIGNIFICANTLY DECREASES THE SECRETION OF IL-6 FROM JAWS II DCS

To further elucidate and confirm the role of STX3 in secretion of cytokines and chemokines from JAWSII DCs, STX3 was neutralised using specific STX3 monoclonal antibody, which binds to the cytoplasmic NH₂-terminal region required for SNARE binding. JAWS II DCs were cultured for seven days in the presence of r-GM-CSF (Sigma ®) and plated at 1 x 10⁶ cell/ml overnight. The cells were then temporarily permeabilised with bacterial derived toxin SLO (20 µg/ml) for 15 minutes to deliver the STX3 neutralising antibody (20 µg/ml). Fresh media was then added to the cells and either left for 4 hours [Figure 5.3] or stimulated with 100 ng/ml LPS for 4h [Figure 5.4]. Supernatants were subsequently removed and analysed for the levels of, IL-1β, IL-6, TNF and MIP-1α with or without LPS stimulation. When STX3 was neutralised IL-6 secretion was significantly decreased both in unstimulated cells (**p* ≤ 0.05) [Figure 5.3] and 4 hours post LPS (**p* ≤ 0.05) [Figure 5.4]. Neutralisation of STX3 did not result in a significant change in IL-1β or TNF-α in unstimulated or stimulated cells. There was a decrease in MIP-1α but it was not statistically significant.

5.2.3 IMMUNOFLUORESCENT ANALYSIS OF THE SNARE STX3 TRANSLOCATES TO THE PLASMA MEMBRANE ONLY IN IL-6 SECRETING JAWSII DCS AND BMDCS

It has been established that the activation of JAWSII DCs with LPS and Loxoribine resulted in up-regulation of STX3 mRNA and IL-6 secretion and that knockdown of STX3 in these cells suppressed secretion of IL-6. Furthermore, it was demonstrated that PGN did not result in up-regulation of STX3 mRNA or IL-6 secretion in JAWSII DCs but in BMDCs PGN stimulation resulted in IL-6 secretion. It was decided to visualise the location of STX3 in JAWSII DCs and BMDCs and therefore, immunofluorescent staining was performed. BMDCs were harvested from C57BL/6 mice and JAWS II DCs were cultured for seven days in the presence of r-GM-CSF (Sigma ®). Cells were then seeded at 0.5×10^6 cell/ml onto 0.13-0.16mm (RA 1.5) cover-slips and left to adhere overnight. Cells were then stimulated with LPS (100 ng/ml), Loxoribine (1 mM) and PGN (5 µg/ml) for 1h. Cover-slips were incubated with STX3 specific monoclonal antibody followed by appropriate fluorescently labelled secondary antibody. In JAWSII DCs the nucleus was stained with PI for 5 minutes, however no nuclear stain was applied to the BMDCs. Slides were then imaged using a Zeiss LSM 710 inverted confocal microscope.

STX3 was detected in the cytoplasm of control JAWSII and following stimulation with LPS and Loxoribine STX3 translocated to the plasma membrane after 1 hour. PGN stimulation in JAWS DCs did not result in translocation of STX3 to the plasma membrane. In BMDCs which do respond to PGN and secrete IL-6, activation with PGN resulted in STX3 translocation [**Figure 5.5**].

Overview of STX3 findings are summarised in **Figure 5.6**.

5.2.4 MEMBERS OF THE IL-12 FAMILY ARE SIGNIFICANTLY UP-REGULATED IN *Stx11*^{-/-} BMDCs COMPARED TO WILD TYPE

It was decided to investigate the role of STX11 in dendritic cell secretion as it was up-regulated in DCs and in disease. This was performed by the use of knockout SNARE mouse model. *Stx11*^{-/-} mice were acquired from Silvia Bulfone-Paus' group in the Borstel Research Institute, Hamburg, Germany.

BMDCs harvested from *Stx11*^{-/-} and Wild type (WT) matched C57BL/6 mice were cultured for seven days in the presence of r-GM-CSF (Sigma ®) and plated at 1 x 10⁶ cell/ml. Cells were then stimulated with 100 ng/ml LPS/100 µg/ml rIL-12, 2µM CpG, 5 µg/ml PGN and 1 µg/ml PAM over a time-course of 2, 6 and 24 hours. Supernatants were removed and analysed for the levels of IL-12p40, IL-23 and IL-27p28 [**Figure 5.7, Figure 5.8 and Figure 5.9**].

IL-12p40 was significantly up-regulated in unstimulated *Stx11*^{-/-} BMDCs compared to control WT ($p \leq 0.05$) [**Figure 5.7**]. Following 2 h, 6 h and 24 h LPS/IL-12 stimulation *Stx11*^{-/-} BMDCs have significantly higher secretion of IL-12p40 compared to WT BMDCs ($p \leq 0.05$, $p \leq 0.001$ and $p \leq 0.01$) [**Figure 5.7**]. 2 and 6 hours post CpG stimulation *Stx11*^{-/-} BMDCs secrete significantly higher amounts of IL-12p40 compared to WT BMDCs ($p \leq 0.05$) [**Figure 5.7**]. 2 and 24 hour stimulation with PGN resulted in significantly higher secretion of IL-12p40 from *Stx11*^{-/-} BMDCs compared to control WT ($p \leq 0.05$) and 2 and 6 hour stimulation with PAM also had significantly higher secretion of IL-12p40 from *Stx11*^{-/-} BMDCs

compared to control WT ($p \leq 0.01$ and $p \leq 0.05$) [Figure 5.7]. Interestingly, secretion of IL-12p40 was down-regulated in *Stx11*^{-/-} BMDCs compared to control WT post 24 hour PAM stimulation ($p \leq 0.01$) [Figure 5.7].

Secretion of IL-23 from *Stx11*^{-/-} BMDCs compared to control WT at basal level was significantly up-regulated ($p \leq 0.05$) [Figure 5.8]. Following stimulation with LPS/IL-12 for 2, 6 and 24 hours, *Stx11*^{-/-} BMDCs had significantly increased secretion of IL-23 compared to WT BMDCs ($p \leq 0.01$ and $p \leq 0.05$) [Figure 5.8]. Similarly following 2, 6 and 24 hours stimulation with CpG *Stx11*^{-/-} BMDCs have significantly higher secretion compared to WT BMDCs ($p \leq 0.01$ and $p \leq 0.05$). Following TLR2 stimulation with PGN *Stx11*^{-/-} BMDCs have significantly higher secretion of IL-23 compared to WT BMDCs at 2, 6 and 24 ($p \leq 0.05$) [Figure 5.8]. Stimulation for 6 hours was the only time point post stimulation with PAM (1 μ g/ml) to show any significant up-regulation of IL-23 from *Stx11*^{-/-} BMDCs compared to control WT ($p \leq 0.01$) [Figure 5.8].

IL-27p28 basal level of secretion was significantly higher in *Stx11*^{-/-} BMDCs compared to control WT ($p \leq 0.01$) [Figure 5.9]. Following stimulation with LPS/IL-12 for 2 and 24 hours, *Stx11*^{-/-} BMDCs had significantly higher secretion of IL-27p28 compared to WT BMDCs ($p \leq 0.05$) [Figure 5.9]. Following 2 hours stimulation with CpG *Stx11*^{-/-} BMDCs had significantly higher secretion compared to WT BMDCs ($p \leq 0.01$). 2, 6 and 24 hour stimulation with PGN, *Stx11*^{-/-} BMDCs had significantly increased levels of IL-27 compared to WT BMDCs ($p \leq 0.05$) and IL-27p28 was also up-regulated in *Stx11*^{-/-} BMDCs compared to control WT post 6 and 24 hour PAM stimulation ($p \leq 0.01$) [Figure 5.9].

5.2.5 IFN- GAMMA IS SIGNIFICANTLY UP-REGULATED IN *STX11*^{-/-} BMDCS COMPARED TO WILD TYPE

IFN- γ secretion had not been measured from DCs during our previous chapters, as IFN- γ has only recently been indicated to be secreted from DCs and does so in small amounts. However IFN- γ has been previously reported to be over expressed from CD8+ CLT in *Stx11*^{-/-} mice (D'Orlando et al., 2013). BMDCs harvested from *Stx11*^{-/-} and WT mice were stimulated and IFN- γ was quantified as previously described [Section 5.2.4].

Secretion of IFN- γ from unstimulated *Stx11*^{-/-} BMDCs compared to control WT was significantly up-regulated ($p \leq 0.01$) [Figure 5.10]. Following stimulation with LPS/IL-12 at 2 and 6 hours, *Stx11*^{-/-} BMDCs had significantly higher secretion of IFN- γ compared to WT BMDCs ($p \leq 0.01$). CpG stimulation also resulted in significantly higher levels of IFN- γ after 2, 4 and 24 hours from *Stx11*^{-/-} BMDCs compared to WT BMDCs ($p \leq 0.001$ and $p \leq 0.05$). Secretion of IFN- γ from *Stx11*^{-/-} BMDCs was significantly increased compared to WT BMDCs following simulation with PGN ($p \leq 0.01$ and $p \leq 0.05$). PAM stimulation for 2, 6 and 24 hours section of IFN- γ did result in a small increase in IFN- γ from *Stx11*^{-/-} BMDCs compared to WT, however, this was not statistically significant [Figure 5.10].

5.2.6 CHEMOKINES ARE SIGNIFICANTLY UP-REGULATED IN *STX11*^{-/-} BMDCS COMPARED TO WT

BMDCs harvested from *Stx11*^{-/-} and WT mice were stimulated and chemokines, MIP-1 α [Figure 5.11] and MIP-2 [Figure 5.12] and quantified as previously described [Section 5.2.4].

MIP-1 α secretion was significantly up-regulated from unstimulated *Stx11*^{-/-} BMDCs when compared to control WT BMDCs at basal level ($p \leq 0.05$) [Figure 5.11]. Following LPS/IL-12 stimulation, *Stx11*^{-/-} BMDCs had significantly up-regulated MIP-1 α secretion at 2, 6 and 24 hours compared to WT BMDC ($p \leq 0.001$ and $p \leq 0.05$). MIP-1 α secretion following activation with CpG was significantly up-regulated at 2 and 6 hours from *Stx11*^{-/-} BMDCs compared to WT BMDCs ($p \leq 0.01$ and $p \leq 0.05$). MIP-1 α secretion was also significantly increased from *Stx11*^{-/-} BMDCs compared to WT BMDCs following 6 and 12 hours PGN and PAM stimulation ($p \leq 0.01$ and $p \leq 0.001$) [Figure 5.11].

At basal level MIP-2 secretion was significantly up-regulated from control *Stx11*^{-/-} BMDCs compared to control WT BMDCs ($p \leq 0.01$) [Figure 5.12]. MIP-2 secretion following activation with LPS/IL-12 was significantly up-regulated at 2 and 6 hours from *Stx11*^{-/-} BMDCs compared to WT BMDCs ($p \leq 0.05$). Following CpG stimulation of *Stx11*^{-/-} BMDCs had significantly up-regulated MIP-2 secretion at 2, 6 and 24 hours compared to WT BMDC ($p \leq 0.05$ and $p \leq 0.01$). A significant increase in MIP-2 was also observed at 2, 4 and 24 hours post stimulation with PGN and 2 hours with PAM stimulation from *Stx11*^{-/-} BMDCs compared to WT BMDCs ($p \leq$

0.01 and $p \leq 0.05$). There was also a significant down-regulation of MIP-2 following 24 hours PAM stimulation from *Stx11*^{-/-} BMDCs compared to WT BMDCs ($p \leq 0.001$) [Figure 5.12].

5.2.7 CYTOKINES IL-6, IL-10 AND TNF-ALPHA FROM *STX11*^{-/-} BMDCS COMPARED TO WT

BMDCs harvested from *Stx11*^{-/-} and WT mice were stimulated and cytokines quantified as previously described [Section 5.2.4].

There were no significant differences in basal level of IL-6 secretion from *Stx11*^{-/-} BMDCs when compared to WT BMDCs [Figure 5.13]. There was only significant up-regulation of IL-6 production following 2 hours stimulation of CpG, 24 hours PGN stimulation and 6 hours PAM stimulation from *Stx11*^{-/-} BMDCs when compared to WT BMDCs ($p \leq 0.05$ and $p \leq 0.001$). Otherwise IL-6 secretion was not significantly changed or was down-regulated in the cases of 24 h LPS/IL12 stimulation, 2 h PGN stimulation and 24 hour PAM stimulation from *Stx11*^{-/-} BMDCs when compared to WT BMDCs ($p \leq 0.05$, $p \leq 0.001$ and $p \leq 0.01$) [Figure 5.13].

There was a significant up-regulation of basal IL-10 from *Stx11*^{-/-} BMDCs when compared to WT BMDCs ($p \leq 0.01$) [Figure 5.14]. Significant up-regulation of IL-10 was also observed 2 hours post LPS/IL-12 stimulation, 24 hours post CpG stimulation, 6 hours post PGN and PAM stimulation from *Stx11*^{-/-} BMDCs when compared to WT BMDCs ($p \leq 0.01$, $p \leq 0.05$ and $p \leq 0.001$) [Figure 5.14]. Otherwise

IL-10 secretion was not significantly different between *Stx11*^{-/-} BMDCs and WT BMDCs [Figure 5.14].

TNF- α secretion at basal level was not significantly different between *Stx11*^{-/-} BMDCs and WT BMDCs [Figure 5.15]. Significant up-regulation of TNF- α was observed 2 hours post CpG and PAM stimulation and 6 hour post PGN stimulation from *Stx11*^{-/-} BMDCs when compared to WT BMDCs ($p \leq 0.001$ and $p \leq 0.05$). TNF- α was significantly down-regulated in response to 24 hours LPS/IL-12, 6 hours CpG, 2 hours PAM and PGN stimulation from *Stx11*^{-/-} BMDCs when compared to WT BMDCs ($p \leq 0.01$, $p \leq 0.05$ and $p \leq 0.001$). [Figure 5.15].

5.2.8 HIGHER BASAL LEVEL SURFACE MARKER EXPRESSION ON *STX11*^{-/-} BMDCS COMPARED TO WT AND MODULATION OF THE DENDRITIC CELL MARKER CD11C

BMDCs harvested from *Stx11*^{-/-} BMDCs and WT matched C57BL/6 mice were cultured for seven days in the presence of r-GM-CSF (Sigma ®) and plated at 1×10^6 cell/ml. Cells were then stimulated with 100 ng/ml LPS/100 μ g/ml rIL-12, 2 μ M CpG, 5 μ g/ml PGN and 1 μ g/ml PAM over a time-course of 2, 6 and 24 hours. Cells were subsequently washed and stained with fluorochrome-labelled monoclonal antibodies to the cell surface markers, TLR-4-MD-2 [Figure 5.16], CD14, [Figure 5.17] CD40 [Figure 5.18], CD80 [Figure 5.19], CD86 [Figure 5.20], MHC II [Figure 5.21] and CD11c [Figure 5.22].

There was a higher expression of TLR-4-MD-2 on unstimulated *Stx11*^{-/-} BMDCs when compared to WT BMDCs at basal levels. **[Figure 5.16]**. Post stimulation with CpG TLR-4-MD-2 expression was increased at 2, 6 and 24 hour time points in WT BMDCs which was comparable to *Stx11*^{-/-} BMDCs, However, *Stx11*^{-/-} BMDCs expression was not as high. TLR-4-MD-2 was down-regulated on both WT BMDCs and *Stx11*^{-/-} BMDCs after LPS stimulation at 2 and 6 hours. However TLR-4-MD2 expression after 24 hours LPS stimulation was up-regulated on both WT BMDCs and *Stx11*^{-/-} BMDCs compared to control cells. Expression of TLR-4-MD2 was higher on WT BMDCs after 24 hours when compared to *Stx11*^{-/-} BMDCs. Post PAM stimulation TLR-4-MD2 expression remained relatively un-changed on WT BMDCs. *Stx11*^{-/-} BMDCs showed down-regulated expression of TLR-4-MD-2 following 2, 6 and 24 hours of PAM stimulation. 24 hours post PGN stimulation WT BMDCs up-regulated TLR-4-MD-2 compared to control cells, in contrast *Stx11*^{-/-} BMDCs down-regulated expression of TLR-4-MD-2 at 24 hours. Expression of TLR-4-MD2 in *Stx11*^{-/-} BMDCs was also down-regulated at 2 and 6 hours post PGN this was comparable in WT cells. **[Figure 5.16]**.

Expression of CD14 at basal level was up-regulated in *Stx11*^{-/-} BMDCs when compared to WT. **[Figure 5.17]**. Following CpG stimulation at 2 hours WT and *Stx11*^{-/-} BMDCs up-regulated CD14 expression compared to control cells. However, at 6 and 24 hours post CpG stimulation CD14 expression was up-regulated in both *Stx11*^{-/-} BMDCs and WT BMDCs, and was higher in the *STX11*^{-/-} BMDCs. 24 hours post LPS/IL12 stimulation CD14 was up-regulated compared to control and was

higher in the *Stx11*^{-/-} BMDCs. CD14 was incrementally increased over time in the WT BMDCs, at 2, 6 and 24 hours. However, in *Stx11*^{-/-} BMDCs CD14 expression was down-regulated at 2 and 6 hours compared to control before being up-regulated at 24 hours. Following PAM stimulation CD14 expression increased over the time course of 2, 6 and 24 hours in WT BMDCs and *Stx11*^{-/-} BMDCs was comparable. Following PGN stimulation over the time-course, WT BMDC expression of CD14 increased over time. This expression was similar in *Stx11*^{-/-} BMDCs with the exception of a down-regulation at 2 hours compared to control. 24 hours stimulation with PGN had a higher expression in WT BMDCs when compared to in *Stx11*^{-/-} BMDCs [Figure 5.17].

CD40 expression on *Stx11*^{-/-} BMDCs was much higher than WT BMDCs on unstimulated cells [Figure 5.18]. Following a time-course of stimulation with CpG, CD40 expression increased over time in both in *Stx11*^{-/-} BMDCs and WT. However expression was higher overall in *Stx11*^{-/-} BMDCs. The CD40 expression following LPS/IL-12 stimulation over 2, 6 and 24 hours also increased over time in both in *Stx11*^{-/-} BMDCs and WT. However, expression was higher overall in *Stx11*^{-/-} BMDCs with the exception of a slight down-regulation of the 2 hour LPS/IL-12 stimulation in *Stx11*^{-/-} BMDCs. Post PAM stimulation over the time-course WT BMDCs had increased the expression of CD40 whereas in *Stx11*^{-/-} BMDCs CD40 expression was down-regulated compared to controls. PGN stimulation resulted in up-regulation of expression of CD40 in a time dependant manner in WT BMDCs. However, *Stx11*^{-/-} BMDCs expression of CD40 was down-regulated in response to 2 hour stimulation of CpG compared to control and its expression at 6 and 24 hours was then up-regulated compared to control [Figure 5.18].

CD80 was up-regulated on unstimulated *Stx11*^{-/-} BMDCs compared to WT BMDCs [Figure 5.19]. Activation with CpG, LPS, PAM and PGN resulted in a time-dependant up-regulation of CD80 at 2, 6 and 24 hours in WT BMDCs. In *Stx11*^{-/-} BMDCs expression of CD80 was highly up-regulated in basal levels. There was an initial down-regulation of CD80 expression in response to CpG, LPS and PGN at 2 hours and 2 and 6 hours following PAM stimulation but subsequently up-regulated its expression was increased compared to control *Stx11*^{-/-} BMDCs [Figure 5.19].

Expression of CD86 was up-regulated in *Stx11*^{-/-} BMDCs when compared to WT BMDCs [Figure 5.20]. Activation with CpG, LPS, PAM and PGN resulted in a time-dependant up-regulation of CD86 at 2, 6 and 24 hours in WT BMDCs. There was also an up-regulation of *Stx11*^{-/-} BMDCs CD86 expression over the time-course of TLR stimulation when compared to controls with the exception of a down-regulation at 12 hours in response to CpG, PAM and PGN stimulation [Figure 5.20].

MHCII expression in *Stx11*^{-/-} BMDCs compared to WT BMDCs was up-regulated at basal levels [Figure 5.21]. Following activation with CpG, LPS, PAM and PGN, *Stx11*^{-/-} BMDCs and WT BMDCs at 2 and 6 hours had up-regulated MHCII expression in a time dependant manner with a slight fall off in expression at 24 hours. MHCII in *Stx11*^{-/-} BMDCs was higher than WT BMDCs at every time point [Figure 5.21].

To assess the DC phenotype we assessed the dendritic cell marker, CD11c. CD11c expression was significantly decreased in *Stx11*^{-/-} BMDCs compared to WT BMDCs ($p \leq 0.01$) [Figure 5.22].

5.2.8 STX11 EXPRESSION IS SIGNIFICANTLY UP-REGULATED AT THE SAME TIMEPOINT IFN-GAMMA IS UP-REGULATED

In an attempt to correlate STX11 requirement and cytokine or chemokine secretion data, the mRNA profile of STX11 was examined in WT BMDCs in response to TLR ligands. Since IFN- γ was significantly up-regulated from *Stx11*^{-/-} BMDCs when compared to WT BMDCs and has reported to be overexpressed from CD8⁺ CLT in *Stx11*^{-/-} mice, it was decided to investigate IFN- γ expression, which we confirmed with the previous IFN- γ data at protein level.

Stx11^{-/-} BMDCs and WT BMDCs were cultured for seven days in the presence of murine rGM-CSF (Sigma ®) and plated at 1 x 10⁶ cell/ml. Cells were then stimulated with 100 ng/ml LPS/100 μ g/ml rIL-12, 2 μ M CpG, 5 μ g/ml PGN and 1 μ g/ml PAM for 6 hours. Total RNA was extracted, converted to cDNA, which was then subjected to quantitative real-time PCR. $2^{-\Delta\Delta Cq}$ formula of the delta-delta Cq method was used and a fold change in expression of STX11 and IFN- γ genes was normalized against that of endogenous control S18. SNARE mRNA levels were determined as expression in the absence of stimulation, which is given an arbitrary value of 1.

STX11 expression in WT BMDCs was seen to be significantly up-regulated 6 hours after LPS/IL-12 stimulation ($p \leq 0.05$) [Figure 5.23(A)]. This correlated with increased mRNA expression of IFN- γ in *Stx11*^{-/-} BMDCs and WT BMDCs, with an increase in IFN- γ expression following stimulation with PGN ($p \leq 0.05$) and LPS/IL-12 (not statistically significant) from *Stx11*^{-/-} BMDCs when compared to WT BMDCs [Figure 5.23(B)]. This correlated well with the increased production of

IFN- γ that was shown from *Stx11*^{-/-} BMDCs when compared to WT BMDCs at 6 hours in a previous experiment [Figure 5.23].

5.2.9 WT BMDCS UP-REGULATE THEIR EXPRESSION OF SURFACE MARKERS WHEN DIFFERENTIATED IN THE PRESENCE OF IFN-GAMMA

The previous data suggested that STX11 has a possibly having a regulatory role in IFN- γ secretion from BMDCs. The next step was to assess the effect IFN- γ would have on BMDC surface marker expression in order to see if it produced a DC with similar phenotypes to the *Stx11*^{-/-} BMDCs.

BMDCs were harvested from WT mice, cultured for three days in the presence of r-GM-CSF (Sigma ®) and in high or low levels of r-IFN- γ (200pg/ml or 10ng/ml). Cells were subsequently washed and stained with fluorochrome-labelled monoclonal antibodies to the cell surface markers, TLR-4-MD-2, CD14, CD40 [Figure 5.24], CD80, CD86, MHC II [Figure 5.25] and CD11c [Figure 5.26].

Expression of TLR-4-MD-2, CD14, CD4, CD80, CD86 and MHC II were all up-regulated at basal level when differentiated in the presence of low or high levels of IFN- γ [Figure 5.24, Figure 5.25]. Expression of these markers were also up-regulated in a dose-dependant manner which was dependant on the concentration of IFN- γ the BMDCs were grown in. BMDCs cultured in high levels of IFN- γ had higher expression of surface markers when compared to BMDCs grown in lower

levels of IFN- γ [Figure 5.24, Figure 5.25]. CD11c expression was significantly down-regulated in BMDCs grown in low and high levels of IFN- γ ($p \leq 0.001$) [Figure 5.26].

5.2.10 WT BMDCS UP-REGULATE THEIR EXPRESSION OF IL-12 WHEN DIFFERENTIATED IN THE PRESENCE OF IFN-GAMMA

It was of interest to assess the effect of BMDCs grown in IFN- γ would have on cytokine secretion of the IL-12 family in order to see if it resulted in a phenotype similar to *Stx11*^{-/-} BMDCs. The IL-12 family were one of the groups of cytokines to be most significantly up-regulated in *Stx11*^{-/-} BMDCs when compared to WT BMDCs. BMDCs harvested from WT mice, cultured for seven days in the presence of r-GM-CSF (Sigma ®) and in high or low levels of r-IFN- γ (200 pg/ml or 10 ng/ml). Cells were then plated at 1×10^6 cell/ml and left to rest overnight. Cells were then stimulated with LPS (100ng/ml) for 24 hours. Supernatants were removed and analysed for the levels of IL-12p40 and IL-23 [Figure 5.27].

IL-12p40 and IL-23 were significantly up-regulated following LPS stimulation in BMDCs grown in low levels of IFN- γ ($p \leq 0.001$) [Figure 5.27]. Conversely IL-12p40 and IL-23 were significantly down-regulated following LPS stimulation in BMDCs cultured in high levels of IFN- γ ($p \leq 0.001$) [Figure 5.27].

5.2.11 THE ADDITION OF AN ANTI-IFN-GAMMA NEUTRALIZING ANTIBODY TO *STX11*^{-/-} BMDCS RESULTED IN A PHENOTYPE SIMILAR TO WT BMDCS

Since WT BMDCs cultured in IFN- γ had similar characteristics to that of *Stx11*^{-/-} BMDCs, it was decided to investigate whether or not an α -IFN- γ antibody would restore the phenotype of *Stx11*^{-/-} BMDCs to WT BMDCs.

BMDCs were harvested from *Stx11*^{-/-} BMDCs and WT matched C57BL/6 mice were cultured for seven days in the presence of r-GM-CSF (Sigma ®) and plated at 1×10^6 cell/ml. Cells were then stimulated with 100 ng/ml LPS/100 μ g/ml rIL-12 for 24 hours. Cells were subsequently washed and stained with fluorochrome-labelled monoclonal antibodies to the cell surface markers, CD40, CD80, CD86 and MHC II [Figure 5.28].

CD40 expression was higher in *Stx11*^{-/-} BMDCs when compared to WT BMDCs following LPS stimulation. In the presence of an α -IFN- γ antibody *Stx11*^{-/-} BMDCs surface expression was down-regulated to similar levels observed in WT BMDCs [Figure 5.28]. This pattern was also observed for CD80, CD86 and MHCII expression [Figure 5.28].

5.2.11 EXPRESSION OF THE MATURATION MARKER CCR5 IS DOWN-REGULATED IN *STX11*^{-/-} BMDCs AND REVERSED IN THE PRESENCE OF AN ANTI-IFN-GAMMA ANTIBODY

The CCR5 surface marker is known to be lost from the surface of a maturing DC. To examine where or not the *Stx11*^{-/-} BMDCs have a more mature phenotype when compared to WT BMDCs the CCR5 expression was assessed in *Stx11*^{-/-} BMDCs and compared to WT BMDCs. In addition, it was of interest whether the *Stx11*^{-/-} BMDCs CCR5 expression could be reversed with an α -IFN- γ antibody.

BMDCs harvested from *Stx11*^{-/-} BMDCs and WT matched C57BL/6 mice were cultured for seven days in the presence of r-GM-CSF (Sigma ®) and plated at 1×10^6 cell/ml. Cells were then stimulated with 100 ng/ml LPS/100 μ g/ml rIL-12, CpG (2 μ M) and PGN (5 μ g/ml) for 24 hours. Cells were subsequently washed and stained with fluorochrome-labelled monoclonal antibodies to the cell surface marker, CCR5 [Figure 5.29].

CCR5 expression was down-regulated on the surface of unstimulated *Stx11*^{-/-} BMDCs compared to WT BMDCs [Figure 5.29]. Following LPS/IL-12 stimulation CCR5 was down-regulated on *Stx11*^{-/-} BMDCs and WT BMDCs. CCR5 expression on LPS/IL-12 stimulated *Stx11*^{-/-} BMDCs was lower than LPS/IL-12 stimulated WT BMDCs. In the presence of an α -IFN- γ antibody, CCR5 expression on *Stx11*^{-/-} BMDCs was comparable to WT BMDC level [Figure 5.29]. This pattern of LPS

stimulation and reversal of CCR5 expression with α -IFN- γ antibody was also observed with CpG and PAM stimulation.

5.2.12 EXPRESSION OF PD-L1 IS UP-REGULATED IN *STX11*^{-/-} BMDCs AND REVERSED IN THE PRESENCE OF AN ANTI-IFN-GAMMA ANTIBODY

Expression of PD-L1 has previously been reported to be up-regulated in response to IFN- γ in BMDCs. PD-L1 is an inhibitory receptor expressed on APCs, such as DCs which regulates tolerance and autoimmunity.

PD-L1 expression was up-regulated on the surface of LPS/IL-12 stimulated WT BMDCs when compared to unstimulated WT BMDCs (MFI 1009 v 682) and LPS/IL12 stimulated *Stx11*^{-/-} BMDCs compared to unstimulated *Stx11*^{-/-} BMDCs (MFI 1204 v 428) [Figure 5.30]. PD-L1 expression on LPS/IL-12 stimulated *Stx11*^{-/-} BMDCs was higher than LPS/IL-12 stimulated WT BMDCs (MFI 1204 v 1009). In the presence of an α -IFN- γ antibody, PD-L1 expression was reduced on *Stx11*^{-/-} BMDCs (MFI 854 v 1204) [Figure 5.30].

5.2.12 *STX11*^{-/-} BMDCs HAVE IMPAIRED ABILITY TO PRIME T CELLS BY INHIBITION OF CYTOKINE SECRETION

It is known that PD-L1 is up-regulated on the *Stx11*^{-/-} BMDCs, which is associated with impaired DC-T cell activation (Shen et al. 2010) and bone marrow pre-cursors

which are differentiated in the presence of GM-CSF and IFN- γ induce T cells hyporesponsiveness (Rongcun et al. 1998). To this end it was of interest to examine the ability of *Stx11*^{-/-} BMDCs to prime T cells by analysing T cell proliferation in a T cell:*Stx11*^{-/-} BMDC co-culture and cytokine production of the T-cells.

WT and *STX11*^{-/-}BMDCs were cultured in r-GM-CSF for seven days and subsequently were plated (1×10^6 cells/ml) and left to rest overnight. Cells were then stimulated with LPS (100 ng/ml) for 4 hours.

CD4⁺ T cells were isolated using a Stemcell Easysep™ system. This system removes unwanted cells by negative selection of non-CD4⁺ T-cells using biotinylated antibody cocktails. The cells suspension was then placed into a magnetic field which holds the non-CD4⁺ T-cells and the un-labelled CD4⁺ T cells are decanted.

CD4⁺ T cells were then stained with CFSE and co-cultured with control and LPS stimulated *Stx11*^{-/-} BMDCs and WT BMDCs for 72 hours. Cells were removed from plate, washed and stained with a CD4 antibody and PI and analysed on FACS Aria. The data was then analysed using FlowJo analysis software (Treestar). Cells were gated on PI negative, CD4⁺ positive cells. CFSE data was plotted and analysed using the proliferation algorithm on FlowJo in order to calculate the percentage of divided cells, and number of cells in each generation after 72 hours of co-culture.

DC differentiated in the presence of IFN- γ have been reported to inhibit the proliferation of T cells (Rojas and Krishnan 2010). Interestingly, proliferation of the T cells showed no differences between *Stx11*^{-/-} BMDCs and WT BMDCs [**Figure 5.31**]. Secretion of IL-2 from T cells co-cultured with control and LPS-stimulated

Stx11^{-/-} BMDCs was however significantly down regulated ($p \leq 0.05$) [Figure 5.32], TNF- α secretion significantly down-regulated from T cells co-cultured with control *Stx11*^{-/-} BMDCs ($p \leq 0.05$) and there was significant down-regulation of IL-4 secretion from T cells co-cultured with LPS stimulated *Stx11*^{-/-} BMDCs ($p \leq 0.05$) [Figure 5.32].

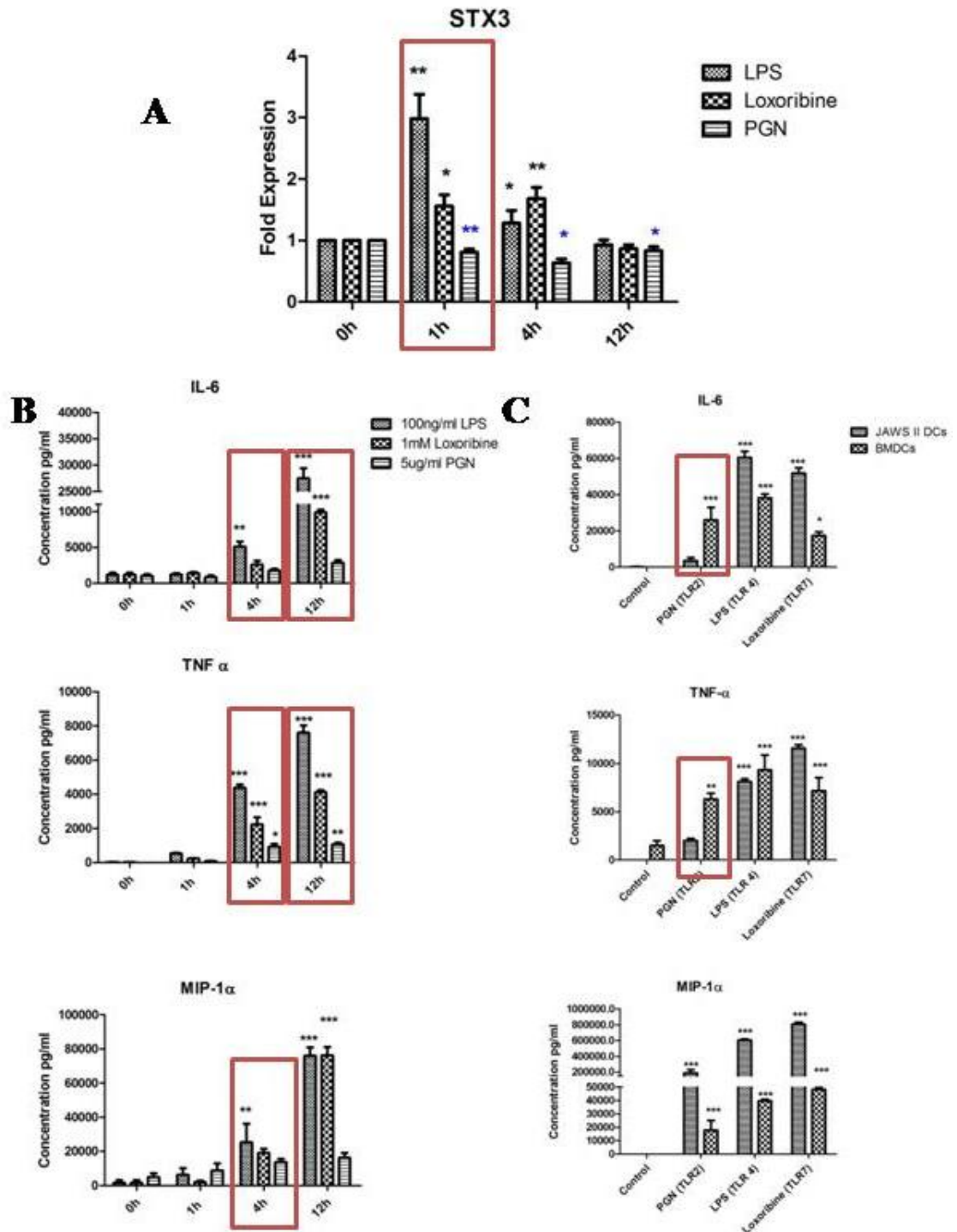


Figure 5.1: Indication for STX3 involvement in cytokine or chemokine secretion overview. (A) Recap of STX3 mRNA data (B). Time-course of cytokine and chemokine secretion from JAWSII DCs in response to TLR2, TLR4 and TLR7 data and (C) cytokine secretion from BMDC v JAWSII DC in response to TLR2, TLR4 and TLR7. Results are mean \pm SEM of triplicate assays. $*p \leq 0.05$, $**p \leq 0.01$ and $***p \leq 0.001$ comparing control to TLR stimulated treated JAWSII DCs as determined by a two-tailed t-test for (A) and (C) whereas in (B) $***p \leq 0.001$, $**p \leq 0.01$, $*p \leq 0.05$ comparing CTL vs 1h, 4h, 12h TLR stimulated groups as determined by one-way ANOVA test.

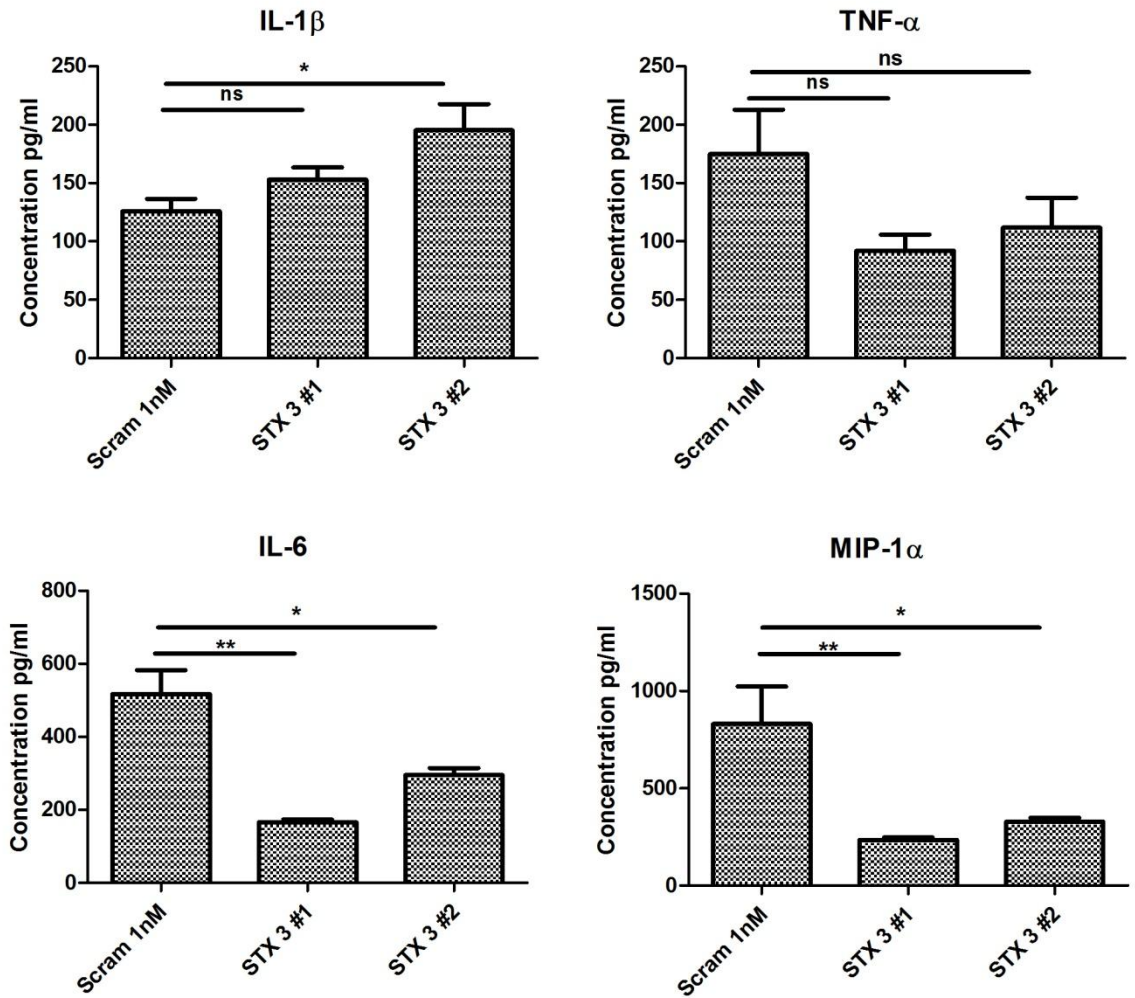


Figure 5.2: Knockdown of STX3 by siRNA. JAWSII DCs were transfected with siRNA against STX3 or a negative control non-silencing siRNA. 24h after the transfection, fresh media was put on the cells and incubated for 4h. This media was then harvested and basal levels of cytokines or chemokines were assessed using specific immunoassays. Results are mean \pm SEM of triplicate assays. * $p \leq 0.05$ and ** $p \leq 0.01$ comparing control versus STX3 siRNA transfected JAWSII DCs as determined by a two-tailed t-test.

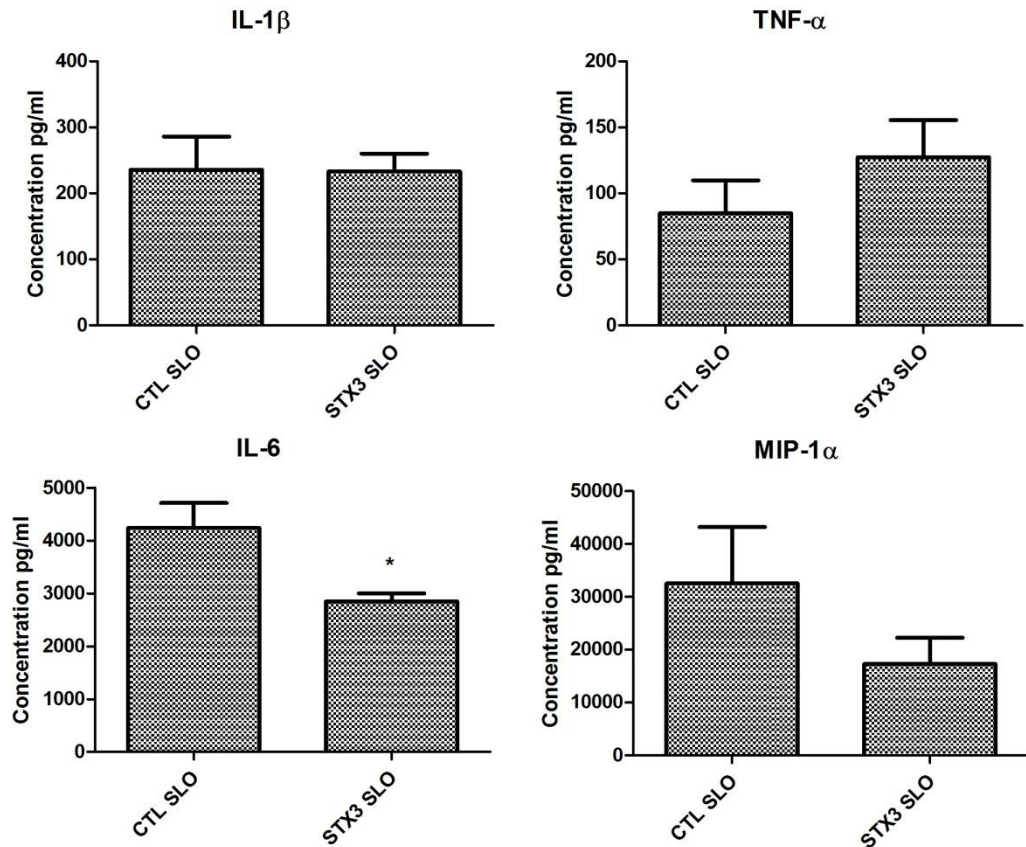


Figure 5.3: Neutralisation of STX3 with STX3 specific monoclonal antibody. JAWSII DCs were temporarily permeabilised for 15 minutes with SLO (20 μ g/ml) and which delivered the STX3 neutralising antibody (20 μ g/ml). After 4 hours the media was then harvested and basal levels of cytokines or chemokines was assessed using specific immunoassays. Results are mean \pm SEM of triplicate assays. * $p \leq 0.05$ comparing control versus STX3 neutralising antibody treated JAWSII DCs as determined by a two-tailed t-test.

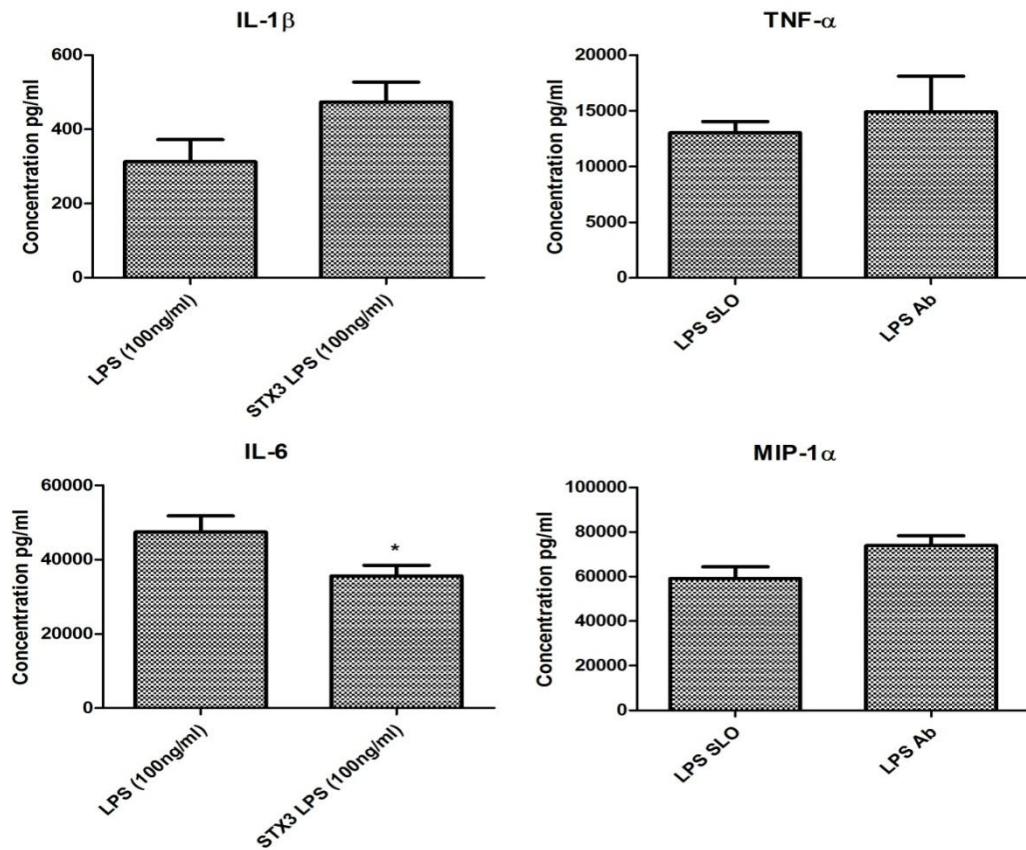


Figure 5.4: Neutralisation of STX3 with STX3 specific monoclonal antibody. JAWSII DCs were temporarily permeabilised for 15 minutes with SLO (20 μ g/ml) and which delivered the STX3 neutralising antibody (20 μ g/ml). Cells were then stimulated with 100 ng/ml LPS for 4 hours. Supernatants were harvested and levels of cytokines or chemokines was assessed using specific immunoassays. Results are mean \pm SEM of triplicate assays. * $p \leq 0.05$ comparing control versus STX3 neutralising antibody treated JAWSII DCs as determined by a two-tailed t-test.

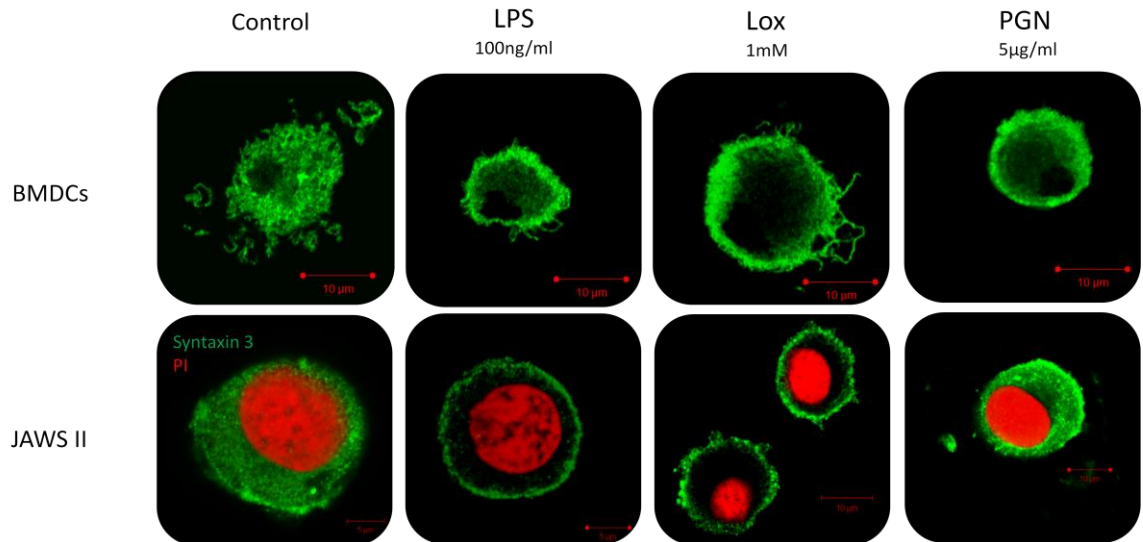


Figure 5.5: Localisation of STX3 to the Plasma Membrane in JAWSII DCs and BMDCs. JAWS II DCs and BMDCs were plated 1×10^6 /ml and stimulated with 5 μ g/ml PGN, 100 ng/ml LPS and 1mM Loxoribine for 1 hour. Immunofluorescent indirect double staining of STX3 (Green) and nuclei (red) in TLR 4, TLR7 and TLR 2 stimulated JAWS II DCs and BMDCs to show localisation of STX3 within the cells.

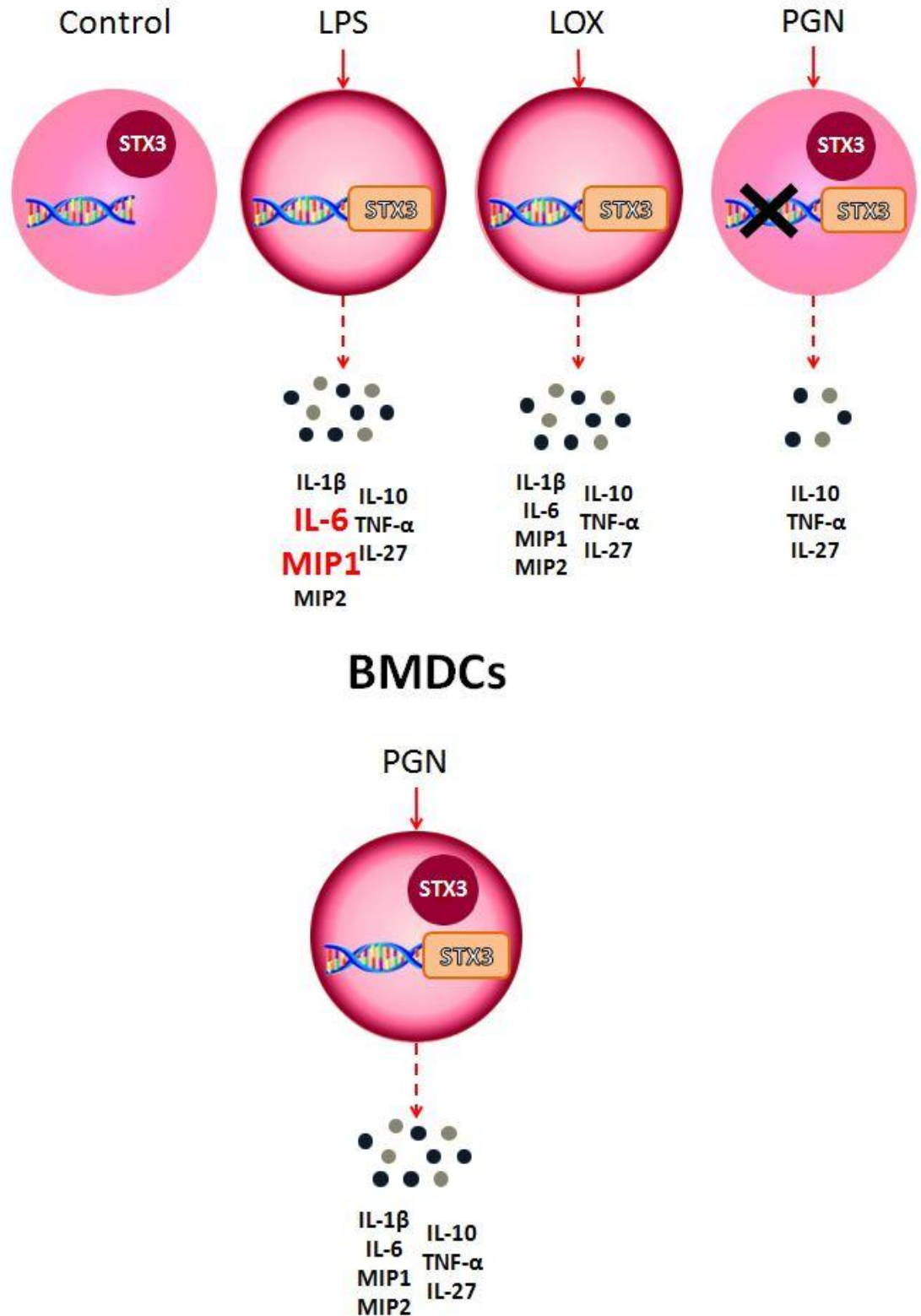


Figure 5.6: Schematic representation of secretion of cytokines and chemokines, mRNA transcription and localisation of STX3 in JAWS II DCs and BMDCs.

IL-12p40

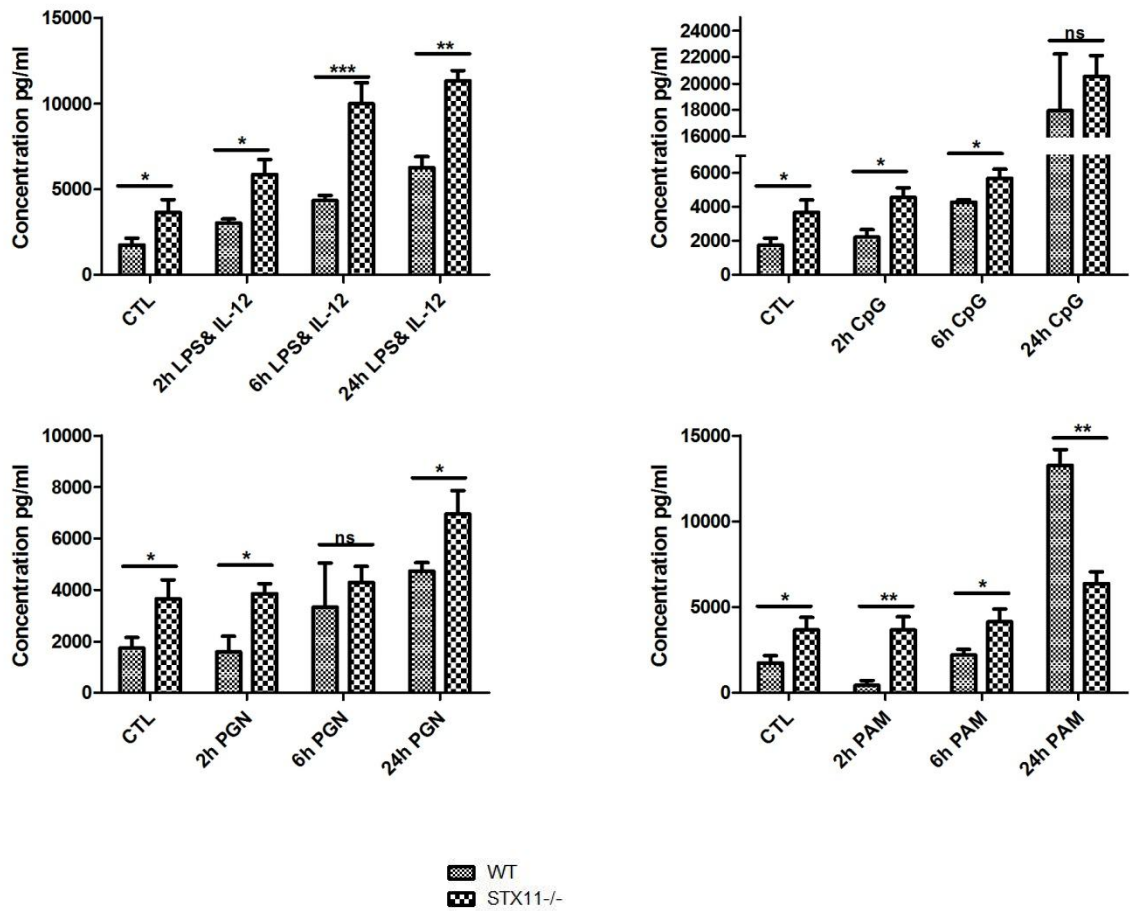


FIGURE 5.7: Comparison of IL-12p40 secretion from WT and *Stx11*^{-/-} BMDCs following activation with a panel of ligands over a time-course. DCs were cultured in r-GM-CSF for seven days and subsequently were plated (1×10^6 cells/ml) and left to rest overnight. Cells were then stimulated with 100 ng/ml LPS and 100 μ g/ml rIL-12, 2 μ M CpG, 5 μ g/ml PGN or 1 μ g/ml PAM. Supernatants were recovered after 24 h and assessed for levels of IL-12p40 using specific immunoassays. Results are \pm SEM of quadruplicate assays. * $p \leq 0.05$, ** $p \leq 0.01$ and *** $p \leq 0.001$ as determined by a two-tailed t-test.

IL-23

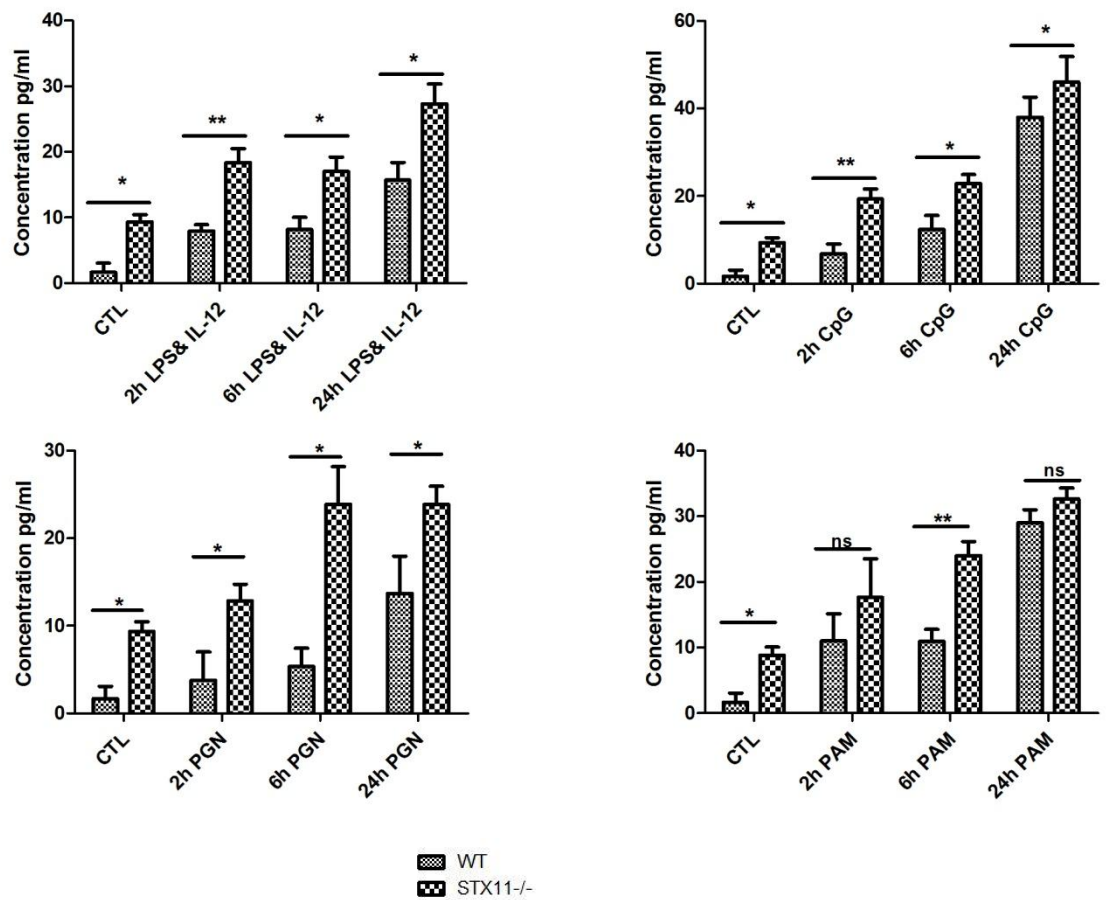


FIGURE 5.8: Comparison of IL-23 secretion from WT and *Stx11*^{-/-} BMDCs following activation with a panel of ligands over a time-course. DCs were cultured in r-GM-CSF for seven days and subsequently were plated (1×10^6 cells/ml) and left to rest overnight. Cells were then stimulated with 100 ng/ml LPS and 100 μ g/ml rIL-12, 2 μ M CpG, 5 μ g/ml PGN or 1 μ g/ml PAM. Supernatants were recovered after 24 h and assessed for levels of IL-23 using specific immunoassays. Results are \pm SEM of quadruplicate assays. * $p \leq 0.05$, ** $p \leq 0.01$ and *** $p \leq 0.001$ as determined by a two-tailed t-test.

IL-27p28

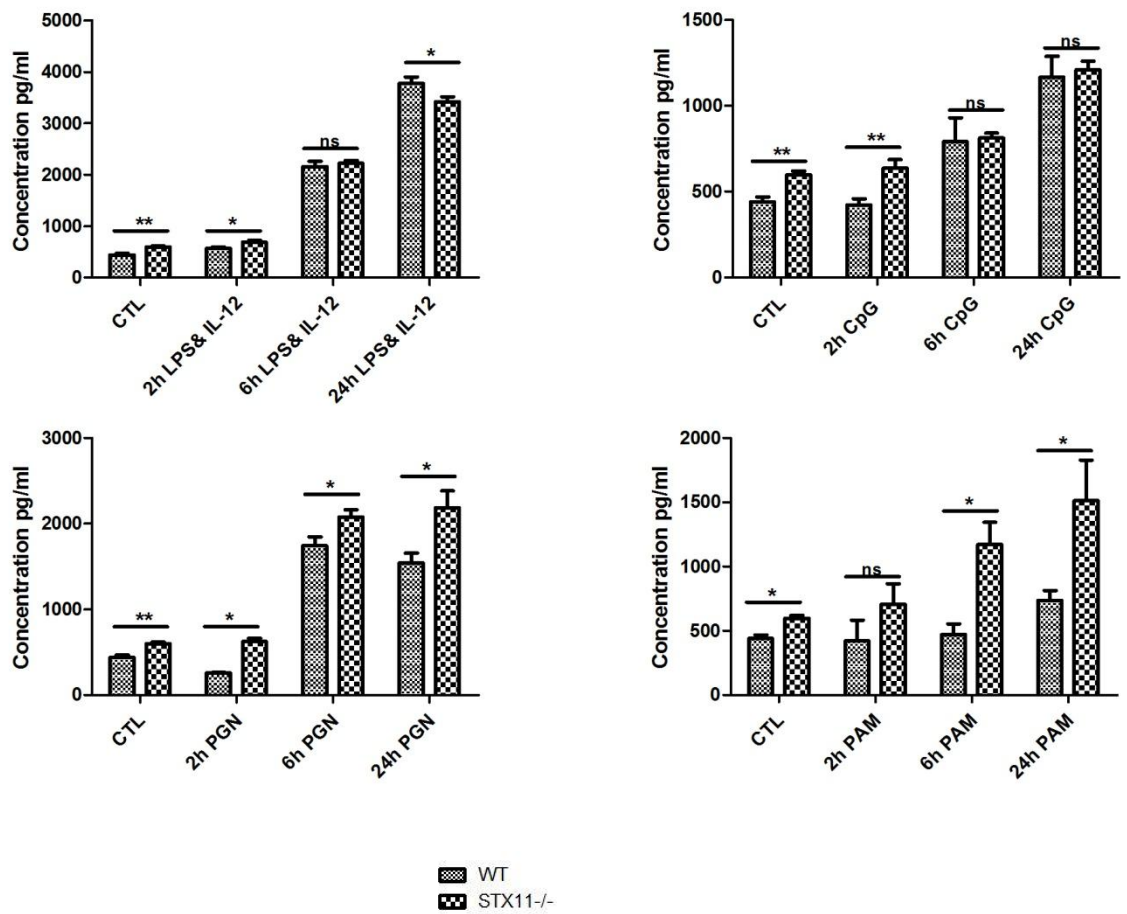


FIGURE 5.9: Comparison of IL-27p28 secretion from WT and *Stx11*^{-/-} BMDCs following activation with a panel of ligands over a time-course. DCs were cultured in r-GM-CSF for seven days and subsequently were plated (1×10^6 cells/ml) and left to rest overnight. Cells were then stimulated with 100 ng/ml LPS and 100 μ g/ml rIL-12, 2 μ M CpG, 5 μ g/ml PGN or 1 μ g/ml PAM. Supernatants were recovered after 24 h and assessed for levels of IL-27p28 using specific immunoassays. Results are \pm SEM of quadruplicate assays. * $p \leq 0.05$, ** $p \leq 0.01$ and *** $p \leq 0.001$ as determined by a two-tailed t-test.

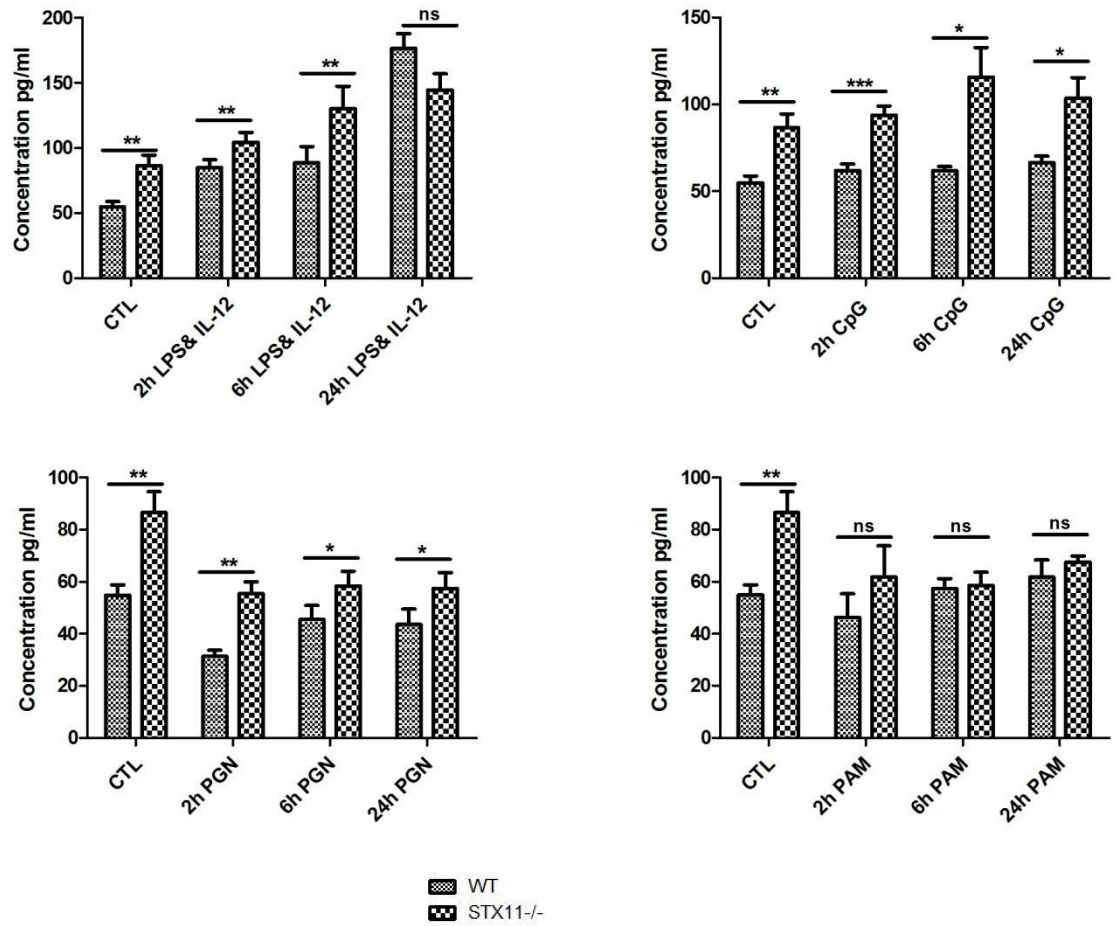
IFN- γ 

FIGURE 5.10: Comparison of IFN- γ secretion from WT and *Stx11*^{-/-} BMDCs following activation with a panel of ligands over a time-course. BMDCs were cultured in r-GM-CSF for seven days and subsequently plated (1×10^6 cells/ml) and left to rest overnight. Cells were then stimulated with 100 ng/ml LPS and 100 μ g/ml rIL-12, 2 μ M CpG, 5 μ g/ml PGN or 1 μ g/ml PAM. Supernatants were recovered after 24 h and assessed for levels of IFN- γ using specific immunoassays. Results are \pm SEM of quadruplicate assays. * $p \leq 0.05$, ** $p \leq 0.01$ and *** $p \leq 0.001$ as determined by a two-tailed t-test.

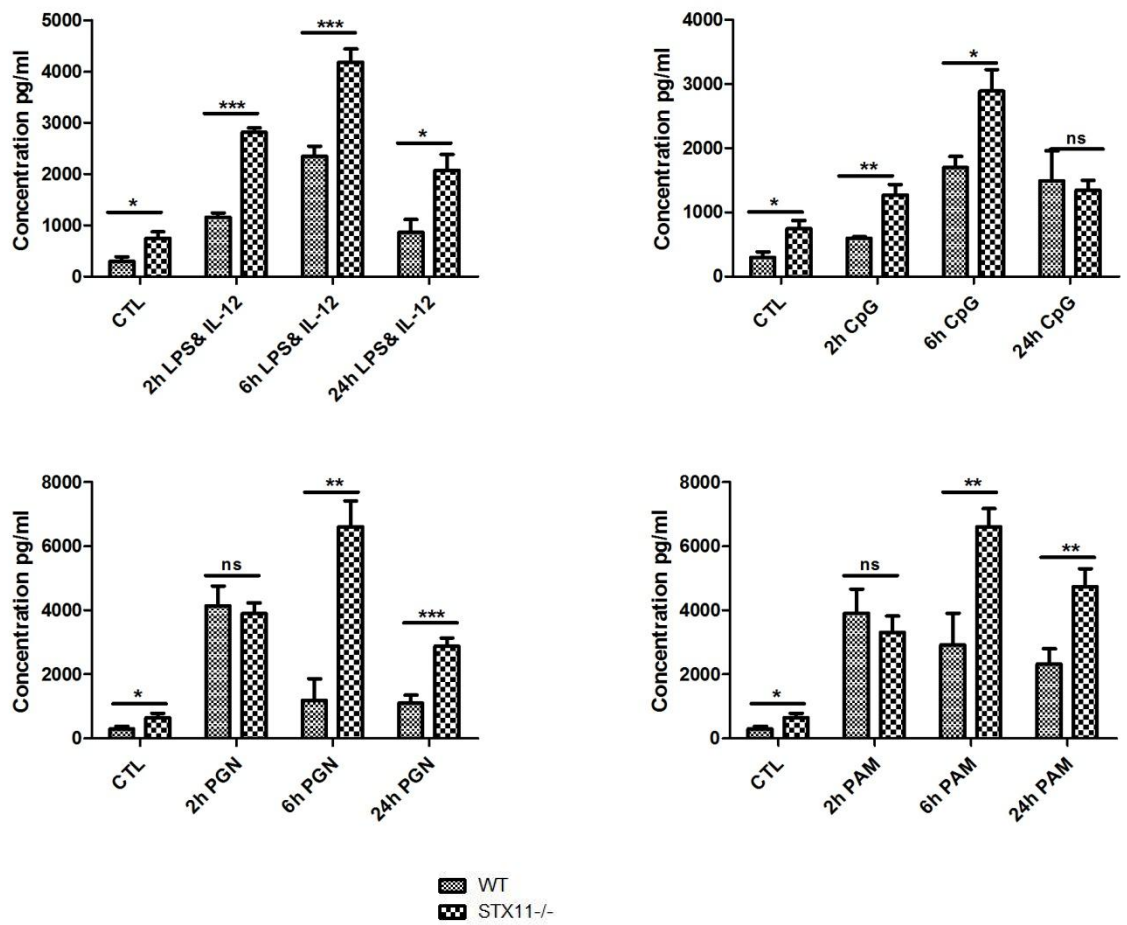
MIP-1 α 

FIGURE 5.11: Comparison of MIP-1 α secretion from WT and *Stx11*^{-/-} BMDCs following activation with a panel of ligands over a time-course. BMDCs were cultured in r-GM-CSF for seven days and subsequently were plated (1×10^6 cells/ml) and left to rest overnight. Cells were then stimulated with 100 ng/ml LPS and 100 μ g/ml rIL-12, 2 μ M CpG, 5 μ g/ml PGN or 1 μ g/ml PAM. Supernatants were recovered after 24 h and assessed for levels of MIP-1 α using specific immunoassays. Results are \pm SEM of quadruplicate assays. * $p \leq 0.05$, ** $p \leq 0.01$ and *** $p \leq 0.001$ as determined by a two-tailed t-test.

MIP-2

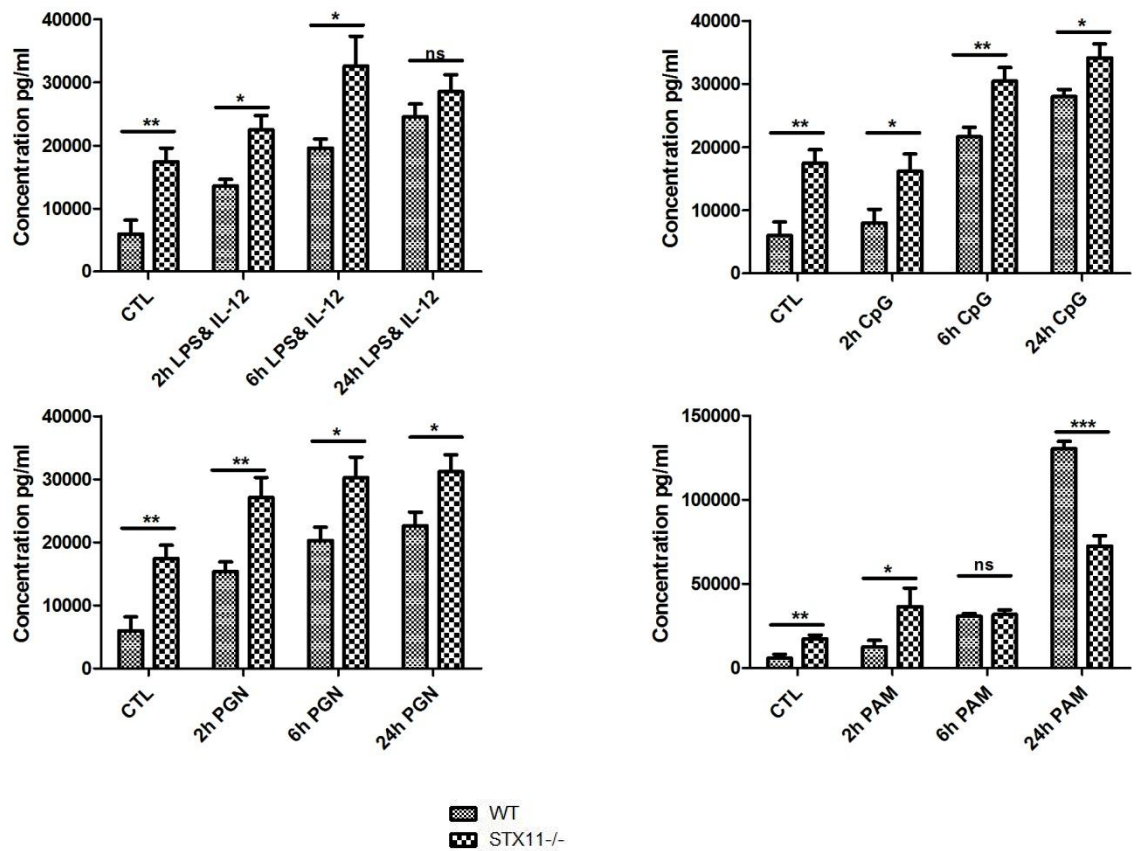


FIGURE 5.12: Comparison of MIP-2 secretion from WT and *Stx11*^{-/-} BMDCs following activation with a panel of ligands over a time-course. BMDCs were cultured in r-GM-CSF for seven days and subsequently were plated (1×10^6 cells/ml) and left to rest overnight. Cells were then stimulated with 100 ng/ml LPS and 100 μ g/ml rIL-12, 2 μ M CpG, 5 μ g/ml PGN or 1 μ g/ml PAM. Supernatants were recovered after 24 h and assessed for levels of MIP-2 using specific immunoassays. Results are \pm SEM of quadruplicate assays. * $p \leq 0.05$, ** $p \leq 0.01$ and *** $p \leq 0.001$ as determined by a two-tailed t-test.

IL-6

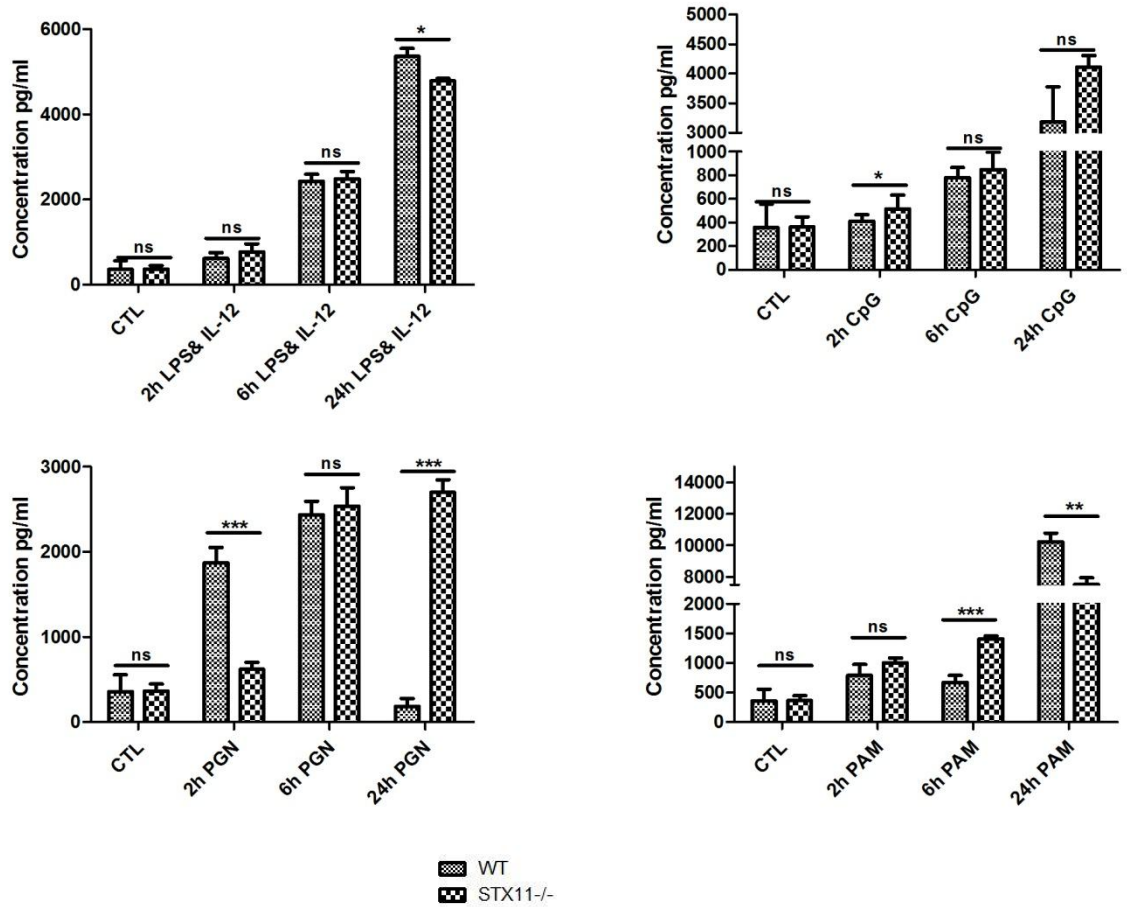


FIGURE 5.13: Comparison of IL-6 secretion from WT and *Stx11*^{-/-} BMDCs following activation with a panel of ligands over a time-course. BMDCs were cultured in r-GM-CSF for seven days and subsequently were plated (1×10^6 cells/ml) and left to rest overnight. Cells were then stimulated with 100 ng/ml LPS and 100 μ g/ml rIL-12, 2 μ M CpG, 5 μ g/ml PGN or 1 μ g/ml PAM. Supernatants were recovered after 24 h and assessed for levels of IL-6 using specific immunoassays. Results are \pm SEM of quadruplicate assays. * $p \leq 0.05$, ** $p \leq 0.01$ and *** $p \leq 0.001$ as determined by a two-tailed t-test.

IL-10

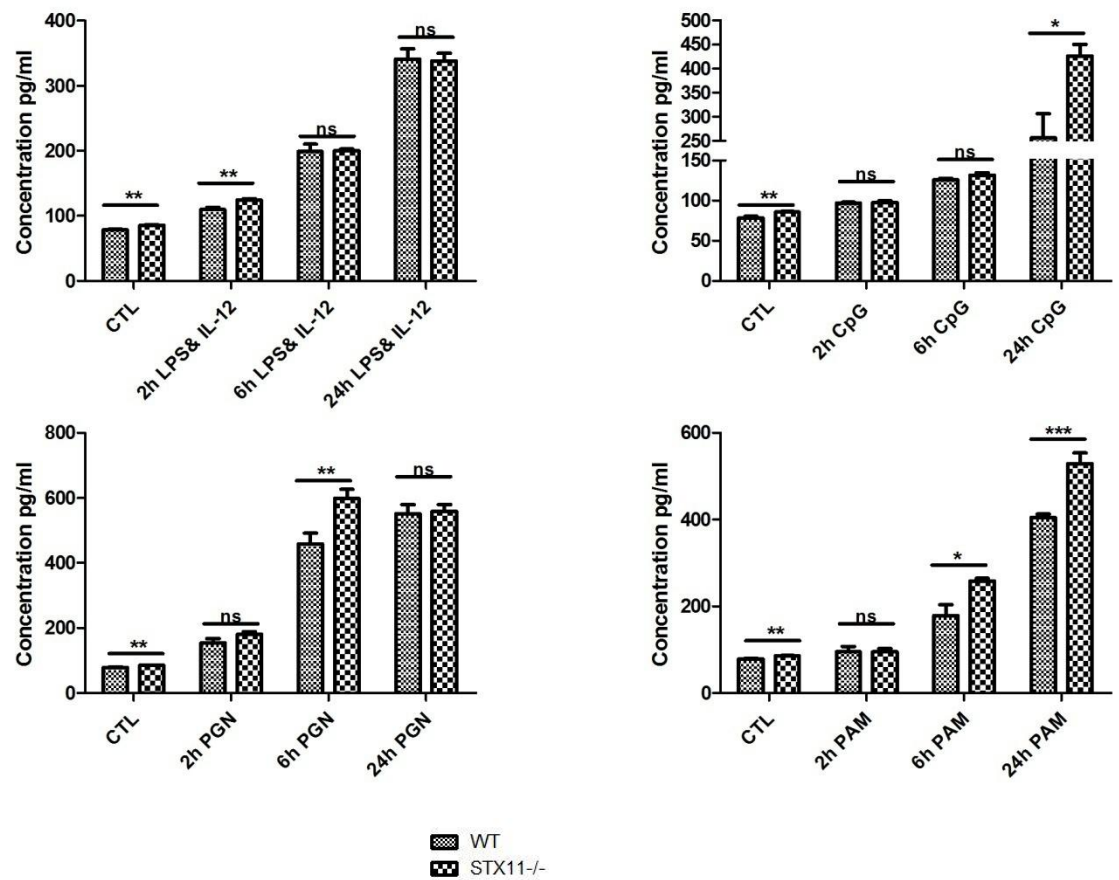


FIGURE 5.14: Comparison of IL-10 secretion from WT and *Stx11*^{-/-} BMDCs following activation with a panel of ligands over a time-course. BMDCs were cultured in r-GM-CSF for seven days and subsequently were plated (1×10^6 cells/ml) and left to rest overnight. Cells were then stimulated with 100 ng/ml LPS and 100 μ g/ml rIL-12, 2 μ M CpG, 5 μ g/ml PGN or 1 μ g/ml PAM. Supernatants were recovered after 24 h and assessed for levels of IL-10 using specific immunoassays. Results are \pm SEM of quadruplicate assays. * $p \leq 0.05$, ** $p \leq 0.01$ and *** $p \leq 0.001$ as determined by a two-tailed t-test.

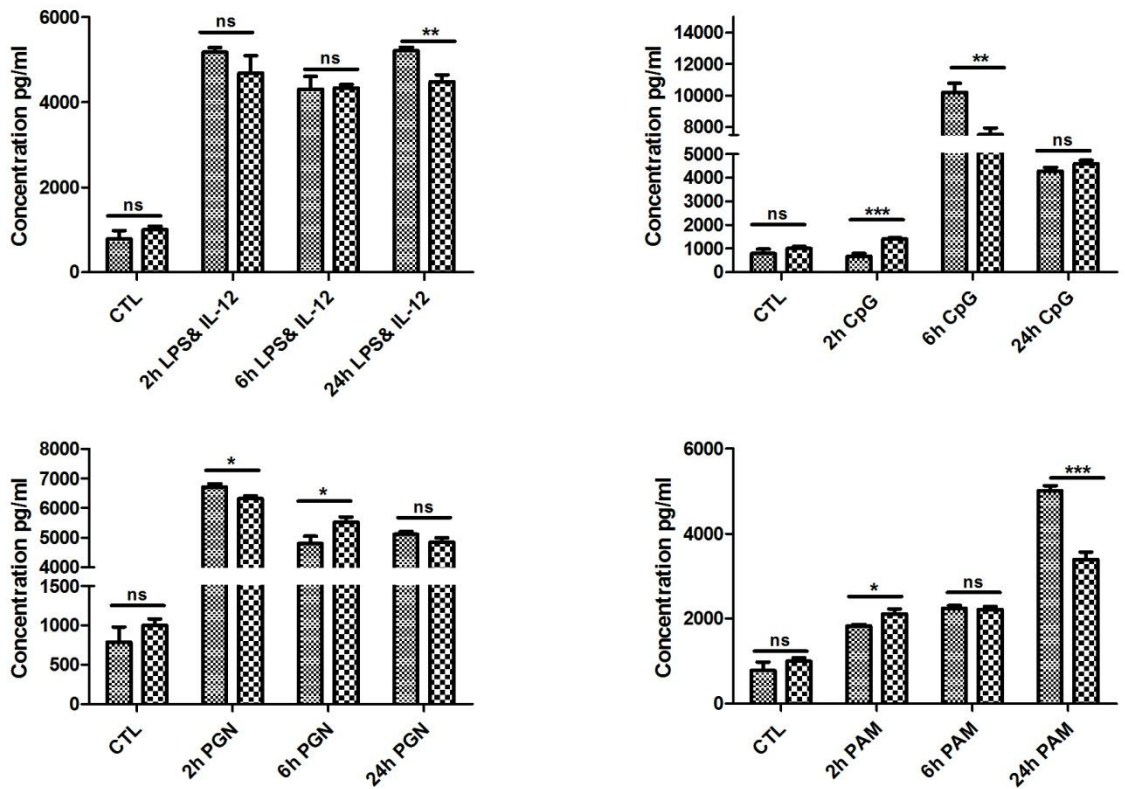
TNF- α 

FIGURE 5.15: Comparison of TNF- α secretion from WT and *Stx11*^{-/-} BMDCs following activation with a panel of ligands over a time-course. BMDCs were cultured in r-GM-CSF for seven days and subsequently were plated (1×10^6 cells/ml) and left to rest overnight. Cells were then stimulated with 100 ng/ml LPS and 100 μ g/ml rIL-12, 2 μ M CpG, 5 μ g/ml PGN or 1 μ g/ml PAM. Supernatants were recovered after 24 h and assessed for levels of TNF- α specific immunoassays. Results are \pm SEM of quadruplicate assays. * $p \leq 0.05$, ** $p \leq 0.01$ and *** $p \leq 0.001$ as determined by a two-tailed t-test

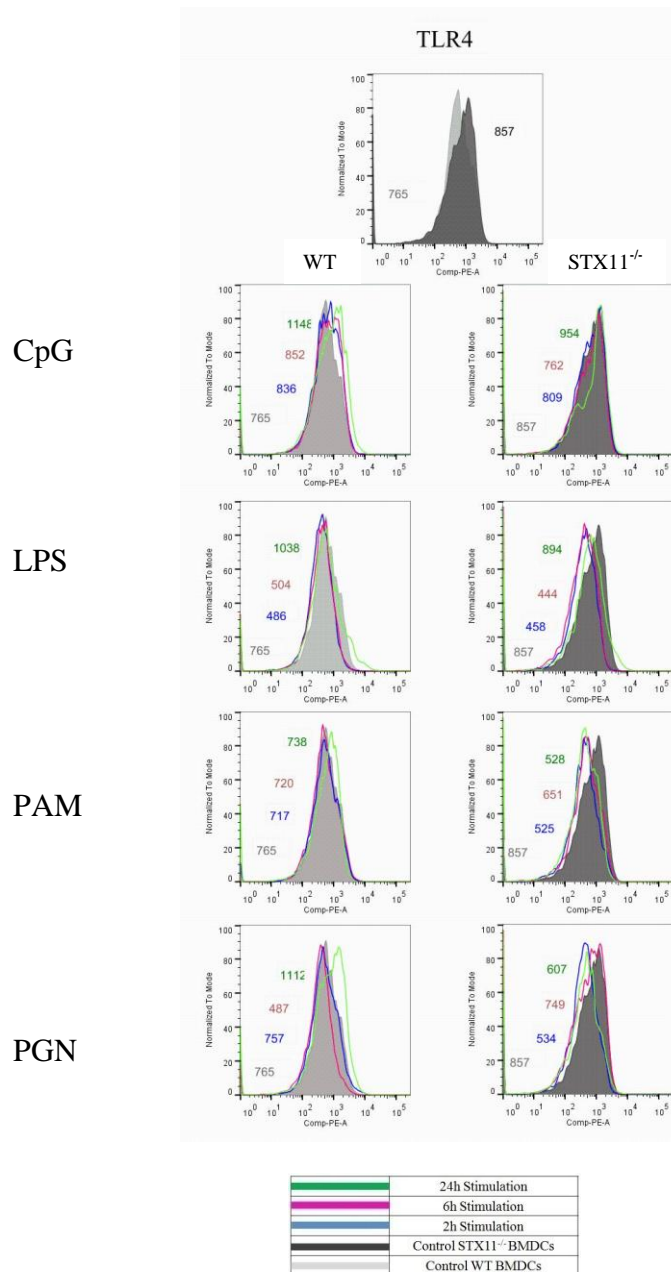


FIGURE 5.16: Comparison of TLR-4 expression on WT and *Stx11*^{-/-} BMDCs following activation. WT and *Stx11*^{-/-} BMDCs were differentiated in the presence of r-GMCSF for seven days and then stimulated with 100 ng/ml LPS and 100 µg/ml rIL-12, 2 µM CpG, 5 µg/ml PGN or 1 µg/ml PAM. Subsequently, cells were washed and stained with specific antibodies. Results of flow cytometric analysis and corresponding Mean Fluorescence Intensity (MFI) values are shown.

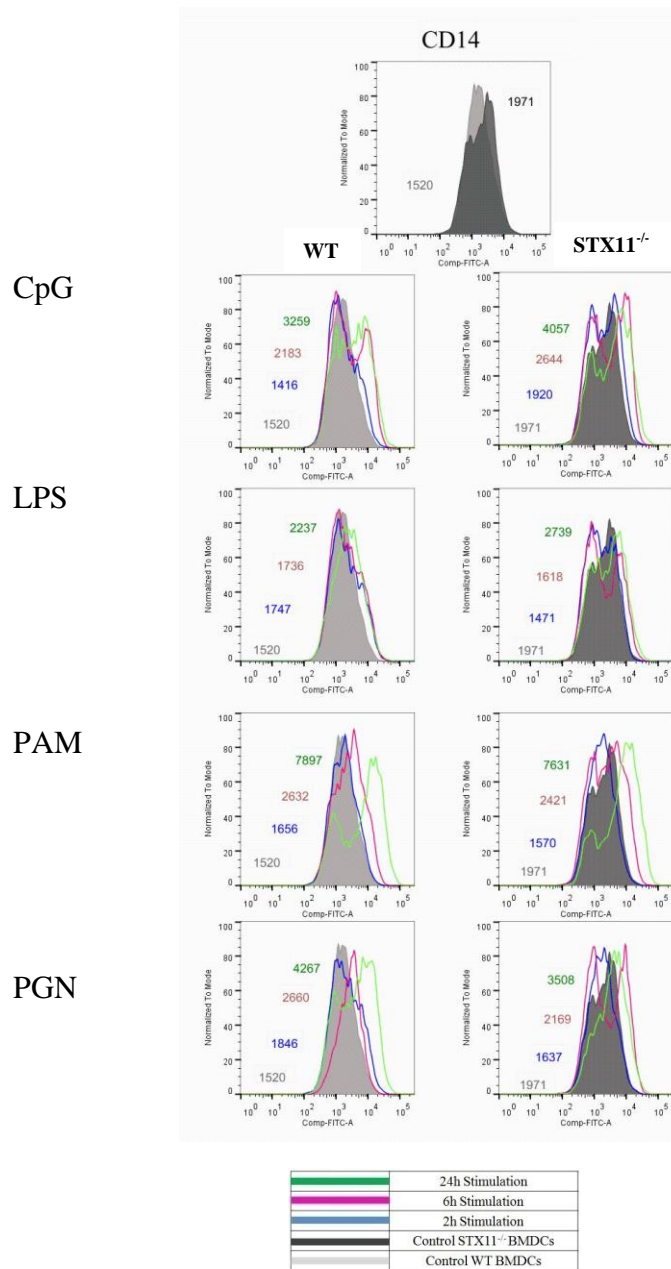


FIGURE 5.17: Comparison of CD14 expression on WT and *Stx11*^{-/-} BMDCs following activation. WT and *Stx11*^{-/-} BMDCs were differentiated in the presence of r-GMCSF for seven days and then stimulated with 100 ng/ml LPS and 100 µg/ml rIL-12, 2 µM CpG, 5 µg/ml PGN or 1 µg/ml PAM. Subsequently, cells were washed and stained with specific antibodies. Results of flow cytometric analysis and corresponding MFI values are shown.

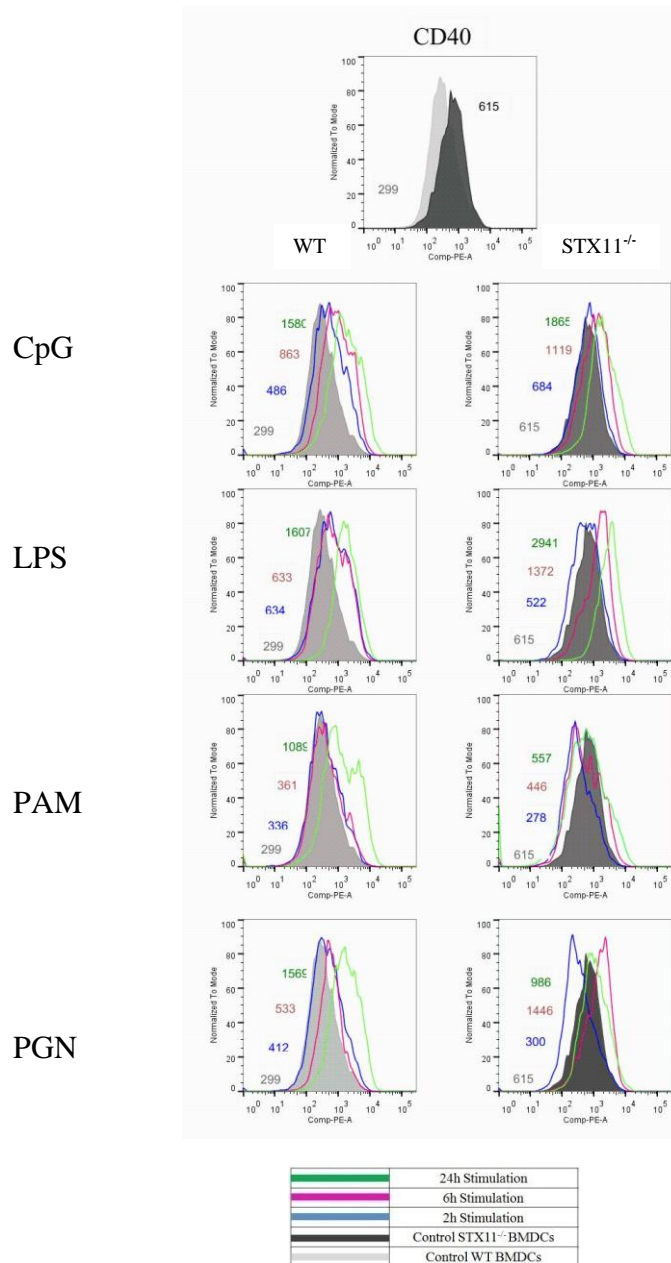


FIGURE 5.18: Comparison of CD40 expression on WT and *Stx11*^{-/-} BMDCs following activation. WT and *Stx11*^{-/-} BMDCs were differentiated in the presence of r-GMCSF for seven days and then stimulated with 100 ng/ml LPS and 100 µg/ml rIL-12, 2 µM CpG, 5 µg/ml PGN or 1 µg/ml PAM. Subsequently, cells were washed and stained with specific antibodies. Results of flow cytometric analysis and corresponding MFI values are shown.

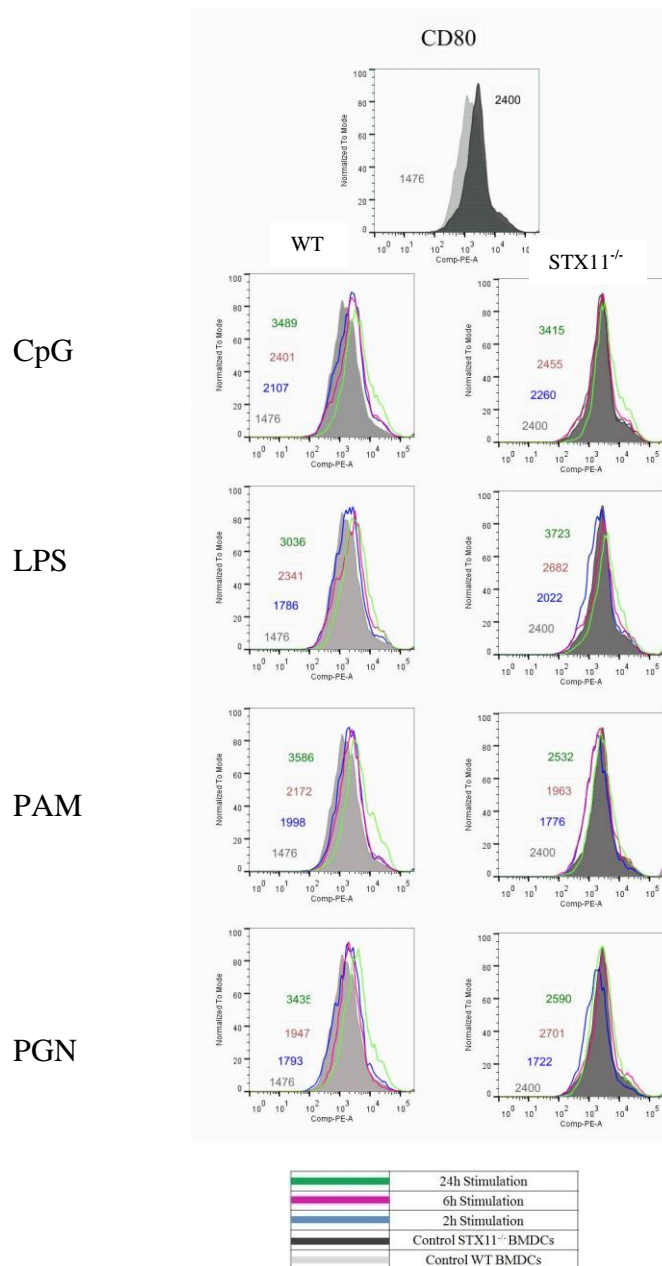


FIGURE 5.19: Comparison of CD80 expression on WT and *Stx11*^{-/-} BMDCs following activation. WT and *Stx11*^{-/-} BMDCs were differentiated in the presence of r-GMCSF for seven days and then stimulated with 100 ng/ml LPS and 100 µg/ml rIL-12, 2 µM CpG, 5 µg/ml PGN or 1 µg/ml PAM. Subsequently, cells were washed and stained with specific antibodies. Results of flow cytometric analysis and corresponding MFI values are shown.

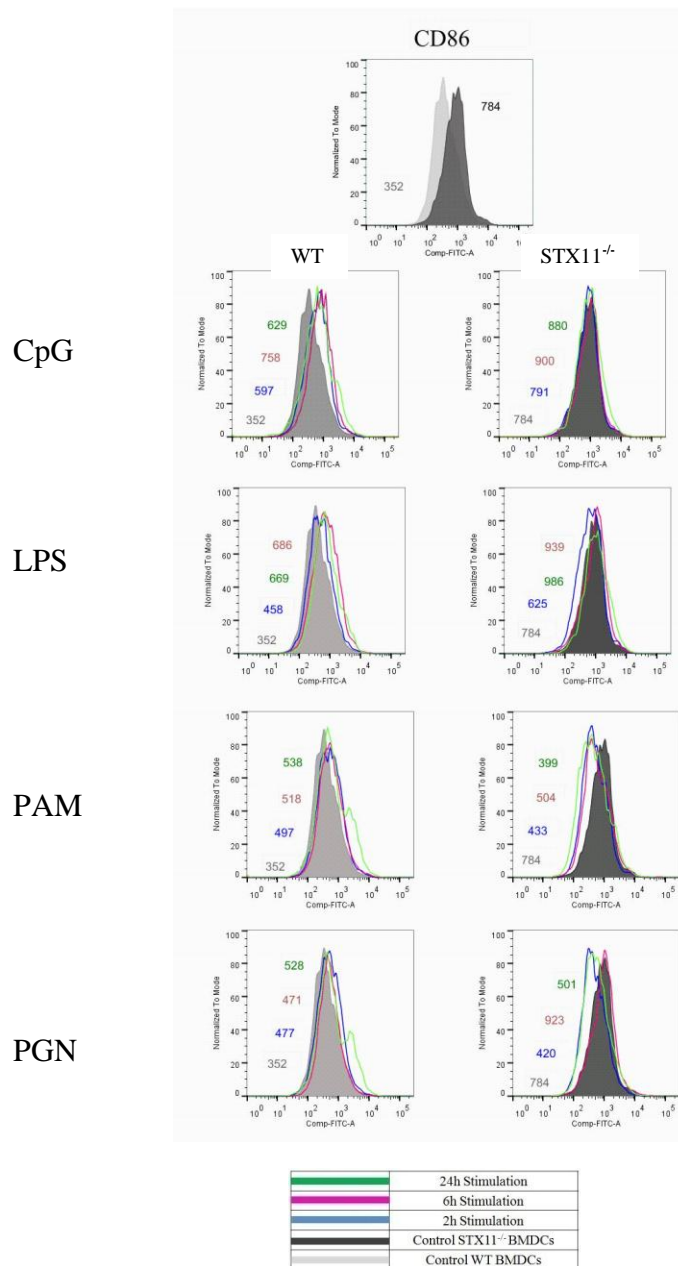


FIGURE 5.20 Comparison of CD86 expression on WT and *Stx11*^{-/-} BMDCs following activation. WT and *Stx11*^{-/-} BMDCs were differentiated in the presence of r-GMCSF for seven days and then stimulated with 100 ng/ml LPS and 100 μg/ml rIL-12, 2 μM CpG, 5 μg/ml PGN or 1 μg/ml PAM. Subsequently, cells were washed and stained with specific antibodies. Results of flow cytometric analysis and corresponding MFI values are shown.

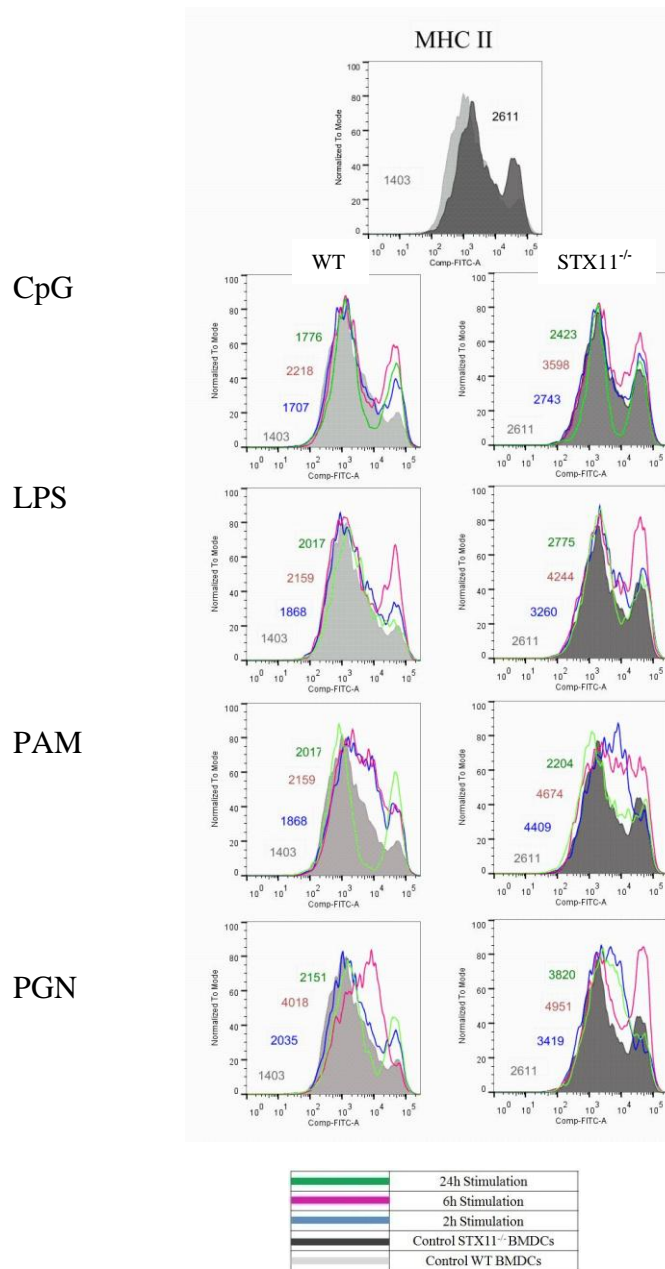


FIGURE 5.21: Comparison of MHCII expression on WT and *Stx11*^{-/-} BMDCs following activation. WT and *Stx11*^{-/-} BMDCs were differentiated in the presence of r-GMCSF for seven days and then stimulated with 100 ng/ml LPS and 100 µg/ml rIL-12, 2 µM CpG, 5 µg/ml PGN or 1 µg/ml PAM. Subsequently, cells were washed and stained with specific antibodies. Results of flow cytometric analysis and corresponding MFI values are shown.

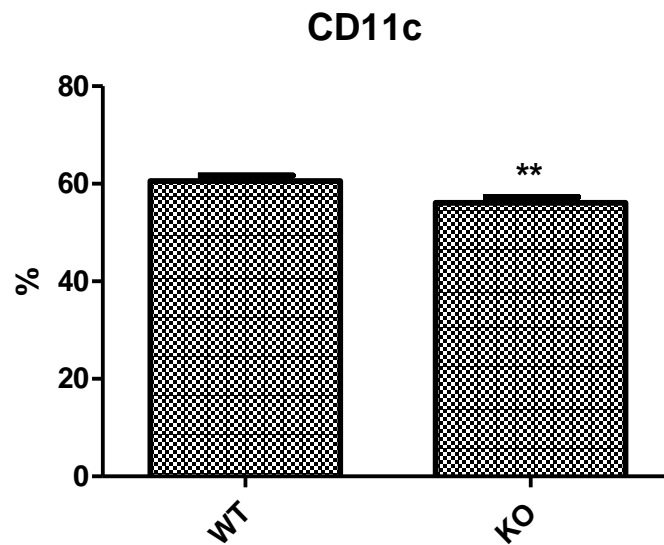


FIGURE 5.22 Comparison of CD11c expression on WT and *Stx11*^{-/-} BMDCs following activation. WT and *Stx11*^{-/-} BMDCs were differentiated in the presence of r-GMCSF for seven days and then stimulated. Subsequently, cells were washed and stained with specific CD11c antibody. Results of flow cytometric analysis and corresponding Percentage fluorescence of CD11c is displayed. ** $p \leq 0.01$ comparing control versus *Stx11*^{-/-} KO) as determined by a two-tailed t-test.

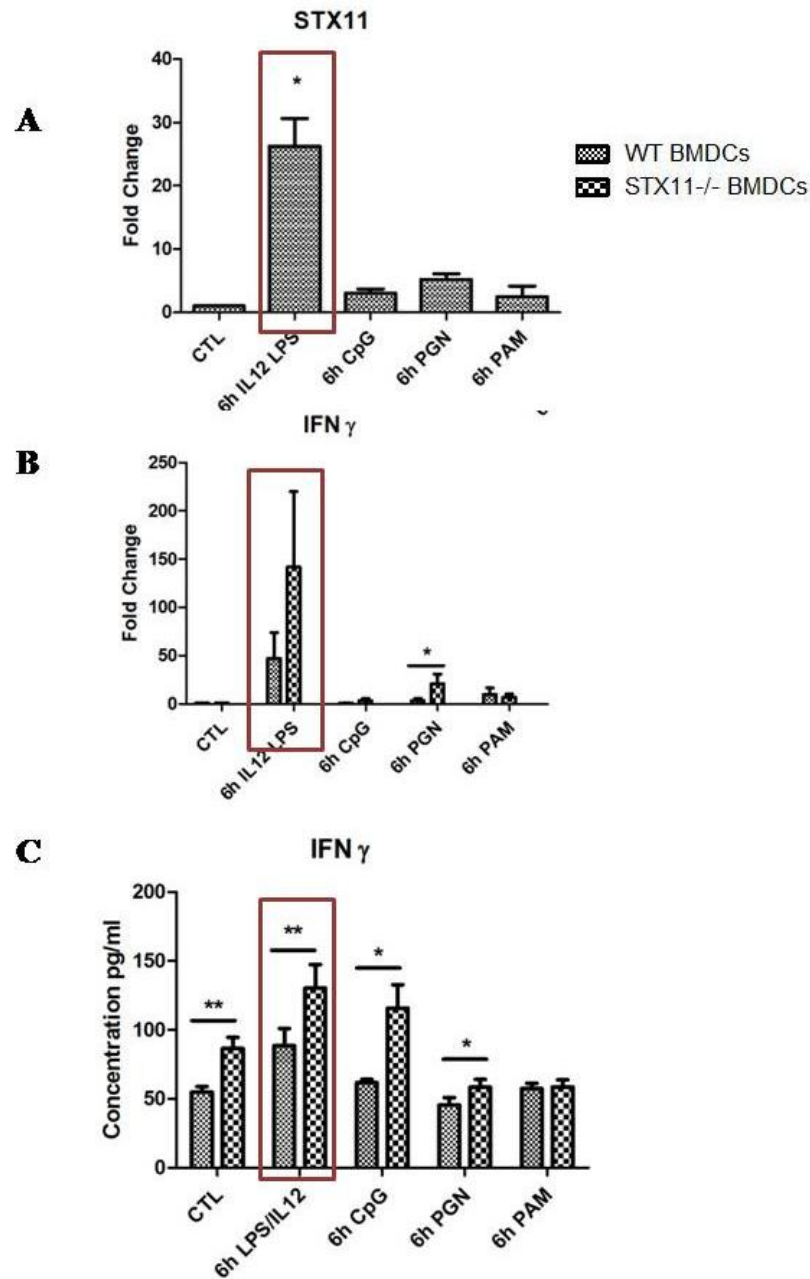


FIGURE 5.23: mRNA expression of (A) STX11 and (B) IFN- γ , WT and STX11^{-/-} BMDCs following activation and (C) a re-cap of IFN- γ secretion from WT and *Stx11*^{-/-} BMDCs following activation. BMDCs were plated 1×10^6 cells/ml and stimulated with 100 ng/ml LPS and 100 μ g/ml rIL-12, 2 μ M CpG, 5 μ g/ml PGN or 1 μ g/ml PAM for 6 hours. The amount of target mRNA was quantified by reverse transcription followed by RT-qPCR using an ABI 7900 HT detection system. mRNA target levels were assayed in triplicate (using SYBR green technology) and normalised with S18 levels. Fold differences were calculated relative to target levels at time zero (assigned value of 1). Results are \pm SEM of quadruplicate assays. * $p \leq 0.05$, ** $p \leq 0.01$ and *** $p \leq 0.001$ as determined by a two-tailed t-test comparing WT versus *Stx11*^{-/-} BMDCs. In the case of STX11 * $p \leq 0.05$ comparing control vs treated groups as determined by one-way ANOVA test.

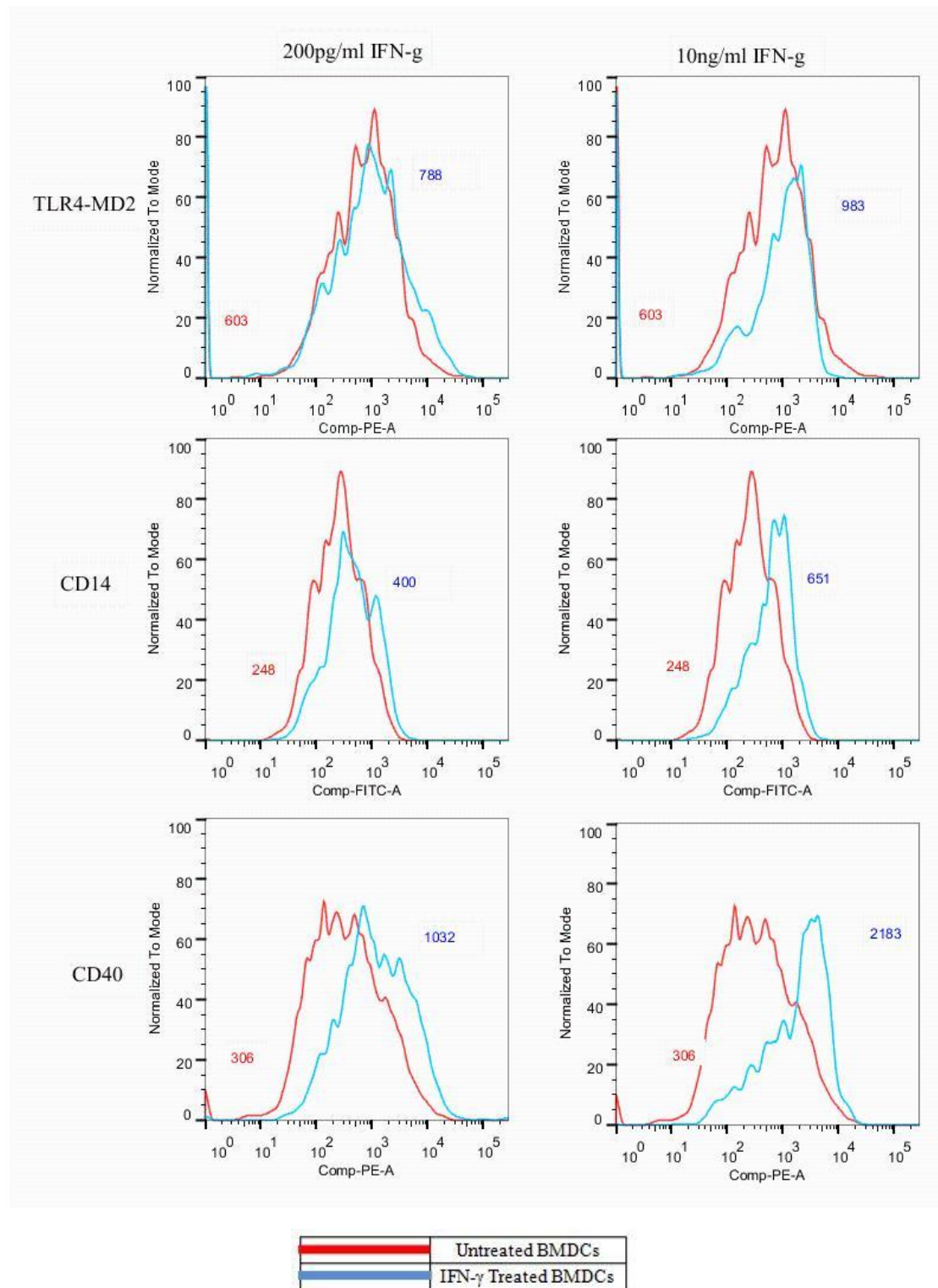


FIGURE 5.24: Comparison of basal TLR4-MD2, CD14 and CD40 expression on BMDCs grown in different concentrations of IFN- γ . BMDC were differentiated in the presence of r-GMCSF with or without varying concentrations of IFN- γ (200pg/ml or 10ng/ml) for three days. Subsequently, cells were washed and stained with specific antibodies. Results of flow cytometric analysis and corresponding MFI values are shown. BMDCs without IFN- γ (red line) vs. BMDCs with varying concentrations of IFN- γ (200 pg/ml or 10 ng/ml) (blue line).

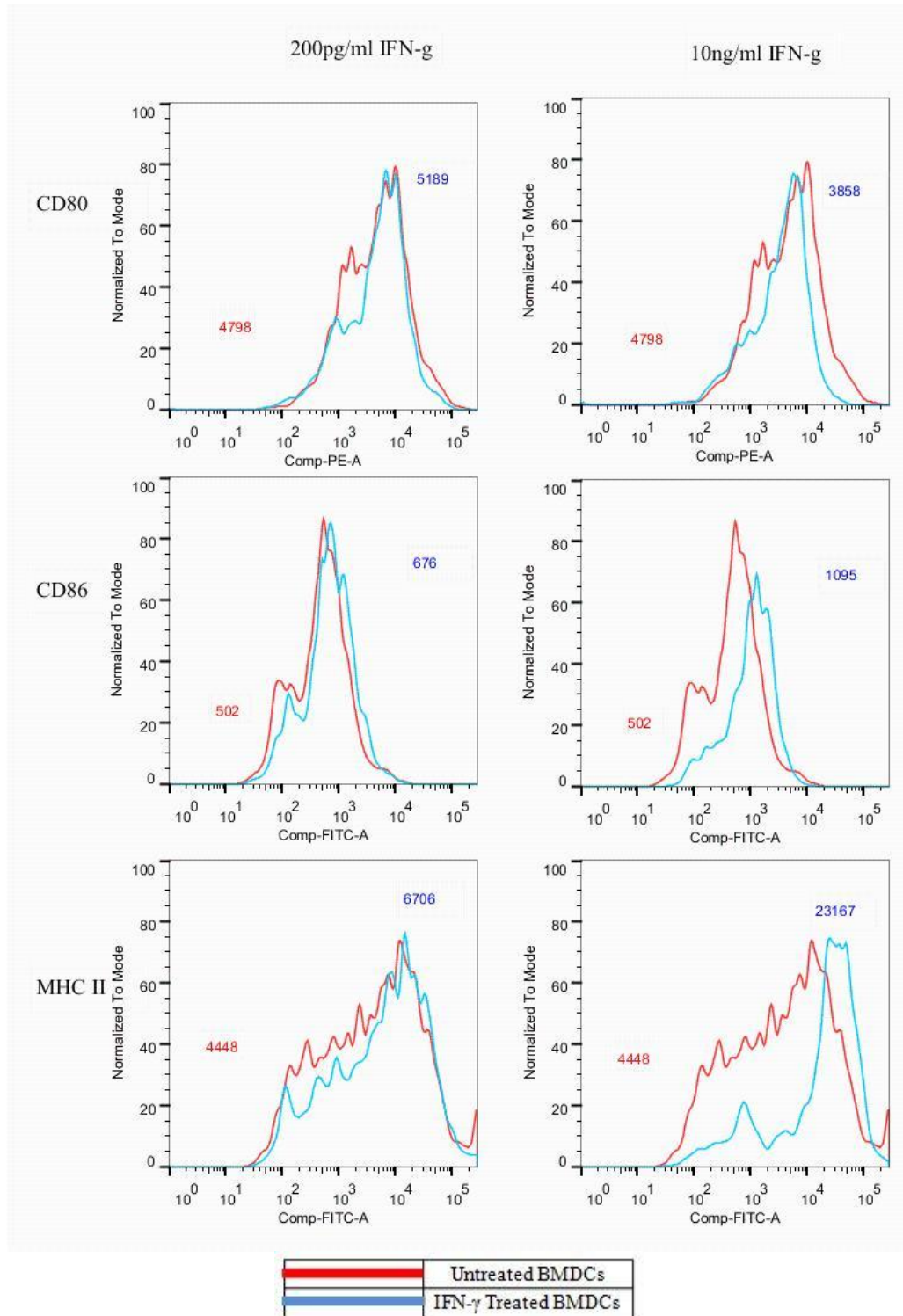


FIGURE 5.25: Comparison of basal CD80, CD86 and MHCII expression on BMDCs grown in different concentrations of IFN- γ . BMDC were differentiated in the presence of r-GMCSF with or without varying concentrations of IFN- γ (200pg/ml or 10ng/ml) for three days. Subsequently, cells were washed and stained with specific antibodies. Results of flow cytometric analysis and corresponding MFI values are shown. BMDCs without IFN- γ (red line) vs. BMDCs with varying concentrations of IFN- γ (200 pg/ml or 10 ng/ml) (blue line).

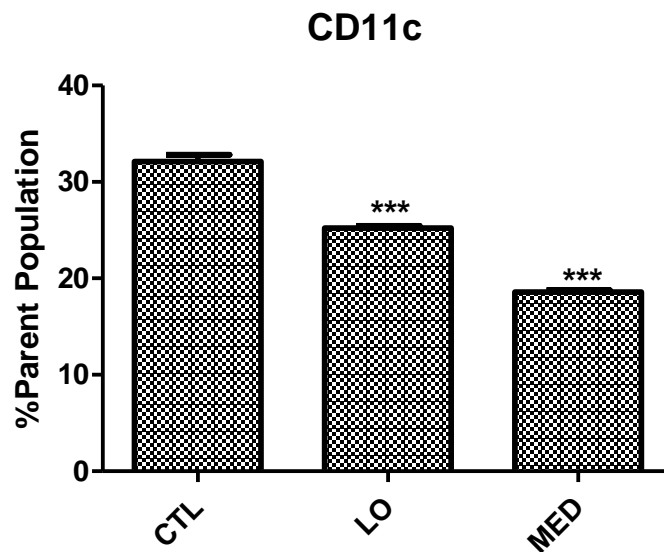


FIGURE 5.26: Comparison of CD11c expression on on BMDCs grown in different concentrations of IFN- γ . BMDCs were differentiated in the presence of r-GMCSF with or without varying concentrations of IFN- γ (200 pg/ml or 10 ng/ml) for three days. Subsequently, cells were washed and stained with CD11c antibody. Results of flow cytometric analysis and corresponding percentage fluorescence of CD11c is displayed. * $p \leq 0.05$, ** $p \leq 0.01$ and *** $p \leq 0.001$ comparing control versus IFN- γ treated BMDCs as determined by a two- tailed t-test.

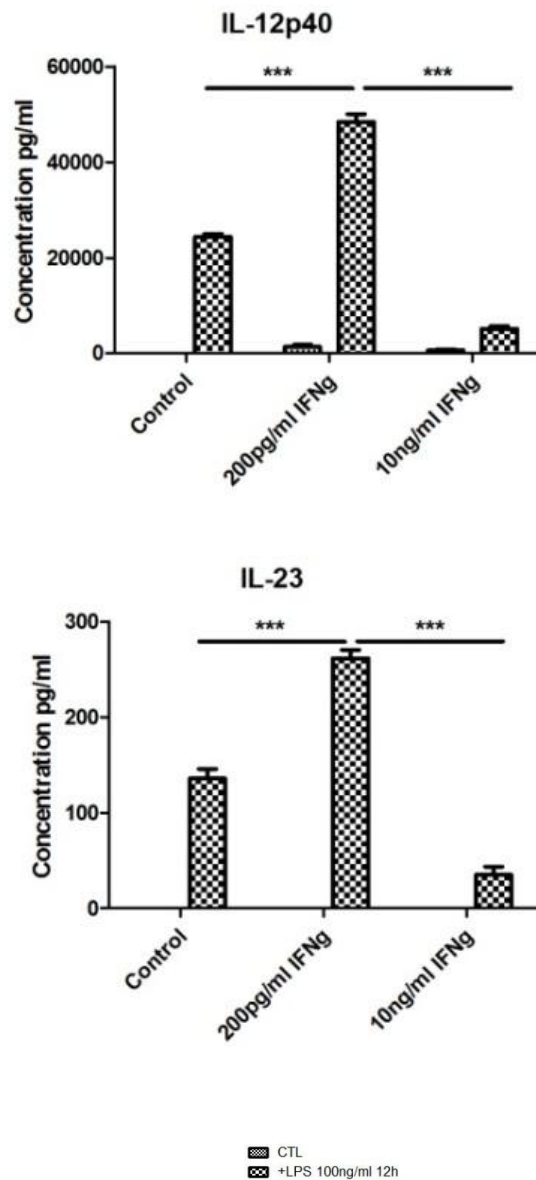


FIGURE 5.27: Comparison of IL-12p40 and IL-23 secretion following activation with LPS from BMDCs grown in different concentrations of IFN- γ . BMDCs were differentiated in the presence of r-GMCSF with or without varying concentrations of IFN- γ (200 pg/ml or 10 ng/ml) for seven days. Cells were then stimulated with 100ng/ml LPS. Supernatants were recovered after 24h and assessed for levels of IL-12p40 and IL-23 using specific immunoassays. Results are \pm SEM of quadruplicate assays. *** $p \leq 0.001$ comparing control versus IFN- γ treated BMDCs as determined by a two-tailed t-test.

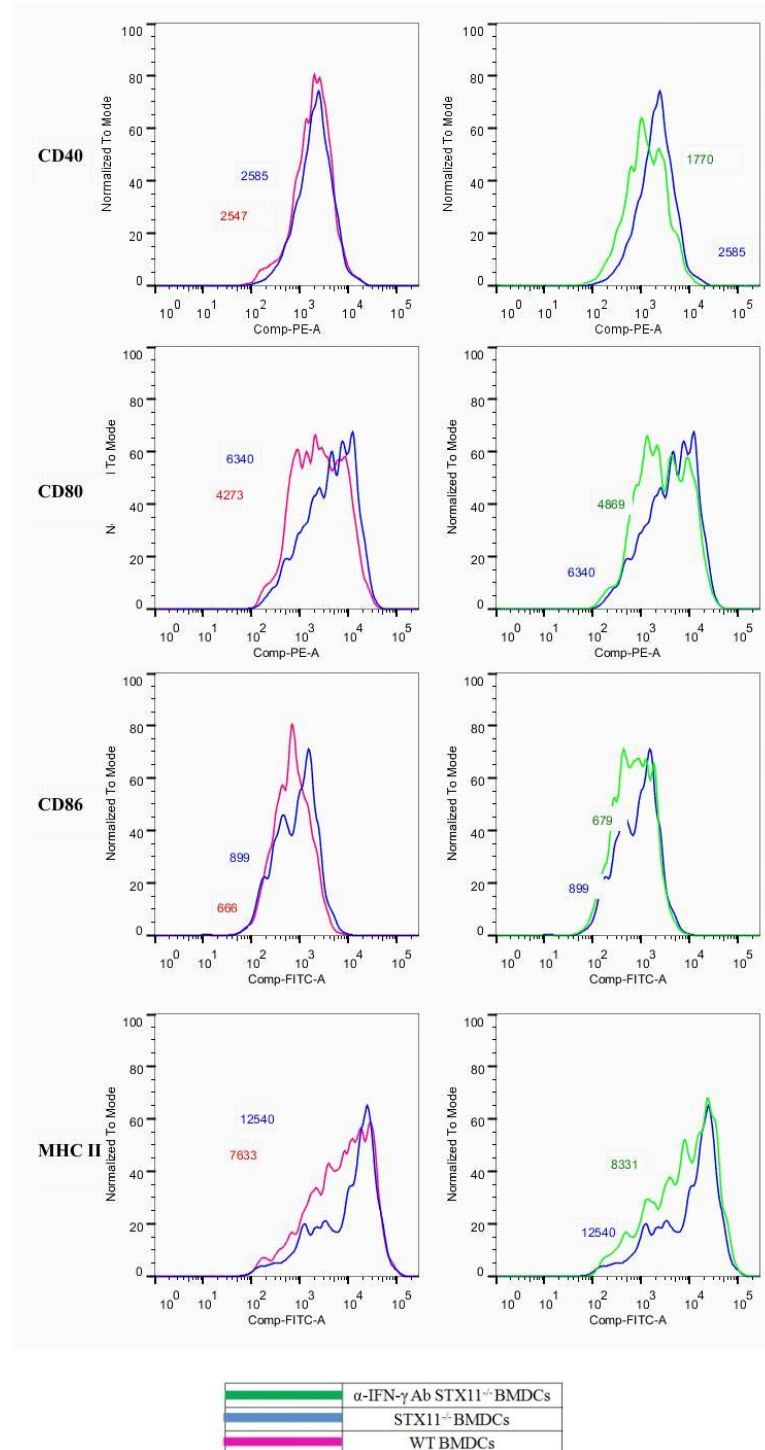
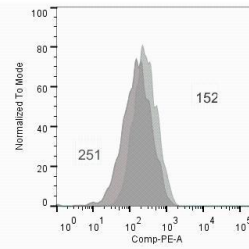
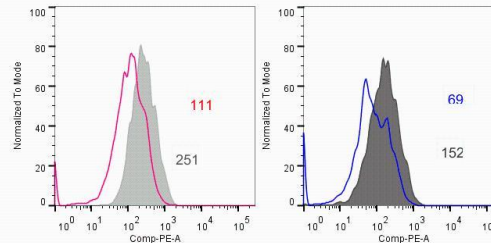


FIGURE 5.28: Comparison of CD40, CD80, CD86 and MHC II and expression on WT and STX11^{-/-} BMDCs following activation with LPS/IL12 (100ng/ml:100μg/ml) in the presence or absence of IFN-γ neutralising antibody. WT and STX11^{-/-} BMDCs were differentiated in the presence of r-GMCSF for seven days and then stimulated with LPS/IL12 (100 ng/ml:100 μg/ml). Subsequently, cells were washed and stained with specific antibodies. Results of flow cytometric analysis and corresponding MFI values are shown.

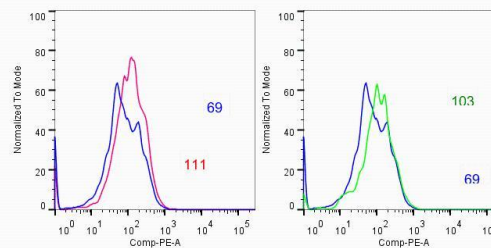
Control BMDCs



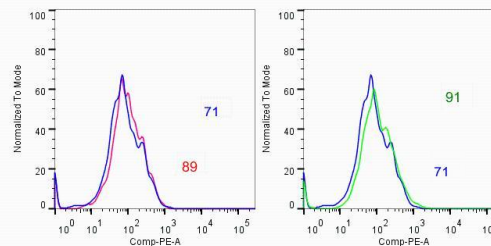
CTL/LPS:IL-12



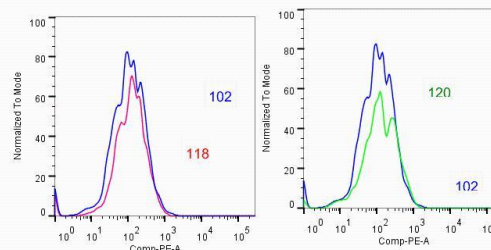
LPS:IL-12



CpG



PAM



	α -IFN- γ Ab STX11 ^{-/-} BMDCs + TLR Ligand Stimulation
	STX11 ^{-/-} BMDCs + TLR Ligand Stimulation
	WT BMDCs + TLR Ligand Stimulation
	Control STX11 ^{-/-} BMDCs
	Control WT BMDCs

FIGURE 5.29: Comparison of CCR5 expression on WT and *Stx11*^{-/-} BMDCs following activation with 100 ng/ml LPS and 100 μ g/ml rIL-12, 2 μ M CpG, 5 μ g/ml PGN or 1 μ g/ml PAM in the presence or absence of IFN- γ neutralising antibody. WT and *Stx11*^{-/-} BMDCs were differentiated in the presence of r-GMCSF for seven days and then stimulated with ligands outlined. Subsequently, cells were washed and stained with specific antibodies. Results of flow cytometric analysis and corresponding MFI values are shown.

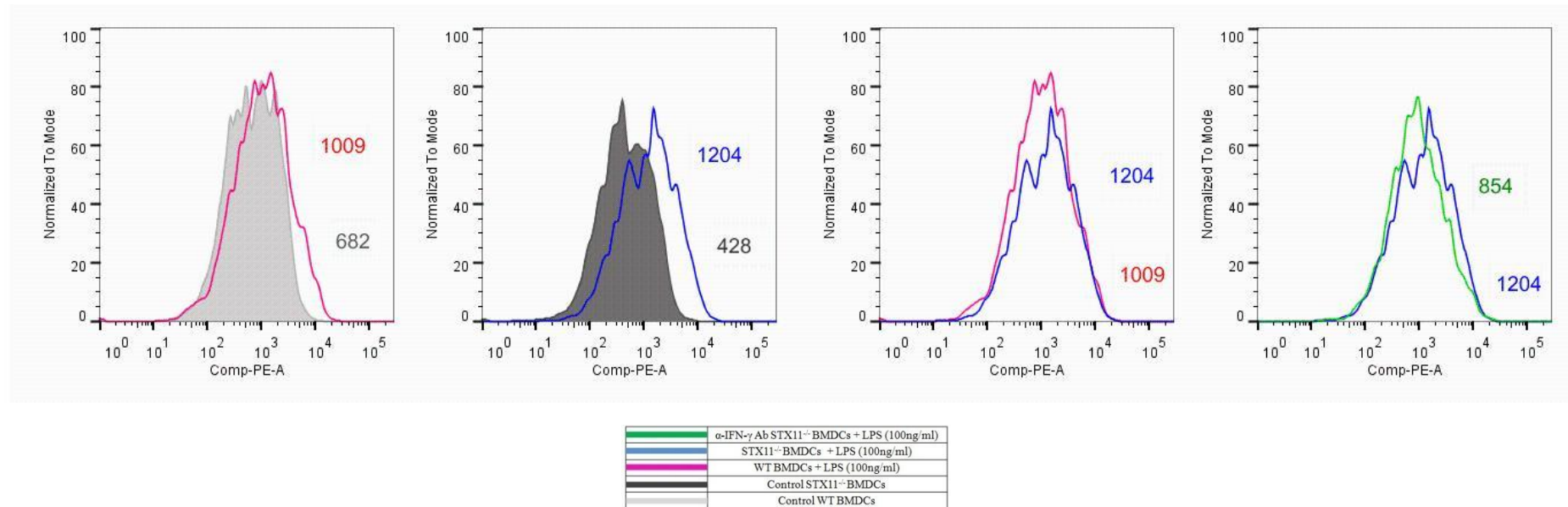


FIGURE 5.30: Comparison of PD-L1 expression on WT and *Stx11*^{-/-} BMDCs following activation with 100 ng/ml LPS and 100 μ g/ml rIL-12, 2 μ M CpG, 5 μ g/ml PGN or 1 μ g/ml PAM in the presence or absence of IFN- γ neutralising antibody. WT and *Stx11*^{-/-} BMDCs were differentiated in the presence of r-GMCSF for seven days and then stimulated with LPS (100 ng/ml) and rIL-12 (100 μ g/ml). Subsequently, cells were washed and stained with specific antibody to PD-L1. Results of flow cytometric analysis and corresponding MFI values are shown.

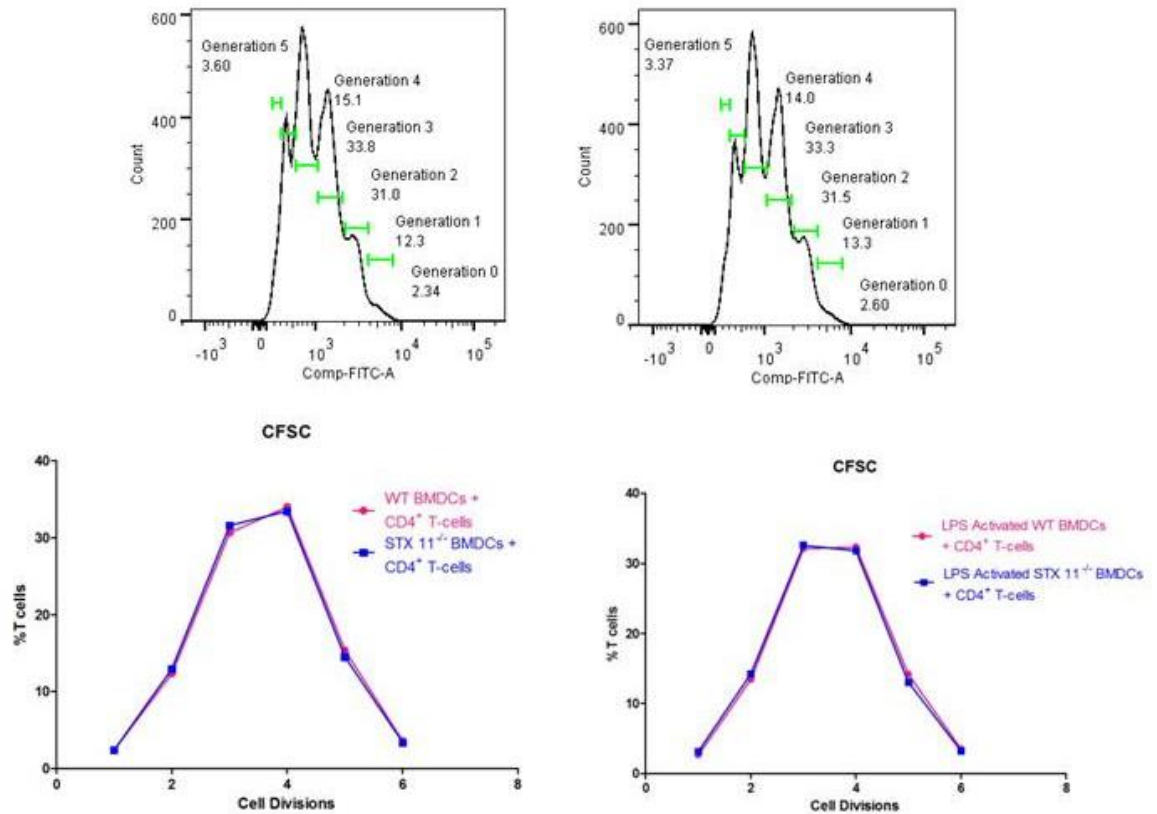


FIGURE 5.31: T-cell *Stx11*^{-/-} BMDC co culture

WT and *Stx11*^{-/-} BMDCs were cultured in r-GM-CSF for seven days and subsequently were plated (1×10^6 cells/ml) and incubated overnight. Cells were then stimulated with 100 ng/ml LPS for 4 hours before being co-cultured with CD4⁺ T cells (stained with CFSE) for 72 hours. Cells were removed from the plate, washed and stained with CD4 antibody and PI and analysed on FACS Aria. The data was then analysed using FlowJo analysis software (Treestar). Cells were gated on PI negative, CD4 positive cells. CFSE data was plotted and analysed using the proliferation algorithm on FlowJo in order to calculate the percentage of divided cells, and number of cells in each generation after 72 hours of co-culture.

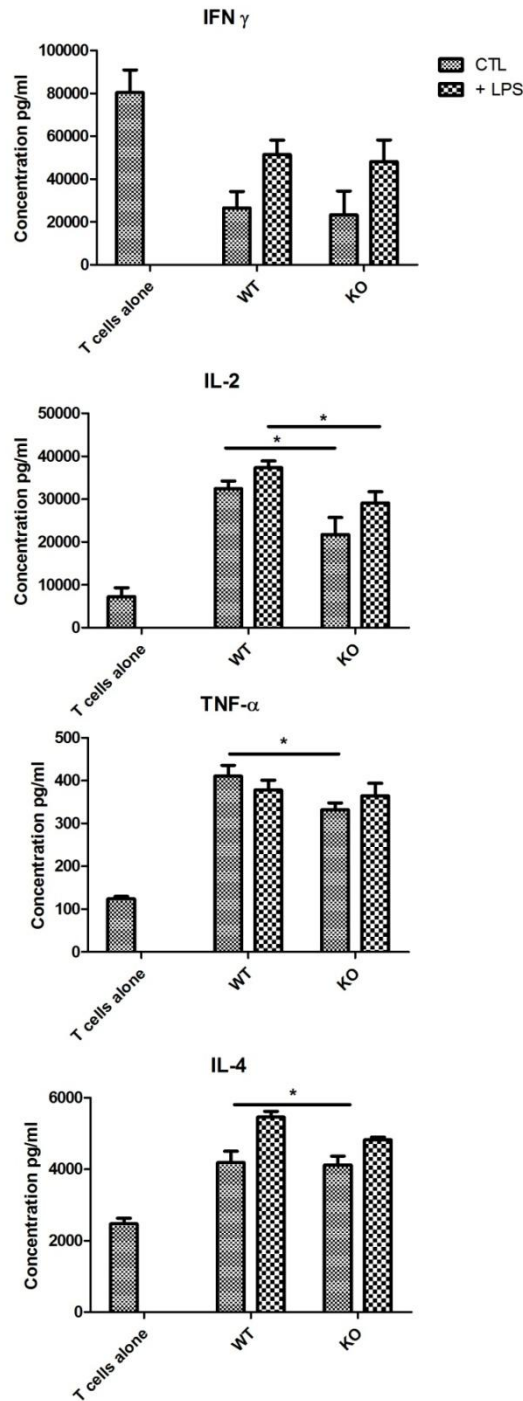


FIGURE 5.32: T-cell *Stx11*^{-/-} BMDC co-culture

WT and *Stx11*^{-/-} BMDCs were cultured in r-GM-CSF for seven days and subsequently were plated (1×10^6 cells/ml) and left to rest overnight. Cells were then stimulated with 100 ng/ml LPS for 4 hours before being co-cultured with CD4⁺ T cells for 72 h and assessed for levels of cytokines using specific immunoassays. Results are \pm SEM of triplicate assays. ** $p \leq 0.01$ and *** $p \leq 0.001$ comparing WT BMDCs versus *STX11*^{-/-} BMDCs as determined by a two-tailed t-test.

5.4 DISCUSSION

Several studies have addressed the role of SNARE involvement in cytokine release from immune cells, however to our knowledge no study has identified the specific SNAREs involved in dendritic cell cytokine and chemokine secretion. In this chapter we focused on two SNAREs, STX3 and STX11 to elucidate their functional roles in dendritic cells. They were identified as candidates as we showed that they were significantly up-regulated after immune activation in DCs *in vitro* and they were also expressed *in vivo* in colitis models of disease. Furthermore they have been previously identified as a requirement for secretion of immune mediators from other cells of the immune system and in the case of STX11 has been implicated in the hyperinflammatory disease, FHL-4 (D'Orlando et al. 2013, Frank et al. 2011).

We firstly looked at STX3 and its role in JAWSII DCs secretion of cytokines and chemokines. We depleted the levels of STX3 in two separate ways by means of an siRNA specific to STX3 and with the administration of a neutralising antibody. In both of these situations IL-6 secretion was significantly down-regulated. MIP-1 α was also down-regulated when STX3 was depleted by using RNAi. This correlates with recent data from mast cells where STX3 was reported to be involved in chemokine release from mast cells (Frank et al. 2011). Using confocal microscopy we assessed the cellular location of STX3 during activation with TLR ligands in both JAWSII DCs and BMDCs, interestingly only in cells where IL-6 was secreted there was a translocation of STX3. This data indicates that STX3 has a role in IL-6 secretion (and possibly MIP-1 α) from dendritic cells and is an important SNARE in dendritic cell function.

There was not complete abolishment of IL-6 levels from the JAWSII and this may be explained as loss of SNAREs can be compensated by other members of the SNARE family which have only 30% amino acid similarity (Atlashkin et al. 2003). However cytokines such as IL-6 are critical mediators of the autoimmune diseases and IL-6 implicated in several disease processes. Increased levels of IL-6 have been observed IBD, RA, systemic-onset juvenile chronic arthritis (JCA), osteoporosis and psoriasis (Ishihara and Hirano 2002). IL-6 blockade has been reported successful in autoimmune diseases and with humanized anti-IL-6 receptor antibody in patients with RA and JCA was noted to have remarkable clinical effects (Yoshizaki 2009). In the past decade IL-6 has been indicated to have a role in differentiation of Th17 subset with TGF- β , therefore its blockade may potentially improve these diseases at the pathogenic initiation phase (Park et al. 2005). Targeted therapeutic of SNAREs in inflammatory disease, such as STX3, may be a novel therapeutic tool for secretion of cytokines like IL-6.

A STX11 deficient (*Stx11*^{-/-}) mouse was recently developed to investigate the role of STX11 played in the immune disease FHL-4. The *Stx11*^{-/-} mouse model was developed by Udo Zur Stadt and were acquired through collaboration with Silvia Bulfone-Paus in the Borstel Research Centre, Hamburg, Germany. The data we present here suggests that *Stx11*^{-/-} BMDCs display significant phenotypical differences when compared with WT BMDCs. IL-12 family was up-regulated, the expression of important cell surface markers were up-regulated and CD11c expression was significantly down regulated in *Stx11*^{-/-} BMDCs compared to WT BMDCs. A study by D'Orlando stated that *Stx11* deletion did not significantly affect the secretion of TNF, IL-6 or IL-12p70 from BMDCs in response to LPS, Poly (I:C)

or CpG for 24 or 48 hours (D'Orlando et al. 2013). This correlated with our data in terms of TNF- α and IL-6 secretion however was not in agreement with the IL-12 data. This conflicting data may be accounted for due to the duration of stimulation between the studies and the fact that we saw more significant differences were seen at early time points, which they do not include in their study. Importantly the study did not measure IFN- γ production from BMDCs. This may be for two reasons. The fact DCs have only recently been identified as a source of IFN- γ as it conflicts with the initial paradigm in which IFN- γ production was restricted to lymphoid cells and that inbred mice strains vary in their ability to produce IFN- γ due to the complexity of its regulation and subsequently is not always measured from dendritic cells (Frucht et al. 2001, Stober, Schirmbeck and Reimann 2001, Schroder et al. 2004). As IFN- γ secretion was up-regulated from CTLs and NK cells isolated from *Stx11*^{-/-} mouse we measured its secretion from BMDCs from *Stx11*^{-/-} mice and WT matched controls. We found that IFN- γ was significantly up-regulated from *Stx11*^{-/-} BMDCs compared to WT BMDCs in both unstimulated BMDCs and post TLR stimulation. Interestingly we also report that increased mRNA levels of STX11 from WT BMDCs correlated with increased expression of IFN- γ mRNA along with secreted IFN- γ . IFN- γ has been widely reported as a mediator of dendritic cell maturation, up-regulating the expression of surface markers MHCII, CD40, CD80 and CD86 molecules on BMDCs while inducing higher levels of IL-12 (Pan et al. 2004, Xue et al. 2013). This up-regulation of basal levels of cytokines, chemokines and surface markers in *Stx11*^{-/-} BMDCs compared to WT BMDCs agrees with previously published data on IFN- γ maturation of BMDCs.

Previous studies have shown that, in the lymph nodes *Stx11*^{-/-} mice expressed CD11c similar levels compared to wild-type expression. This study also reported that

compared with wild-type mice, *Stx11*^{-/-} mice showed no differences in cell number, percentages in cell populations, specific cell surface marker expression or activation marker expression in lymph nodes or splenic cells (D'Orlando et al., 2013). However we saw significant down regulation of CD11c on *Stx11*^{-/-} DCs and WT DCs which interested us. As CD11c has classically been indicated as a DC marker we proposed that the phenotype of the *Stx11*^{-/-} BMDCs was changing. However, a recent study by Singh-Jasuja *et al.*, stated that CD11c is down-regulated upon cell activation, which would correlate with up-regulation of basal surface marker expression of the *Stx11*^{-/-} BMDCs compared to WT BMDCs. This further supported our hypothesis that *Stx11*^{-/-} DCs become activated during differentiation. Indeed this study goes as far as to suggest that down-regulation of CD11c might be used as a new activation marker for mouse DCs (Singh-Jasuja et al. 2013).

As this data indicates that the *Stx11*^{-/-} BMDCs have a more mature phenotype than the WT DCs, it would suggest that some agent is being released from the DC to act as a maturation stimulus. In a study looking at the role of STX11 in macrophage Offenhauser *et al.*, indicated a novel regulatory role for STX11 by binding to SNARE Vti1b in a non-traditional *trans*-SNARE complex (Offenhaeuser et al. 2011). Given that IFN- γ has been previously reported to be over expressed from CTLs and NK cells in *Stx11*^{-/-} mice (D'Orlando et al., 2013) as it is from the *Stx11*^{-/-} BMDCs in this study, we proposed that the altered phenotype of *Stx11*^{-/-} BMDCs is due to un-regulated production of IFN- γ due to lack of STX11 regulation.

To examine whether *Stx11*^{-/-} BMDCs are maturing during differentiation due to un-regulated IFN- γ production, we grew WT BMCDs in the presence of rIFN- γ to see if this would mimic the *Stx11*^{-/-} BMDC phenotype. We observed up-regulation of the same markers surface markers in unstimulated cells, up-regulation of the IL-12

family post LPS stimulation and down-regulation of CD11c which correlates with our *Stx11*^{-/-} BMDC data. We then added an α -IFN- γ neutralising antibody to the *Stx11*^{-/-} BMDC to see if this would restore the phenotype to resemble the WT cells. Surface level expression of CD40, CD80, CD86 and MHCII were up-regulated in *Stx11*^{-/-} BMDC compared to WT, however with the addition of an α -IFN- γ neutralising antibody this decreased surface marker expression to levels similar to that of WT BMDCs. We then assessed the expression of CCR5 as immature DCs express chemokine receptors which are lost of upon maturation, due to the chemokines that are being produced from the maturing DC (Sallusto et al. 1998). Thus we wanted to assess the levels of CCR5 on *Stx11*^{-/-} BMDC compared to WT, which unsurprisingly was decreased on unstimulated *Stx11*^{-/-} BMDC (suggesting a mature BMDC phenotype). Classically LPS/IL-12 stimulation down-regulated CCR5 expression on both *Stx11*^{-/-} BMDCs and WT BMDCs, but it was more down-regulated on *Stx11*^{-/-} BMDCs. Addition of an α -IFN- γ neutralising antibody to the *Stx11*^{-/-} BMDC reversed the down-regulation of CCR5 on the *Stx11*^{-/-} BMDCs to WT BMDC levels.

To further test the hypothesis that the phenotype of *Stx11*^{-/-} BMDCs is due to un-regulated production of IFN- γ due to lack of STX11 to regulate its secretion, we examined the expression of the surface marker PD-L1, T cell proliferation and cytokine secretion in a T cell:*Stx11*^{-/-} BMDC co-culture. We did this as bone marrow pre-cursors which are differentiated in the presence of GM-CSF and IFN- γ induce T cells hyporesponsiveness (Rongcun et al. 1998). PD-L1 is an inhibitory receptor expressed on APCs, such as DCs which regulates tolerance and autoimmunity. Expression of PD-L1 has previously been reported to be up-regulated in response to IFN- γ in BMDCs (Rojas and Krishnan 2010) We reported an up-regulation of PD-L1

expression in *Stx11*^{-/-} BMDCs and a reversal with IFN- γ antibody. Interestingly there were no changes to T cell proliferation, which was in agreement with previously published data. This study stated no impairment of *Stx11*^{-/-} BMDC-mediated induction of CD8⁺ and CD4⁺ T-cell proliferation data (D'Orlando et al. 2013). However the *Stx11*^{-/-} BMDCs appear to be impaired to prime T cells by inhibition of cytokine secretion of IL-2, IL-4 and TNF- α . IL-2 has been reported to be implicated in the generation and maintenance of Treg cells. Treg cells have an important function in inhibition of the function of antigen presenting cells and effector T cells. Due to this function Tregs maintain immune homeostasis, prevent autoimmunity, moderate inflammation and minimise tissue damage. Blockade of IL-2 receptor completely abrogates suppression (de la Rosa et al. 2004). Therefore a decrease in the secretion of this cytokine may impact on T cell function.

Overall this study suggests the STX3 may have a role in the secretion of IL-6 and possible MIP-1 α from DCs and lack of *Stx11* results in DCs with a semi-mature phenotype at basal level due to the uncontrolled expression of IFN- γ production, indicating a role for both SNAREs in dendritic cell secretion.

CHAPTER 6

GENERAL DISCUSSION

6.1 GENERAL DISCUSSION

DCs have the ability to link the innate and adaptive immunity. The profile of cytokines that they secrete in response to specific pathogens polarize specific Th differentiation and thus are a potential target for manipulating the immune system. To examine these immune modulating mediators and their potential for targeting in inflammatory disease, we established a cytokine secretion model using JAWSII DCs. This choice, uncommon in DC research compared to use of primary derived DCs, provided us with a homogeneous population that had previously been shown to be receptive to transfection with RNAi, which would be beneficial for functional studies (Pajtasz-Piasecka et al. 2007) This immature DC cell line has also been previously reported to be capable of maturation and subsequently capable of stimulating T cells to proliferate (Mackay and Moore 1997). We concluded that while similar to primary DCs, JAWSII DCs have significant differences to that of BMDCs when stimulated with TLR ligands, and we demonstrated different patterns of cytokine and chemokine expression in the JAWSII DCs post activation.

In order to target the cytokines and chemokines that are involved in the pathogenesis of many inflammatory diseases, we sought to investigate how they are trafficked out of the cell and to identify possible therapeutic targets. The significance of trafficking machinery in eukaryotic cells was highlighted recently by the award of the 2013 Noble Prize for Physiology and Medicine to James Rothman, Randy Schekman and Thomas Sudhof. Combined, the discoveries of these researchers have shaped our understanding of the building blocks of trafficking networks such as SNARE

discovery and its subsequent regulation (Stow 2013). Based on their work, functional roles for SNAREs in secretion of critical mediators from immune cells, such as TNF- α from macrophage have been identified (stow 2009). Furthermore, it is now clear that understanding these complex trafficking pathways and the proteins that regulate them will be important in defining their role in inflammatory diseases. Indeed to date, their expression in such disease has not yet been investigated.

To investigate the role of SNAREs in DC secretion we firstly examined mRNA expression following activation with a panel of TLR ligands. Our objective was to identify SNAREs that are up-regulated following TLR activation, which may indicate their involvement in the trafficking of cytokines or chemokines that the cell secretes in response to the particular TLR ligand. We demonstrate differential expression of SNARE mRNA in response TLR ligands. Interestingly, not all SNARE expression was modulated. Apart from the obvious lack of involvement in functional SNARE complexes in DC secretion, we propose this may be due to other reasons. For example, VAMP8 has previously been implicated in DC function however we showed that there was no change in its expression (Ho et al. 2008). This may be explained by the fact that VAMP8 expression has been reported to be regulated by caspases and degraded by microRNA-96 (Ho et al. 2009, Kondkar et al. 2010). Thus post transcriptional regulation may be involved in SNARE expression. It has also been reported that SNAREs involved in membrane fusion are recycled many times before being used up (Malsam, Kreye and Soellner 2008), therefore it may not be necessary for the cell to turn on transcription.

STX3 expression was up-regulated following DC activation. Indeed, STX3 expression was significantly increased *in vivo* and *in vitro*. Of particular interest to us was the fact that STX3 expression in JAWSII DCs was up-regulated significantly in response to LPS and Loxoribine but not to PGN stimulation. Given our data on the cytokines and chemokines that these cells secreted in response to these ligands, we were able to correlate expression of STX3 with IL-6 secretion. STX3 was also identified to be significantly up-regulated *in vivo* in colitis models of disease which interestingly correlated with increased mRNA expression of IL-6, TNF- α , MIP-1 α , MIP-2 and MCP in the colon. The concept of SNARE up-regulation paralleled with cytokine up-regulation has proven useful in other studies. The novel SNARE complex involved in the secretion of TNF- α in macrophage, STX6 and Vti1b was also identified in this manner (Murray et al. 2005b). We then went on to prove a role for STX3 in IL-6 (and partially MIP-1 α) secretion through abolishment of STX3 in DCs by means of neutralising antibodies and RNAi, and investigation of subcellular STX3 in IL-6 secreting DCs.

IL-6 is a multifunctional cytokine that regulates the immune response, hematopoiesis, the acute phase response and inflammation. It has been implicated in several disease processes such as IBD, RA, systemic-onset juvenile chronic arthritis (JCA), osteoporosis and psoriasis ((Ishihara and Hirano 2002). These studies suggest that blockade of IL-6 may represent a potential therapeutic target in inflammatory disease. Indeed, administration of an anti-IL-6 monoclonal antibody to patients with refractory RA has been shown to improve patient pain in a number of arthritic joints, which lasted for two months (Feldmann, Brennan and Maini 1996). Recently, IL-6

has been indicated to have a role in differentiation of Th17 subset with TGF- β , and its blockade may also be an advantage in Th17-related diseases (Park et al. 2005).

We did observe some evidence to suggest that MIP-1 α secretion may also be mediated by STX3. This was of interest to us as a previous group identified that STX3 and SNAP-23 were required for chemokine release from human mast cells (Frank et al). MIP-1 proteins are involved in the pathogenesis of diseases such as asthma, granuloma formation, wound healing, arthritis and multiple sclerosis (Maurer and von Stebut 2004). MIP-1 α has also been indicated in IBD. Systemic administration of MIP-1 α has been shown to exacerbate colitis in a mouse model, increasing the numbers of infiltrating CD4 cells and increased IFN- γ and TNF- α levels (Pender et al. 2005). The CCR1 and CCR3 antagonist, UCB35625, has been developed which changes the responses of MIP-1 α and MCP-4 from eosinophils and is currently in clinical trials for the treatment of eosinophil-mediated inflammatory disorders, such as asthma (Sabroe et al. 2000).

Given the evidence to show that IL-6 and MIP-1 α are involved in the pathogenesis of inflammatory disease, and now our findings that STX3 is involved in their secretion from DCs, blockade of their secretion from DCs through inhibition of this SNARE protein may prove an effective therapy in such diseases. Interestingly in RA, which is characterised by up-regulation of pro-inflammatory cytokines, patients have been treated successfully with intra-articular Botulinum Toxin (BoNT) A (Feldmann, Brennan and Maini 1996, Mahowald, Singh and Dykstra 2006). BoNTs are produced by various species of species of *Clostridia* and cleave specific proteins of SNARE

complexes. BoNT/A injections significantly improved joint pain by up to 55%, with no immediate or delayed adverse reactions to the injections of toxin which further supports our idea that regulation of cytokine secretion by SNARE inactivation may yield effective therapies in inflammatory disease (Borodic, Acquadro and Johnson 2001).

The importance of SNAREs proteins is further highlighted by the disease, familial hemophagocytic lymphohistiocytosis type-4 (FHL-4), which is the result of STX11 protein dysregulation. Patients with this disease present with FHL-4 with symptoms including high levels of pro-inflammatory cytokines (IFN- γ , IL-6, TNF and IL-18), higher numbers of activated, incorrectly phagocytosing macrophage and defective CTL and NK cells (D'Orlando et al. 2013, Gholam et al. 2011).

For this reason and the fact that we showed STX11 expression to be highly up-regulated *in vivo* and *in vitro*, we identified STX11 as another important SNARE in DC secretion. Following TLR2, 4 and 7 activation there was significant up-regulation of STX11 in JAWSII DCs and during early acute inflammation of DSS its expression was up-regulated in parallel with IL-6, TNF- α , IFN- γ , MIP-1 α , MIP-2 and MCP. Furthermore, in the *C. rodentium* model of colitis, STX11 was up-regulated in parallel with IL-6, TNF- α , IFN- γ and MCP-1. To investigate the role of this SNARE further, we employed the use of a STX11 deficient mouse model. Unlike STX3 where abolishment resulted in suppression of cytokine and chemokine secretion, STX11 deficiency resulted in a significant up-regulation of the IL-12 family and the expression of important cell surface markers and down-regulation of

CD11c DC surface marker in un-stimulated *Stx11*^{-/-} BMDCs compared to WT BMDCs. These significant phenotypical changes in un-stimulated resting *Stx11*^{-/-} BMDCs compared to WT BMDCs led us to believe that *Stx11*^{-/-} BMDCs display a more mature phenotype than WT BMDCs.

IFN- γ , a known DC modulator, was up-regulated in resting and stimulated *Stx11*^{-/-} BMDCs compared to WT BMDCs. We, in this study, and others show that BMDCs grown in IFN- γ have characteristics similar to *Stx11*^{-/-} BMDCs. Given the fact that IFN- γ has previously been reported to be up-regulated in CTLs and NK cells isolated from *Stx11*^{-/-} mouse and as STX11 has been reported to act as a negative regulator by binding to the SNARE Vti1b in a non-traditional *trans*-SNARE complex (Offenhaeuser et al. 2011), we proposed that STX11 negatively regulates IFN- γ secretion from BMDCs.

To support this hypothesis we demonstrated that STX11 expression was up-regulated in parallel with IFN- γ expression and secretion in WT BMDCs. This was further supported by our data showing the reversal of the *Stx11*^{-/-} BMDCs phenotype with an α -IFN- γ antibody. IFN- γ primed BMDCs have been reported to have an impaired ability to prime T cells, therefore we examined a number of parameters relevant to this. We showed that expression of PD-L1, a co-inhibitory marker on DCs for T cell activation was more highly up-regulated on *Stx11*^{-/-} BMDCs compared to WT DCs. This expression was reversed to normal levels with addition of an α -IFN antibody. In a T cell:*Stx11*^{-/-} BMDC co-culture, proliferation remained

unchanged but importantly T cell cytokines such as IL-2, important in the growth and proliferation of T cells, were significantly down-regulated.

T cells are reported to be tolerogenic or anergic when they fail to respond to their specific antigen (Schwartz 2003). We showed that *Stx11*^{-/-} BMDCs had increased levels of the co-inhibitory marker PD-L1 and the co-cultured T cells showed inhibition of cytokine secretion. However, these hyporesponsive T cells did not show any signs of inhibition of proliferation or arrested growth, both signs of T cells anergy. Hence more work in this area would need to be carried out to fully define the consequences of lack of regulated IFN γ in DCs for subsequent T cell activation.

Other work in our lab has pointed to a role for STX11 in T helper cells. We have identified differential expression of STX11 in Th1 and Th17 cells. High levels of STX11 and IFN γ in Th17 cells suggested a role for STX11 in Th17 differentiation as suppression of IFN γ is necessary for efficient Th17 differentiation. Indeed STX11 deficient mice were unable to differentiate into a Th17 subset due to the aberrant expression of IFN- γ . (DeCoursey, Unpublished).

IFN- γ has been implicated in many inflammatory diseases, indeed we identified it to its expressed in two mouse models of disease that we examined. Administration of IFN- γ to mouse models of CIA has been shown to accelerate disease onset and incidence, and treatment of CIA with an α -IFN- γ antibody resulted in reduced severity of disease and lower anti-collagen antibody levels (Chen and Liu 2009).

However, this was dependant on the stage of treatment; at later stages of disease treatment with this antibody aggravated the arthritis. We have shown that IFN- γ treatment can promote the expression of the suppressive molecule PD-L1 and which has the ability to antagonize Th17 cell development. This could conversely be a treatment of Th17 mediated diseases such as psoriasis, RA, MS, IBD and asthma. Subsequently, further investigation of IFN γ role in disease and its regulation in these Th17 mediated diseases could provide insight to its therapeutic potential.

It is important to note that secretion of the negative regulator of inflammation, Flightless (Flii), a gelsolin superfamily protein member has been reported to be regulated by Rab7 and STX11 in macrophage (Lei et al. 2012, Dai et al. 2009). It does so through a number of intracellular mechanisms including directly interfering with the formation of the TLR4-MyD88 signalling complex, resulting in reduced activation of NF- κ B (Dai et al. 2009, Wang et al. 2006). Lei et al., also suggest that Flii is secreted and can bind to LPS acting as a scavenger mopping up excess LPS and preventing hyper-activation of the immune system. In the absence of extracellular Flii, LPS activation of macrophage leads to increased TNF secretion and enhanced macrophage activation. (Lei et al. 2012). Although we didn't report a change in TNF- α expression in the *Stx11*^{-/-} BMDCs compared to WT BMDCs, Flii's secretion is regulated by STX11 and as Flii is indicated to negatively regulate inflammation, it would be interesting to look at Flii expression in the *Stx11*^{-/-} BMDCs compared to WT BMDCs.

In conclusion we have identified two important SNARE proteins that play key roles in DCs. STX3 mediates secretion of IL-6 from DCs. Given the significance of IL-6 in mediating inflammatory disease, our findings suggest that STX3 could be a potential target in such diseases to block secretion of this important cytokine. We also provided evidence that STX3 may also play a role in MIP-1 α secretion which could also provide useful in regulating inflammation. We also present a negative regulatory role for STX11 in IFN γ secretion and demonstrate an altered DC phenotype in STX11 deficient mice which may have consequences for subsequent T cell activation. Further characterisation of SNARE proteins in inflammatory disease may uncover a novel group of proteins which can be targeted to regulate inflammation.

The importance of future work into the SNARE complexes is highlighted by the award of a Nobel Prize to the initial researchers in this area who identified and functionally characterised these proteins and their involvement in trafficking. As trafficking underpins nearly all cell functions in particular the secretion of immune mediators, it would also be medically important to fully elucidate all steps involved in immune trafficking. As this work has identified two SNAREs, STX3 and STX11 involved in pathways of DC secretion, more work looking at their SNARE partners by means of co precipitation, location identification within the post-golgi domain (on secretory vesicles or the plasma membrane) would help elucidate the entire trafficking pathways of the cytokines or chemokines such as IL-6 and IFN- γ . This consequently could be used for therapeutic targets in the treatment of Th17 or Th1 mediated immune diseases where secretion of these cytokines from DCs contributes to the differentiation of T helper cell subsets.

APPENDICES

APPENDIX A**MEDIA AND BUFFERS****CELL CULTURE MEDIA****COMPLETE α -MEM**

500ml

Non-heat inactivated Foetal Calf Serum (FCS)

10%

Penicillin/Streptomycin/L-glutamine

100 μ g/ml:100 μ g/ml:2mM

Gentamycin

50 μ g/ml

rGMCSF

5ng/ml

COMPLETE RPMI 1640

500ml

Heat inactivated Foetal Calf Serum (FCS)

5%

Penicillin/Streptomycin/L-glutamine

100 μ g/ml:100 μ g/ml:2mM**10X PHOSPHATE BUFFERED SALINE (PBS)**Na₂HPO₄.2H₂O

8 mM

KH₂PO₄

1.5 mM

NaCl

137 mM

KCl

2.7 mM

Dissolved in dH₂O to a pH of 7.4**10 X TRIS BUFFERED SALINE (TBS) pH 7.6**

NaCl	1.5M
------	------

Trizma Base	0.2M
-------------	------

Dissolve dH₂O pH to 7.6

2N H₂SO₄

H ₂ SO ₄ (36 N)	11.1 ml
---------------------------------------	---------

dH ₂ O	88.9 ml
-------------------	---------

FACS BUFFER

FCS	2%
-----	----

NaN ₃	0.05%
------------------	-------

EDTA	0.5M
------	------

Dissolved PBS and 0.2μM filtered before use

NP-40 LYSIS BUFFER

Tris HCL (pH 7.5)	50mM
-------------------	------

NaCl	150mM
------	-------

Igepal	0.5%
--------	------

Protease Inhibitor Cocktail	1%
-----------------------------	----

Phosphatase Inhibitor Cocktail	1%
--------------------------------	----

5X SAMPLE BUFFER

125 mM Tris	6.25 ml 1M Tris HCl pH 6.8
10 % Glycerol	5 ml
2 % Sodium dodecyl sulphate (SDS)	10 ml (10 % (w/v) SDS)
0.05% (w/v) Bromophenol Blue	0.01 g
dH ₂ O	28.75 ml
0.25 M Dithiothreitol (DTT)*	250 µl 1 M DTT

* Added to 1 ml 5X Sample Buffer just before use

SEPARATING GEL (10% (v/v))

Acrylamide/Bisacrylamide (30% stock)	33% w/v
Tris-HCl pH8.8	1.5M
SDS	1% w/v
Ammonium persulphate	0.5% w/v
TEMED	0.1% v/v
Dissolved in dH ₂ O	

STACKING GEL

Acrylamide/Bisacrylamide (30% stock)	6.5% v/v
Tris-HCl pH6.8	0.5M
SDS	1% w/v
Ammonium persulphate	0.5% w/v
TEMED	0.1% v/v
Dissolved in dH ₂ O	

ELECTRODE RUNNING BUFFER

Tris base	25mM
Glycine	200mM
SDS	17mM
Dissolved in dH ₂ O	

50X TAE Buffer

Tris Base	40mM
Glacial Acetic Acid	20mM
EDTA	1mM
Dissolved in dH ₂ O and pH to 8.5	

PARFORMALDEHYDE

Paraformaldehyde	3% (w/v)
0.1M NaOH	500 ml

Place in a 70°C shaking water bath until dissolved (15mins). Cool to room temperature and pH with HCl to 7.2.

PERMABLOCK SOLUTION

Saponin	0.1% (v/v)
Fish gelatine	0.25% (v/v)
Sodium Azide	0.02% (w/v)
PBS	10 ml
All microscopy solutions were 0.2µM filtered before use.	

APPENDIX B

PRIMER TEMPERATURE GRADIENTS

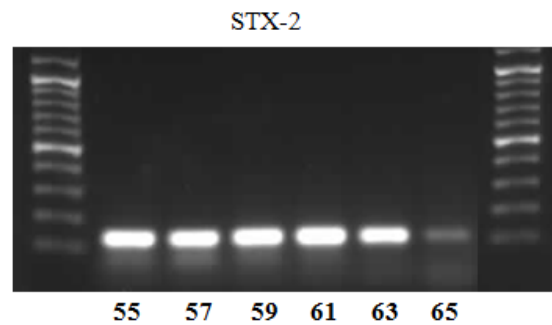


FIGURE A: Assay Validation: Primer Temperature Gradient for STX-2. RT-qPCR was performed using STX-2 primers. Master mix was prepared and split into six individual PCR tubes containing cDNA of LPS 100 ng/ml JAWS II DCs. Each mix was subjected to different temperatures ranging from 55-65 °C degrees.

TABLE A: Assay Validation: Primer Temperature Gradient for all primers. RT-qPCR was performed using specific primers. Master mix was prepared and split into six individual PCR tubes containing cDNA of LPS 100 ng/ml JAWS II DCs. Each mix was subjected to different temperatures ranging from 55-65°C degrees

Primer	Temperature Gradient producing product	Temperature used in RT-qPCR
SNAP-23	55-63°C	60°C
STX-2	55-63°C	60°C
STX-3	55-61°C	60°C
STX-4	55-63°C	60°C
STX-5	55-63°C	60°C
STX-6	55-63°C	60°C
STX-7	55-63°C	60°C
STX-11	55-61°C	60°C
STX-12	55-63°C	60°C
STX-16	55-63°C	60°C
Vti1a	55-61°C	60°C
Vti1b	55-61°C	60°C
Vamp-1	55-61°C	60°C
Vamp-2	59-65°C	60°C
Vamp-3	59-65°C	60°C
Vamp-4	59-65°C	60°C
Vamp-7	55-61°C	60°C
Vamp-8	55-65°C	60°C
Mip-1 α	55-61°C	60°C
Mip-2	55-61°C	60°C
MCP	55-61°C	60°C
IL-6	55-61°C	60°C
IFN- γ	55-61°C	60°C
S18	55-63°C	60°C

APPENDIX C

STX 3 TRANSFECTION DATA

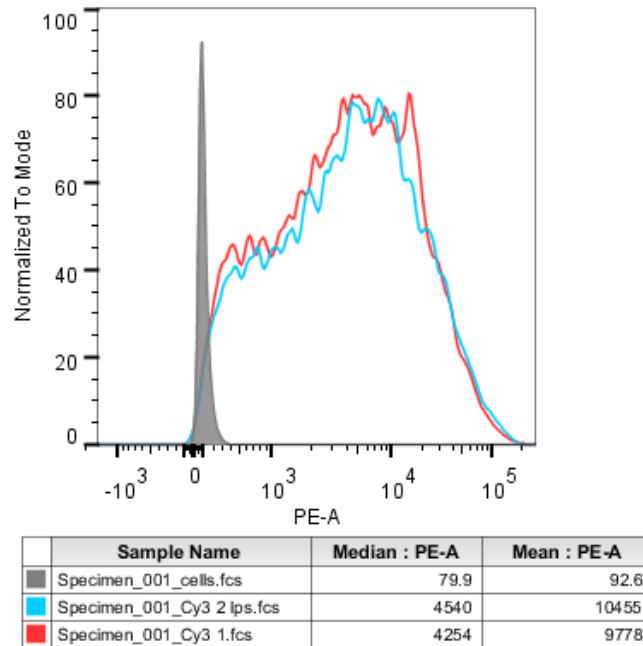


FIGURE B: Transfection Efficiency: JAWS II were differentiated in the presence of r-JAWSII DCs were transfected with siRNA against negative control non-silencing Cy-3 postivesiRNA. At 24h after the transfection cells were washed and read by FACS Aria. Results of flow cytometric analysis and corresponding MFI values are shown. Control DCs (grey filled histogram) vs Cy3-postiive transfected stimulated DCs (red/blue line). Profiles are shown for a single experiment and are representative of three experiments.

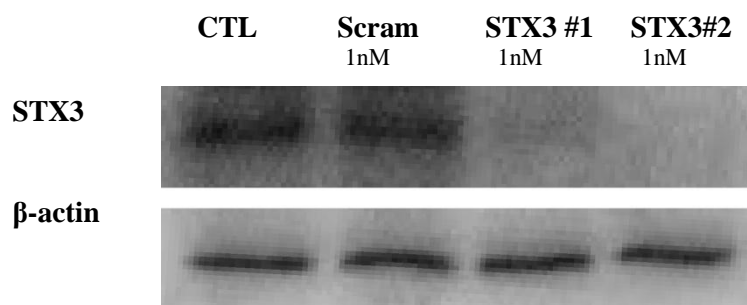


FIGURE C: Knockdown Efficiency: JAWS II were differentiated in the presence of r-JAWSII DCs were transfected with siRNA against negative control non-silencing Cy-3 postivesiRNA. At 24h after the transfection cells were lysed and immunoblotted for STX-3 (β -actin used as a loading control). Profiles are shown for a single experiment and are representative of three experiments.

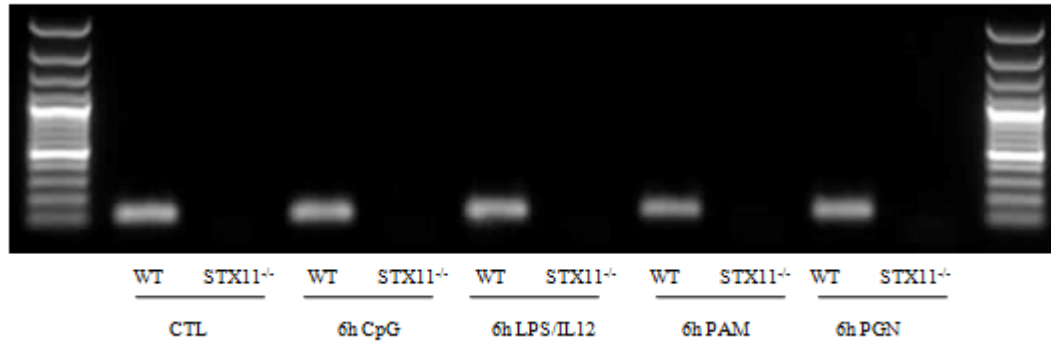
APPENDIX D STX-11 EXPRESSION IN WT AND STX-11^{-/-} BMDCs

FIGURE D: mRNA expression of STX-11 in WT AND STX-11^{-/-} BMDCs. WT and STX 11^{-/-} BMDCs were plated 1x10⁶/ml and stimulated with 100ng/ml LPS and 100µg/ml rIL-12, 2µM CpG, 5µg/ml PGN or 1µg/ml PAM for 6 hours. The amount of target mRNA was quantified by reverse transcription followed by RT-qPCR using an ABI 7900 HT detection system. PCR products were run out on a 1% agarose gel and STX-11 was detected at its respective bp product size.

BIBLIOGRAPHY

BIBLIOGRAPHY

Akira, S. and Hemmi, H. 2003. Recognition of pathogen-associated molecular patterns by TLR family. *Immunology Letters*, 85(2), pp.85-95.

Alex, P., Zachos, N.C., Nguyen, T., Gonzales, L., Chen, T., Conklin, L.S., Centola, M. and Li, X. 2009. Distinct cytokine patterns identified from multiplex profiles of murine DSS and TNBS-induced colitis. *Inflammatory Bowel Diseases*, 15(3), pp.341-352.

Atlashkin, V., Kreykenbohm, V., Eskelinen, E.L., Wenzel, D., Fayyazi, A. and von Mollard, G.F. 2003. Deletion of the SNARE *vti1b* in mice results in the loss of a single SNARE partner, syntaxin 8. *Molecular and Cellular Biology*, 23(15), pp.5198-5207.

BALCH, W., DUNPHY, W., BRAELL, W. and ROTHMAN, J. 1984. Reconstitution of the transport of protein between successive compartments of the golgi measured by the coupled incorporation of N-acetylglucosamine. *Cell*, 39(2), pp.405-416.

Banchereau, J. and Steinman, R.M. 1998a. Dendritic cells and the control of immunity. *Nature*, 392(6673), pp.245-252.

Banchereau, J. and Steinman, R. 1998b. Dendritic cells and the control of immunity. *Nature*, 392(6673), pp.245-252.

Baumgarth, N. and Roederer, M. 2000. A practical approach to multicolor flow cytometry for immunophenotyping. *Journal of Immunological Methods*, 243(1-2), pp.77-97.

BIBLIOGRAPHY

- Bennett, M.K., Garciaarraras, J.E., Elferink, L.A., Peterson, K., Fleming, A.M., Hazuka, C.D. and Scheller, R.H. 1993. The syntaxin family of vesicular transport receptors. *Cell*, 74(5), pp.863-873.
- Berndt, B.E., Zhang, M., Chen, G., Huffnagle, G.B. and Kao, J.Y. 2007. The role of dendritic cells in the development of acute dextran sulfate sodium colitis. *Journal of Immunology*, 179(9), pp.6255-6262.
- Bhinder, G., Sham, H.P., Chan, J.M., Morampudi, V., Jacobson, K. and Vallance, B.A. 2013. The citrobacter rodentium mouse model: Studying pathogen and host contributions to infectious colitis. *Journal of Visualized Experiments : JoVE*, (72), pp.e50222-e50222.
- Blanco, P., Palucka, A.K., Pascual, V. and Banchereau, J. 2008. Dendritic cells and cytokines in human inflammatory and autoimmune diseases. *Cytokine & Growth Factor Reviews*, 19(1), pp.41-52.
- Block, M., Glick, B., Wilcox, C., Wieland, F. and Rothman, J. 1988. Purification of an N-ethylmaleimide-sensitive protein catalyzing vesicular transport. *Proceedings of the National Academy of Sciences of the United States of America*, 85(21), pp.7852-7856.
- Boismenu, R. and Chen, Y.P. 2000. Insights from mouse models of colitis. *Journal of Leukocyte Biology*, 67(3), pp.267-278.
- Borodic, G.E., Acquadro, M. and Johnson, E.A. 2001. Botulinum toxin therapy for pain and inflammatory disorders: Mechanisms and therapeutic effects. *Expert Opinion on Investigational Drugs*, 10(8), pp.1531-1544.

BIBLIOGRAPHY

- Bostrom, P., Andersson, L., Vind, B., Haversen, L., Rutberg, M., Wickstrom, Y., Larsson, E., Jansson, P., Svensson, M.K., Branemark, R., Ling, C., Beck-Nielsen, H., Boren, J., Hojlund, K. and Olofsson, S. 2010. The SNARE protein SNAP23 and the SNARE-interacting protein Munc18c in human skeletal muscle are implicated in insulin Resistance/Type 2 diabetes. *Diabetes*, 59(8), pp.1870-1878.
- Bustin, S.A., Benes, V., Garson, J.A., Hellems, J., Huggett, J., Kubista, M., Mueller, R., Nolan, T., Pfaffl, M.W., Shipley, G.L., Vandesompele, J. and Wittwer, C.T. 2009. The MIQE guidelines: Minimum information for publication of quantitative real-time PCR experiments. *Clinical Chemistry*, 55(4), pp.611-622.
- Cai, D.T., Ho, Y.H.S., Chiow, K.H., Wee, S.H., Han, Y., Peh, M.T. and Wong, S.H. 2011. Aspirin regulates SNARE protein expression and phagocytosis in dendritic cells. *Molecular Membrane Biology*, 28(2), pp.90-102.
- Carmosino, M., Valenti, G., Caplan, M. and Svelto, M. 2010. Polarized traffic towards the cell surface: How to find the route. *Biology of the Cell*, 102(2), pp.75-91.
- Chan, V.W.F., Kothakota, S., Rohan, M.C., Panganiban-Lustan, L., Gardner, J.P., Wachowicz, M.S., Winter, J.A. and Williams, L.T. 1999. Secondary lymphoid-tissue chemokine (SLC) is chemotactic for mature dendritic cells. *Blood*, 93(11), pp.3610-3616.
- Chen, J. and Liu, X. 2009. The role of interferon gamma in regulation of CD4(+) T-cells and its clinical implications. *Cellular Immunology*, 254(2), pp.85-90.

BIBLIOGRAPHY

- Clary, D.O., Griff, I.C. and Rothman, J.E. 1990. Snaps, a family of nsf attachment proteins involved in intracellular membrane-fusion in animals and yeast. *Cell*, 61(4), pp.709-721.
- Collison, L.W., Workman, C.J., Kuo, T.T., Boyd, K., Wang, Y., Vignali, K.M., Cross, R., Sehy, D., Blumberg, R.S. and Vignali, D.A.A. 2007. The inhibitory cytokine IL-35 contributes to regulatory T-cell function. *Nature*, 450(7169), pp.566-U19.
- Creagh, E.M. and O'Neill, L.A.J. 2006. TLRs, NLRs and RLRs: A trinity of pathogen sensors that co-operate in innate immunity. *Trends in Immunology*, 27(8), pp.352-357.
- Cua, D.J., Sherlock, J., Chen, Y., Murphy, C.A., Joyce, B., Seymour, B., Lucian, L., To, W., Kwan, S., Churakova, T., Zurawski, S., Wiekowski, M., Lira, S.A., Gorman, D., Kastelein, R.A. and Sedgwick, J.D. 2003. Interleukin-23 rather than interleukin-12 is the critical cytokine for autoimmune inflammation of the brain. *Nature*, 421(6924), pp.744-748.
- Dai, P., Jeong, S.Y., Yu, Y., Leng, T., Wu, W., Xie, L. and Chen, X. 2009. Modulation of TLR signaling by multiple MyD88-interacting partners including leucine-rich repeat fli-I-interacting proteins. *Journal of Immunology*, 182(6), pp.3450-3460.
- De Koker, S., Lambrecht, B.N., Willart, M.A., van Kooyk, Y., Grooten, J., Vervaet, C., Remon, J.P. and De Geest, B.G. 2011. Designing polymeric particles for antigen delivery. *Chemical Society Reviews*, 40(1), pp.320-339.

BIBLIOGRAPHY

- de la Rosa, M., Rutz, S., Dorninger, H. and Scheffold, A. 2004. Interleukin-2 is essential for CD4(+)CD25(+) regulatory T cell function. *European Journal of Immunology*, 34(9), pp.2480-2488.
- Dearman, R.J., Cumberbatch, M., Maxwell, G., Basketter, D.A. and Kimber, I. 2009. Toll-like receptor ligand activation of murine bone marrow-derived dendritic cells. *Immunology*, 126(4), pp.475-484.
- Didierlaurent, A., Ferrero, I., Otten, L.A., Dubois, B., Reinhardt, M., Carlsen, H., Blomhoff, R., Akira, S., Kraehenbuhl, J.P. and Sirard, J.C. 2004. Flagellin promotes myeloid differentiation factor 88-dependent development of Th2-type response. *Journal of Immunology*, 172(11), pp.6922-6930.
- D'Orlando, O., Zhao, F., Kasper, B., Orinska, Z., Mueller, J., Hermans-Borgmeyer, I., Griffiths, G.M., Stadt, U.Z. and Bulfone-Paus, S. 2013. Syntaxin 11 is required for NK and CD8(+) T-cell cytotoxicity and neutrophil degranulation. *European Journal of Immunology*, 43(1), pp.194-208.
- Dowling, D., Hamilton, C.M. and O'Neill, S.M. 2008. A comparative analysis of cytokine responses, cell surface marker expression and MAPKs in DCs matured with LPS compared with a panel of TLR ligands. *Cytokine*, 41(3), pp.254-262.
- Dziarski, R. 2003. Recognition of bacterial peptidoglycan by the innate immune system. *Cellular and Molecular Life Sciences*, 60(9), pp.1793-1804.
- Egger, B., Bajaj-Elliott, M., MacDonald, T., Inglin, R., Eysselein, V. and Buchler, M. 2000. Characterisation of acute murine dextran sodium sulphate colitis: Cytokine profile and dose dependency. *Digestion*, 62(4), pp.240-248.

BIBLIOGRAPHY

- Farquhar, M.G. and Palade, G.E. 1998. The golgi apparatus: 100 years of progress and controversy. *Trends in Cell Biology*, 8(1), pp.2-10.
- Feldmann, M., Brennan, F. and Maini, R. 1996. Role of cytokines in rheumatoid arthritis. *Annual Review of Immunology*, 14pp.397-440.
- Frank, S.P.C., Thon, K., Bischoff, S.C. and Lorentz, A. 2011. SNAP-23 and syntaxin-3 are required for chemokine release by mature human mast cells. *Molecular Immunology*, 49(1-2), pp.353-358.
- Frucht, D., Fukao, T., Bogdan, C., Schindler, H., O'Shea, J. and Koyasu, S. 2001. IFN-gamma-production by antigen-presenting cells: Mechanisms emerge. *Trends in Immunology*, 22(10), pp.556-560.
- Galli, S., Kalesnikoff, J., Grimbaldston, M., Piliponsky, A., Williams, C. and Tsai, M. 2005. Mast cells as "tunable" effector and immunoregulatory cells: Recent advances. *Annual Review of Immunology*, 23pp.749-786.
- Gee, K., Guzzo, C., Mat, N.F.C., Ma, W. and Kumar, A. 2009. The IL-12 family of cytokines in infection, inflammation and autoimmune disorders. *Inflammation & Allergy Drug Targets*, 8(1), pp.40-52.
- Gholam, C., Grigoriadou, S., Gilmour, K.C. and Gaspar, H.B. 2011. Familial haemophagocytic lymphohistiocytosis: Advances in the genetic basis, diagnosis and management. *Clinical and Experimental Immunology*, 163(3), pp.271-283.
- Girolomoni, G., Lutz, M.B., Pastore, S., Abmann, C.U., Cavani, A. and Ricciardicastagnoli, P. 1995. Establishment of a cell-line with features of early

BIBLIOGRAPHY

dendritic cell precursors from fetal mouse skin. *European Journal of Immunology*, 25(8), pp.2163-2169.

Gorden, K.B., Gorski, K.S., Gibson, S.J., Kedl, R.M., Kieper, W.C., Qiu, X.H., Tomai, M.A., Alkan, S.S. and Vasilakos, J.P. 2005. Synthetic TLR agonists reveal functional differences between human TLR7 and TLR8. *Journal of Immunology*, 174(3), pp.1259-1268.

Guo, Z.H., Turner, C. and Castle, D. 1998. Relocation of the t-SNARE SNAP-23 from lamellipodia-like cell surface projections regulates compound exocytosis in mast cells. *Cell*, 94(4), pp.537-548.

Haase, C., Michelsen, B.K. and Jorgensen, T.N. 2004. CD40 is necessary for activation of naive T cells by a dendritic cell line in vivo but not in vitro. *Scandinavian Journal of Immunology*, 59(3), pp.237-245.

Hamerman, J.A., Ogasawara, K. and Lanier, L.L. 2005. NK cells in innate immunity. *Current Opinion in Immunology*, 17(1), pp.29-35.

Hartgers, F., Figdor, C. and Adema, G. 2000. Towards a molecular understanding of dendritic cell immunobiology. *Immunology Today*, 21(11), pp.542-545.

Hay, J. 2001. SNARE complex structure and function. *Experimental Cell Research*, 271(1), pp.10-21.

Higgins, L.M., Frankel, G., Douce, G., Dougan, G. and MacDonald, T.T. 1999. *Citrobacter rodentium* infection in mice elicits a mucosal Th1 cytokine response and lesions similar to those in murine inflammatory bowel disease. *Infection and Immunity*, 67(6), pp.3031-3039.

BIBLIOGRAPHY

- Ho, Y.H.S., Cai, D.T., Huang, D., Wang, C.C. and Wong, S.H. 2009. Caspases regulate VAMP-8 expression and phagocytosis in dendritic cells. *Biochemical and Biophysical Research Communications*, 387(2), pp.371-375.
- Ho, Y.H.S., Cai, D.T., Wang, C., Huang, D. and Wong, S.H. 2008. Vesicle-associated membrane protein-8/endobrevin negatively regulates phagocytosis of bacteria in dendritic cells. *Journal of Immunology*, 180(5), pp.3148-3157.
- Hue, S., Ahern, P., Buonocore, S., Kullberg, M.C., Cua, D.J., McKenzie, B.S., Powrie, F. and Maloy, K.J. 2006. Interleukin-23 drives innate and T cell-mediated intestinal inflammation. *Journal of Experimental Medicine*, 203(11), pp.2473-2483.
- Huizing, M., Anikster, Y. and Gahl, W. 2000. Hermansky-pudlak syndrome and related disorders of organelle formation. *Traffic*, 1(11), pp.823-835.
- Ierino, F.L., Mulley, W., Dodge, N., Li, Y.Q., Mouhtouris, E., Christiansen, D. and Sandrin, M.S. 2010. Dendritic cells expressing soluble CTLA4Ig prolong antigen-specific skin graft survival. *Immunology and Cell Biology*, 88(8), pp.846-850.
- Ishihara, K. and Hirano, T. 2002. IL-6 in autoimmune disease and chronic inflammatory proliferative disease. *Cytokine & Growth Factor Reviews*, 13(4-5), pp.357-368.
- Jahn, R. and Scheller, R.H. 2006. SNAREs - engines for membrane fusion. *Nature Reviews Molecular Cell Biology*, 7(9), pp.631-643.
- Jiang, X., Shen, C., Rey-Ladino, J., Yu, H. and Brunham, R.C. 2008. Characterization of murine dendritic cell line JAWS II and primary bone marrow-

BIBLIOGRAPHY

derived dendritic cells in chlamydia muridarum antigen presentation and induction of protective immunity. *Infection and Immunity*, 76(6), pp.2392-2401.

Jorgensen, T.N., Haase, C. and Michelsen, B.K. 2002. Treatment of an immortalized APC cell line with both cytokines and LPS ensures effective T-cell activation in vitro. *Scandinavian Journal of Immunology*, 56(5), pp.492-503.

Kawai, T. and Akira, S. 2006. TLR signaling. *Cell Death and Differentiation*, 13(5), pp.816-825.

Kenny, E.F. and O'Neill, L.A.J. 2008. Signalling adaptors used by toll-like receptors: An update. *Cytokine*, 43(3), pp.342-349.

Kimbrell, D.A. and Beutler, B. 2001. The evolution and genetics of innate immunity. *Nature Reviews Genetics*, 2(4), pp.256-267.

Kondkar, A.A., Bray, M.S., Leal, S.M., Nagalla, S., Liu, D.J., Jin, Y., Dong, J.F., Ren, Q., Whiteheart, S.W., Shaw, C. and Bray, P.F. 2010. VAMP8/endobrevin is overexpressed in hyperreactive human platelets: Suggested role for platelet microRNA. *Journal of Thrombosis and Haemostasis*, 8(2), pp.369-378.

Kondo, Y., Tachikawa, E., Ohtake, S., Kudo, K., Mizuma, K., Kashimoto, T., Irie, Y. and Taira, E. 2010. Inflammatory cytokines decrease the expression of nicotinic acetylcholine receptor during the cell maturation. *Molecular and Cellular Biochemistry*, 333(1-2), pp.57-64.

Lacy, P. 2006. Mechanisms of degranulation in neutrophils. *Allergy, Asthma, and Clinical Immunology : Official Journal of the Canadian Society of Allergy and Clinical Immunology*, 2(3), pp.98-108.

BIBLIOGRAPHY

- Laroui, H., Ingersoll, S.A., Liu, H.C., Baker, M.T., Ayyadurai, S., Charania, M.A., Laroui, F., Yan, Y., Sitaraman, S.V. and Merlin, D. 2012. Dextran sodium sulfate (DSS) induces colitis in mice by forming nano-lipocomplexes with medium-chain-length fatty acids in the colon. *Plos One*, 7(3), pp.e32084.
- Lavelle, E.C., Murphy, C., O'Neill, L.A.J. and Creagh, E.M. 2010. The role of TLRs, NLRs, and RLRs in mucosal innate immunity and homeostasis. *Mucosal Immunology*, 3(1), pp.17-28.
- Lee, J., Chuang, T.H., Redecke, V., She, L.P., Pitha, P.M., Carson, D.A., Raz, E. and Cottam, H.B. 2003. Molecular basis for the immunostimulatory activity of guanine nucleoside analogs: Activation of toll-like receptor 7. *Proceedings of the National Academy of Sciences of the United States of America*, 100(11), pp.6646-6651.
- Lei, N., Franken, L., Ruzehaji, N., Offenhaeuser, C., Cowin, A.J. and Murray, R.Z. 2012. Flightless, secreted through a late endosome/lysosome pathway, binds LPS and dampens cytokine secretion. *Journal of Cell Science*, 125(18), pp.4288-4296.
- Lorentz, A., Baumann, A., Vitte, J. and Blank, U. 2012. The SNARE machinery in mast cell secretion. *Frontiers in Immunology*, 3pp.143.
- Low, S.H., Chapin, S.J., Weimbs, T., Komuves, L.G., Bennett, M.K. and Mostov, K.E. 1996. Differential localization of syntaxin isoforms in polarized madin-darby canine kidney cells. *Molecular Biology of the Cell*, 7(12), pp.2007-2018.
- Luckashenak, N., Schroeder, S., Endt, K., Schmidt, D., Mahnke, K., Bachmann, M.F., Marconi, P., Deeg, C.A. and Brocker, T. 2008. Constitutive crosspresentation

BIBLIOGRAPHY

of tissue antigens by dendritic cells controls CD8(+) T cell tolerance in vivo.

Immunity, 28(4), pp.521-532.

Lutz, M., Kukutsch, N., Ogilvie, A., Rossner, S., Koch, F., Romani, N. and Schuler, G. 1999. An advanced culture method for generating large quantities of highly pure dendritic cells from mouse bone marrow. *Journal of Immunological Methods*, 223(1), pp.77-92.

Macdonald, T.T. 2011. New cytokine targets in inflammatory bowel disease.

Gastroenterology & Hepatology, 7(7), pp.474-6.

Mackay, V.L. and Moore, E.E.1997. *Immortalized dendritic cells*, 3.

Mahowald, M., Singh, J. and Dykstra, D. 2006. Long term effects of intra-articular botulinum toxin A for refractory joint pain. *Neurotoxicity Research*, 9(2-3), pp.179-188.

Malsam, J., Kreye, S. and Soellner, T.H. 2008. Membrane fusion: SNAREs and regulation. *Cellular and Molecular Life Sciences*, 65(18), pp.2814-2832.

Marcet-Palacios, M., Odemuyiwa, S.O., Coughlin, J.J., Garofoli, D., Ewen, C., Davidson, C.E., Ghaffari, M., Kane, K.P., Lacy, P., Logan, M.R., Befus, A.D., Bleackley, R.C. and Moqbel, R. 2008. Vesicle-associated membrane protein 7 (VAMP-7) is essential for target cell killing in a natural killer cell line. *Biochemical and Biophysical Research Communications*, 366(3), pp.617-623.

Marsh, R.A., Satake, N., Biroschak, J., Jacobs, T., Johnson, J., Jordan, M.B.,

Bleesing, J.J., Filipovich, A.H. and Zhang, K. 2010. STX11 mutations and clinical

BIBLIOGRAPHY

phenotypes of familial hemophagocytic lymphohistiocytosis in north america.

Pediatric Blood & Cancer, 55(1), pp.134-140.

Martin-Martin, B., Nabokina, S.M., Lazo, P.A. and Mollinedo, F. 1999. Co-expression of several human syntaxin genes in neutrophils and differentiating HL-60 cells: Variant isoforms and detection of syntaxin 1. *Journal of Leukocyte Biology*, 65(3), pp.397-406.

Maurer, M. and von Stebut, E. 2004. Macrophage inflammatory protein-1. *International Journal of Biochemistry & Cell Biology*, 36(10), pp.1882-1886.

McGettrick, A.F. and O'Neill, L.A.J. 2004. The expanding family of MyD88-like adaptors in toll-like receptor signal transduction. *Molecular Immunology*, 41(6-7), pp.577-582.

McGettrick, A.F. and O'Neill, L.A.J. 2010. Localisation and trafficking of toll-like receptors: An important mode of regulation. *Current Opinion in Immunology*, 22(1), pp.20-27.

Means, T.K., Hayashi, F., Smith, K.D., Aderem, A. and Luster, A.D. 2003. The toll-like receptor 5 stimulus bacterial flagellin induces maturation and chemokine production in human dendritic cells. *Journal of Immunology*, 170(10), pp.5165-5175.

Michelsen, K.S., Aicher, A., Mohaupt, M., Hartung, T., Dimmeler, S., Kirschning, C.J. and Schumann, R.R. 2001. The role of toll-like receptors (TLRs) in bacteria-induced maturation of murine dendritic cells (DCs) - peptidoglycan and lipoteichoic acid are inducers of DC maturation and require TLR2. *Journal of Biological Chemistry*, 276(28), pp.25680-25686.

BIBLIOGRAPHY

- Mills, K.H.G. 2011. TLR-dependent T cell activation in autoimmunity. *Nature Reviews Immunology*, 11(12), pp.807-822.
- Mollinedo, F., Calafat, J., Janssen, H., Martin-Martin, B., Canchado, J., Nabokina, S.M. and Gajate, C. 2006. Combinatorial SNARE complexes modulate the secretion of cytoplasmic granules in human neutrophils. *Journal of Immunology*, 177(5), pp.2831-2841.
- Mundy, R., MacDonald, T., Dougan, G., Frankel, G. and Wiles, S. 2005. *Citrobacter rodentium* of mice and man. *Cellular Microbiology*, 7(12), pp.1697-1706.
- Murphy, C.A., Langrish, C.L., Chen, Y., Blumenschein, C., McClanahan, T., Kastelein, R.A., Sedgwick, J.D. and Cua, D.J. 2003. Divergent pro- and antiinflammatory roles for IL-23 and IL-12 in joint autoimmune inflammation. *Journal of Experimental Medicine*, 198(12), pp.1951-1957.
- Murray, R.Z., Kay, J.G., Sangermani, D.G. and Stow, J.L. 2005a. A role for the phagosome in cytokine secretion. *Science*, 310(5753), pp.1492-1495.
- Murray, R.Z., Wylie, F.G., Khromykh, T., Hume, D.A. and Stow, J.L. 2005b. Syntaxin 6 and Vti1b form a novel SNARE complex, which is up-regulated in activated macrophages to facilitate exocytosis of tumor necrosis factor-alpha. *Journal of Biological Chemistry*, 280(11), pp.10478-10483.
- Ni, K. and O'Neill, H.C. 1997. The role of dendritic cells in T cell activation. *Immunology and Cell Biology*, 75(3), pp.223-230.

BIBLIOGRAPHY

- Offenhaeuser, C., Lei, N., Roy, S., Collins, B.M., Stow, J.L. and Murray, R.Z. 2011. Syntaxin 11 binds Vti1b and regulates late endosome to lysosome fusion in macrophages. *Traffic*, 12(6), pp.762-773.
- Ohtsuka, Y. and Sanderson, I.R. 2003. Dextran sulfate sodium-induced inflammation is enhanced by intestinal epithelial cell chemokine expression in mice. *Pediatric Research*, 53(1), pp.143-147.
- O'Neill, L.A.J., Golenbock, D. and Bowie, A.G. 2013. The history of toll-like receptors - redefining innate immunity. *Nature Reviews Immunology*, 13(6), pp.453-460.
- Pagan, J.K., Wylie, F.G., Joseph, S., Widberg, C., Bryant, N.J., James, D.E. and Stow, J.L. 2003. The t-SNARE syntaxin 4 is regulated during macrophage activation to function in membrane traffic and cytokine secretion. *Current Biology*, 13(2), pp.156-160.
- Pajtasz-Piasecka, E., Rossowska, J., Szyda, A., Krawczenko, A. and Dus, D. 2007. Generation of anti-tumor response by JAWS II mouse dendritic cells transduced with murine interleukin 12 genes. *Oncology Reports*, 17(5), pp.1249-1257.
- Pan, J., Zhang, M., Wang, J., Wang, Q., Xia, D., Sun, W., Zhang, L., Yu, H., Liu, Y. and Cao, X. 2004. Interferon-gamma is an autocrine mediator for dendritic cell maturation. *Immunology Letters*, 94(1-2), pp.141-151.
- Park, H., Li, Z., Yang, X., Chang, S., Nurieva, R., Wang, Y., Wang, Y., Hood, L., Zhu, Z., Tian, Q. and Dong, C. 2005. A distinct lineage of CD4 T cells regulates

BIBLIOGRAPHY

tissue inflammation by producing interleukin 17. *Nature Immunology*, 6(11), pp.1133-1141.

Parkin, J. and Cohen, B. 2001. An overview of the immune system. *Lancet*, 357(9270), pp.1777-1789.

Pender, S.L.F., Chance, V., Whiting, C.V., Buckley, M., Edwards, M., Pettipher, R. and MacDonald, T.T. 2005. Systemic administration of the chemokine macrophage inflammatory protein 1 alpha exacerbates inflammatory bowel disease in a mouse model. *Gut*, 54(8), pp.1114-1120.

Perse, M. and Cerar, A. 2012. Dextran sodium sulphate colitis mouse model: Traps and tricks. *Journal of Biomedicine and Biotechnology*, pp.718617.

Pickett, J. and Edwardson, J. 2006. Compound exocytosis: Mechanisms and functional significance. *Traffic*, 7(2), pp.109-116.

Pinchuk, L.M., Lee, S. and Filipov, N.M. 2007. In vitro atrazine exposure affects the phenotypic and functional maturation of dendritic cells. *Toxicology and Applied Pharmacology*, 223(3), pp.206-217.

Pulendran, B. 2004. Modulating vaccine responses with dendritic cells and toll-like receptors. *Immunological Reviews*, 199(1), pp.227-250.

Puri, N., Kruhlak, M.J., Whiteheart, S.W. and Roche, P.A. 2003. Mast cell degranulation requires N-ethylmaleimide-sensitive factor-mediated SNARE disassembly. *Journal of Immunology*, 171(10), pp.5345-5352.

BIBLIOGRAPHY

Rakoff-Nahoum, S., Paglino, J., Eslami-Varzaneh, F., Edberg, S. and Medzhitov, R. 2004. Recognition of commensal microflora by toll-like receptors is required for intestinal homeostasis. *Cell*, 118(2), pp.229-241.

Rinehart, JJ., Keville, L. 1997. Effects of endotoxin on proliferation of human cell precursors. *Cytotechnology*, 24 (2), pp 153-9.

Rojas, D. and Krishnan, R. 2010. IFN-gamma generates maturation-arrested dendritic cells that induce T cell hyporesponsiveness independent of Foxp3(+) T-regulatory cell generation. *Immunology Letters*, 132(1-2), pp.31-37.

Rongcun, Y., Maes, H., Corsi, M., Dellner, F., Wen, T. and Kiessling, R. 1998. Interferon gamma impairs the ability of monocyte-derived dendritic cells to present tumour-specific and allo-specific antigens and reduces their expression of CD1A, CD80 and CD4. *Cytokine*, 10(10), pp.747-755.

Ruedl, C. and Hubele, S. 1997. Maturation of peyer's patch dendritic cells in vitro upon stimulation via cytokines or CD40 triggering. *European Journal of Immunology*, 27(6), pp.1325-1330.

Sabroe, I., Peck, M., Van Keulen, B., Jorritsma, A., Simmons, G., Clapham, P., Williams, T. and Pease, J. 2000. A small molecule antagonist of chemokine receptors CCR1 and CCR3 - potent inhibition of eosinophil function and CCR3-mediated HIV-1 entry. *Journal of Biological Chemistry*, 275(34), pp.25985-25992.

Sallusto, F., Palermo, B., Lenig, D., Miettinen, M., Matikainen, S., Julkunen, I., Forster, R., Burgstahler, R., Lipp, M. and Lanzavecchia, A. 1999. Distinct patterns

BIBLIOGRAPHY

and kinetics of chemokine production regulate dendritic cell function. *European Journal of Immunology*, 29(5), pp.1617-1625.

Sallusto, F., Schaerli, P., Loetscher, P., Schaniel, C., Lenig, D., Mackay, C.R., Qin, S.X. and Lanzavecchia, A. 1998. Rapid and coordinated switch in chemokine receptor expression during dendritic cell maturation. *European Journal of Immunology*, 28(9), pp.2760-2769.

Schekman, R. and Orci, L. 1996. Coat proteins and vesicle budding. *Science*, 271(5255), pp.1526-1533.

Schroder, K., Hertzog, P.J., Ravasi, T. and Hume, D.A. 2004. Interferon-gamma: An overview of signals, mechanisms and functions. *Journal of Leukocyte Biology*, 75(2), pp.163-189.

Schwartz, R. 2003. T cell anergy. *Annual Review of Immunology*, 21pp.305-334.

Shen, T., Chen, X., Chen, Y., Xu, Q., Lu, F. and Liu, S. 2010. Increased PD-L1 expression and PD-L1/CD86 ratio on dendritic cells were associated with impaired dendritic cells function in HCV infection. *Journal of Medical Virology*, 82(7), pp.1152-1159.

Shiffman, D., Rowland, C.M., Louie, J.Z., Luke, M.M., Bare, L.A., Bolonick, J.I., Young, B.A., Catanese, J.J., Stiggins, C.F., Pullinger, C.R., Topol, E.J., Malloy, M.J., Kane, J.P., Ellis, S.G. and Devlin, J.J. 2006. Gene variants of VAMP8 and HNRPUL1 are associated with early-onset myocardial infarction. *Arteriosclerosis Thrombosis and Vascular Biology*, 26(7), pp.1613-1618.

BIBLIOGRAPHY

- Shirakawa, R., Higashi, T., Tabuchi, A., Yoshioka, A., Nishioka, H., Fukuda, M., Kita, T. and Horiuchi, H. 2004. Munc13-4 is a GTP-Rab27-binding protein regulating dense core granule secretion in platelets. *Journal of Biological Chemistry*, 279(11), pp.10730-10737.
- Singh-Jasuja, H., Thiolat, A., Ribon, M., Boissier, M., Bessis, N., Rammensee, H. and Decker, P. 2013. The mouse dendritic cell marker CD11c is down-regulated upon cell activation through toll-like receptor triggering. *Immunobiology*, 218(1), pp.28-39.
- Smith, A.D., Botero, S., Shea-Donohue, T. and Urban, J.F.,Jr. 2011. The pathogenicity of an enteric citrobacter rodentium infection is enhanced by deficiencies in the antioxidants selenium and vitamin E. *Infection and Immunity*, 79(4), pp.1471-1478.
- Steinman, R.M. 1998. Dendritic cells and the control of immunity. *Experimental Hematology*, 26(8), pp.681-681.
- Steinman, R.M. and Cohn, Z.A. 1973. Identification of a novel cell type in peripheral lymphoid organs of mice. *Journal of Experimental Medicine*, 137(5), pp.1142-1162.
- Stober, D., Schirmbeck, R. and Reimann, J. 2001. IL-12/IL-18-dependent IFN-gamma release by murine dendritic cells. *Journal of Immunology*, 167(2), pp.957-965.
- Stow, J.L. 2013. Nobel prize discovery paves the way for immunological traffic. *Nature Reviews.Immunology*, 13(12), pp.839-841.

BIBLIOGRAPHY

- Stow, J.L., Low, P.C., Offenhaeuser, C. and Sangermani, D. 2009. Cytokine secretion in macrophages and other cells: Pathways and mediators. *Immunobiology*, 214(7), pp.601-612.
- Stow, J.L., Manderson, A.P. and Murray, R.Z. 2006a. SNAREing immunity: The role of SNAREs in the immune system. *Nature Reviews Immunology*, 6(12), pp.919-929.
- Stow, J.L. and Murray, R.Z. 2013. Intracellular trafficking and secretion of inflammatory cytokines. *Cytokine & Growth Factor Reviews*, 24(3), pp.227-239.
- Sudhof, T.C. 1995. The synaptic vesicle cycle - a cascade of protein-protein interactions. *Nature*, 375(6533), pp.645-653.
- Sutton, R., Fasshauer, D., Jahn, R. and Brunger, A. 1998. Crystal structure of a SNARE complex involved in synaptic exocytosis at 2.4 angstrom resolution. *Nature*, 395(6700), pp.347-353.
- Taylor, P.C. and Feldmann, M. 2009. Anti-TNF biologic agents: Still the therapy of choice for rheumatoid arthritis. *Nature Reviews Rheumatology*, 5(10), pp.578-582.
- Tchernev, V.T., Mansfield, T.A., Giot, L., Kumar, A.M., Nandabalan, K., Li, Y., Mishra, V.S., Detter, J.C., Rothberg, J.M., Wallace, M.R., Southwick, F.S. and Kingsmore, S.F. 2002. The chediak-higashi protein interacts with SNARE complex and signal transduction proteins. *Molecular Medicine*, 8(1), pp.56-64.
- Ungar, D. and Hughson, F.M. 2003. SNARE protein structure and function. *Annual Review of Cell and Developmental Biology*, 19pp.493-517.

BIBLIOGRAPHY

- Villadangos, J.A. and Schnorrer, P. 2007. Intrinsic and cooperative antigen-presenting functions of dendritic-cell subsets in vivo. *Nature Reviews Immunology*, 7(7), pp.543-555.
- Wang, T., Chuang, T., Ronni, T., Gu, S., Du, Y., Cai, H., Sun, H., Yin, H. and Chen, X. 2006. Flightless I homology negatively modulates the TLR pathway. *Journal of Immunology*, 176(3), pp.1355-1362.
- Weimbs, T., Low, S.H., Chapin, S.J., Mostov, K.E., Bucher, P. and Hofmann, K. 1997. A conserved domain is present in different families of vesicular fusion proteins: A new superfamily. *Proceedings of the National Academy of Sciences of the United States of America*, 94(7), pp.3046-3051.
- Williams, R.O., Paleolog, E. and Feldmann, M. 2007. Cytokine inhibitors in rheumatoid arthritis and other autoimmune diseases. *Current Opinion in Pharmacology*, 7(4), pp.412-417.
- Wong, S., Zhang, T., Xu, Y., Subramaniam, V., Griffiths, G. and Hong, W. 1998. Endobrevin, a novel synaptobrevin/VAMP-like protein preferentially associated with the early endosome. *Molecular Biology of the Cell*, 9(6), pp.1549-1563.
- Woska, J.R., Jr. and Gillespie, M.E. 2011. Small-interfering RNA-mediated identification and regulation of the ternary SNARE complex mediating RBL-2H3 mast cell degranulation. *Scandinavian Journal of Immunology*, 73(1), pp.8-17.
- Xie, L., de la Iglesia-Vicente, J., Fang, Y. and Mollinedo, F. 2009. Expression and subcellular localization of syntaxin 11 in human neutrophils. *Inflammation Research*, 58(7), pp.407-412.

BIBLIOGRAPHY

Xue, M., Zhu, L., Meng, Y., Wang, L., Sun, H., Wang, F., Wang, E. and Shan, F. 2013. Detailed modulation of phenotypes and functions of bone marrow dendritic cells (BMDCs) by interferon-gamma (IFN-gamma). *International Immunopharmacology*, 17(2), pp.366-372.

Yan, Y., Kolachala, V., Dalmaso, G., Nguyen, H., Laroui, H., Sitaraman, S.V. and Merlin, D. 2009. Temporal and spatial analysis of clinical and molecular parameters in dextran sodium sulfate induced colitis. *Plos One*, 4(6), pp.e6073.

Yoshizaki, K. 2009. A new therapeutic strategy for autoimmune and chronic inflammatory disease based on clinical results using IL-6 blocking therapy with a humanized anti-IL-6 receptor antibody. *Yakugaku Zasshi-Journal of the Pharmaceutical Society of Japan*, 129(6), pp.667-674.

Zapala, L., Drela, N., Bil, J., Nowis, D., Basak, G.W. and Lasek, W. 2011. Optimization of activation requirements of immature mouse dendritic JAWSII cells for in vivo application. *Oncology Reports*, 25(3), pp.831-840.

zur Stadt, U., Schmidt, S., Diler, A.S., Henter, J.I., Kabisch, H., Schneppenheim, R., Nurnberg, P., Janka, G. and Hennies, H.C. 2005. Linkage of familial hemophagocytic lymphohistiocytosis (FHL) type-4 to chromosome 6q24 and identification of mutations in syntaxin 11. *Human Molecular Genetics*, 14(6), pp.827-834.